Fe-Catalyzed Cross-Coupling
of 1-Substituted Cyclopropyl Tosylates
&
Rh(III) Complexes in Carbene Transfer Reactions:
Development of an Azo Metathesis

Dissertation

zur Erlangung des akademischen Grades eines

Doktors der Naturwissenschaften

(Dr. rer. nat.)

des Fachbereichs Chemie und chemische Biologie

der Technischen Universität Dortmund

vorgelegt von

Daniel James Tindall

geboren am 26.11.1989

in Peine

Mülheim a. d. Ruhr, 2018

Eidesstattliche Versicherung (Affidavit)

Tindall, Daniel James_____
Name, Vorname
(Surname, first name)

182981_____
Matrikel-Nr.
(Enrolment number)

Mülheim a. d. Ruhr, 11.04.2018_
Ort, Datum
(Place, date)

_____
Unterschrift
(Signature)

Titel der Dissertation:
(Title of the thesis):

Fe-Catalyzed Cross-Coupling of 1-Substituted Cyclopropyl Tosylates &_____

Rh(III) Complexes in Carbene Transfer Reactions: Development of an Azo Metathesis_____

*Please be aware that solely the German version of the affidavit ("Eidesstattliche Versicherung") for the PhD thesis is the official and legally binding version.

Mülheim a. d. Ruhr, 11.04.2018_
Ort, Datum
(Place, date)

_____
Unterschrift
(Signature)

Die vorliegende Arbeit entstand unter Anleitung von Prof. Dr. Alois Fürstner in der Zeit von Februar 2015 bis März 2018 am Max-Planck-Institut für Kohlenforschung in Mülheim an der Ruhr. Teile dieser Arbeit wurden bereits in folgenden Beiträgen veröffentlicht:

„Iron-Catalyzed Cross-Coupling of 1-Alkynylcyclopropyl Tosylates and Related Substrates"

D. J. Tindall, H. Krause, A. Fürstner

Adv. Synth. Catal. **2016**, *358*, 2398–2403.

„Structure and Reactivity of Half-Sandwich Rh(+3) and Ir(+3) Carbene Complexes. Catalytic Metathesis of Azobenzene Derivatives"

D. J. Tindall, C. Werlé, R. Goddard, P. Philipps, C. Farès, A. Fürstner

J. Am. Chem. Soc.. **2018**, *140*, 1884–1893.

Die praktischen Arbeiten erfolgten zum Teil in Zusammenarbeit mit Helga Krause (Kapitel 2.2.1) und Dr. Christophe Werlé (Kapitel 3.2.1). Die beschriebenen Ergebnisse bilden eine vollständige Darstellung dieser gemeinsamen Arbeiten. Die von diesen Mitarbeitern alleinverantwortlich erzielten Ergebnisse wurden als solche an entsprechender Stelle gekennzeichnet.

1. Berichterstatter: Herr Prof. Dr. Alois Fürstner

2. Berichterstatter: Herr Prof. Dr. Norbert Krause

Meinen Eltern

Life is too long to be taken seriously all the time.

A little bit of humour helps!

I   Abstract

A novel Fe-catalyzed cross-coupling of 1-alkynylcyclopropyl tosylates **37** and alkyl Grignard reagents was developed, which represents the first Fe-catalyzed cross-coupling of *tert*-alkyl electrophiles. The protocol allows regioselective access to the direct (S_N2-type) substitution products **38** (Scheme 1, top), in contrast to related Fe-catalyzed processes involving propargylic substrates which furnish exclusively the S_N2'-type allene products. In addition, 1-vinyl-cyclopropyl tosylates **170** afforded the desired cross-coupling products **171** when reacted with MeMgCl. If β-hydrogens were available on the nucleophile, mixtures of the cross-coupling product **172** along with the reduced and the dimerized starting material (**45** and **46**, respectively) were obtained (Scheme 1, bottom). 1-Aryl- and 1-alkylcyclopropyl tosylates do not undergo this transformation which suggests that coordination of the substrate to the iron catalyst is necessary to allow for successful cross-coupling. Based on this observation, the more efficient reaction of **37** compared to that of **170** is explained by the higher binding affinity of the alkyne to the iron catalyst, thereby suppressing side reactions.
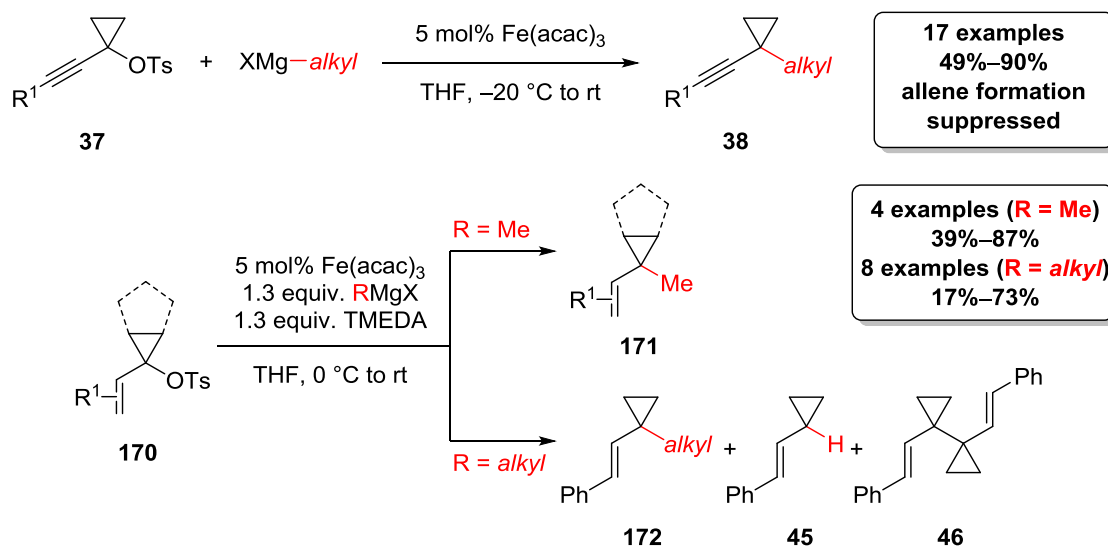
Scheme 1: Fe-catalyzed cross-coupling of 1-alkynyl- and 1-vinylcyclopropyl tosylates with alkylmagnesium halides.

Secondly, studies on Rh(III) complexes in carbene transfer reactions showed that carbene formation and migratory insertion are likely to be fast steps in Rh(III)-mediated C–H functionalization of arenes (Scheme 2, left). The presence of a labile ligand and the absence of inorganic impurities were essential for the conversion of **99** into **101**. Additionally, piano-stool complexes of the type [Cp*MX₂]₂ (M = Rh, Ir; X = Cl, Br, I) were shown to catalyze a representative set of carbene transfer reactions. Only [Cp*RhCl₂]₂ was found to be a poor catalyst, which is explained by the formation of C-metalated rhodium enolate **89** rather than the expected carbene complex **94** (Scheme 2, right).
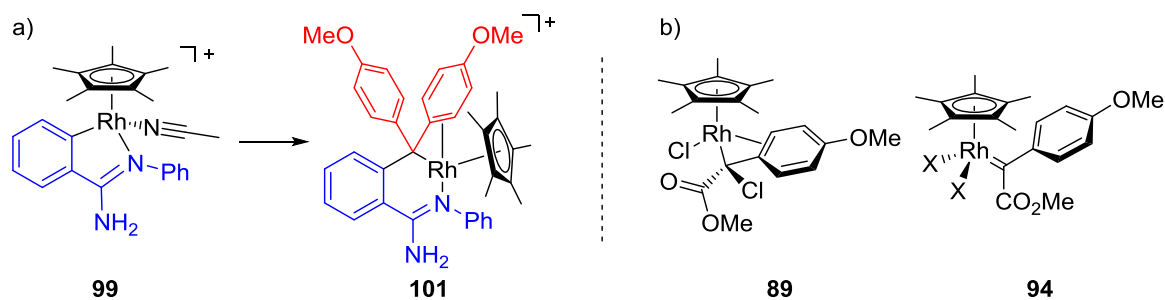
Scheme 2: a) Synthesis of a cyclometalated Rh(III) complex (**101**) though migratory insertion of a carbene derived from bis(4-methoxyphenyl)diazomethane (**100**, red). b) Rh(III) carbenoid complex **89** and Rh(III) carbene complex **94**.

Thirdly, a Rh(III)-catalyzed metathesis of diazo compounds **173** and azoarenes **174** affording α-imino esters **175** was developed (Scheme 3, top). Key to the success and scalability of the reaction was irradiation of the reaction mixture with blue LEDs which facilitate the *E→Z* isomerization of the azoarene and sets the scene for the metathesis to occur. This transformation represents a new type of reaction of donor/acceptor carbenes and shows a broad scope with high yields and an appreciable compatibility with polar and apolar substituents giving rise to α-imino esters which could not easily be synthesized by traditional means.

Mechanistic investigations argue against the intermediacy of a metal nitrene formed *via* the archetypal [2+2]/retro-[2+2] cycloaddition mechanism. Instead, reaction of rhodium carbene complex **95** and (*Z*)-azobenzene (**117**) forms a transient diaziridine **157** which was characterized by X-ray crystallography (Scheme 3, bottom). This intermediate can form the α-imino esters through two possible pathways: either a metal-free (bimolecular) decay of the three-membered ring releases the product **175** alongside (*E*)-azobenzene, which then re-enters the catalytic cycle, or the diaziridine **157** reacts with another rhodium carbene complex **95** leading to the product and regeneration of the catalyst, presumably *via* a cheletropic process.
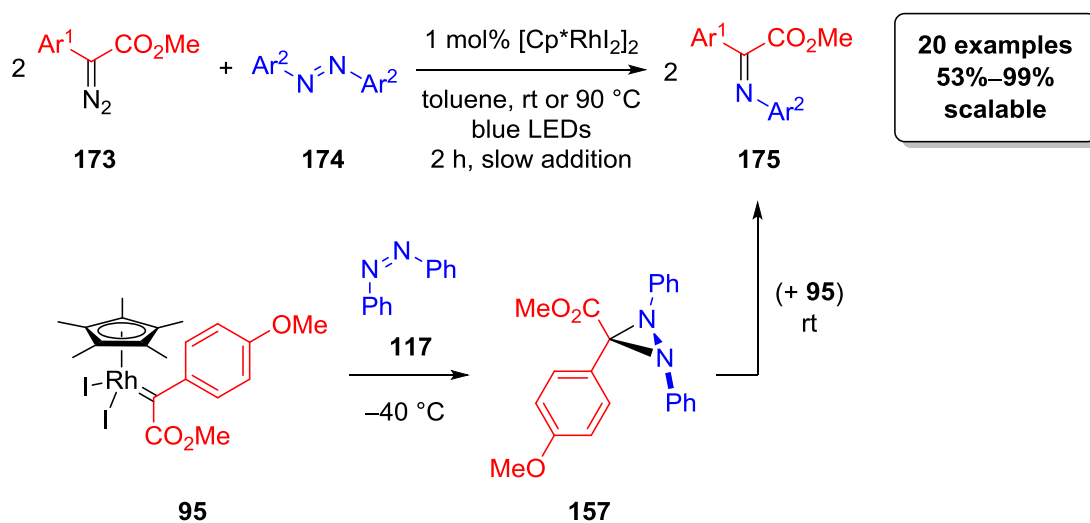
Scheme 3: Rh(III)-catalyzed metathesis of diazo compounds **173** and azoarenes **174**.

II Übersicht

Es wurde eine neuartige Fe-katalysierte Kreuzkupplung entwickelt, die zum ersten Mal tertiäre Elektrophile (1-Alkinylcyclopropyltosylate **37**) mit Alkyl-Grignard-Verbindungen kreuzkuppelt (Schema 1, oben). Sie erlaubt den regioselektiven Zugang zu den S_N2-artigen Substitutions-produkten **38**, während vergleichbare Fe-katalysierten Kreuzkupplungen mit propargylischen Substraten ausschließlich Allene (S_N2'-Produkte) liefern. Weiterhin wurden aus 1-Vinylcyclo-propyltosylaten **170** mit MeMgCl die Kreuzkupplungsprodukte **171** erhalten (Schema 1, unten). Die höheren homologen Alkyl-Grignard-Verbindungen lieferten die Kreuzkupplungsprodukte **172** zusammen mit dem reduzierten (**45**) und dem dimerisierten Startmaterial (**46**). 1-Aryl- und 1-Alkylcyclopropyltosylate ließen sich nicht kreuzkuppeln, sodass vermutet wird, dass eine Koordination des Substrats an den Eisenkatalysator erforderlich ist. Dies liefert einen Erklärungsansatz für das unterschiedliche Reaktionsverhalten von **37** und **170**: Alkine **37** binden stärker an den Eisenkatalysator, was zur Unterdrückung von Nebenprodukten führt. Dagegen binden Alkene **170** schwächer an den Eisenkatalysator, was Nebenreaktionen wahrscheinlicher macht und zu den Nebenprodukten **45** und **46** führt.
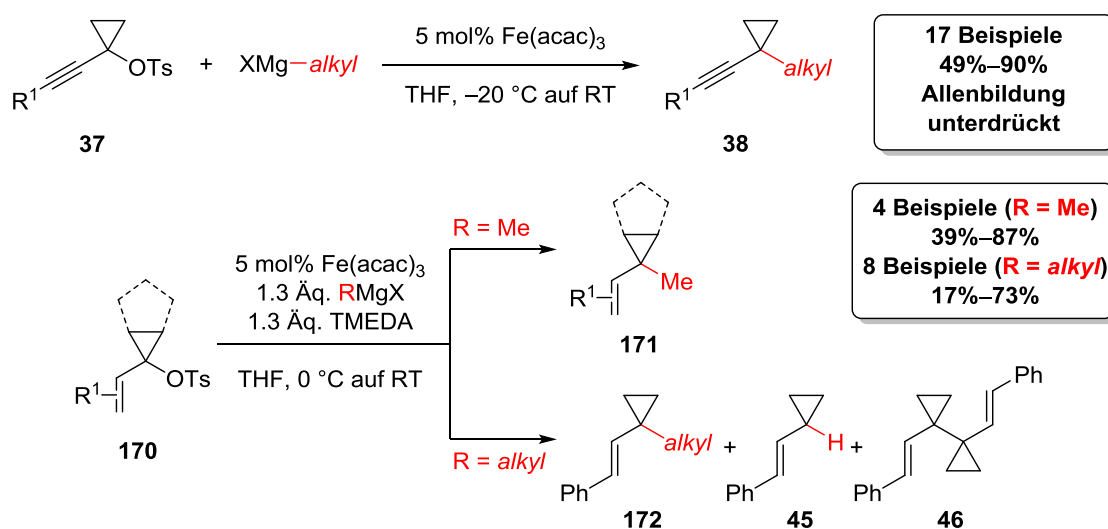
Schema 1: Fe-katalysierte Kreuzkupplungen von 1-Alkinyl- und 1-Vinylcyclopropyltosylaten mit Alkyl-Grignard-Verbindungen.

Im zweiten Teil zeigten Studien an Rh(III)-Komplexen in Carben-Übertragungsreaktionen, dass in Rh(III)-vermittelten C–H-Funktionalisierungen die Carben-Bildung und Carben-Insertion wahrscheinlich schnell ablaufen (Schema 2, links). Um den Komplex **101** zu erhalten, musste der Startkomplex **99** frei von anorganischen Verunreinigungen sein und einen leicht dissoziierenden Liganden besitzen. Weiterhin konnte gezeigt werden, dass neutrale Komplexe des Typs [Cp*MX$_2$]$_2$ (M = Rh, Ir; X = Cl, Br, I) verschiedene repräsentative Carben-Übertragungsreaktionen katalysieren. Einzig [Cp*RhCl$_2$]$_2$ stellte sich als ungeeignet heraus. Dies wurde damit erklärt,

dass [Cp*RhCl$_2$]$_2$ statt des zu erwartenden Carben-Komplexes **94** ein C-metalliertes Rhodium-Enolat **89** bildet (Schema 2, rechts).
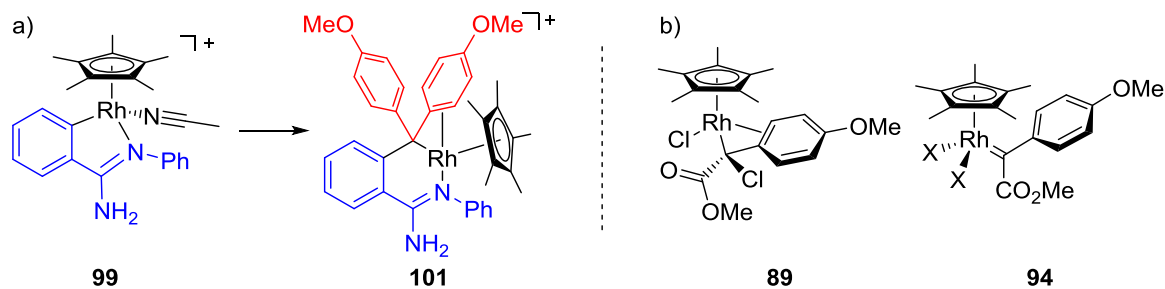
Schema 2: a) Synthese eines zyklometallierten Rh(III)-Komplexes (**101**) durch Insertion eines Carbens abgeleitet von Bis(4-methoxyphenyl)diazomethan (**100**, rot). b) Rh(III)-Carbenoid-Komplex **89** und Rh(III)-Carben-Komplex **94**.

Im dritten Teil wurde eine Rh(III)-katalysierte Metathese von Diazoverbindungen **173** und Azoarenen **174** entwickelt, welche einen neuen Reaktionstyp für Donor/Akzeptor-Carbene darstellt (Schema 3, oben). Kern der milden und skalierbaren Methode ist die Bestrahlung der Reaktionsmischung mit blauen LEDs, um die $E{\rightarrow}Z$-Isomerisierung der Azoarene zu ermöglichen. Die Reaktion liefert gute Ausbeuten und zeigt eine hohe Toleranz gegenüber verschiedenen polaren und unpolaren Gruppen. Damit erlaubt sie den Zugang zu α-Iminoestern **175**, die mit traditionellen Methoden schwer zu synthetisieren sind.

Detaillierte Untersuchungen sprechen gegen einen Mechanismus analog zu dem der Alken-metathese unter Bildung von Metallnitrenen als Zwischenprodukte. Stattdessen reagiert ein Rhodium-Carben-Komplex **95** mit (*Z*)-Azobenzol (**117**) unter Bildung eines instabilen Diaziridins **157**, welches kristallografisch charakterisiert wurde (Schema 3, unten). Für die Bildung der α-Iminoester werden zwei Reaktionswege vorgeschlagen: Entweder zerfällt **157** (bimolekular) unter Freisetzung von **175** und (*E*)-Azobenzol, welches wieder in den Katalysezyklus eintritt, oder **157** reagiert mit einem weiteren Äquivalent des Rhodium-Carben-Komplexes **95** unter Bildung einer Spezies, die in einem vermutlich cheletropen Prozess das Produkt **175** und den Katalysator freisetzt.
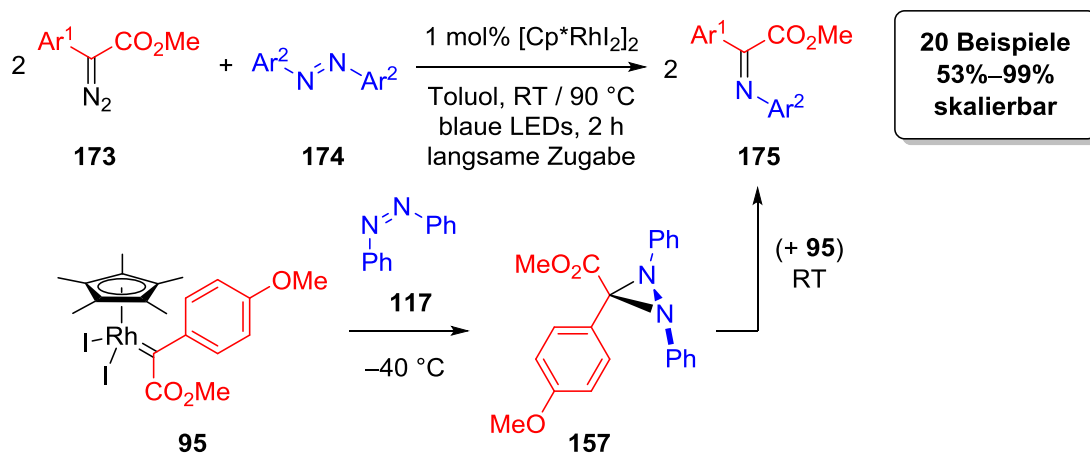
Schema 3: Rh(III)-katalysierte Metathese von Diazoverbindungen **173** und Azoarenen **174**.

III List of Abbreviations

2c/2e	two-center/two-electron		EI	electron impact
3c/4e	three-center/four-electron		EPR	electron paramagnetic resonance
Ac	acetyl		equiv.	equivalent
acac	acetylacetonate		ESI	electrospray ionization
APPI	atmospheric pressure photo ionization		Et	ethyl
aq.	aqueous		eV	electron volts
Ar	aryl		EWG	electron withdrawing group
Bn	benzyl		EXAFS	extended X-ray absorption fine structure
br	broad			
brsm	based on recovered starting material		g	gram
cat.	catalytic		GC	gas chromatography
cf.	*confer* (compare or consult)		h	hour
Cp*	1,2,3,4,5-pentamethylcyclopentadienyl		HIV	human immunodeficiency virus
cm	centimeter		HMBC	heteronuclear multiple-bond correlation
cod	1,5-cyclooctadiene			
COSY	correlation spectroscopy		HMTA	hexamethylenetetramine
CPME	cyclopentyl methyl ether		HPLC	high performance liquid chromatography
δ	chemical shift			
d	doublet		HRMS	high resolution mass spectrometry
dd	doublet of doublets		HSQC	heteronuclear single quantum coherence/correlation
ddd	doublet of doublet of doublets			
ddt	doublet of doublet of triplets		Hz	hertz
dt	doublet of triplets		*i*-Pr	isopropyl
DABCO	1,4-diazabicyclo[2.2.2]octane		IR	infrared
dba	dibenzylideneacetone		I_V	luminous intensity
dbm	dibenzoylmethide		J	coupling constant
DCE	1,2-dichloroethane		L	neutral ligand
DEAD	diethyl azodicarboxylate		λ	wavelength
DFT	density functional theory		LED	light-emitting diode
DG	directing group		LUMO	lowest unoccupied molecular orbital
DMAP	4-dimethylaminopyridine		µL	microliter
dppe	1,2-bis(diphenylphosphino)ethane		µm	micrometer
E	nonmetal		µmol	micromole
Ed(s).	editor(s)		m	multiplet
EDA	ethyl diazo acetate		*m*	mass
EDG	electron donating group		M	metal
			M	molecular peak

M	molarity	sat.	saturated
mcd	millicandela	SE	*societas Europaea*
MCD	magnetic circular dichroism	sept	septet
Me	methyl	SET	single electron transfer
MeCN	acetonitrile	SHOP	Shell Higher Olefin Process
mg	milligram	SIPr	1,3-bis(2,6-diisopropylphenyl)-imidazolidene
MHz	megahertz		
min	minute	SKU	stock keeping unit
mL	milliliter	S_N	nucleophilic substitution
mmol	millimole	t	triplet
M.p.	melting point	*t*	time
MS	mass spectrometry	*T*	temperature
n-Bu	*n*-butyl	TBDPS	*tert*-butyldiphenylsilyl
NHC	N-heterocyclic carbene	TBS	*tert*-butyldimethylsilyl
nm	nanometer	*t*-Bu	*tert*-butyl
NMR	nuclear magnetic resonance	td	triplet of doublets
NMP	*N*-methyl-2-pyrrolidone	*tert*	tertiary
№	numero sign	Tf	trifluoromethylsulfonyl (triflyl)
NOESY	nuclear Overhauser enhancement and exchange spectroscopy	THF	tetrahydrofurane
		TLC	thin layer chromatography
q	quartet	TMEDA	tetramethylethylenediamine
quint	quintet	tpa	triphenylacetate
Ph	phenyl	Ts	*p*-toluenesulfonyl (tosyl)
Phen	phenanthroline	$\tilde{\nu}$	wavenumber
Piv	pivalate	V	volt
ppm	parts per million	W	watt
p-tol	*para*-tolyl	X	halogen or halide
R	residue	Xantphos	4,5-bis(diphenylphosphino)-9,9-dimethylxanthene
rt	room temperature		
s	singlet	Y	heteroatom
S	spin	*z*	charge number

IV Table of Contents

1 General Introduction

Catalysis, a term derived from the ancient Greek κατάλυσις, English 'a dissolving, dissolution', is defined as the process in which "a substance [the catalyst] increases the rate of a reaction without modifying the overall standard Gibbs energy change in the reaction. The catalyst is both a *reactant* and *product* of the reaction".[1] Although this term was coined by Berzelius in the 19th century,[2] many other people have contributed to the development of the concept of catalysis (*e.g.*, Faraday, Davy, Döbereiner, Dulong, Thénard, Phillips, Ostwald, Henry, Wilhelmy, and Kuhlmann).[3] Applications of catalysis predate its naming. The point when mankind began to produce alcohol by fermentation (*i.e.*, biocatalysis) is most likely the first exploitation of catalysis.

Catalysts render reactions feasible as well as selective.[4] Feasibility refers not only to the occurrence of a reaction in the first place, but also to lowering the temperature, pressure, and time required for the reaction to take place. In addition, the selectivity of complex chemical transformations is important as completely different products might be obtained from the same starting materials by choosing an appropriate catalytic system.

In the past century, catalysis has undergone massive development.[5] At the beginning of the century, the growing academic knowledge in chemistry began to be translated into industrial applications. Processes for the production of fertilizers (*e.g.*, Haber–Bosch process) and fuels for machinery (*e.g.*, Fischer–Tropsch process) were needed for a growing (industrialized) population. Furthermore, the World Wars demanded processes for the production of explosives for weapons. Later, various catalytic processes for the manufacturing of synthetic polymers were developed (*e.g.*, Ziegler–Natta process) while the petrochemical industry provided many of the feedstocks needed (*e.g.*, SHOP process). Nowadays, approximately 85–90% of the products in the chemical industry are made *via* catalytic processes. In addition, the negative impact of industrial chemistry on the environment is increasingly recognized and the development of new technologies to mitigate this began in earnest at the end of the last century.

The development of industrial chemistry is closely related to the development of catalysis.[6] Modern research approaches catalysis in two ways: firstly, established methods are modified to match them with today's requirements—especially with respect to their environmental impact. Secondly, it seeks for further exploration of space beyond the one covered by the existing catalytic reactions.

In relation to the latter, the first chapter of this thesis is concerned with the development of a Kumada–Tamao–Corriu-type cross-coupling reaction of *tert*-alkyl electrophiles and Grignard reagents catalyzed by an iron catalyst of low environmental impact. The second chapter is concerned with the exploration of neutral piano-stool complexes of rhodium and iridium as catalysts in carbene transfer reactions. The subsequent development of a metathesis of azoarenes and diazo compounds represents an expansion of the known space of carbene transfer reactions.

2 Fe-Catalyzed Cross-Coupling Reactions of 1-Substituted Cyclopropyl Tosylates

2.1 Introduction

Modern synthetic chemistry benefits from a wide range of chemical transformations. Among these, transition metal-catalyzed cross-coupling represents one of the most successful reactions. Cross-couplings have found wide applications in the industrial synthesis of fine chemicals, pharmaceuticals,[7] agricultural chemicals,[8] and synthetic polymers,[9] as well as in natural product synthesis.[10] The awarding of the Nobel Prize in Chemistry to Heck, Negishi, and Suzuki in 2010 "for palladium-catalyzed cross couplings in organic synthesis" further emphasizes the importance of this methodology.[11]

Palladium plays a dominant role in cross-coupling, but other transition metals such as nickel are also often used in catalytic systems. This is attributed to their versatility, high functional group tolerance, and their selective reaction towards electrophiles. Despite their advantages, these metals have drawbacks: they are not bio-compatible and are often highly toxic. In addition, the natural abundance of palladium is low and, consequently, it is expensive. Therefore, researchers are increasingly exploring alternatives to avoid these disadvantages. One excellent candidate for this purpose is iron. Its abundance in the Earth's crust is the second highest of the metals after aluminium (Fe: 41×10^3 ppm, Pd: 6×10^{-6} ppm, Ni: 80 ppm)[12] and is, consequently, much cheaper (Fe: ≈ 0.09 €/kg, Pd: $\approx 28,000$ €/kg, Ni: ≈ 10 €/kg).[13] In addition, iron is an integral part of many biological systems and its toxicity is low. This is reflected in the classification by the European authorities of iron being a "metal of minimal safety concern" (the permitted oral exposure concentrations in drug substances are given: Fe: 1300 ppm, Pd: 10 ppm, Ni: 25 ppm).[14] Therefore, its low toxicity makes iron especially attractive for the pharmaceutical and the food industry.[15]

In addition to these economic considerations, Fe-catalyzed cross-coupling reactions show a remarkable functional group tolerance, short reaction times, and mild reaction conditions. A selected example is given in Scheme 4, in which Fürstner *et al.* performed a Kumada–Tamao–Corriu-type cross-coupling of an aryl chloride in the presence of an ester group within minutes on a gram-scale.[16] The reaction is fast enough to outcompete the Grignard addition to the carbonyl, which occurs in the absence of the iron catalyst.
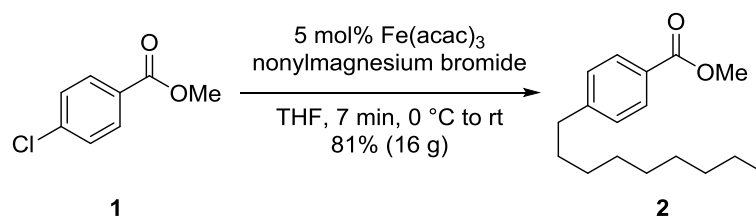
Scheme 4: Gram-scale synthesis of the liquid crystalline material methyl 4-nonylbenzoate (**2**).

In addition, iron serves not only as a simple replacement for other transition metals, but it also offers new modes of reactivity. For example, Sun and Fürstner reported an Fe-catalyzed ring-opening/cross-coupling reaction of 2-pyrones to furnish stereodefined dienyl carboxylates.[17] This methodology was mild and selective enough to be applied in total synthesis (Scheme 5): the *Z,E*-configured dienoate subunit (blue) in **4** was accessed by this method from the 2-pyrone ring (blue) in **3**. A subsequent Mukaiyama-type macrolactonization afforded macrocycle **5**.[18]
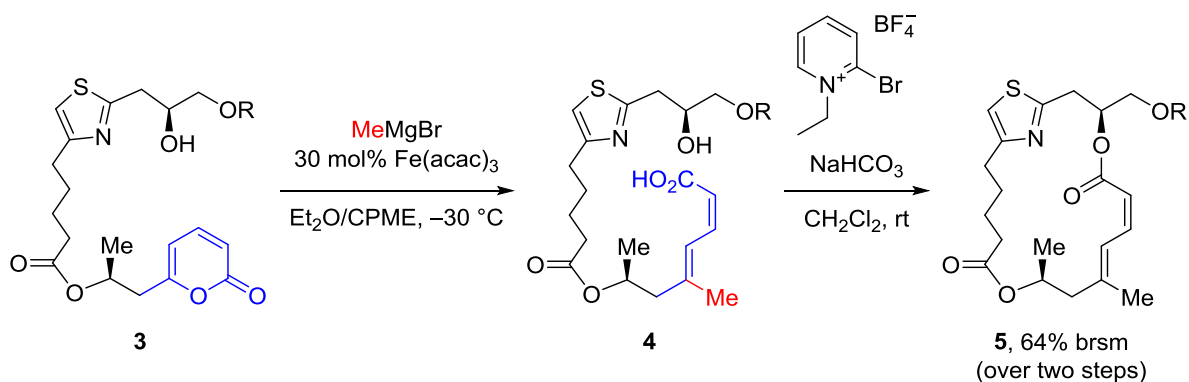
Scheme 5: Two-step macrolactonization in the total synthesis of a pateamine A analogue: Fe-catalyzed pyrone ring-opening/cross-coupling sequence, followed by a Mukaiyama-type macrolactonization (R = TBDPS).

These are only two examples in the field of iron catalysis which has grown massively since the turn of the millennium. Iron has not yet gained the same efficiency and broad applications as palladium, but, the reviews of the growing numbers of publications on iron catalysis—which do not only deal with cross-couplings—showcase that iron is rapidly catching up.[19–29]

2.1.1 Historic Development

The first couplings mediated by iron date back to the early 1940s, when Kharasch and Fields described the homocoupling of aryl Grignard reagents in the presence of an aryl halide as the terminal oxidant.[30,31] The reaction was catalyzed by various metal salts, such as $CoCl_2$, CuCl, $MnCl_2$, $NiCl_2$, $CrCl_3$, and $FeCl_3$. Around this time, Vavon *et al.* reported the first Fe-catalyzed cross-coupling of arylmagnesium bromides and *n*-alkyl halides (Scheme 6, top).[32]

In 1953, Cook and co-workers reported the synthesis of aliphatic ketones from acid chlorides and aliphatic Grignard reagents, catalyzed by $FeCl_3$ (Scheme 6, center).[33] This reaction represents an early example of iron's excellent reactivity profile, outperforming the un-catalyzed

reduction of the carbonyl to the corresponding alcohol. Later, Cason and Kraus investigated the mechanism of this transformation.[34,35]

Vavont, 1944

$$Et{-}Br \quad + \quad BrMg{-}\langle\rangle{-}OMe \quad \xrightarrow[\substack{Et_2O,\ rt \\ 58\%}]{cat.\ FeCl_3} \quad Et{-}\langle\rangle{-}OMe$$

Cook, 1953

$$\underset{Me}{\overset{O}{\|}}{Cl} \quad + \quad ClMg{\diagup}{\diagdown}{Me} \quad \xrightarrow[\substack{Et_2O,\ -70\ °C \\ 72\%}]{cat.\ FeCl_3} \quad \underset{Me}{\overset{O}{\|}}{\diagup}{\diagdown}{Me}$$

Kochi, 1971

$$3\ equiv. \quad Me{\diagup}{\diagdown}{Br} \quad + \quad MeMgBr \quad \xrightarrow[\substack{THF,\ 25\ °C \\ >95\%}]{5\ mol\%\ FeCl_3} \quad Me{\diagup}{\diagdown}{Me}$$
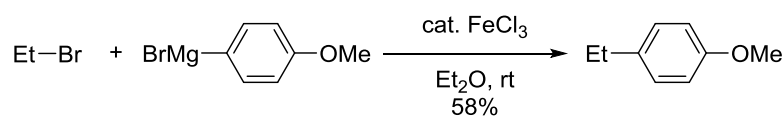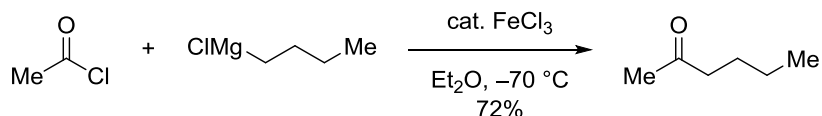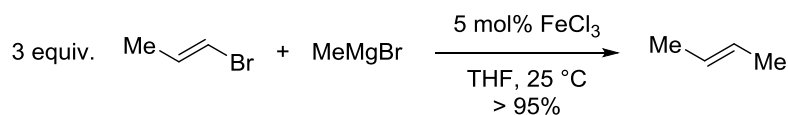
Scheme 6: Early examples of Fe-catalyzed cross-coupling reactions.

Almost 20 years later, Kochi *et al.* reported the Fe-mediated cross-coupling of alkenyl bromides and alkylmagnesium halides under mild reaction conditions (Scheme 6, bottom).[36] Several iron salts and complexes were found to be suitable pre-catalysts, of which tris(dibenzoyl-methide)iron(III) (Fe(dbm)$_3$) was found to be most effective with regards to reaction rate and catalyst stability.[37] *E*-Configured alkenyl bromides were found to react faster than their *Z*-configured isomers, with stereoretention of the double bond geometry observed in both cases.

One year after Kochi's report, Kumada and Corriu published their studies on the Ni-catalyzed reactions of Grignard reagents with vinyl and aryl halides, which can be seen as the foundation of transition metal cross-coupling chemistry.[38] Somehow, Kochi's work was not well received by the chemical community at the time and Fe-catalyzed cross-coupling remained a curiosity until the mid-1990s. Up to that point, the modest yields, low selectivities, and the limited substrate scope (*e.g.*, alkenyl halides,[39] alkenyl sulfones,[40] acid chlorides,[34,35,41] thiolesters,[42] and allylic phosphates[43])[44] are reasons why Fe-catalyzed cross-coupling reactions have not found many applications as opposed to the related Pd-catalyzed reactions. In the following years, several advances began to address these issues.

One major advance was the introduction of *N*-methyl-2-pyrrolidone (NMP) as a co-solvent by Cahiez and co-workers in 1998 (Scheme 7, top).[45] The use of NMP, which was first reported for the Fe-catalyzed alkenylation of organomanganese reagents,[39f] led to higher yields and an

extended functional group tolerance. The advances in the synthesis of functionalized Grignard reagents increased the synthetic versatility again.[46]

In 2002, Fürstner *et al.* expanded the scope of Fe-catalyzed cross-coupling of alkyl Grignard reagents to include aryl halides as the reaction partner (Scheme 7, center).[47] In contrast to what is usually observed in palladium and nickel catalysis, this methodology provides better results with aryl chlorides and triflates than with the corresponding bromides or iodides. Although the reaction was shown to be widely applicable to various electron poor and electron rich (hetero-) aromatic electrophiles,[48] only alkyl Grignard reagents were found to be suitable coupling partners. Aryl, allyl, and alkenyl Grignard reagents gave poor results, which was attributed to the formation of significant quantities of homocoupled biaryls or dienes under the catalytic conditions .[49]

Cahiez, 1998

THF: 5%
THF/NMP (9 equiv.):   85%

Fürstner, 2002

X = I   27%
X = Br   38%
X = Cl   > 95%
X = OTf   > 95%
X = OTs   > 95%

Nakamura, 2007

FeCl₃: 32%   32%
FeF₃·3H₂O: 98%   4%
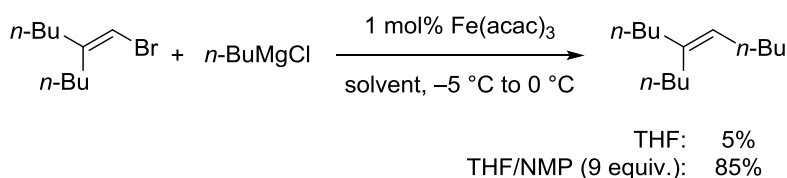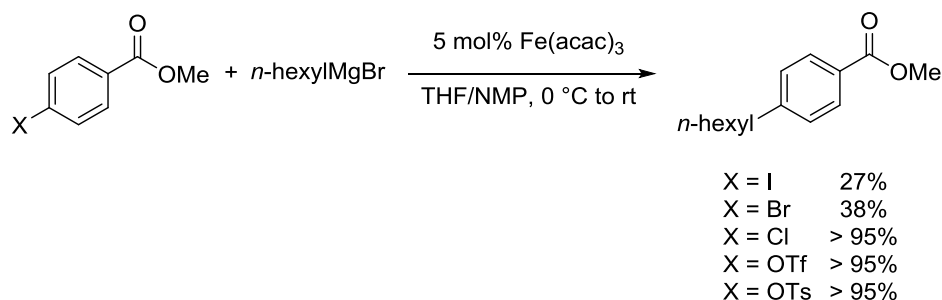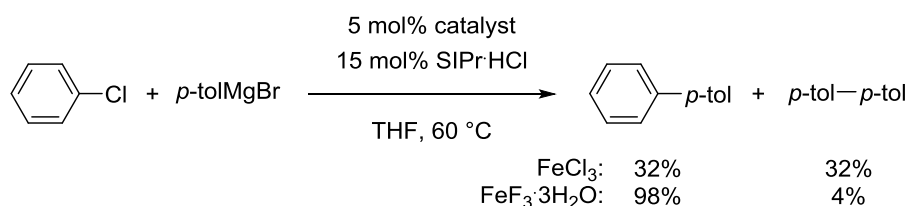
Scheme 7: Selected key developments in Fe-catalyzed cross-couplings.

The homocoupling of aryl Grignard reagents under iron catalysis remained a challenge until 2007, when the group of Nakamura presented a catalytic system (*i.e.*, a combination of FeF$_3$·3H$_2$O and an NHC-ligand) that efficiently suppressed the homocoupling of the aryl-magnesium halide (Scheme 7, bottom).[50] This so-called "catalytic fluoride effect" was explained computationally by the fluoride ion coordinating so strongly to the iron center that reduction of the metal center is suppressed (*vide infra*), thereby inhibiting subsequent oxidative homo-coupling of the aryl Grignard.[51]

2.1.2 Mechanistic Aspects of Fe-Catalyzed Cross-Coupling Reactions

Although the field of Fe-catalyzed cross-couplings is continuously expanding and the state of the art has improved significantly over the past 20–30 years, the mechanisms of these reactions are still not fully understood. While the mechanisms in palladium or nickel catalysis have been studied extensively and are well understood in most of the cases, reactions mediated by iron have only recently been subjected to detailed studies. Iron catalysis is more challenging to study for a variety of reasons:[52] first of all, iron's formal oxidation states can range from −II to +VI and, therefore, different redox manifolds can occur in catalytic cycles. In the same manner as in classical Pd(0)/Pd(II) cross-coupling, two-electron oxidative addition/reductive elimination pathways are possible. In addition, iron is capable of undergoing facile single electron transfer (SET) processes which allow odd-numbered redox manifolds to be accessed.[53] On the one hand, a diverse reactivity profile could be harnessed if it were possible to control iron's formal oxidation states in a given reaction. On the other hand, it can be a curse when one seeks to obtain a clear picture of the mechanism if different cycles are interconnected (*vide infra*) or intermediates involve multiple spin states.[54] Furthermore, the paramagnetism of many iron compounds makes it difficult to study their reactivity by standard NMR spectroscopy. Fortunately, other spectroscopic techniques are available (*e.g.*, Mössbauer, EPR, and MCD spectroscopy accompanied by DFT calculations) and help to study and understand Fe-catalyzed transformations.[55]

So far, the available data suggest that the active species and the resulting catalytic cycle can differ in every reaction.[56] The mechanism may depend on the nature of the pre-catalyst (*i.e.*, a simple iron salt or a well-defined iron complex, in which the formal oxidation state from iron can range from −II to +III), the structure of the nucleophile (*i.e.*, aryl, alkenyl, or alkyl Grignard reagents and, in the latter case, with or without β-hydrogen atoms) as well as the structure of the electrophile (*i.e.*, primary, secondary, or tertiary alkyl as well as aryl and alkenyl derivatives bearing different leaving groups). Even (co-) solvents (*e.g.*, THF, Et$_2$O, NMP, etc.) and additives (*e.g.*, NHCs, phosphines, TMEDA, etc.) have been shown to have a significant influence on the mechanistic scenario.

The earliest investigations on the mechanism of the Fe-catalyzed cross-coupling reaction between vinyl bromides and alkyl Grignard reagents were conducted by the group of Kochi. An $S = {}^1/_2$ species was observed in the catalytic reaction by EPR spectroscopy and an Fe(I) species was therefore proposed to be "the catalyst".[57] At the time, it was already known that high valent transition metals can be reduced by Grignard reagents. In line with this, Kochi *et al.* proposed that the Fe(III) pre-catalyst **6** is reduced to the Fe(I) complex **7** (Scheme 8). Oxidative addition of (*E*)-1-bromoprop-1-ene (**8**) affords the Fe(III) complex **9** which undergoes transmetalation with

RMgBr to give Fe(III) complex **10**. Reductive elimination leads to re-formation of complex **7** and the cross-coupling product **11**.
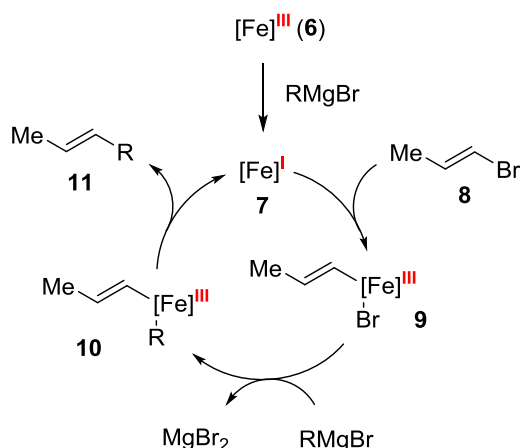
Scheme 8: Kochi's proposed catalytic cycle for the Fe-catalyzed cross-coupling of (*E*)-1-bromoprop-1-ene and RMgBr. It is important to mention that in reference 57 the authors state in footnote 10: "Iron(0) species cannot be ruled out unequivocally, but replacement of Iron(I) with Iron(0) does not change the following discussion materially."

Despite years of debate and extensive experimental and computational studies, it is still not clear if complex **7** is actually a mononuclear Fe(I) species or a more complex polynuclear species.[58]

Several groups have isolated potential intermediates in iron catalysis. In 2006, the Fürstner group reported the synthesis of the homoleptic tetramethyliron(II) ferrate complex [Li(OEt$_2$)]$_2$[(FeMe$_4$)(MeLi)] (**12**) from the reaction of MeLi with FeCl$_x$ (x = 2 or 3) in Et$_2$O.[59] They characterized this highly pyrophoric complex in the solid state (Figure 1, left).
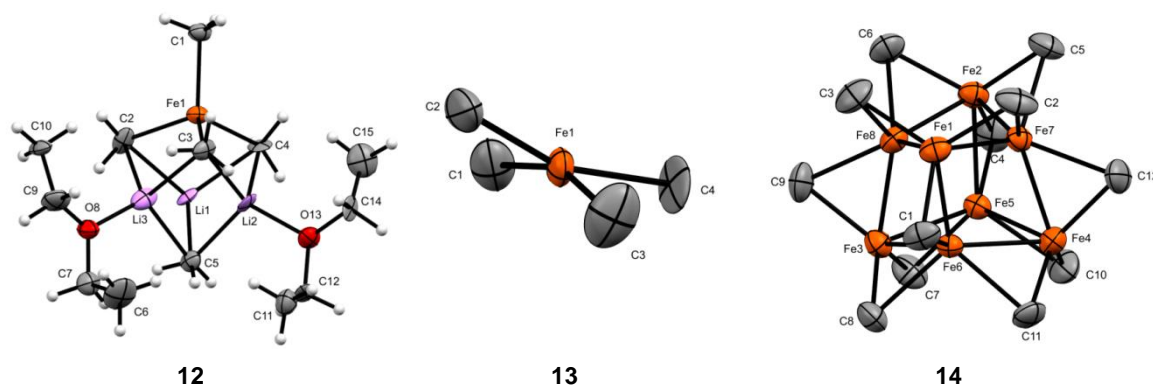
Figure 1: Molecular structures of homoleptic methyl ferrate complexes in the solid state with ellipsoids depicted at the 50% probability level: complex **12** was reported by the Fürstner group.[59] Complexes **13** and **14** were reported by the Neidig group.[60,61] The [MgCl(THF)$_5$]$^+$ counter ions, hydrogen atoms, and co-crystallized THF in **13** and **14** are omitted for clarity.

Complex **12** did not undergo the expected methyl group transfer to alkenyl halides such as (2-bromovinyl)benzene. However, an efficient (even catalytic) methyl transfer to more activated substrates such as aryl triflates was possible.

In 2014, Neidig and co-workers sought to characterize Kochi's methylated iron complex from "catalytically relevant reagents" (*i.e.*, THF as a solvent and MeMgBr as the nucleophile).[60] At −80 °C, they were able to isolate the homoleptic tetramethyliron(III) ferrate complex [MgCl(THF)$_5$][Me$_4$Fe]·THF (**13**). Its structure in the solid state features a distorted square planar, monoanionic [FeMe$_4$]$^-$ complex (Figure 1, center). EPR and DFT studies revealed that **13** is an intermediate spin ($S = {}^3/_2$) system.

Warming a freeze-trapped sample of complex **13** to room temperature inside an EPR spectrometer resulted in the disappearance of **13** and observation of an $S = {}^1/_2$ species (**14**) in line with the report by Kochi from 1976.

Two years later, Neidig's group succeeded in structurally characterizing **14** by warming a sample of **13** to 0 °C and immediately cooling it to −80 °C.[61] The analysis of the isolated material by X-ray crystallography revealed the formation of an unusual monoanionic, mixed-valent octairon cluster, [Fe$_8$Me$_{12}$]$^-$, in which the 12 bridging methyl groups are the only supporting ligands (Figure 1, right).

However, complex **14** did not react efficiently with (2-bromovinyl)benzene (**15**) to give prop-1-en-1-ylbenzene (**16**). Only 5% and 6% of **16** were obtained after a reaction time of 40 s and 120 s, respectively. Remarkably, addition of an excess of MeMgBr to a mixture of **14** and **15** resulted in quantitative formation of **16** (Scheme 9).
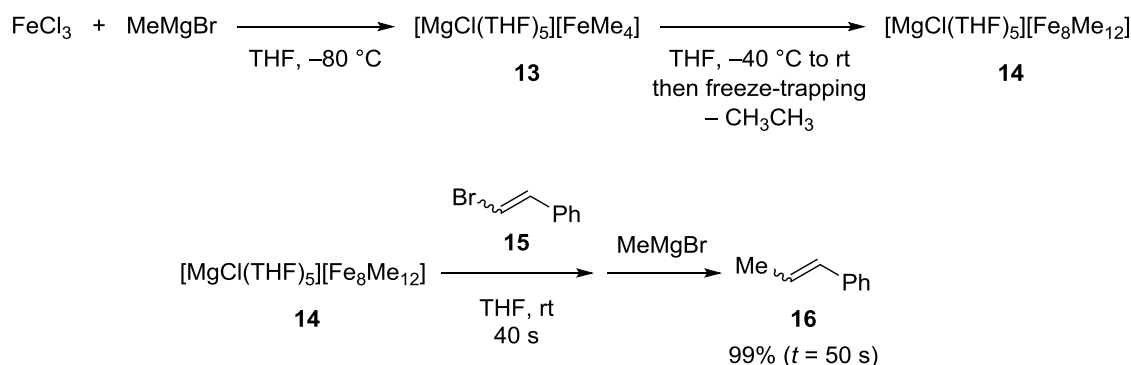
Scheme 9: Summary of the work done by Neidig and co-workers on Kochi's Fe-catalyzed cross-coupling of MeMgBr and (2-bromovinyl)benzene (**15**).

This work exemplifies how intriguing iron catalysis can be. Neidig and co-workers managed to cut the Gordian knot and provided a cornerstone of the longstanding (*i.e.*, 40 years!) mystery of the species involved in Kochi's iron cross-coupling: instead of a "simple" mononuclear iron complex, a mixed-valent octairon cluster appears to play an important role as the resting state of the catalyst. This finding also highlights the importance of the interplay between multiple analytical techniques to get insights into an Fe-catalyzed reaction mechanism.[55]

While Neidig's group dealt with a single catalytic transformation, the Fürstner group has conducted extensive work on a much broader space of Fe-catalyzed cross-coupling reactions.[47,59,62,63] Their data led to the proposal that several mechanisms may occur, involving multiple redox couples with the formal oxidation states Fe(I)/Fe(III), Fe(0)/Fe(II), and Fe(−II)/Fe(0).[63] These different redox cycles were suggested to be interconnected and, although one pathway might be dominant in any particular reaction, it will be difficult to identify which one this may be. All of the cycles begin with the reduction of the pre-catalyst (*i.e.*, Fe(II) or Fe(III) salt) to the Fe(0) species by the Grignard reagent (Scheme 10). This can then enter the Fe(0)/Fe(II) redox manifold (cycle B) or it can be further reduced by two equivalents of Grignard reagent to the low-valent Fe(−II) species (cycle C). The Fe(I)/Fe(III) redox cycle (cycle A) can be accessed when the Fe(II) species in cycle B undergoes a homolytic Fe–R cleavage to form an Fe(I) species.
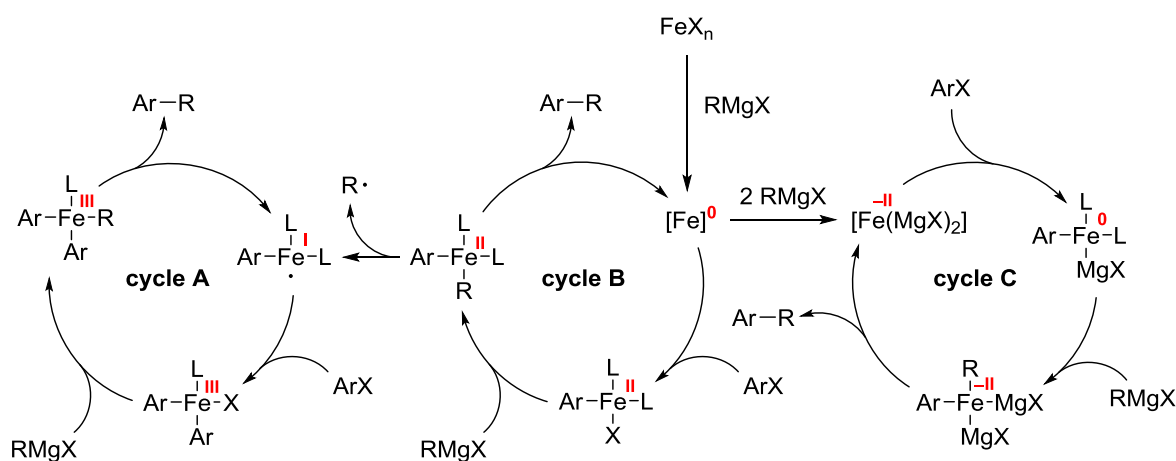
Scheme 10: Interconnected mechanisms of Fe-catalyzed cross-coupling reactions as proposed by Fürstner *et al.*

In support of this mechanistic scheme, Fürstner and co-workers demonstrated that well-defined iron complexes with oxidation states +III, +II, +I, 0, and −II all serve as competent (pre-) catalysts in cross-coupling reactions of both primary and secondary alkyl halides with aromatic Grignard reagents.[63]

In contrast to the two-electron oxidative addition/reductive elimination mechanism of traditional cross-coupling reactions, the mechanisms of Fe-catalyzed cross-coupling reactions show a greater diversity and are still not well understood. Future detailed studies of the active catalysts' structures as well as solvent, ligand, and additive effects will not only help to understand the mechanisms, but will also provide the tools to improve current catalytic systems and to develop new catalysts and methodologies.[52,58]

2.1.3 Cross-Coupling Reactions with Alkyl Substrates

The majority of cross-coupling reactions is conducted on substrates bearing sp or sp^2 hybridized carbons at the site of reaction. Although progress towards alkyl cross-coupling has been made recently, reactions involving sp^3 hybridized substrates are still rare.[64,65] While Pd- or Ni-catalyzed reactions of alkyl substrates require careful optimization of the reaction conditions (*i.e.*, catalyst and ligand structure), even simple iron salts such as $FeCl_3$ are successful (pre-) catalysts for sp^3 cross-coupling reactions.[66] In 2004, the first systematic studies on Fe-catalyzed Kumada–Tamao–Corriu-type cross-couplings with alkyl halides were reported[62,67,68] and, subsequently, numerous (functionalized) primary and secondary (cyclo)alkyl halides have been successfully cross-coupled with this type of transformation.[19–29] However, *tert*-alkyl halides are very poor substrates for Fe-catalyzed cross-coupling.[65,69] The only example of an all-carbon quaternary sp^3 center being formed by iron catalysis involves the reaction of *gem*-dichloro-cyclopropanes such as **17** and MeMgBr in the presence of 4-methoxytoluene as an additive (Scheme 11).[70]
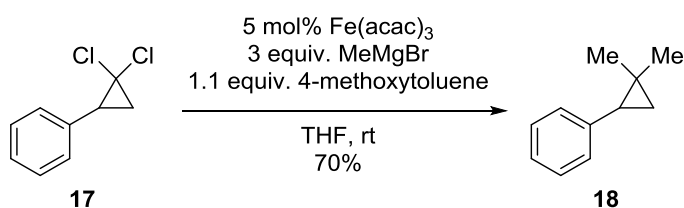
Scheme 11: Dimethylation of *gem*-dichlorocyclopropanes by the group of Tanabe.

Another group of tertiary alkyl substrates which do react under iron cross-coupling conditions are propargylic electrophiles. The groups of Pasto,[71] Szeimies[72] and Bäckvall[73] have reported reactions of propargylic chlorides and propargylic acetates with Grignard reagents, affording a broad range of the corresponding allene products in an S_N2'-type manner (Scheme 12). Fürstner and Méndez showed that under similar conditions enantiopure oxiranes are stereospecifically converted into chiral 2,3-allenols (*e.g.*, **25**; Scheme 12).[74] The observed *syn*-configuration of the product is opposite to that usually observed in reactions of propargylic oxiranes with organo-copper reagents.[75] In their report on an Fe-catalyzed addition of Grignard reagents to activated vinylcyclopropanes, Sherry and Fürstner showed that propargyl derivative **26** underwent a 1,7-addition to furnish the corresponding allene **27**.[76]

Pasto, 1978

19

cat. FeCl$_3$
1 equiv. n-BuMgBr

Et$_2$O/THF, 0 °C
87%

20

Szeimies, 1994

0.5 mol% Fe(acac)$_3$

BrMg—◁ **22**

Et$_2$O/1,4-dioxane, 0 °C
36%

21

23

Fürstner, 2003

5 mol% Fe(acac)$_3$
1.3 equiv. i-PrMgCl

toluene, −5 °C
94%

24

25

Fürstner, 2009

10 mol% Fe(acac)$_3$
1.5 equiv. i-PrMgCl

toluene, −30 °C
60%

26

27

Bäckvall, 2016

5 mol% Fe(acac)$_3$
1.25 equiv. PhMgCl

Et$_2$O, −20 °C
92%

28

29
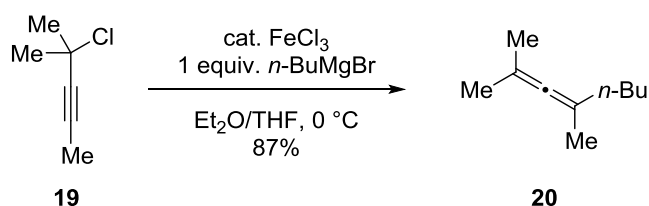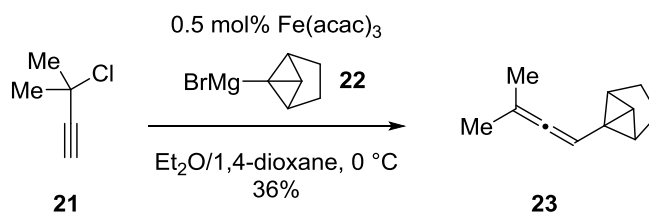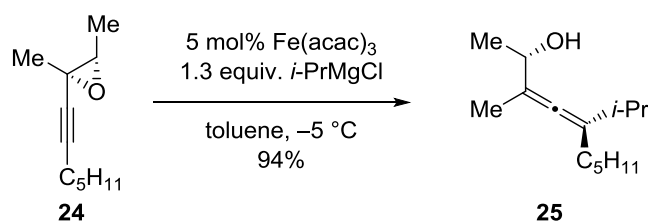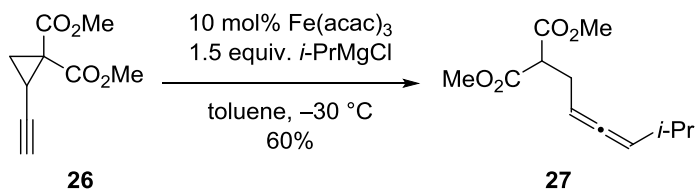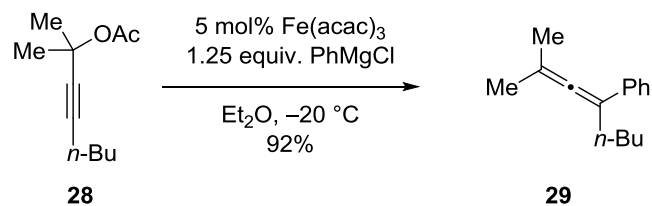
Scheme 12: Literature examples of Fe-catalyzed allene formation from propargylic derivatives.

In some of the outlined examples, the isomeric alkyne derivatives (*i.e.*, the S$_N$2-type products) have been isolated as minor by-products. Until now, no general Fe-catalyzed method to synthesize the alkyne cross-coupling products in high regioselectivities has been developed. Even other metals have not been reported to allow selective access to the alkyne products. It seems that only one example exists in which Salaün and de Meijere reported the Pd-catalyzed cross-coupling of propargylic electrophiles to furnish significant amounts of the direct substitution products (Scheme 13): for example, the Pd(dba)$_3$-catalyzed reaction between 1-alkynylcyclopropyl chlorides (**30**) and PhZnCl afforded mixtures of allenes (**31**) as well as

reduced and/or substituted cyclopropane derivatives (**32** and **33**, respectively) in varying ratios.[77,78]
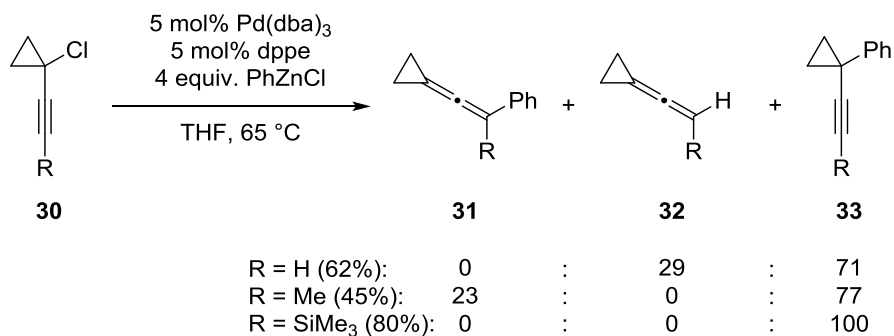
Scheme 13: Examples of nucleophilic substitutions of 1-alkynylcyclopropyl chlorides catalyzed by palladium(0). Yields refer to the total amount of isolated products (**31** + **32** + **33**). Ratios refer to the isolated material.

Given the aforementioned literature reports, the lack of a regioselective Fe-catalyzed method to access substituted alkyne derivatives such as **33** from propargylic derivatives makes the development of such a process highly desirable.

2.2 Results and Discussion

2.2.1 Fe-Catalyzed Cross-Coupling of 1-Alkynylcyclopropyl Tosylates

The following project was conducted in cooperation with Helga Krause. Her contributions are highlighted.

In 2003, Fürstner and Méndez studied the reaction of propargylic bromide **34** with *p*-MeOC$_6$H$_4$MgBr in the presence of catalytic amounts of Fe(acac)$_3$ in analogy to Pasto's report (Scheme 14).[71] Although the obtained yield of the desired allene **35** was low (12%), the direct S$_N$2-substitution product **36** was obtained in 50% yield. After screening different propargylic derivatives, propargylic oxiranes were found to perform very well to furnish the corresponding 2,3-allenol derivatives (*cf.* Scheme 12) and no further attention was payed to the formation of compound **36**.[74]
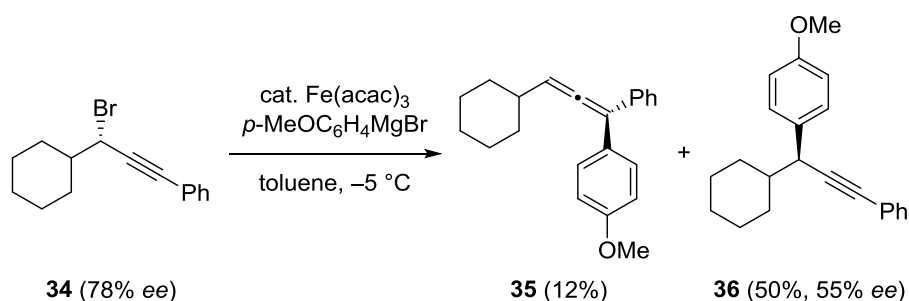
Scheme 14: Fe-catalyzed reaction of **34** with *p*-MeOC$_6$H$_4$MgBr by Fürstner and Méndez.

In light of the literature reports on the selective formation of allenes from propargylic electrophiles (*cf.* Section 2.1.3), the observation of **36** being formed as a major product served as an entry point to develop an Fe-catalyzed cross-coupling of propargylic derivatives with Grignard reagents by direct S$_N$2-type substitution.

This study commenced by screening different leaving groups on the propargylic substrate **37-R** (Table 1).[79] Fe(acac)$_3$ was chosen as the iron source because it is cheap and non-hygroscopic and therefore easier to handle than iron chlorides. Reaction conditions were chosen based on previous Fe-catalyzed methodologies developed in the Fürstner group: a solution of *n*-hexylMgBr in Et$_2$O was added dropwise to a THF solution of substrate **37-R** at −20 °C. The substrates **37-R** were designed with a cyclopropyl moiety to avoid decomposition during their syntheses or purification on silica (*e.g.*, the dimethyl derivative of **37-Ts** was prone to undergo E2-type elimination to furnish the corresponding olefin after deprotonation of one of the geminal methyl groups). Only in the synthesis of triflate **37-Tf** was a complex mixture obtained and **37-Tf** could therefore not be used in this study.

The results of the screening reactions are summarized in Table 1. Although the starting material was quantitatively consumed in all cases, the reactions of pivalate **37-Piv** and carbonate **37-**

CO$_2$Me gave complex mixtures (entries 1 and 2). When phosphate **37-P(O)(OEt)$_2$** was subjected to the reaction conditions, a single product, the desired substitution product **38a**, was obtained in 48% yield (entry 3). In the case of the tosylate **37-Ts**, a higher yield of **38a** was obtained (80%, entry 4). In the absence of Fe(acac)$_3$, no reaction of **37-Ts** was observed with the Grignard reagent under otherwise identical conditions (entry 5).

Table 1: Results of the screening reactions of the leaving group for the Fe-catalyzed cross-coupling reaction. The solution of the Grignard reagent (1.3 equiv. relative to **37-R**) was added to the solution of **37-R** (0.14–0.46 mmol) and Fe(acac)$_3$ (5 mol%) in THF (c = 0.1 M) at −20 °C over ≈ 5 min *via* syringe. [a] A complex mixture was obtained. [b] No Fe(acac)$_3$ was used.

entry	R	isolated yield (%)
1	Piv	—[a]
2	CO$_2$Me	—[a]
3	P(O)(OEt)$_2$	48
4	Ts	80
5	Ts	0[b]

The Fe-catalyzed process forms a quaternary center under mild conditions with the cyclopropane ring intact. Alkyne **38a** was the only product arising from the substrate **37-Ts**—no allene formation was observed. The only observed side products are derived from the Grignard reagent (*i.e.*, *n*-hexane, hex-1-ene, and dodecane).[80]

The fact that the substrate lacks a halide leaving group differentiates this reaction from all other Fe-catalyzed alkyl–alkyl cross-coupling reactions reported in the literature.[66,81,82] Although several examples of Fe-catalyzed cross-couplings of aryl and alkenyl sulfonates are known,[47,83] Nakamura and co-workers showed that primary and secondary alkyl tosylates are unreactive under iron catalysis unless the mixture contains halide ions that substitute the sulfonate before the actual cross-coupling takes place.[84] Substitution of the tosylate group of **37-Ts** by a halide is excluded on the basis of the control experiment in the absence of the iron complex as well as the fact that no traces of cyclopropyl halides were observed during the entire study.

Under the established reaction conditions, the influences of different substituents on the alkyne and of different Grignard reagents on the Fe-catalyzed cross-coupling of 1-alkynylcyclopropyl tosylates were investigated (Table 2).[85]

Table 2: Fe-catalyzed cross-coupling of different Grignard reagents with 1-alkynyl-cyclopropyl tosylates **37**. The solution of the Grignard reagent (1.3–1.5 equiv. relative to **37**) was added to the solution of **37** (0.2–1.1 mmol) and Fe(acac)$_3$ (5 mol%) in THF (c = 0.1 M) at −20 °C over ≈ 5 min *via* syringe. [a] Isolated yield of pure **38**. [b] The corresponding allene by-product **39** was isolated by HPLC.
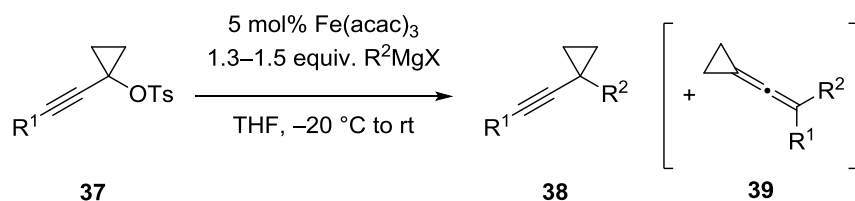
entry	product		R^1	isolated yield (%)[a]
1		**38a**	(CH$_2$)$_3$OTBS	80
2		**38b**	(CH$_2$)$_2$OBn	74
3	*n*-hexyl	**38c**	*n*-Bu	88
4		**38d**	Ph	86
5		**38e**	SiMe$_3$	78
6		**38f**	(CH$_2$)$_3$OTBS	83
7	Me	**38g**	(CH$_2$)$_2$OBn	76
8		**38h**	Ph	70
9		**38i**	(CH$_2$)$_3$OTBS	87
10	SiMe$_3$	**38j**	(CH$_2$)$_2$OBn	86
11		**38k**	Ph	90
12		**38l**	(CH$_2$)$_3$OTBS	57
13		**38m**	(CH$_2$)$_2$OBn	73
14		**38n**	CH$_2$OPh	76 (traces[b])
15		**38o**	Ph	76
16	Ph	**38p**	(CH$_2$)$_3$OTBS	49 (12[b])
17		**38q**	(CH$_2$)$_3$OTBS	59
18		**38r**	(CH$_2$)$_2$OBn	37 (29[b])
19		**38s**	Ph	64 (9[b])

Similarly to alkylsilyl ether derivative **38a**, the alkylbenzyl ether derivative **38b** and the *n*-alkyl derivative **38c** were obtained in excellent isolated yields through cross-coupling with *n*-hexylmagnesium bromide (80%, 74%, and 88%, respectively, entries 1–3). Additionally, replacement of the alkyl substituents by a phenyl and a trimethylsilyl group on the alkyne did not affect the yields (86% and 78%, respectively; entries 4 and 5).

A methyl Grignard reagent underwent efficient cross-coupling with three different substrates (70–83% isolated yield, entries 6–8). The methyl Grignard reagent could be replaced by MeLi, although the yield was much lower (44%). The fact that an efficient Fe-catalyzed cross-coupling takes place under mild reaction conditions contrasts the related Pd-catalyzed process developed by Salaün and de Meijere who reported that the same tosylate **37d** provided mixtures of unidentified products when treated with MeZnCl and $Pd(dba)_2$/dppe in various refluxing solvents for extended amounts of time.[77]

The reactions of substrates **37a**, **37b**, and **37c** with trimethylsilylmethylmagnesium chloride required much longer reaction times (4–48 h) than the corresponding reactions with MeMgX (<1 h), although they were similarly clean and productive (86–90% isolated yield, entries 9–11). The slower reaction is attributed to the β-silicon effect:[86] a metal complex formed with the trimethylsilylmethyl anion will exhibit a higher thermal stability resulting from hyper-conjugation between the occupied σ orbital of the M–C bond and the empty σ* orbital of the C–Si bond if they adopt an antiperiplanar conformation. This may be manifested in poor trans-ferability of the trimethylsilylmethyl group from the Grignard reagent itself or the subsequently formed iron (ate) complex (*cf.* Section 2.1.2)[59–61,63] and explains the slower reaction compared to the methyl Grignard reagent. An additional factor could be the lower nucleophilicity of the trimethylsilylmethyl anion due to a distribution of the negative charge through silicon's polarizability (α-silicon effect) in contrast to that of lighter atoms such as hydrogen or carbon.

A Grignard reagent bearing an acetal furnished the cross-coupling products **38l–38o** in 57%, 73%, 76%, and 76% isolated yield, respectively (entries 12–15). In the case of the CH_2OPh-substituted alkyne **37n** (entry 14), traces of the allene by-product **39n** were observed by GC-MS for the first time in this study. Significantly more allene was formed in the cross-coupling of **37a** and 2-phenylethylmagnesium chloride (entry 16). After column chromatography, the products **38p** and **39p** were obtained as a ≈ 4:1 mixture which gave both compounds in 49% and 12% isolated yield, respectively, after HPLC separation. Cyclopropylmagnesium bromide reacted with **37a** to furnish bicyclopropane **38q** in 59% isolated yield (entry 17).

While the alkyl Grignard reagents resulted in formation of the desired S_N2-type substitution products **38** in the majority of the cases, the reactions of arylmagnesium halides resulted in

much more diverse outcomes.[87] Entries 18 and 19 are representative: the alkylbenzyl ether derivatives **38r** and **39r** were obtained as a ≈ 1.3:1 mixture (entry 18) and hydrocarbons **38s** and **39s** were isolated as a ≈ 7.3:1 mixture (entry 19) in 66% and 73% combined yield, respectively, after column chromatography.

The poor regioselectivities of these *aryl* Grignard reagents contrast the excellent regioselectivities of the *alkyl* Grignard reagents in this methodology. Sherry and Fürstner reported similarly poor regioselectivities (between 1,5- and 1,7-addition) for *aryl* Grignard reagents in their Fe-catalyzed addition to activated vinylcyclopropanes. In the case of *alkyl* Grignard reagents, the 1,7-addition products were obtained selectively.[76] On the other hand, Bäckvall's group showed that *phenyl*magnesium bromide cross-couples with propargylic acetates in the presence of Fe(acac)$_3$ to furnish substituted allenes with the same regioselectivity as *alkyl* Grignard reagents.[73]

Szeimies and co-workers argued that "stereoelectronic factors" control the regioselectivities in their Fe-catalyzed cross-coupling of propargylic electrophiles with tricyclo[3.1.0.0^{2,6}]hexan-1-ylmagnesium bromide (**22**).[72] Although it could be argued that this might play a role in the Fe-catalyzed cross-coupling of 1-alkynylcyclopropyl tosylates **37** with *aryl*magnesium halides, this study shows that smaller *alkyl* Grignard reagents selectively add to the most sterically encumbered end of the alkyne.

The contrasting results in the literature show that both the nature of the Grignard and the steric environment of the propargylic electrophile can have a role in influencing the regioselectivity. That this study shows a high selectivity for the direct substitution products **38** points to the presence of an over-riding factor. Given the sensitivity of the results to the nature of the leaving group (*cf.* Table 1), it seems likely that propargylic *tosylates* are privileged substrates for this mode of reactivity.

2.2.2 Fe-Catalyzed Cross-Coupling of 1-Alkenylcyclopropyl Tosylates

The Fe-catalyzed cross-coupling reaction developed in Section 2.2.1 successfully reacted 1-alkynylcyclopropyl tosylates with various alkyl Grignard reagents to furnish the direct S_N2-type substitution products. Variation of the 1-substituent of the cyclopropane to a functional group other than alkynyl would lead to an extended scope and broader applications of this transformation. Therefore, a range of 1-vinyl, 1-alkyl, and 1-aryl derivatives was tested in the Fe-catalyzed cross-coupling.

While the methodology described in Section 2.2.1 furnished the desired cross-coupling products in high yields from 1-alkynylcyclopropyl tosylates, the corresponding 1-vinylcyclopropyl tosylates did not undergo this reaction in high yields under the same conditions, showing the substrate dependence of this type of chemistry. Extensive optimization was necessary to obtain a 58% yield of the cross-coupling product **42** from 1-vinylcyclopropyl tosylate (**40**) and 2-(4-methoxyphenyl)ethylmagnesium chloride (**41**; Table 3, entry 1). These optimized conditions feature an prolonged addition time of the Grignard reagent (*cf*. entry 2) which was premixed with equimolar amounts of *N*,*N*,*N*′,*N*′-tetramethylethylenediamine (TMEDA). An increase in yield of Fe-catalyzed cross-couplings of secondary electrophiles in the presence of TMEDA was first reported by Nakamura *et al*.; the effect relies on reducing side reactions such as olefin formation by the loss of hydrogen halide from the halide substrate.[53d,68]

A selected set of variations on the optimized conditions is given in Table 3. As expected, conducting the reaction in the absence of Fe(acac)$_3$ led to no conversion (entry 3). Although the presence of TMEDA and its premixing with the Grignard reagent seem to have a minor influence on the reaction outcome (entries 4–6), it was left as part of the optimized reaction conditions because it was found to have a beneficial influence on cross-couplings with other Grignard reagents (for example, cross-coupling of **43** with cyclopropylmagnesium bromide resulted in a 59% yield without TMEDA, but in a 73% yield with TMEDA; *cf*. Table 4, entry 6). Addition of NMP as a co-solvent had a negative effect on the formation of **42** (39%, entry 7).[45,47] Several additives such as DABCO and phenanthroline,[88] HMTA,[89] PPh$_3$, Xantphos,[90] and LiCl[91] were also tested because they have been reported to be beneficial to the yields of Fe-catalyzed cross-coupling reactions. However, none of them were found to improve the yield or selectivity of this reaction (entries 8–13).

Table 3: Selected optimization experiments for the Fe-catalyzed cross-coupling of tosylate **40** and Grignard reagent **41**. [a] The premixed solution of the Grignard reagent and TMEDA (1.2 equiv. of each relative to **40**) was added to the solution of **40** (0.5 mmol) and Fe(acac)$_3$ (5 mol%) in THF ($c = 0.1$ M) at 0 °C over 30 min *via* syringe pump. [b] The yields were determined by ^{1}H NMR spectroscopy from the crude mixture using 1,3,5-trimethoxybenzene as an internal standard which was added after completion of the reaction.

entry	additive (equiv.)	variation of the standard conditions[a]	yield (%)[b]
1	—	—	58
2	—	dropwise addition over ≈ 5 min	45
3	—	no Fe(acac)$_3$	0
4	—	no TMEDA	56
5	—	TMEDA was added to the reaction mixture before **41**	56
6	—	0.1 equiv. of TMEDA	48
7	NMP (1.0)	no TMEDA	39
8	DABCO (0.05)	no TMEDA	55
9	HMTA (0.05)	no TMEDA	55
10	Phen (0.05)	no TMEDA	31
11	PPh$_3$ (0.1)	no TMEDA	46
12	Xantphos (0.1)	no TMEDA	51
13	LiCl (1.0)	—	58

Next, several Grignard reagents were cross-coupled with (*E*)-1-styrylcyclopropyl tosylate (**43**) under the optimized conditions (Table 4). In general, the yields of the cross-coupling products **44** were significantly lower than of the related alkyne derivatives **38**. For example, the Fe-catalyzed cross-coupling of **43** and *n*-hexylmagnesium bromide resulted in a 19% isolated yield of **44a** (entry 1). In contrast, **43**'s analogous alkyne derivative **37d** had given an 86% yield of **38d** (*cf.* Table 2, entry 4).

Table 4: Fe-catalyzed cross-coupling of different Grignard reagents with (*E*)-1-styrylcyclopropyl tosylate (**43**). The premixed solution of the Grignard reagent and TMEDA (1.2 equiv. of each relative to **43**) was added to the solution of **43** (0.2 mmol) and Fe(acac)$_3$ (5 mol%) in THF (*c* = 0.1 M) at 0 °C over 30 min *via* syringe pump.

entry	RMgX	product	isolated yield (%)
1	*n*-hexylMgBr	**44a**	19
2	EtMgBr	**44b**	17
3	*t*-BuCH$_2$MgCl	**44c**	30
4	Me$_3$SiCH$_2$MgCl	**44d**	36
5	(1,3-dioxan-2-ylethyl)MgBr	**44e**	37
6	*i*-PrCH$_2$MgCl	**44f**	54
7	cyclopropylMgBr	**44g**	73
8	MeMgCl	**44h**	80

Although the yields of the desired products (**44**) were generally low, no starting material was recovered in any of these reactions. A further analysis of the reaction mixtures led to identification of two additional products derived from **43**. The reaction of tosylate **43** with EtMgBr serves as a representative example (Scheme 15, top). In addition to **44b** being isolated in 17% yield, (*E*)-(2-cyclopropylvinyl)benzene (**45**), which represents the reduced starting material, and 1,1'-di((*E*)-styryl)-1,1'-bi(cyclopropane) (**46**), which represents a dimerization product, were isolated in 12% and 26% yield, respectively.

Hydrocarbon **45** was identified unambiguously by comparison with literature data.[92] The amount of reduced starting material varied depending on the nature of the Grignard reagent. Whereas substantial amounts of **45** were formed when a Grignard reagent bearing β-hydrogen atoms was used (Table 4, entry 1: 43%, entry 2: 12%, entry 5: 40%, entry 6: 23%), only traces of

45 were detected when a Grignard reagent without β-hydrogen atoms was used (entries 4 and 8: <1%, entries 3 and 7: <5%). This suggests that the reduction of **43** occurs through a β-hydride elimination of an organometallic intermediate (derived from the Grignard reagent) to furnish a metal hydride. Because a hydrogen abstraction from the solvent could also be envisioned, deuterated ethylmagnesium bromide ([D$_5$]-EtMgBr) was prepared and subjected to the cross-coupling with **43** (Scheme 15, bottom). A very similar outcome as for EtMgBr was observed and the reduced product **[D]-45** showed full (≥95%) deuterium incorporation as determined by NMR spectroscopy, providing strong evidence for the β-hydride elimination pathway.
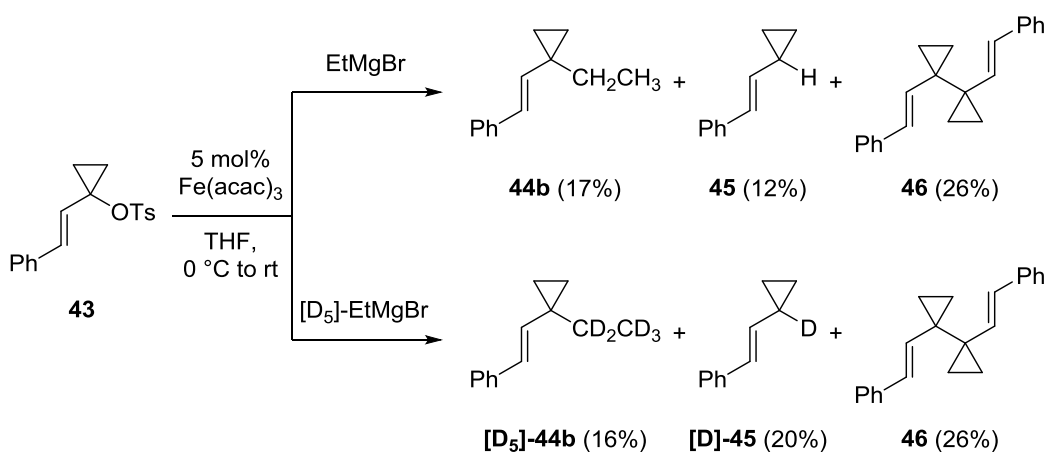
Scheme 15: Fe-catalyzed cross-coupling of undeuterated and deuterated EtMgBr with (*E*)-1-styrylcyclopropyl tosylate (**43**). The solution of the Grignard reagent (1.2 equiv. relative to **43**) was added to the solution of **43** (0.2 mmol) and Fe(acac)$_3$ (5 mol%) in THF (*c* = 0.1 M) at 0 °C over 30 min *via* syringe pump.

The occurrence of a β-hydride elimination process competing with the desired cross-coupling reaction also explains why higher yields are obtained for the cyclopropyl (73%, entry 7, Table 4) and the methyl Grignard reagent (80%, entry 8) of which the former is less likely to undergo β-hydride elimination due to formation of a strained cyclopropene and the latter does not even carry any β-hydrogens.

Dimer **46** was fully characterized by NMR and IR spectroscopy, mass spectrometry, and X-ray crystallography (Figure 2). The latter unambiguously proved the constitution of **46** with both cyclopropyl rings intact. Compound **46** was unknown to the literature, but two related dimers had been reported: firstly, the Ma group observed **49** as a minor by-product (2%) upon un-catalyzed lithiation of 1-cyclopropyl-2-phenylacetylene (**47**; Scheme 16).[93] Szeimies and co-workers isolated dimer **53** in 24% yield from their Fe-catalyzed cross-coupling of Grignard reagent **51** with propargylic chloride **50**.[72] They explained the formation of **53** by the steric repulsion between the SiMe$_3$ group and the sterically demanding Grignard reagent **51** suppressing the usually observed allene formation. A cross-coupling is therefore only possible at the propargylic position of **50** which is also difficult for the Grignard reagent to access because of the two germinal methyl groups, resulting in a very low yield of **52** (3%). Instead, dimer **53** is

formed from two propargylic intermediates whose nature is not further described by the authors.
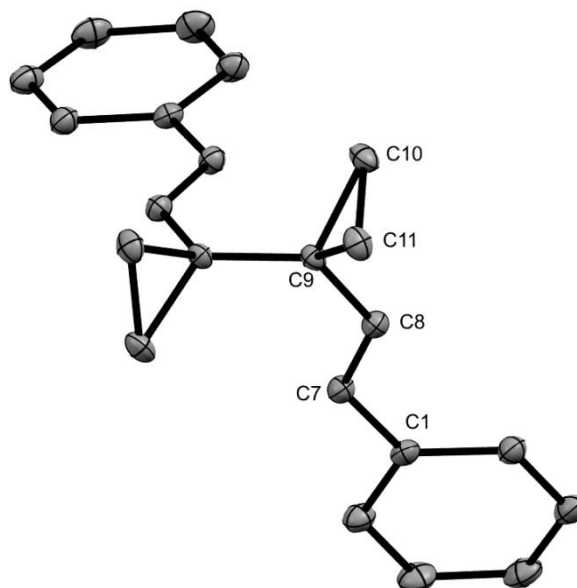
Figure 2: Molecular structure of **46** in the solid state with ellipsoids depicted at the 50% probability level. Hydrogen atoms are omitted for clarity. Selected distances (in Å): C1–C7 1.468(2), C7–C8 1.339(2), C8–C9 1.479(2), C9–C9′ 1.500(2), C9–C10 1.524(2), C10–C11 1.496(2), C11–C9 1.522(2).
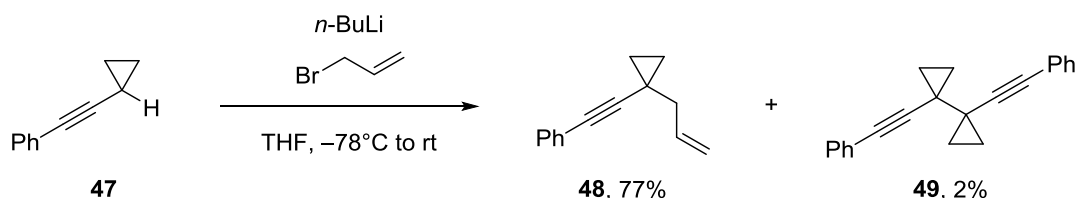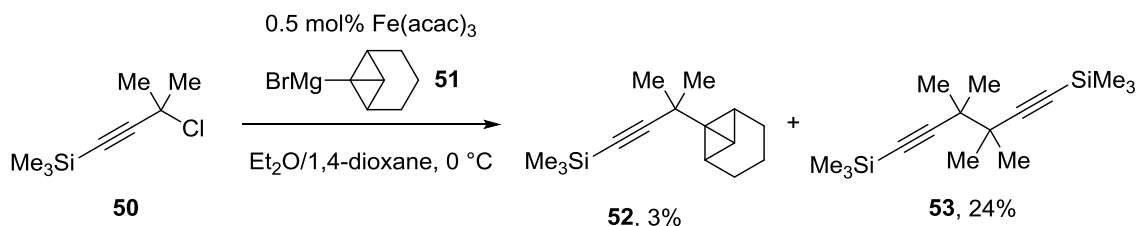
Scheme 16: Coupling reactions that produced dimerized starting materials which are related to dimer **46**.

Methylmagnesium chloride, with no β-hydrogens, had given the highest yield in the Fe-catalyzed cross-coupling of 1-styrylcyclopropyl tosylate (**43**) and was therefore chosen for cross-coupling with other 1-vinylcyclopropyl tosylates (Scheme 17). All reactions resulted in clean formation of the desired cross-coupling product; no reduced or dimerized starting materials were detected by GC-MS or NMR spectroscopy. Compounds **54**, **55**, and **56** were obtained in 87%, 48%, and

39% isolated yield, respectively. The lower yields of the latter two are attributed to their volatility as they are low molecular weight hydrocarbons.

44h, 80%   **54**, 87%   **55**, 48%   **56**, 39%
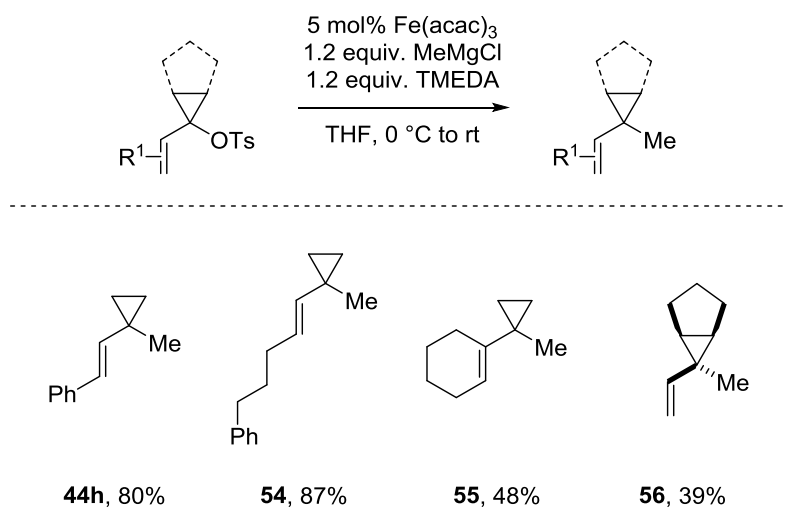
Scheme 17: Fe-catalyzed cross-coupling of MeMgCl with different vinylcyclopropyl tosylates. The premixed solution of the Grignard reagent and TMEDA (1.2 equiv. of each relative to the tosylate) was added to the solution of the tosylate (0.5 mmol) and Fe(acac)$_3$ (5 mol%) in THF (c = 0.1 M) at 0 °C over 30 min *via* syringe pump.

Product **56** was isolated as a single isomer with an *exo*-orientated methyl group (as assigned by ^{1}H/^{1}H NOESY NMR spectroscopy; Figure 3, left) from the corresponding *exo*-tosylate **57** (as established unambiguously by X-ray crystallography; Figure 3, right). This result indicates a stereospecific cross-coupling with retention at the C1 carbon, at least when MeMgCl is used as the nucleophile. Kochi *et al*. noted the same behavior under similar conditions for the Fe-catalyzed cross-coupling of alkenyl bromides and alkylmagnesium halides.[36]
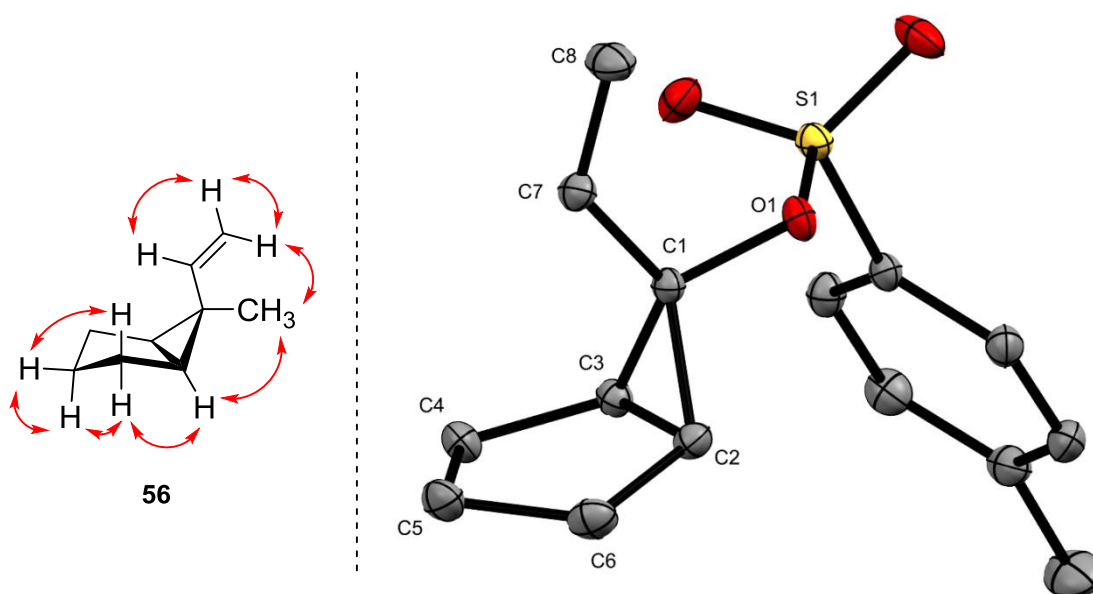
Figure 3: Left: contacts observed by ^{1}H/^{1}H NOESY NMR spectroscopy in the cross-coupling product **56.** Right: molecular structure of **57** in the solid state with ellipsoids depicted at the 50% probability level. Hydrogen atoms are omitted for clarity. Selected distances (in Å): C1–O1 1.4548(9), O1–S1 1.5868(6), C1–C2 1.5212(9), C2–C3 1.5105(9), C3–C4 1.522(1), C4–C5 1.553(1), C5–C6 1.548(1), C6–C2 1.519(1), C1–C7 1.4788(9), C7–C8 1.331(1).

Besides 1-alkynyl- and 1-vinylcyclopropyl tosylates, 1-alkyl- and 1-arylcyclopropyl tosylates were also tested in the Fe-catalyzed cross-coupling reaction. Neither the alkyl derivative **58** nor the aryl derivative **59** underwent any cross-coupling, even when employing more forcing conditions (Scheme 18, left). This indicates that the double bond and the triple bond are not just innocent bystanders and a coordination of the substrate to the iron catalyst is required for cross-coupling to take place. This proposal is supported by the fact that complexes of olefins and iron in low oxidation states are well known.[63,94]
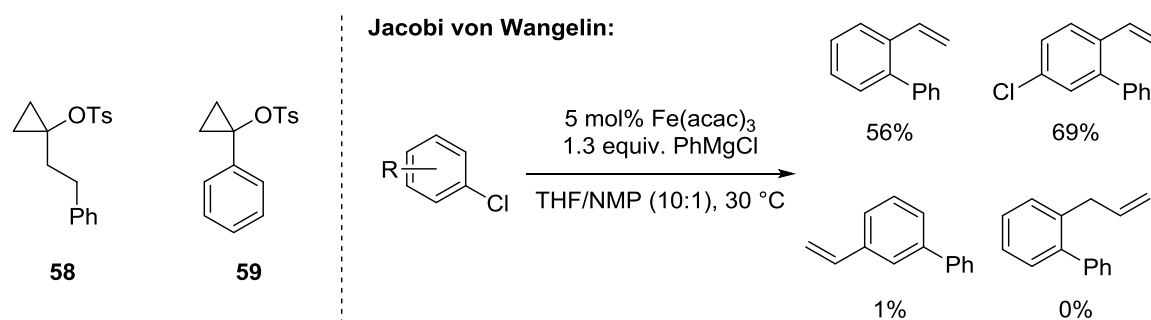
Scheme 18: Left: Unreactive substrates in the Fe-catalyzed cross-coupling with alkyl Grignard reagents: 1-phenethylcyclopropyl tosylate (**58**) and 1-phenylcyclopropyl tosylate (**59**). Right: Fe-catalyzed cross-coupling of deactivated chlorostyrenes with PhMgCl by the group of Jacobi von Wangelin.

In 2012, the group of Jacobi von Wangelin used vinyl directing groups to facilitate the Fe-catalyzed cross-coupling of deactivated chlorostyrenes and arylmagnesium halides (Scheme 18, right). They found that it was important to place the vinyl group *ortho* to the chloro substituent to obtain a high yield and explained this by an activation process through a rate-determining coordination of the catalyst to the vinyl substituent and subsequent so-called haptotropic migration[95] along the conjugated π system to the site of C–Cl bond cleavage.[96]

2.2.3 Mechanistic Considerations

The Fe-catalyzed cross-coupling reactions of the closely related 1-alkynyl- and 1-vinylcyclopropyl tosylates (*e.g.*, **37d** and **43**, respectively) with alkyl Grignard reagents have shown a dramatic difference in the products that are formed: while alkynyl derivative **37d** resulted in exclusive formation of the desired cross-coupling products **38**, reduced and dimerized starting material were observed during the cross-coupling of the vinyl derivative **43**. The degree of unsaturation of the substituent in the 1-position of the cyclopropane must play an important role in the reactivity. Two aspects are discussed to aid in understanding this behavior.

Crystal structures were obtained for tosylates **37d** and **43** (Figure 4) and both show a periplanar alignment of the 1-substituent with the C–O bond. From this finding, it is suggested that the tosylate leaving group might be more labile in the alkyne derivative due to a destabilizing interaction between the filled π bonding orbital of the C–C triple bond (which is orthogonal to the π system of the phenyl group) and the empty antibonding σ* orbital of the C–O single bond

(π(C≡C) → σ*(C–O) donation; Scheme 19, left). The weakening of the C–O bond would facilitate a faster cross-coupling reaction which, therefore, outcompetes side reactions such as β-hydride elimination. A similar hyperconjugative interaction in the vinyl derivative **43** is not present in the solid state because the π orbital of the C–C double bond is orthogonal to the C–O bond (Scheme 19, right). However, if the C–O bond is significantly weakened, this would be reflected in significantly different C–O distances of the two substrates. Because this is not the case (**37d**: 1.441(2) Å; **43**: 1.449(2) Å), this effect is not believed to have a strong contribution, although it might indeed turn out to be more relevant during the course of the reaction (*e.g.*, after coordination to the catalyst).
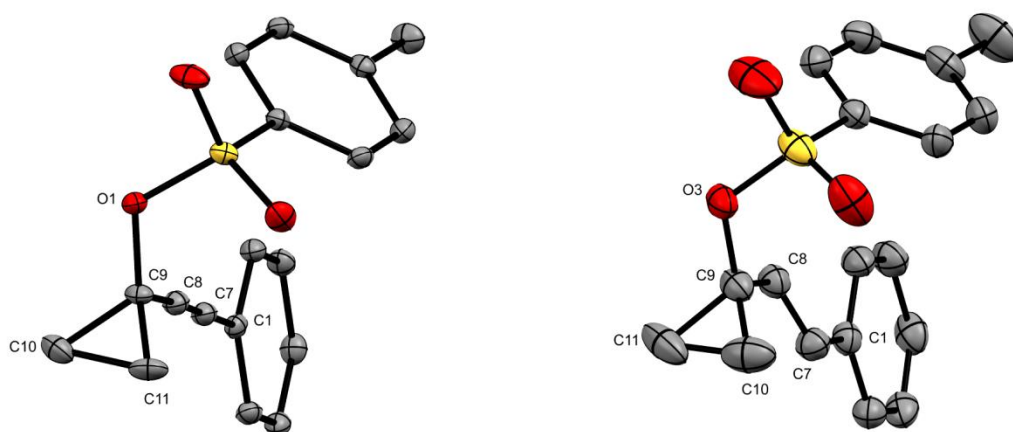
Figure 4: Molecular structures of **37d** (left) and **43** (right) in the solid state with ellipsoids depicted at the 50% probability level. Hydrogen atoms are omitted for clarity. Selected distances for **37d** (in Å): C9–O1 1.441(2), C9–C8 1.438(2), C8–C7 1.198(2), C7–C1 1.433(2), C9–C10 1.506(2), C9–C11 1.500(2), C10–C11 1.498(3). Selected distances for **43** (in Å): C9–O3 1.449(2), C9–C8 1.478(2), C8–C7 1.328(2), C7–C1 1.474(2), C9–C10 1.486(2), C9–C11 1.502(2), C10–C11 1.492(3).
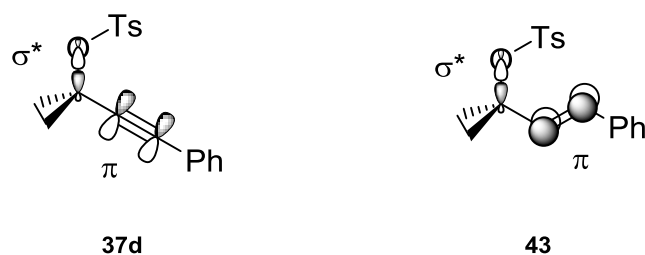
Scheme 19: Orbital depictions of tosylates **37d** and **43** which are considered to explain the reactivity differences of the two differently substituted cyclopropyl tosylates.

A second aspect refers to the ability of alkynes and olefins to coordinate to metals. Alkynes can donate up to four electrons, while olefins can act only as two-electron donors. The Holland group has studied the binding affinities of alkynes and alkenes to low-coordinate, low-valent (β-diketiminato)iron(I) complexes and found that alkynes exhibit a higher binding affinity to the iron complex than olefins.[97] In light of this report, it is reasonable to assume that the stronger binding of the alkyne substrate to the iron catalyst (**61** → **60** in Scheme 20)—regardless of **61**'s detailed structure (*cf.* Section 2.1.2)—occupies what would otherwise be a vacant site

(represented by the grey square) on the metal of alkyl complex **61** and prevents β-hydride elimination. Due to the lower binding affinity of the olefin to complex **61**, the vacant site is more likely to be available to participate in β-hydride elimination furnishing the metal hydride complex **62**. Further steps would lead eventually to the reduced tosylate instead of the desired cross-coupling product.
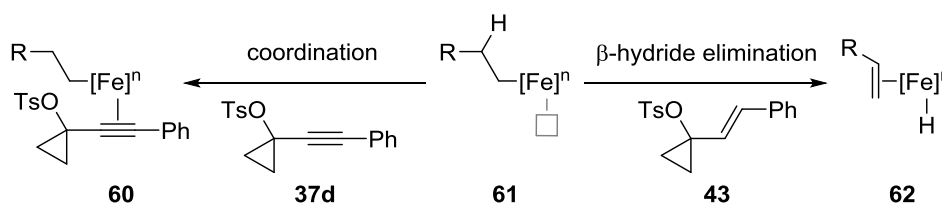
Scheme 20: Depiction of two mechanistic scenarios depending on the coordinating ability of the substrate. The grey square represents a vacant site on the metal center.

Because Fe-catalyzed alkyl–alkyl cross-couplings are still in its infancy, the mechanistic understanding of these processes is minimal.[56,58] Càrdenas and co-workers have published one of the few studies on this particular type of transformation.[82] In analogy to their proposed mechanism, Scheme 21 shows a mechanistic scenario which includes all of the available data from this study and is intended to serve as a starting point for further detailed mechanistic studies.
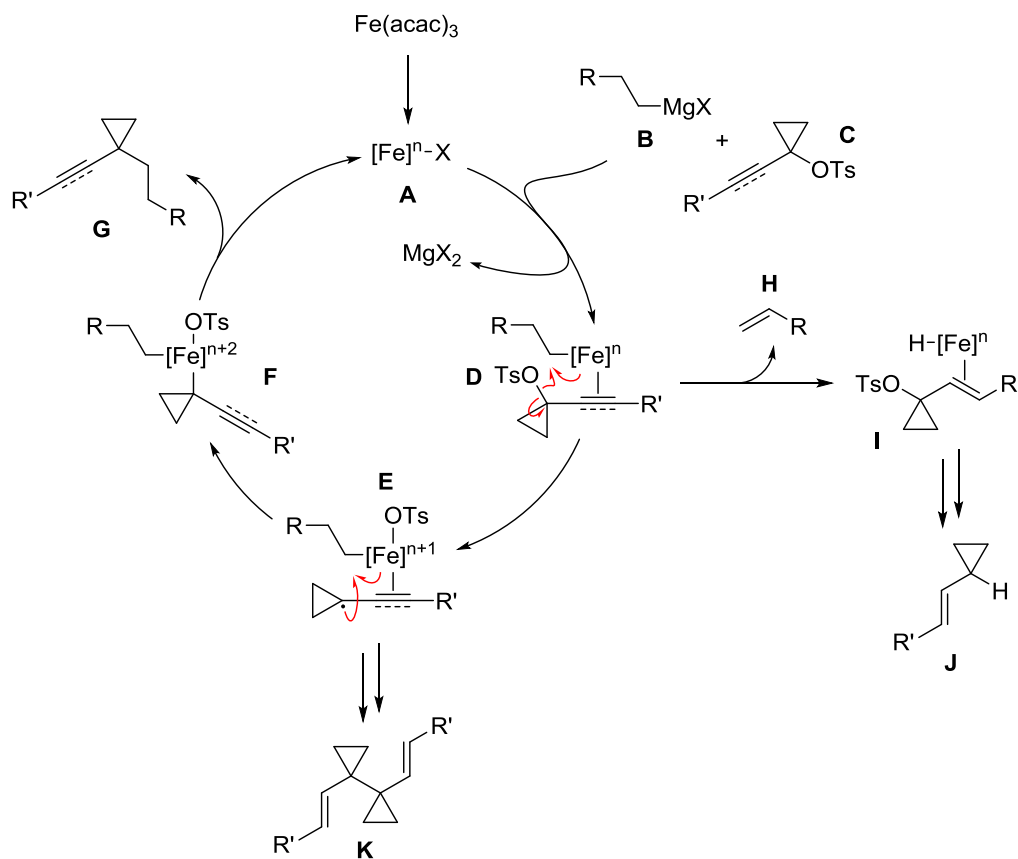
Scheme 21: A possible mechanistic scenario for the Fe-catalyzed cross-coupling of 1-alkynyl- and 1-vinylcyclopropyl tosylates.

Herein, reduction of the pre-catalyst Fe(acac)$_3$ leads to formation of a low-valent iron species **A** whose structure cannot be specified with the available data (*cf.* Section 2.1.2). Complex **A** undergoes ligand exchange with the Grignard reagent **B** and coordination of the substrate **C** or *vice versa* to give complex **D**. Homolytic C–O bond cleavage of **D** results in formation of iron complex **E** bearing a coordinated propargylic or allylic radical which then undergoes an one-electron oxidation of the metal center to furnish the dialkyl iron complex **F**. Reductive elimination from complex **F** re-forms the catalyst **A** and the cross-coupling product **G**.

If substrate **B** is a 1-vinylcyclopropyl tosylate which coordinates weaker than its alkyne counterpart (*vide supra*), **D** can undergo a β-hydride elimination after dissociation of the substrate to form the metal hydride complex **I** which leads to the reduced starting material **J**.

Furthermore, the intermediacy of complex **E** may also explain the formation of the dimerized starting material **46**. Due to the lower binding affinity of the olefin derivatives (*i.e.*, allylic radicals) to the metal center, they may dissociate more easily and recombine to give **K** as opposed to propargylic radicals which are more tightly bound to the metal center.

Lastly, the retention of the configuration of **57** in the Fe-catalyzed cross-coupling with MeMgCl could be a result of steric repulsion in the step **E**→**F**. Two possible products may be formed from the planar intermediate **65** (**64** and **66**, Scheme 22). On steric grounds, the formation of complex **66** is favored over the formation of complex **64** and, therefore, after reductive elimination, only the cross-coupling product **56** is formed with the *exo*-methyl group. A more thorough mechanistic probe would be to use a chiral 1-vinylcyclopropane tosylate with another substituent in the 2-position of the cyclopropane without the over-riding steric bias as in **57**. This type of substrate would allow distinguishing a stereospecific mechanism (retentive or double invers cross-coupling) from a substrate controlled mechanism as depicted in Scheme 22.
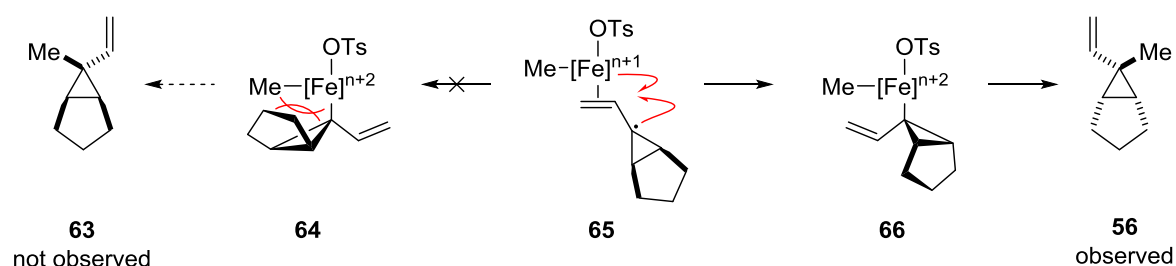
Scheme 22: Possible explanation for the observed stereoretentive Fe-catalyzed cross-coupling of 1-vinylcyclopropyl tosylate **57** and MeMgCl.

In conclusion, the developed Fe-catalyzed cross-coupling of 1-substituted cyclopropyl tosylates and alkyl Grignard reagents shows unique and unusual mechanistic features for Fe-catalyzed cross-couplings which require further mechanistic studies. Although the *in situ* generation of the active iron catalyst may make such mechanistic investigations more difficult, the present system

is, on the other hand, highly practical because it uses no ligands and a cheap, non-hygroscopic pre-catalyst. Furthermore, the methodology shows mild reaction conditions and short reaction times.

2.3   Conclusions and Outlook

The first example of an Fe-catalyzed Kumada–Tamao–Corriu-type cross-coupling reaction of *tert*-alkyl electrophiles was developed. With alkyl Grignard reagents as the cross-coupling partner, this reaction represents a rare method for $C(sp^3)$–$C(sp^3)$ bond formations, catalyzed by the simple iron complex, Fe(acac)$_3$. In contrast to the reported literature, cross-coupling of 1-alkynylcyclopropyl tosylates occurs with alkylmagnesium halides in excellent regioselectivity, furnishing the direct substitution products. Mixtures of these products and their corresponding allene isomers were obtained when aryl Grignard reagents were used.

Cross-coupling of 1-vinylcyclopropyl tosylates with Grignard reagents bearing no β-hydrogen atoms gave very good yields, whereas the cross-coupling of Grignard reagents which have hydrogen atoms available for β-hydride elimination resulted in lower yields along with formation of substantial amounts of reduced and dimerized starting material.

In addition, it was found that the triple and double bonds of the substrates are essential for a successful cross-coupling: analogous alkyl and aryl derivatives do not undergo Fe-catalyzed cross-coupling with the current system.

The presented method opens opportunities for the installation of the (1-methylcyclo-propyl)ethynyl group which has recently attracted the attention of the pharmaceutical industry.[98] In contrast to a *tert*-butyl group, this structural motif offers metabolic advantages and can enhance the stability of pharmaceutical drugs. This is illustrated by a series of anti-HIV drug candidates (**67**) which are related to Efavirenz.[99] Compounds of type **68** or **69** were patented for the potential treatment of hepatitis C[100] or cystic fibrosis[101] as well as for crop protection purposes[102] (Scheme 23).

Scheme 23: Representative examples of bioactive compounds comprising a (1-methylcyclopropyl)ethynyl group.

In addition, the cross-coupling products which are now accessible under mild reaction conditions are potential precursors for the synthesis of more complex structures. For example, Kim *et al.* reported the Rh(I)-catalyzed carbonylative [3+3+1] cycloaddition of 1-cyclopropyl-bicyclo[4.1.0]hept-2-ene derivatives (**70**) to form 4-vinylcyclohept-4-en-1-ones (**71**, Scheme 24).[103] The new Fe-catalyzed methodology allows access to more structurally divers 1-substituted cyclohept-4-en-1-ones (*e.g.*, **72** and **74**, Scheme 25, left) and is not restricted to the bicyclo[4.1.0]heptane structure of **70** because the 3,4-dihydro-2*H*-pyran substructure was necessary to access derivatives of **70** through Pt-catalyzed cycloisomerization reactions of cyclopropylenynes.
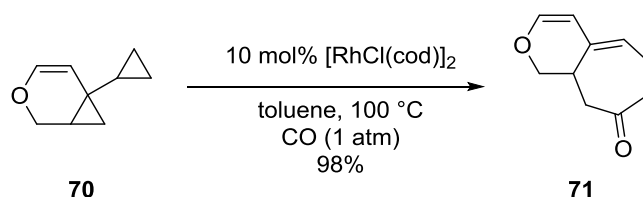
Scheme 24: Rh(I)-catalyzed carbonylative [3+3+1] cycloaddition of a bicyclopropane (**70**) with a vinyl substituent.

Another direction could be intra-/intermolecular [5+2] cascade reactions to access bicyclo[5.3.0]decatrienes (**73**)[104] and bicyclo[5.3.0]decadienes (**75**)[105] from **38q** and **44g**, respectively, when reacted with an alkyne (Scheme 25, right).
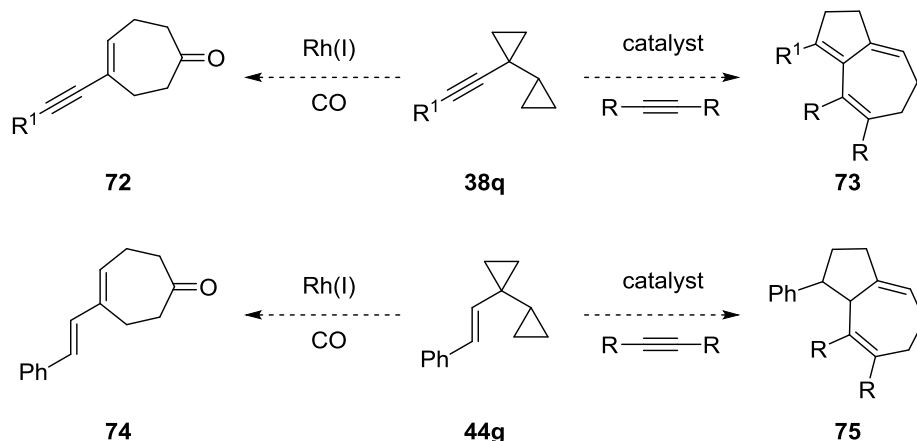
Scheme 25: Potential transformations in which bicyclopropanes **38q** (R^1 = (CH$_2$)$_3$OTBS) and **44g** serve as precursors.

Besides these synthetic possibilities, future work will focus on detailed mechanistic studies combining multiple analytical techniques to rationalize the different behavior of 1-alkynylcyclopropyl tosylates and 1-vinylcyclopropyl tosylates with the goal of extending this methodology even further.

3 Reactivity of Piano-Stool Rh(III) & Ir(III) Carbene Complexes

3.1 Introduction

3.1.1 Rh(II) Carbene Complexes in Carbene Transfer Reactions

In the early 1970s, $Rh_2(OAc)_4$ was reported to be an effective catalyst for the decomposition of diazo compounds.[106] The resulting carbene intermediates undergo reactions such as insertion into hydroxylic bonds and the cyclopropanation of olefins. Since then, the field of Rh(II)-catalyzed reactions involving diazo compounds has grown dramatically.[107–113] This chemistry gives access to a variety of synthetically useful transformations: insertions into E–H (E = B, C, O, N, Si, and S) and carbon-heteroatom bonds, cyclopropanations, cyclopropenations, [4+3] cyclo-additions and numerous ylide forming reactions. The success of this area of research can be attributed to the easy modification of $Rh_2(OAc)_4$, to yield a plethora of (chiral) catalysts with impressive turnover numbers and frequencies as well as high levels of chemo- regio-, diastereo-, and enantioselectivity.

It is well accepted that these reactions have a metal carbene as a common intermediate. These carbenes have been classified by their substituents to distinguish them from the well-known Fischer and Schrock carbenes (Scheme 26).
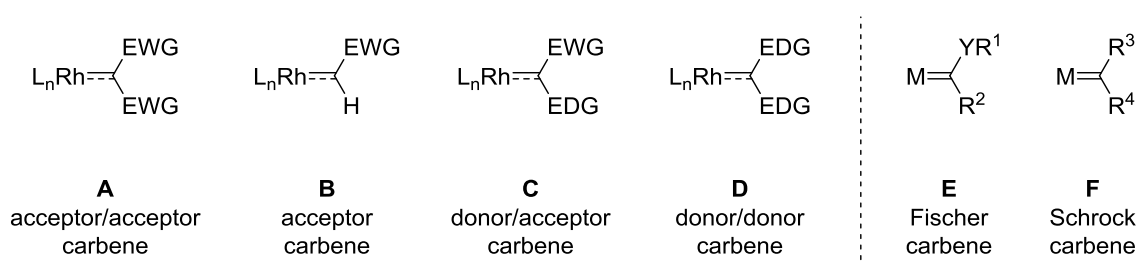
Scheme 26: Classification of rhodium carbene complexes (left). General representation of Fischer and Schrock carbenes (right). L_n = ligand sphere; EWG = CO_2R, COR, NO_2, $PO(OR)_2$, CF_3, SO_2R; EDG = vinyl, aryl, heteroaryl; M = transition metal; Y = O, NR; R, R^{1-4} = H, alkyl, aryl.

Fischer carbene complexes (**E**) feature an α-heteroatom that provides stabilization of the electrophilic carbene. They are often air stable, isolable species which can serve as stoichiometric reagents in reactions such as cyclopropanation.[114] Schrock carbene complexes (**F**) have no stabilizing heteroatom substituents on the carbene carbon and are excellent catalysts in olefin metathesis, exhibiting nucleophilic reactivity at the carbene.[115] Although structurally distinct from Fischer carbenes, complexes **A–D** show electrophilic reactivity. Their stability and reactivity form a spectrum from acceptor/acceptor carbenes (**A**) being the most unstabilized to donor/donor (**D**) being the most stabilized. The intermediate complexes are then referred to as

acceptor carbenes (**B**) or as donor/acceptor carbenes (**C**) and it is often these which provide the best balance between reactivity and stability needed for catalysis. Their corresponding (nucleophilic) precursors show the reverse trend in stability: the acceptor/acceptor diazo compounds are the most stable precursors, while the donor/donor diazo compounds are the most unstable ones.

In addition to their outstanding reactivity profiles, the dirhodium carbene complexes described above have drawn attention because of the interest in understanding their electronic and structural features. This results in a catalyst design which might lead to improved selectivities and new modes of reactivity.

The character of the carbene center has been termed as "superelectrophilic" by Berry in 2012.[116] He described the bonding situation of the Rh–Rh–C core by a three-center/four-electron (3c/4e) model—based on earlier work published by Nakamura and co-workers.[117] Mixing of one of the filled Rh–Rh π* orbitals with the unoccupied p orbital of the carbene results in an energetically low-lying LUMO polarized towards the carbene carbon. Its lower energy makes the LUMO more available for a reaction with an incoming (poor) nucleophile compared to an unoccupied π* antibonding orbital in a localized two-center/two-electron (2c/2e) bond of a mononuclear rhodium carbene complex. In addition, this description suggests a surprisingly low Rh–Rh bond order (<1).

Although several theoretical investigations on complexes such as **76** and **77** have been carried out (Scheme 27), complimentary experimental data was not available for a long time. It was not until 2013 that Davies, Berry, and co-workers managed to characterize a transient dirhodium carbene complex (**77**) for the first time by NMR, EXAFS, and optical spectroscopy (Scheme 27).[118] A highly deshielded ^{13}C{^{1}H} NMR signal was observed at 240.1 ppm for the carbene carbon. This indicates its very electrophilic character which is reflected in the fact that **77** was shown to undergo typical carbene reactivity (*i.e.*, cyclopropanation, C–H functionalization). This is in contrast to what has been found by Synder *et al.* for the dirhodium-NHC complex **78**, which is stable at room temperature and only catalyzes an intramolecular C–H insertion reaction after dissociation of the NHC.[119] A carbene carbon shift of 153.7 ppm was reported, which is in line with the observed reduced electrophilicity. The data obtained by EXAFS and optical spectroscopy by Davies, Berry, and co-workers gave rise to some structural data such as the Rh–Rh distance (*vide infra*), but still could not provide a detailed analysis of all of the geometrical features of the complex.

Two years later, Werlé *et al.* obtained the first crystallographic characterization of a reactive dirhodium carbene complex (**79**) bearing two electron donating substituents.[120] This seminal

report was quickly followed by the characterization of a range of dirhodium complexes in solution and the solid state, including complex **80** with only one stabilizing electron donating group.[121] Its carbene carbon resonance was detected at 237.1 ppm, similar to **77** (240.1 ppm). The $^{13}C\{^1H\}$ shift for the carbene carbon in **79** is observed at 268.9 ppm. This ≈ 30 ppm down-field shift compared to the structurally very similar complexes **77** and **80** can be mainly attributed to the nature of the substituents on the carbene.
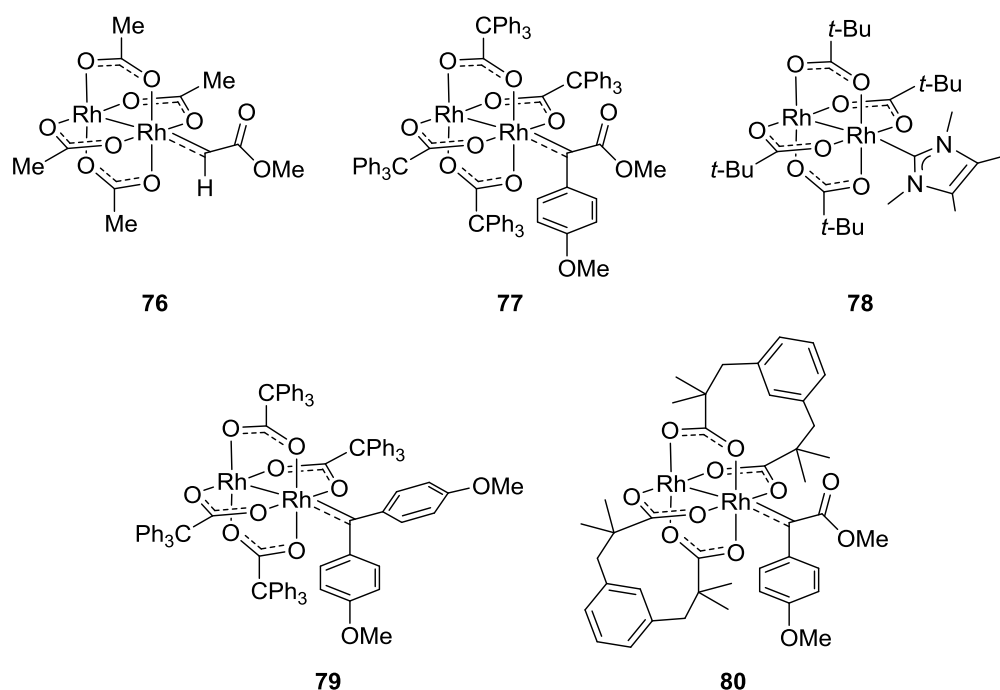
Scheme 27: Examples of dirhodium carbene complexes which were studied by different methods: DFT calculations were performed on **76** and **77**. Experimental data were determined by using optical spectroscopy on **77** or by X-ray crystallography on **78**–**80**.

The calculated Rh–Rh distance of **76** is significantly longer (2.475 Å by DFT) than the ones experimentally determined for **77**–**80** (**77**: 2.434(2) Å by EXAFS), **78**: 2.423(2) Å, **79**: 2.423(1) Å, **80**: 2.423(3) Å), but all of them are elongated compared to the parent dirhodium complexes (*e.g.*, 2.3707(5) Å in Rh$_2$(tpa)$_4$·2CH$_2$Cl$_2$,[116] the parent complex of **77** and **78**). The elongation of the Rh–Rh distances in the carbene complexes compared to their parent complexes is in line with Berry's model of changing from 2c/2e to 3c/4e bonding (*vide supra*). The much longer Rh–Rh distance in **76** seems to be an overestimation by the DFT calculations because a shorter Rh–Rh distance is expected due to an efficient $\pi^*_{Rh–Rh} \rightarrow p_{carbene}$ back bonding.

The Rh–C distances seem more suitable for a discussion because the carbene ligands are flexible and should respond to even subtle changes in the system. Complex **76** features the shortest Rh–C distance (1.939 Å by DFT) of the five complexes. The longest Rh–C distances are observed for the most stable complexes **78** (2.056(9) Å) and **79** (2.061(6) Å). The Rh–C distances of **77** (1.972 Å by DFT) and **80** (2.001(2) Å) lie between these boundaries. These data show a

relationship between Rh–C distances and the electrophilicity of the carbene ligands (Scheme 28): carbene complex **76** represents the most electrophilic carbene in the present series. With no stabilizing groups, the only stabilization can come from a π back donation of the Rh–Rh core, reflected in the contracted Rh–C distance compared to **77–80**. In the complexes **77** and **80** the carbenes carry an additional electron donating group rendering the carbene carbons less electrophilic than in **76** and, consequently, the lower demand for π back donation from rhodium results in a longer Rh–C distance. In continuation of this description, even more stabilized carbene ligands (*i.e.*, complexes **78** and **79**) exhibit the longest Rh–C distances in the present series.
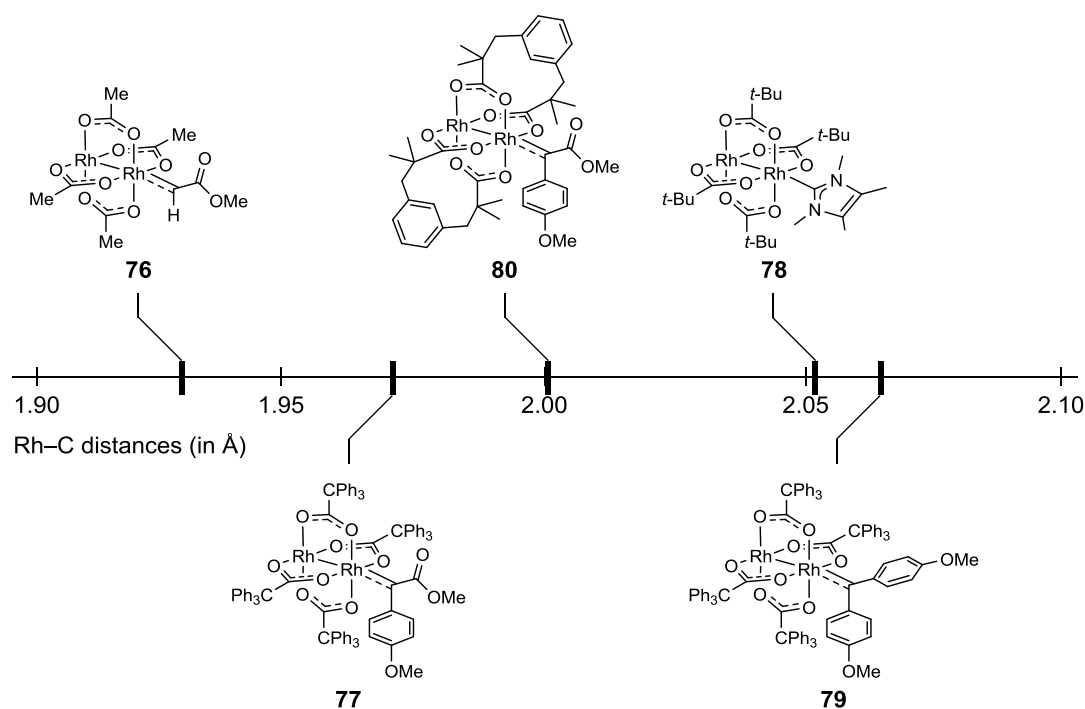
Scheme 28: Comparison of the Rh–C distances in the rhodium(II) carbene complexes **1–5**.

The combination of steric interactions between the carboxylate ligands and the carbenes' substituents and the reduced requirement for π back donation from the Rh–Rh core explains the observation that in **77–80** the carbene adopts a staggered conformation with respect to the O–Rh–O unit. These experimental data are in stark contrast to the theoretical prediction that the carbene ligand in **76** has an eclipsed conformation relative to the same entity and allowing for maximal orbital overlap for stabilization of the electrophilic carbene carbon. Although the eclipsed conformation of **76**, which was first noted by Hansen *et al.*,[122] seems to be an exception at first sight, recent work of the Fürstner group for related Bi–Rh complexes shows that different conformations are observed depending on the carbenes' substituents.[123] A more detailed analysis of this phenomenon is necessary to understand the reasons and therefore will not be discussed any further here.

All available crystallographic data of the dirhodium carbene complexes such as **79** and **80**, as well as other derivatives,[124] show effects of substituents on the geometry of the carbene itself. Firstly, substituents with electron donating groups adopt a coplanar orientation, so that they provide maximum stabilization by electron donation *via* the aromatic π-cloud into the formally vacant p orbital of the singlet carbene. In contrast, electron withdrawing groups exhibit an almost perpendicular conformation with respect to the $Rh-C_{aryl}-C_{Carbonyl}$ plane around the carbene carbon atom to avoid destabilization as much as possible. These conformational features are crucial for the explanation and prediction of stereochemistry in Rh-catalyzed reactions.[120,121,124]

3.1.2   C–H Functionalization with Cationic Rh(III) Complexes

Despite the successful application of Rh(II) complexes in catalysis, represented by the large body of diverse transformations, some key reactivity modes are still challenging for this type of complex. Rh(II) complexes catalyze carbene insertion reactions into (aliphatic) C–H bonds, but, good site-selectivity therein is still rare.[125] In addition, the insertion of carbenes into aromatic C–H bonds catalyzed by Rh(II) complexes is very difficult if not impossible, because the aromatic ring undergoes a Buchner ring expansion instead.[112j] However, Rh(III) complexes of the type $[Cp*RhX_2]_2$ (X = Cl, Br, I) have been used as successful pre-catalysts in C–H functionalization reactions of arenes with diazo compounds of type **A**–**C** (*cf.* Scheme 26).[126,127] Following the initial report by Chan *et al.*,[128] these methods typically use a silver salt to abstract the halide of $[Cp*RhCl_2]_2$ generating an electrophilic complex capable of activating the C–H bond.[129] Scheme 29 depicts a representative catalytic cycle for this type of methodology as proposed by Chan *et al.*
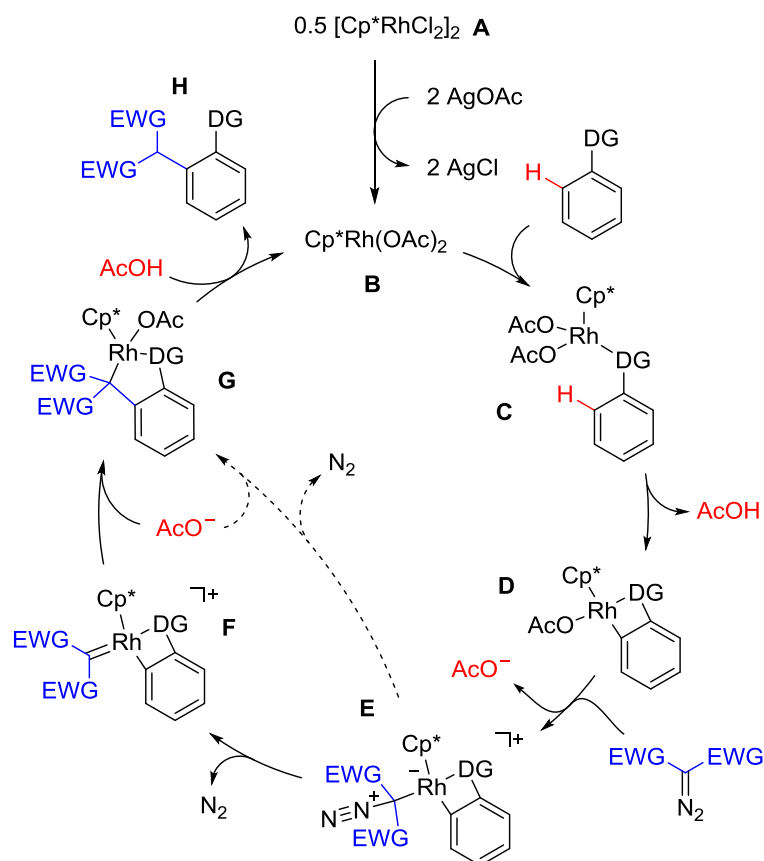
Scheme 29: The catalytic cycle proposed by Chan *et al.* for the Rh-catalyzed intermolecular functionalization of aromatic C–H bonds (DG = directing group).

The reaction of [Cp*RhCl$_2$]$_2$ (**A**) with AgOAc forms the active catalyst **B**. After coordination of the directing group (*e.g.*, oxime, carbonyl, or amine) to the metal center, **C** undergoes base-assisted cyclometalation to form rhodacycle **D**.[130] The directing group is often used to ensure region-selectivity which, in this example, directs the cyclometalation into the *ortho*-position. Rhoda-cycle **D** then reacts with one equivalent of diazo compound, resulting in the formation of a cyclometalated carbene complex **F** after nitrogen extrusion.[121,131] The carbene undergoes migratory insertion into the aryl-C–Rh bond to give **G**. Protodemetalation of **G** results in regeneration of the active catalyst (**B**) and release of the C–H functionalized product **H**. An alternative pathway from **E** to **G** *via* an 1,2-aryl shift from the Rh metal center onto the carbenoid carbon carrying the N$_2$ leaving group was also proposed by the same group.

In the same study, Chan *et al.* performed stoichiometric experiments, providing an insight into the reaction mechanism (Scheme 30). The reaction of benzo[*h*]quinolone (**81**) with [Cp*RhCl$_2$]$_2$ afforded the cyclometalated Rh(III) complex **82** which, upon reaction with dimethyl diazomalonate, gave the *tert*-alkyl complex **83**. The structure of **83** was confirmed unambiguously by X-ray crystallography.
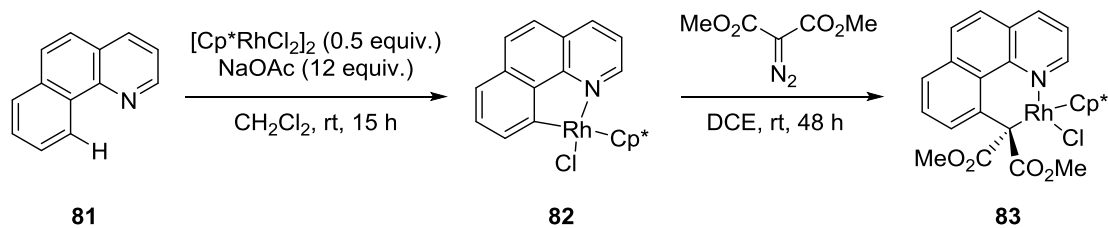
Scheme 30: Stoichiometric experiments performed by Chan *et al.*

Whether the stoichiometric experiments support the proposed mechanism is questionable. First of all, benzo[*h*]quinolone (**81**) was not employed as a substrate in their substrate scope, although the groups of Glorius[132] as well as Li and Wang[133] later proved that **81** is a suitable substrate in catalytic C–H functionalizations with diazo compounds. Secondly, complexes **82** and **83** are a poor model for the proposed intermediates (**D** and **G**, respectively) because they carry different anionic ligands (chloride and acetate, respectively).

In addition, no structural or spectroscopic data were provided for the intermediate cationic Rh(III) carbene complex (**F**). Indeed, no such complex had been characterized at the outset of this study.

3.1.3 Isolation of Piano-Stool Cp*Rh(III) Carbene Complexes

Although the interest in methodologies using cationic Rh(III) complexes as catalysts has increased recently,[134] the parent complexes [Cp*RhX$_2$]$_2$ (X = Cl, Br, I) have not been studied in carbene chemistry in any detail.[135] This is despite neutral, mononuclear Rh(III) complexes having been shown to facilitate reactions between diazo compounds and appropriate substrates.[136] Indeed, as early as 1973, Paulissen *et al.* showed that RhCl$_3$·3H$_2$O catalyzes the insertion of ethyl diazo acetate (EDA) into the O–H bond of EtOH in 64% yield.[106a] Despite dimeric Rh(II) complexes often giving better catalytic performance (Rh$_2$(OAc)$_4$ gave 88% yield in the aforementioned example), mononuclear Rh(III) complexes have not yet been the focus of such intense development as the Rh(II) complexes.[134]

The Fürstner group has shown in a preliminary study that Cp*Rh(III) complexes can serve as competent catalysts in typical transformations with diazo compounds (Scheme 31):[121] cyclopropanation of *p*-methoxystyrene was achieved in 69% (with [Cp*RhI$_2$]$_2$) and 46% (with [Cp*RhCl$_2$]$_2$) yield. The transiently formed carbene underwent insertion into the X–H bonds of HSi(OEt)$_3$ and MeOH in 81% and 88% yield, respectively. Lastly, the reaction with (*p*-methoxyphenyl)acetylene afforded directly the 2-methoxyfuran **88** in 65% yield.[137]
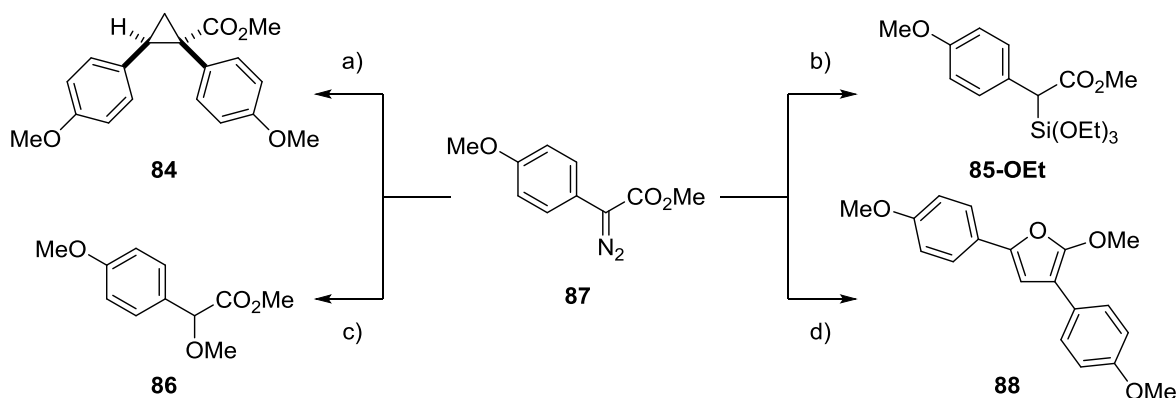
Scheme 31: Preliminary reactivity studies of a piano-stool Rh(III) carbene complex generated *in situ*. Reagents and conditions: a) *p*-methoxystyrene, *n*-pentane, 69% (with [Cp*RhI$_2$]$_2$ (1 mol%)); 46% (with [Cp*RhCl$_2$]$_2$ (1 mol%)). b) HSi(EtO)$_3$, [Cp*RhI$_2$]$_2$ (1 mol%), CH$_2$Cl$_2$, 81%. c) MeOH, [Cp*RhI$_2$]$_2$ (1 mol%), CH$_2$Cl$_2$, 88%. d) (*p*-methoxyphenyl)-acetylene, [Cp*RhI$_2$]$_2$ (1 mol%), CH$_2$Cl$_2$, 65%.

Further work by the Fürstner lab was concerned with characterization of the intermediates in these reactions which were believed to be well-defined piano-stool Rh(III) carbene complexes.[121] In an NMR experiment, the reaction of diazo compound **87** with [Cp*RhCl$_2$]$_2$ at ≈ 8 °C resulted in formation of a species whose ^{1}H NMR spectrum showed a 1:1 ratio of Cp* and carbene fragment resonances. However, the ^{13}C{^{1}H} NMR spectrum lacked any high frequency resonances consistent with a deshielded carbene and instead showed a new signal at 70.6 ppm. Analysis by X-ray crystallography revealed this complex to be a C-metalated rhodium enolate (**89**, Figure 5). The formation of **89** was rationalized as being the product of chloride migration from the intermediate metal carbene complex. The formally 16-valence electron complex appears to be stabilized in the solid state by the *para*-methoxyphenyl ring, as evident from short contacts between rhodium and the carbon atoms C4 and C9 (Rh1–C4: 2.257(1) Å, Rh1–C9 2.419(1) Å; sum of van der Waals radii of Rh and C: 3.80 Å; sum of covalent radii of Rh and C: 2.09 Å).[138] This stabilization persists in solution to a certain extend as seen from the high-field shifts of C4 (96.2 ppm) and C5/C9 (116.6 ppm) in the ^{13}C{^{1}H} NMR spectrum and broadened signals of the *para*-methoxyphenyl group in the ^{1}H NMR spectrum, consistent with restricted rotation about C1–C4.
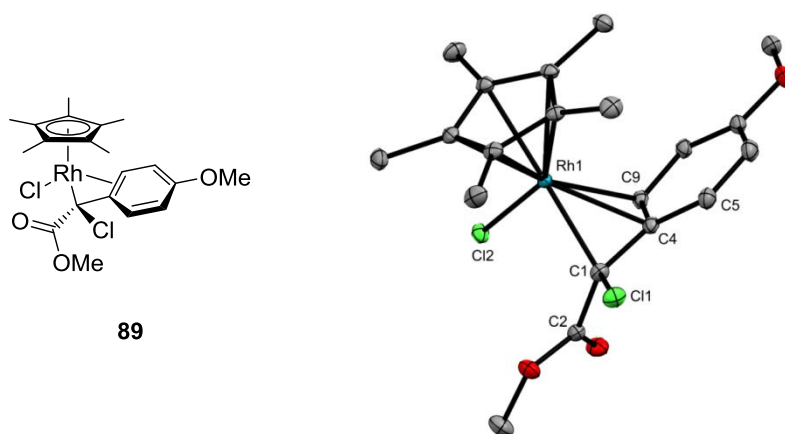
Figure 5: Molecular structure of complex **89** in the solid state with ellipsoids depicted at the 50% probability level. Hydrogen atoms and co-crystallized toluene are omitted for clarity. Selected distances (in Å): Rh1–C1 2.123(1), Rh1–C4 2.257(1), Rh1–C9 2.419(1), Rh1–Cl2 2.4069(7), C1–Cl1 1.779(1), C1–C2 1.499(2), C1–C4 1.467(2), C4–C9 1.421(2), C4–C5 1.431(2).[121]

Although this finding was not expected, there is precedence for the intramolecular insertion of a carbene moiety into a metal–halogen bond (Scheme 32). Based on work by Jennings *et al.*,[139] Bergamini *et al.*[140] reported the synthesis of α-chiral platinum alkyl complexes (**91**) by reaction of EDA with haloplatinum complexes of the type [PtX$_2$L$_2$] (**90**). The report by Maxwell and Kodadek shows that a 1:1 mixture of rhodium porphyrin complex **92** and EDA reacts to form an α-iodo alkyl Rh(III) porphyrin complex (**93**).[141] Complex **93** does not undergo cyclopropanation with styrene whereas **92** catalyzes the cyclopropanation when an 10-fold excess of styrene is used.
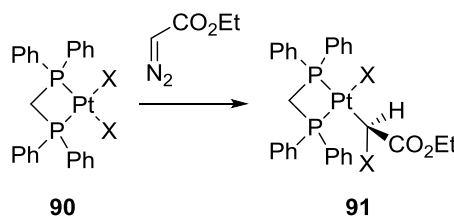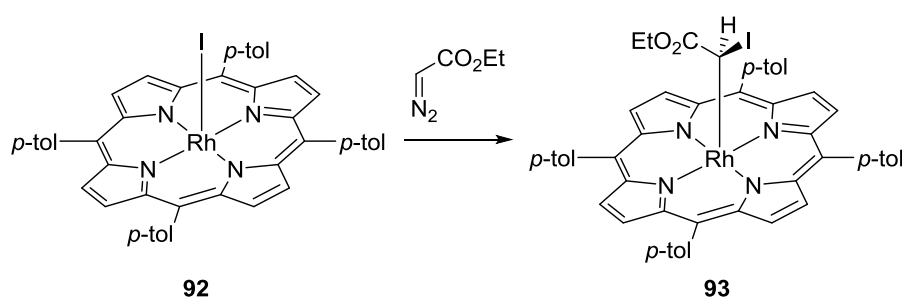
Scheme 32: Literature precedence for carbene insertion into a metal–halogen bond by a) the groups of Jennings and Bergamini (top, X = Cl, Br, I) and by Kodadek *et al.* (bottom).

In contrast to the facile chloride migration observed for **89** and the literature precedence described above, the carbene complexes of [Cp*RhX$_2$]$_2$ (X = Br, I) were isolated when **87** was used as the carbene precursor. Both complexes (X = Br: **94** and X = I: **95**) were stable at ≈ 0 °C

and feature a distinctive resonance for their carbene carbon in the $^{13}C\{^1H\}$ NMR spectrum (**94**: 313.9 ppm; **95**: 316.4 ppm). This represents a pronounced down-field shift compared to dirhodium complex **80** (237.1 ppm). This is attributed to the different oxidation states of the metal centers and the different ligand spheres.[142]
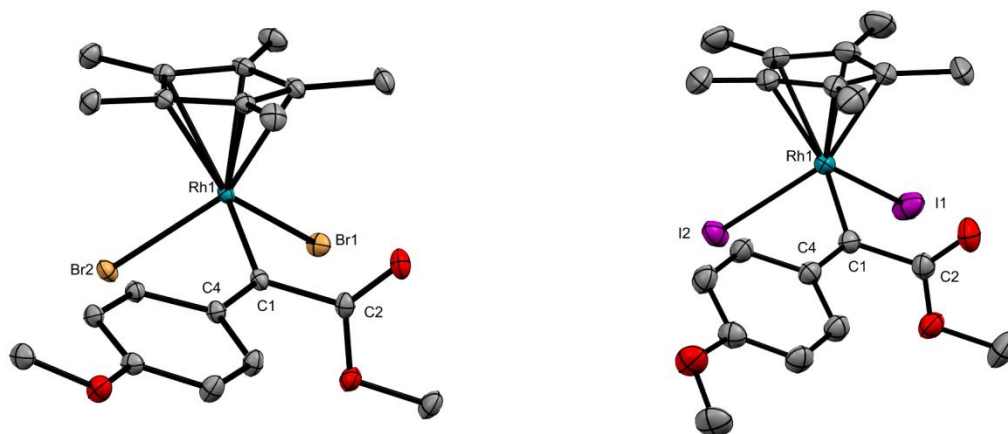
Figure 6: Molecular structures of complexes **94** (X = Br, left) and **95** (X = I, right) in the solid state with ellipsoids depicted at the 50% probability level. Hydrogen atoms, co-crystallized PhF, and co-crystallized toluene are omitted for clarity. Selected distances (in Å): **94**: Rh1–Br1 2.5407(4), Rh1–Br2 2.5303(4), Rh1–C1 1.967(1), C1–C2 1.497(2), C1–C4 1.414(2); **95**: Rh1–I1 2.7067(7), Rh1–I2 2.6920(4), Rh1–C1 1.970(2), C1–C2 1.504(4), C1–C4 1.415(4).[121]

Crystals of **94** and **95** were obtained and subjected to X-ray diffraction analysis confirming the presence of the carbene motif. These complexes represent the first examples of reactive piano-stool Rh(III) carbene complexes that were characterized in the solid state and, therefore, allowed further investigations into the structures of these complexes (Figure 6). In both cases, the carbene substituents adopt a similar conformation to those observed for the dirhodium carbene complexes: the electron donating aryl group is oriented coplanar with the p orbital on the carbene carbon, while the ester group adopts a perpendicular conformation with respect to the Rh-C_{aryl}-$C_{Carbonyl}$ plane around C1. The stabilizing effect is reflected in the C1–C4 bonds (**94**: 1.414(2) Å, **95**: 1.415(4) Å) being significantly shorter than the C1–C2 bonds (**94**: 1.497(2) Å, **95**: 1.504(4) Å).

The Rh1–C1 distances (**94**: 1.967(1) Å, **95**: 1.970(2) Å) are shorter than that of the dirhodium complex **80** (2.001(2) Å), consistent with the proposed increase in metal–carbene bond order for 2c/2e bonding compared to 3c/4e bonding.[116] Although greater deviations are found in linear triatomic model systems (*e.g.*, Br_3^-: 2.6372 Å, Br_2: 2.281 Å[143]),[144] the complexes studied are far more complex and ligand effects can be expected to constrain their geometries.

3.2 Results and Discussion

3.2.1 Studies Towards a Cyclometalated Rh(III) Complex Bearing a Carbene Ligand

The following project was conducted in cooperation with Dr. Christophe Werlé. His contributions are highlighted.

As outlined in Section 3.1.2, the well accepted mechanism of Rh(III)-catalyzed C–H function-nalization reactions of arenes with diazo compounds involves the formation of a cyclometalated complex bearing a carbene moiety as a ligand (**F** in Scheme 29). However, this type of intermediate has not been characterized to date and, thus, this project aimed to isolate such a complex to obtain spectroscopic and structural features for the first time. It was envisaged that a more stable complex could be generated by employing a donor/donor diazo compound as the carbene precursor.

N-Phenylbenzamidine **96** was chosen as a substrate for the synthesis of the cyclometalated complex because the phenyl group could provide steric shielding around the carbene and enhance the complex's stability. A complex with a similar ligand (**98**; Scheme 33, right) has been reported by Li and co-workers.[145] Complex **98** was synthesized from [Cp*RhCl$_2$]$_2$ and *N*-phenylacetimidamide using NaOAc as a base at room temperature in CH$_2$Cl$_2$. The molecular structure was confirmed by X-ray crystallography and revealed that the ligand chelates the rhodium to form a 6-membered rhodacycle.

On the basis of the literature, the same reaction conditions were applied to the synthesis of a complex bearing **96** as the cyclometalating ligand. Although complex **97** was obtained as the major product, the synthesis turned out to be irreproducible and varying mixtures of several Cp* containing species were obtained, as evident from ^{1}H NMR spectra. These isomeric complexes could arise from several modes of chelation of **96** to the rhodium center. It was reasoned that selective formation of the target complex could be achieved by heating the reaction mixture, resulting in the formation of the thermodynamic product. Finally, complex **97** was obtained selectively by conducting the synthesis in toluene at reflux temperature (Scheme 33, left).
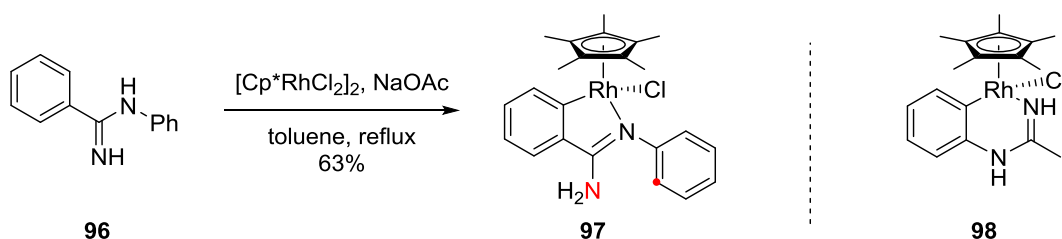
Scheme 33: Left: Synthesis of complex **97**. Right: The related literature known complex **98**. Formation of a 6-membered chelate, analogously to **98**, would occur through metalation and coordination of the atoms marked in red.

Complex **97** was fully characterized by NMR and IR spectroscopy, mass spectrometry, and X-ray crystallography (Figure 7). It shows a significant difference from complex **98** in that formation of a 5-membered chelate is favored over the formation of a 6-membered chelate (in that case, metalation and coordination would occur through the atoms marked in red in **97**; Scheme 33). It is also noteworthy that the *N*-substituted benzamidine moiety has undergone isomerization to the *N'*-substituted benzamidine (C1–N1: 1.315(2) Å, C1–N2: 1.351(3) Å). While the Rh1–C3 distance in **97** is similar to the one found in **98** (**97**: 2.016(2) Å, **98**: 2.024(6) Å), a significant difference is found in the Rh1–N1 distances (**97**: 2.099(2) Å, **98**: 2.043(6) Å). This is attributed to the differing substituent on N1 as well as the different size of the metallacycle. In the ^{1}H and ^{13}C{^{1}H} NMR spectra, broader signals for the *ortho-* and *meta*-positions of the N-phenyl group are observed. This is explained by a hindered rotation about the N1–C8 bond caused by steric repulsion of the phenyl group and the Cp* ligand. The Rh1–C3 $^1J_{RhC}$ coupling constant of 32.2 Hz is almost identical to the one reported for complex **98** (32.6 Hz).
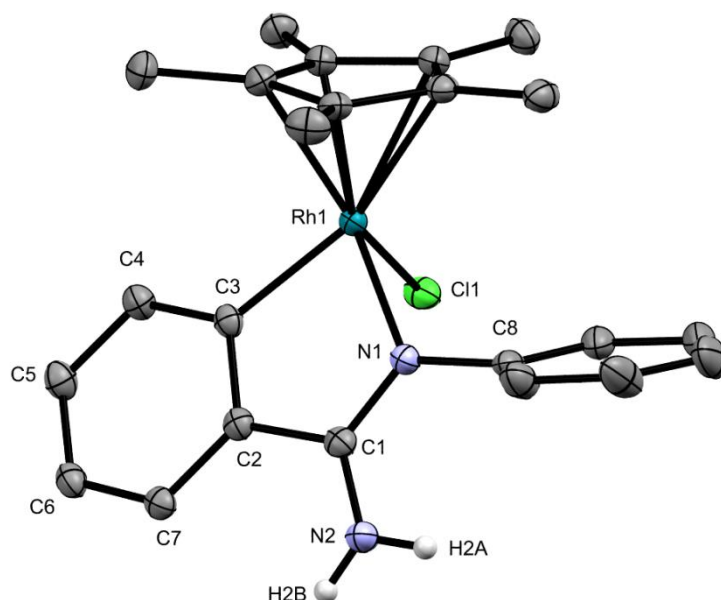
Figure 7: Molecular structure of complex **97** in the solid state with ellipsoids depicted at the 50% probability level. With exception of acidic protons, hydrogen atoms are omitted for clarity. H2A and H2B were found and refined. Selected distances (in Å): Rh1–Cl1 2.4317(7), Rh1–N1 2.099(2), Rh1–C3 2.016(2), C1–N1 1.315(2), C1–N2 1.351(3), C1–C2 1.472(3), C2–C3 1.416(3), C3–C4 1.393(3), C4–C5 1.396(3), C5–C6 1.392(3), C6–C7 1.386(3), C7–C2 1.405(3), N1–C8 1.429(3).

In order to generate the targeted rhodium carbene complex, **97** was reacted with diazo compound **100** at room temperature. No reactivity was observed, which was attributed to the lack of an easily accessible coordination site for coordination of the diazo compound and subsequent dinitrogen extrusion. Therefore, chloride abstraction with AgSbF$_6$ in the presence of MeCN was undertaken to introduce a more labile ligand (MeCN). Surprisingly, the isolated acetonitrile complex also did not undergo any reaction with **100**. The slow formation of a black precipitate during the reaction led to the suggestion that inorganic (*e.g.*, Ag) contaminants

prevented any reactivity. Because different attempts to remove these impurities were not met with success, an alternative synthesis was chosen. In analogy to the selective synthesis of **97**, an MeCN solution of *N*-phenylbenzamidine **96** and [Cp*Rh(MeCN)$_3$](SbF$_6$)$_2$ was heated to reflux in the presence of NaOAc affording the desired complex **99** in 80% isolated yield (Scheme 34, top). Crystals could not be obtained due to the formation of an oil in various solvent mixtures and at different temperatures. Despite that, the complex was fully characterized by NMR and IR spectroscopy, and mass spectrometry. The ^{1}H and ^{13}C{^{1}H} NMR spectra of **99** qualitatively resemble those of **97**, with the exception that the signals for the *ortho*-positions of the N-phenyl group are sharp, indicating free rotation about the N–Ph bond in complex **99**.
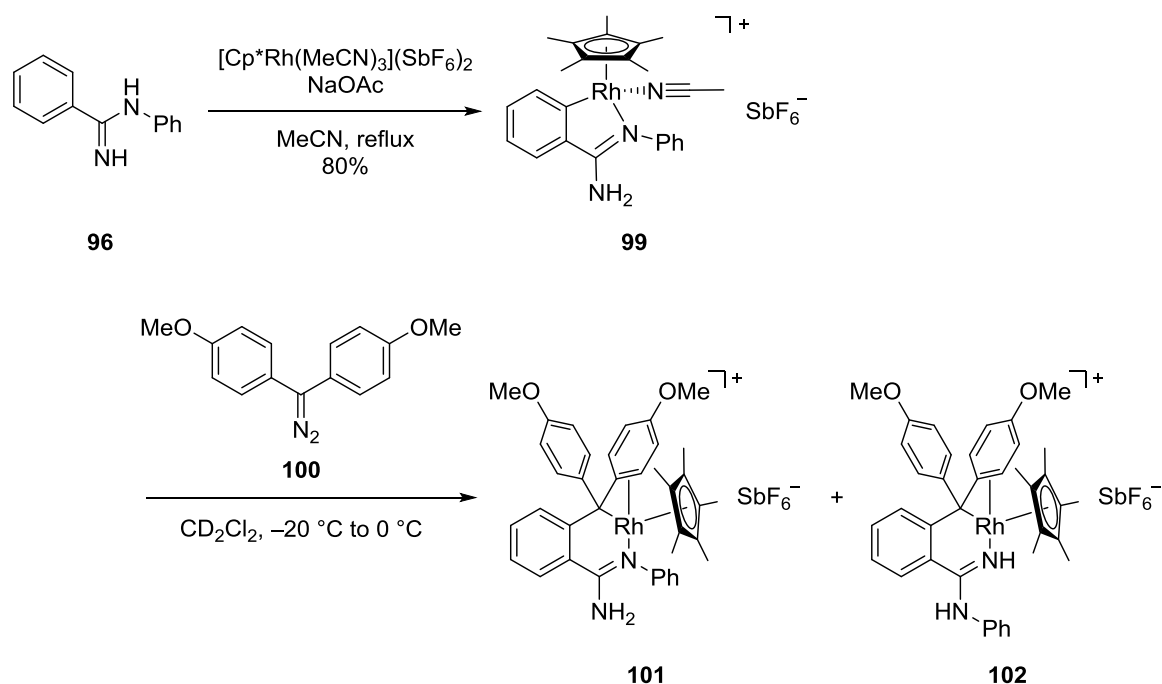
Scheme 34: Synthesis of complex **99** (top) and result of the reaction of **99** with diazo compound **100** at low temperature (bottom).

Gratifyingly, samples of complex **99** generated by this method reacted with diazo compound **100**. In an NMR experiment, **100** was added dropwise to a solution of **99** in CD$_2$Cl$_2$ at −20 °C. Monitoring this mixture at different temperatures showed that, initially, no reaction had occurred and the starting materials were still present. Upon warming the mixture to 0 °C, the signals which had been assigned to the starting materials decreased and two new sets of signals appeared in a ratio of ≈ 2.5:1. These were assigned to complex **101** as the major component and a second isomeric complex **102** (Scheme 34, bottom) as the minor component. Both complexes resemble the products of migratory insertion of a transiently formed carbene into the Rh–C$_{aryl}$ bond and are isomers with respect to the amidine motif. Broader signals in the NMR spectra are observed for the *ortho*-protons of the N-phenyl group in complex **101** due to hindered rotation about the N–Ph bond caused by the closer Cp* ring compared to **102**. Both complexes have

smaller $^1J_{CRh}$ coupling constants (**101**: 14.3 Hz, **102**: 13.2 Hz) than their precursor (**99**: 30.2 Hz). The differences in the observed $^1J_{CRh}$ coupling constants can be explained analogously to the empirical relationship between the s-character of the carbon atom and the magnitude of the $^1J_{CH}$ coupling constant:[146] complexes **101** and **102** show a much smaller $^1J_{CRh}$ coupling constant than **99** (which is sp² hybridized) and therefore, the carbon possess a higher s-character; hence, it is sp³ hybridized.

Furthermore, both complexes show an inequality of the two *para*-methoxyphenyl rings, most distinctly shown by their *ipso*-position $^{13}C\{^1H\}$ NMR shifts (**101**: 138.6 ppm and 106.7 ppm; **102**: 138.0 ppm and 136.6 ppm). In addition, the *para*-methoxyphenyl rings that exhibit the up-field shift at their *ipso*-positions also display desymmetrized AA'XX' spin systems in the ^1H NMR spectrum (Figure 8). This observation is more pronounced in complex **101** and further illustrated by the inequivalence of the *ortho*-carbon $^{13}C\{^1H\}$ chemical shifts (**101**: 131.2 ppm and 105.6 ppm; **101**: 133.0 ppm and 128.7 ppm). Although no scalar coupling of rhodium with any of these carbon atoms is observed, the large up-field shift (over 25 ppm in the case of complex **101**) could be explained by an electronic interaction between the electron rich aromatic ring and the electron deficient metal center.
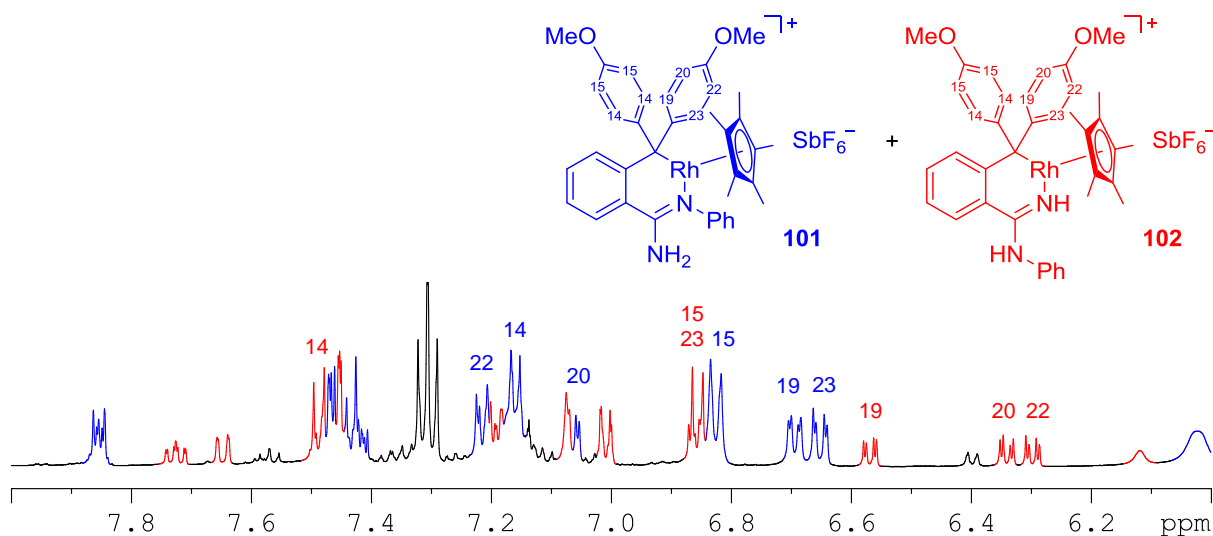
Figure 8: Excerpt of the ^1H NMR spectrum (500 MHz, CD₂Cl₂) of complexes **101** (blue) and **102** (red) showing the desymmetrized AA'XX' spin systems of the *para*-methoxyphenyl rings which interact with the rhodium metal center as is evident from the comparison of the signals of the symmetrical AA'XX' spin system (14 and 15) with the signals of the desymmetrized AA'XX' spin system (19, 20, 22, and 23) for each complex. The apparent triplet at 7.31 ppm was assigned to the *meta*-hydrogens of the N–Ph group of both complexes.

Crystals of the major isomer **101** were obtained and the resulting molecular structure is depicted in Figure 9.[147] In agreement with the NMR data, **101** is seen to be a rare example of a *tert*-alkyl rhodium complex. The X-ray data also corroborate the observed desymmetrization of the *para*-methoxyphenyl rings by showing that one of the aromatic rings is significantly closer to the rhodium center than the other one (Rh1–C22: 2.342(2) Å, Rh1–C15: 3.055(2) Å). Furthermore, the closer ring system shows shorter contacts between the rhodium and one side

of the ring system than the other (Rh1–C27: 2.494(2) Å, Rh1–C23: 3.384(2) Å). The complexes that most closely resemble **101** are complex **89**[121] and chiral complex **103**[148] (Scheme 35), in which both were described to exhibit a coordination of the aryl group to the metal center. The Rh–C distances in **101** (Rh1–C22: 2.342(2) Å, Rh1–C27: 2.494(2) Å) are shorter than in **89** (Rh1–C4: 2.257(1) Å, Rh1–C9: 2.419(1) Å)[121] and in **103** (Rh1–C11: 2.290(2) Å, Rh1–C12: 2.212(3) Å)[148]. Accounting for all of the available data, it is concluded that the aromatic ring coordinates to the rhodium metal center to stabilize complex **101**, in fulfillment of the 18-electron rule.

Figure 9: Molecular structure of complex **101** in the solid state with ellipsoids depicted at the 50% probability level. With exception of acidic protons, hydrogen atoms and the counter ion SbF_6^- are omitted for clarity. H1, H2, and H27 were found and refined. Selected distances (in Å): Rh1–N1 2.105(2), Rh1–C1 2.162(2), Rh1–C22 2.342(2), Rh1–C27 2.494(2), N1–C8 1.308(3), N1–C9 1.439(3), C8–N2 1.347(4), C1–C2 1.503(4), C1–C22 1.486(3), C22–C23 1.422(4), C22–C27 1.402(4), C2–C3 1.409(3), C3–C4 1.378(4), C4–C5 1.377(4), C5–C6 1.376(4), C6–C7 1.404(4), C1–C15 1.506(3).

Scheme 35: Complexes that were characterized in the solid state by Werlé *et al*. (**89**) and Panichakul *et al*. (**103**) and are structurally related to complex **101**.

This first stoichiometric study on the Rh(III)-mediated C–H functionalization of arenes has provided valuable insight into the nature of the catalytic cycle and reactive intermediates. The neutral Rh(III) halide complex **97** does not decompose diazo **100**, and neither does cationic complex **99** when generated *in situ* from **97** by halide abstraction with AgSbF$_6$. With pure **99** in

hand, however, diazo decomposition is facile at 0 °C and leads directly to the isomeric products of migratory insertion **101** and **102**. These results show that carbene formation and migratory insertion are likely to be fast steps in the catalytic cycle and that *in situ* halide abstraction may not always lead to the envisaged reactivity.

3.2.2 Reactivity Studies on Piano-Stool Rh(III) and Ir(III) Carbene Complexes

As outlined in Section 3.1.2, Rh(III) carbene complexes have major applications in C–H functionalization reactions. Neutral $[Cp*RhX_2]_2$ (X = Cl, Br, I) complexes have been far less studied as pre-catalysts than either dimeric Rh(II) complexes or cationic Rh(III) complexes. Initial studies on the neutral complex $[Cp*RhI_2]_2$ were reported by Werlé *et al.* after characterization of the first piano-stool Cp*Rh(III) complexes.[121] It was found that *in situ* generated Rh(III) carbene complexes exhibit decent reactivity in typical carbene transfer reactions.

In continuation of these efforts, this project aimed at gaining further insights into the reactivity of neutral piano-stool Cp* complexes of rhodium and iridium. As analogous iridium complexes $[Cp*IrX_2]_2$ have also been employed as catalysts in carbene transfer reactions.[149] Werlé was able to obtain crystallographic data of the Ir(III) carbene complexes derived from $[Cp*IrCl_2]_2$ and $[Cp*IrI_2]_2$ and diazo compounds **87** and **104**, respectively (*cf.* Table 5).[150] In contrast to the carbene complex derived from $[Cp*RhCl_2]_2$, no iridium chloride migration was observed.

Cyclopropanation of *p*-methoxystyrene was chosen as the starting point for an initial catalyst screening (Table 5). All complexes gave the anticipated products. $[Cp*RhI_2]_2$ (69%, entry 2) performed better than $[Cp*RhCl_2]_2$ (46%, entry 1). $[Cp*IrCl_2]_2$ and $[Cp*IrI_2]_2$ led to isolation of the desired cyclopropane derivatives in 63% and 58% yield, respectively (entries 3 and 4).

Table 5: Results of the catalyst screening for the cyclopropanation of *p*-methoxystyrene. The solution of the diazo compound was added over 3 h *via* syringe pump. The isolated yields are relative to the diazo compound.

87, R^1 = OMe, R^2 = Me
104, R^1 = CO$_2$Me, R^2 = Et

84, R^1 = OMe, R^2 = Me
105, R^1 = CO$_2$Me, R^2 = Et
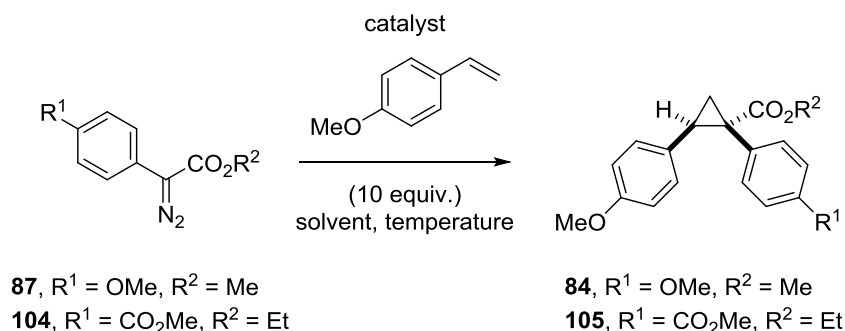
entry	substrate	catalyst (1 mol%)	solvent	T (°C)	yield (%)
1	**87**	[Cp*RhCl$_2$]$_2$	pentane	rt	46
2 [121]	**87**	[Cp*RhI$_2$]$_2$	pentane	rt	69
3	**87**	[Cp*IrCl$_2$]$_2$	CH$_2$Cl$_2$	40	63
4	**104**	[Cp*IrI$_2$]$_2$	CH$_2$Cl$_2$	rt	58

The observation that [Cp*RhCl$_2$]$_2$ resulted in a lower yield than [Cp*RhI$_2$]$_2$ became even more apparent when these complexes were used to catalyze carbene insertion into Si–H bonds (Table 6). The former performed poorly and only traces of the insertion product were detected (entry 1). In contrast, [Cp*RhI$_2$]$_2$ gave an excellent isolated yield of 81% under the exact same reaction conditions (entry 2). [Cp*IrCl$_2$]$_2$ and [Cp*IrI$_2$]$_2$ were moderately successful catalysts for this transformation (49% (entry 3) and 39% yield (entry 4), respectively).

Table 6: Results of the catalyst screening for the carbene insertion into Si–H bonds. The solution of the diazo compound was added over 1 h *via* syringe pump (except for entry 3). The isolated yields are relative to the diazo compound.

87, R^1 = OMe, R^2 = Me
104, R^1 = CO$_2$Me, R^2 = Et

85-Et, R^1 = OMe, R^2 = Me, R = Et
106, R^1 = CO$_2$Me, R^2 = Et, R = Et
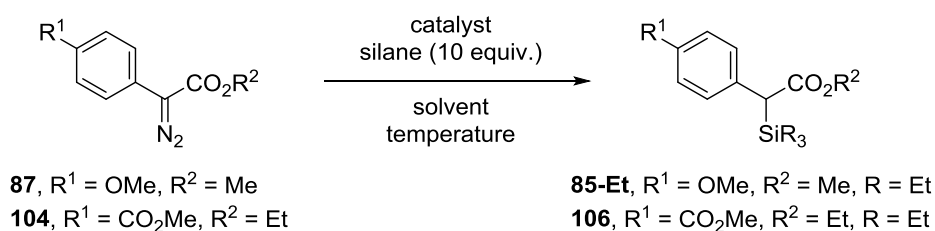
entry	substrate	silane	catalyst (1 mol%)	solvent	T (°C)	yield (%)
1	**87**	HSi(OEt)$_3$	[Cp*RhCl$_2$]$_2$	CH$_2$Cl$_2$	rt	traces
2 [121]	**87**	HSi(OEt)$_3$	[Cp*RhI$_2$]$_2$	CH$_2$Cl$_2$	rt	81
3	**87**	HSiEt$_3$	[Cp*IrCl$_2$]$_2$	DCE	80	49
4	**104**	HSiEt$_3$	[Cp*IrI$_2$]$_2$	DCE	rt	39

Similarly, [Cp*RhCl$_2$]$_2$ led to a low conversion in the (Darzens) oxirane formation from aromatic aldehydes, whereas, [Cp*RhI$_2$]$_2$ performed well.[151] The chloride complex gave only traces of the desired product **107** (7% conversion by GC), whereas, with the iodo complex, an isolated yield of 61% was obtained (Scheme 36). This result turned out to be general for oxirane formation from various aromatic and alkenyl aldehydes with electron donating or withdrawing substituents. Even the poorly nucleophilic methyl 4-formylbenzoate afforded the corresponding oxirane **110** in 85% isolated yield.

Neither aliphatic aldehydes nor acetophenone underwent this transformation which is in line with reports using Rh$_2$(OAc)$_4$ or an NHC-Ag$^+$ based catalyst.[152–154] These substrates seem to be only utilizable by employing Rh$_2$(OAc)$_4$ and a (chiral) sulfide in the synthesis of oxiranes developed by the Aggarwal group in which the intermediate sulfur-ylide—not the Rh(II) carbene complex—transfers the carbene moiety onto the carbonyl substrate.[155]

All oxiranes shown in Scheme 36 were obtained as a single diastereomer with a *cis*-arrangement of the ester and the aromatic or alkenyl moiety, confirmed by ^{1}H/^{1}H NOESY NMR experiments in all cases. Crystals of **109** were obtained and the solid state structure is in line with the findings in solution (Figure 10).
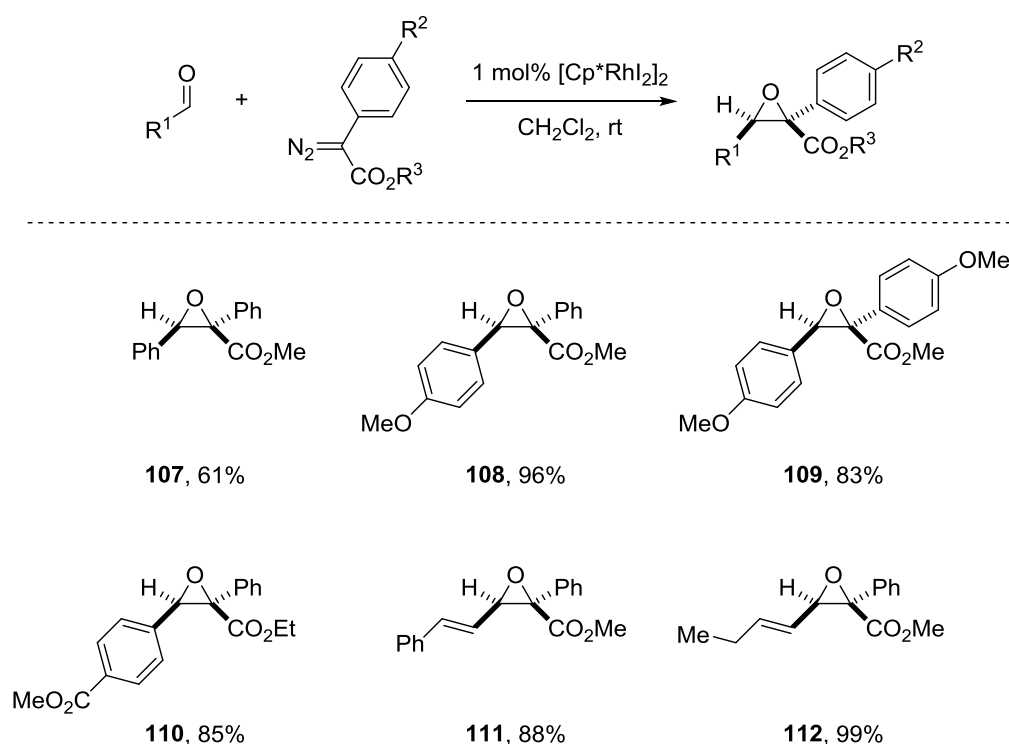
Scheme 36: Scope of the Rh(III)-catalyzed oxirane formation from aldehydes with isolated yields. The solution of the diazo compound (1.5 equiv. relative to the aldehyde) was added to the solution of the aldehyde (0.25 mmol) in CH$_2$Cl$_2$ (*c* = 0.1 M) over 1 h *via* syringe pump.
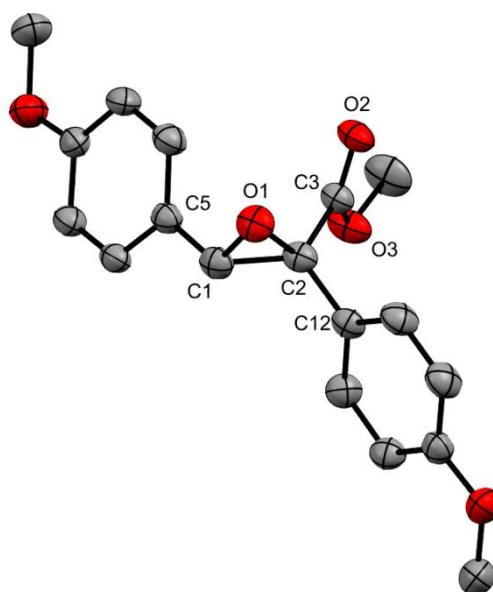
Figure 10: Molecular structure of oxirane **109** in the solid state with ellipsoids depicted at the 50% probability level. Hydrogen atoms are omitted for clarity. Selected distances (in Å): C1–O1 1.444(3), C2–O1 1.434(3), C1–C2 1.475(4), C1–C5 1.490(4), C2–C3 1.510(3), C3–O2 1.197(3), C3–O3 1.329(3), C2–C12 1.491(3).

Next, the catalytic insertion of carbenes into the O–H bond of MeOH was investigated (Table 7). In contrast to the aforementioned reactions, the desired product was obtained in similar isolated yields regardless of whether [Cp*RhCl$_2$]$_2$ (83%, entry 1) or [Cp*RhI$_2$]$_2$ (88%, entry 2) were employed as catalysts. As expected, the analogous iridium complexes [Cp*IrCl$_2$]$_2$ and [Cp*IrI$_2$]$_2$ afforded the insertion product **86** in good isolated yields (74% and 76%, respectively, entries 3 and 4). When the less reactive diazo compound **104** was used, the reaction was slower (18 h instead of 5 h), but an excellent isolated yield of **113** (90%, entry 5) was obtained.

Table 7: Results of the catalyst screening for the O–H insertion reaction. The solution of the diazo compound was added over 3 h *via* syringe pump. The isolated yields are relative to the diazo compound.


87, R^1 = OMe, R^2 = Me **86**, R^1 = OMe, R^2 = Me
104, R^1 = CO$_2$Me, R^2 = Et **113**, R^1 = CO$_2$Me, R^2 = Et

entry	substrate	catalyst (1 mol%)	yield (%)
1	87	[Cp*RhCl$_2$]$_2$	83
2 [121]	87	[Cp*RhI$_2$]$_2$	88
3	87	[Cp*IrCl$_2$]$_2$	74
4	87	[Cp*IrI$_2$]$_2$	76
5	104	[Cp*IrI$_2$]$_2$	90

The observed reactivity trends may be explained based on X-ray diffraction data previously obtained in the Fürstner group (*cf.* Section 3.1.3).[121,150] In the case of [Cp*RhCl$_2$]$_2$, it was not possible to isolate the corresponding carbene complex. Instead, a functionalized C-metalated rhodium enolate complex **89** was isolated (*cf.* Scheme 37). This was interpreted as a result of the electrophilicity of the transiently formed carbene, which then inserts into the Rh–Cl bond. Consequently, the so formed carbenoid carbon is not easily accessible for nucleophiles such as an olefinic double bond or a carbonyl oxygen, leading to low conversions in the catalytic reactions. On the contrary, this halide migration was not observed with the bromo and iodo derivatives and both can catalyze all the studied carbene transfer reactions.

The fact that the halide ligands on rhodium do not exert a difference in the O–H insertion reactions with MeOH, can be interpreted as a kinetic effect: the O–H insertion outcompetes migratory insertion. Alternatively, a different mechanism may be operative. In a stoichiometric NMR experiment, an excess of MeOH was added to preformed complex **89**, resulting in the formation of product **86**. This result shows that complex **89** may be considered to be a sufficiently reactive carbenoid species,[156] in which the carbon bound chloride functions as a leaving group. Substitution with MeOH generates the organic product **86** and re-forms the catalyst which again reacts with another equivalent of a diazo compound (Scheme 37).
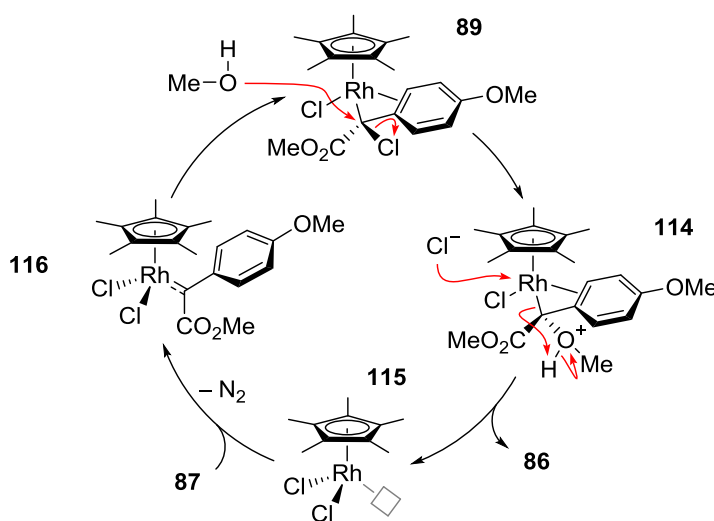
Scheme 37: Mechanistic proposal for the reaction of diazo compound **87** and MeOH catalyzed by [Cp*RhCl$_2$]$_2$. The grey square represents a vacant site on the metal center.

For [Cp*IrCl$_2$]$_2$ and [Cp*IrI$_2$]$_2$ the corresponding carbene complexes were isolated and no halide migration was observed.[150] Therefore, it is not surprising that both serve as good pre-catalysts in all of the reactions studied in this project.

3.2.3 Development of a Catalytic Metathesis of Azoarenes

3.2.3.1 Introduction

In 2015, two independent reports by the groups of Kim[127k] and Lee[157] were published in which cationic Cp*Rh(III) complexes catalyze the derivatization of azoarenes (Scheme 38). Analogously to the description in Section 3.1.2, the azo functionality served as the directing group for a selective *ortho*-functionalization *via* a proposed cyclometalated Rh(III) complex.
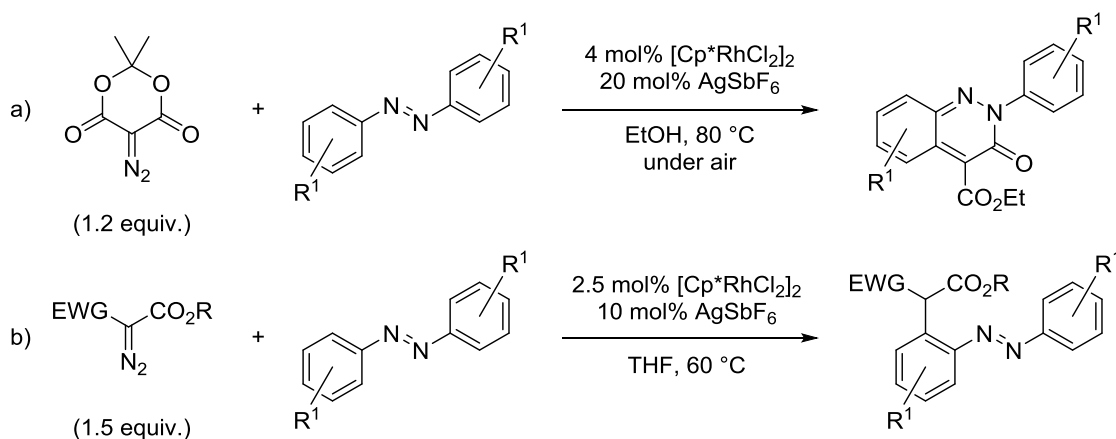
Scheme 38: Examples from the literature where azoarenes are functionalized with diazo compounds in the presence of a cationic Rh(III) complex: a) a methodology by Son *et al.* for the synthesis of cinnolin-3(2*H*)-one derivatives and b) a process developed by Sharma *et al.* to access *ortho*-functionalized azoarenes.

As shown previously, employing the neutral piano-stool Rh(III) complexes could prevent the C–H activation process and potentially lead to a different reaction outcome. Stoichiometric reactions between chromium and tungsten Fischer carbene complexes and azoarenes have precedence in the literature and support the feasibility of this approach.[158–164]

In a preliminary experiment, a CH₂Cl₂ solution of [Cp*RhI₂]₂ (1 mol%) and equimolar amounts of donor/acceptor diazo compound **87** and azobenzene ((*E*)-**117**) was stirred at room temperature overnight (Scheme 39). After workup and purification, α-imino ester **118** was isolated in 38% yield, exclusively as the *Z*-isomer.
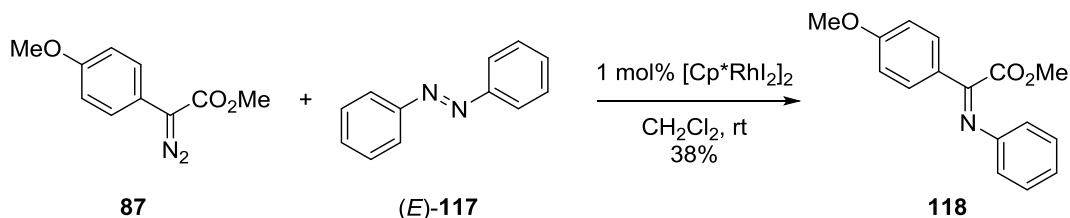
Scheme 39: The initial reaction between diazo compound **87** and azobenzene (**117**) resulted in the formation of α-imino ester **118**.

The structure of the product was assigned on the basis of NMR data, of which the imine carbon ¹³C{¹H} chemical shift is most informative (159.6 ppm). Crystals of **118** were obtained and the

structure in the solid state was in agreement with the NMR analysis (Figure 11). The C1–N1 distance (1.280(1) Å) is in excellent agreement with the X-ray data that can be obtained for C–N double bonds from the Cambridge Structural Database (average distance: 1.279(8) Å).[165]
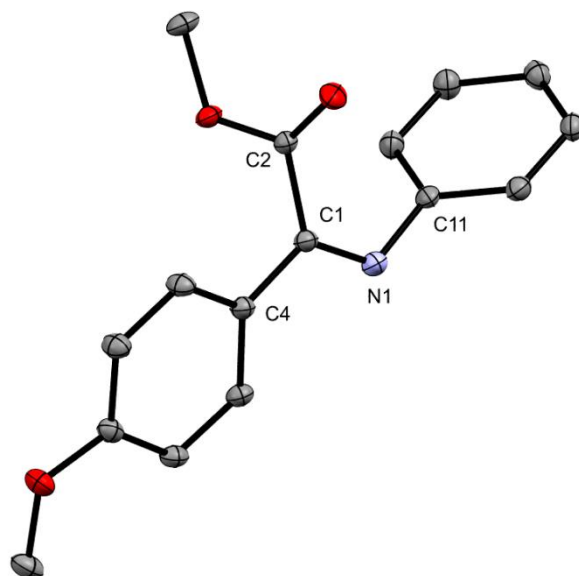
Figure 11: Molecular structure of α-imino ester **118** in the solid state with ellipsoids depicted at the 50% probability level. Hydrogen atoms are omitted for clarity. Selected distances (in Å): N1–C1 1.280(1), N1–C11 1.420(1), C1–C2 1.522(1), C1–C4 1.471(1).

This result confirms the hypothesis, that switching from a cationic Rh(III) catalyst to its neutral analogue gives rise to different reactivity. This reaction is the first catalytic synthesis of α-imino esters from diazo compounds and azoarenes. Although α-imino esters have been synthesized from diazo compounds and azides previously,[166,167] azoarenes offer several advantages over azides because they are stable, safe, and easy to synthesize with a range of functional groups.[168]
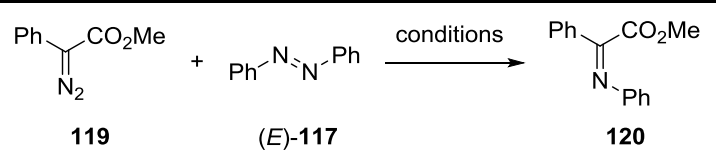
3.2.3.2   *Optimization and Scope*

With the preliminary result in hand, a model reaction was chosen for a series of optimization experiments (Table 8). Herein, diazo compound **87** was replaced by **119**, which was added *via* syringe pump over 5 h to the reaction mixture (entries 1–6). Conducting the reaction at room temperature resulted in a rather low yield (14%, entry 1). This result was improved when the reaction was run at elevated temperature (48%, entry 2). A brief screening of solvents showed that Lewis basic solvents had a negative effect on the reaction outcome (entries 3–4). Toluene gave the best yield of 63% (entry 6) which could be slightly increased by conducting the reaction under reflux conditions (up to 69% yield). Unfortunately, this result was irreproducible upon scale-up where only traces of the desired product formed (for example, on a 1 mmol scale, less than 5% of imine was detected). In light of the literature precedence for this type of transformation (*vide infra*), this observation led to the suggestion that light may play an

important role. The *Z*-isomer of azobenzene is the more nucleophilic and less sterically hindered isomer and therefore likely to be more reactive than the *E*-isomer. Because light facilitates the *E*→*Z* isomerization of azobenzene,[169] it was anticipated that irradiation with a light source should solve the irreproducibility upon scale-up. In accordance with the literature, blue LEDs ($\lambda \approx 470$ nm) were chosen to selectively excite one of the absorption bands that facilitate the *E*→*Z* isomerization.[170] The usage of white LEDs would excite several absorption bands which are responsible for the *E*→*Z* as well as the *Z*→*E* isomerization.[171]

Table 8: Optimization results of the catalytic metathesis of (*E*)-**117** (0.25 mmol, *c* = 0.08 M). The diazo compound **119** (2.8 equiv. relative to (*E*)-**117**) was added over 5 h (entries 1–6) or 2 h (entries 7–12) *via* syringe pump. [a] Irradiation was found to have negligible effects on the internal temperature of the reaction. [b] o: daylight; +: irradiation with light emitted by commercial blue LEDs; −: the reaction was carried out in the dark; [c] NMR yield. [d] Isolated yield.

entry	catalyst (1 mol%)	solvent	*T* (°C)[a]	LED[b]	yield (%)[c]
1	[Cp*RhI₂]₂	CH₂Cl₂	rt	o	14
2	[Cp*RhI₂]₂	DCE	80	o	48
3	[Cp*RhI₂]₂	MeCN	80	o	14
4	[Cp*RhI₂]₂	THF	80	o	traces
5	[Cp*RhI₂]₂	*n*-hexane	80	o	24
6	[Cp*RhI₂]₂	toluene	80	o	63
7	[Cp*RhI₂]₂	toluene	rt	+	98 (91[d])
8	[Cp*RhI₂]₂	toluene	rt	−	8
9	—	toluene	rt	+	0
10	[Cp*RhBr₂]₂	toluene	rt	+	98
11	[Cp*RhCl₂]₂	toluene	rt	+	13
12	Rh₂(OAc)₄	toluene	rt	+	72
13	[Cp*IrI₂]₂	toluene	rt	+	96
14	[Cp*IrCl₂]₂	toluene	rt	+	93

This assumption turned out to be correct. When the reaction mixture was irradiated with commercial blue LEDs, a 91% yield of isolated product was obtained (*cf.* Figure S1 and Figure S2 in the appendix for the experimental set-up).[172] Furthermore, this modification allowed to conduct the reaction at room temperature and the addition time of the diazo compound could be reduced to 2 h without loss to selectivity (entry 7). The excellent yield was well reproducible on a 1 mmol scale (*cf.* Scheme 40). Control experiments showed that both light and the catalyst are essential for this transformation (entries 8 and 9). With respect to the reactivity trends of the

piano-stool Rh(III) complexes discussed in Section 3.2.2, it was not surprising that [Cp*RhBr$_2$]$_2$ performed equally as well as [Cp*RhI$_2$]$_2$ (98%, entry 10), whereas [Cp*RhCl$_2$]$_2$ only gave a low conversion to the imine product (13%, entry 11). For comparison, Rh$_2$(OAc)$_4$, [Cp*IrI$_2$]$_2$, and [Cp*IrCl$_2$]$_2$ were also tested and did catalyze this reaction, although with a slightly lower yield (72%, 96%, and 93%, respectively, entries 12–14).

Next, the scope of this transformation was examined under the optimized reaction conditions. Firstly, different azoarenes were employed to probe steric and electronic parameters (Scheme 40). The presence of electron donating or electron withdrawing groups has only a minor influence on the reaction (**120–125**: 77%–97%), although it is necessary to heat the reaction mixture if the azoarene bears an electron withdrawing substituent in the *para*-position (**124**: 84% and **125**: 89%). This is attributed to the lower nucleophilicity of the azo functionality. In contrast, *meta*-substituted azoarenes do not show this influence and perform very well (**126**: 99%, **127**: 86%, and **128**: 95%). The reaction is sensitive to substitution in the *ortho*-positions of the azoarenes. A single *ortho*-methyl substituent is tolerated (**129**: 85%), whereas 2,2',6,6'-tetramethylazobenzene is unreactive (**130**: 0%). The proximity of steric bulk to the azo bridge might disfavor *E→Z*-isomerization as well as the approach of the electrophile to the nitrogen atoms. The high yielding, one step synthesis of α-imino ester **131** (83%) exemplifies the utility of the developed method since such substrates with carbonyl groups cannot be synthesized by classical methods (*i.e.*, a condensation reaction of an α-keto ester and an aniline derivative). The azo metathesis also tolerates internal alkynes (**132**: 65%).[173] In addition, a substrate with an azide group afforded imine **133** in 71% isolated yield—highlighting the different reactivity profile of [Cp*RhI$_2$]$_2$ compared to dimeric Rh(II) complexes.[174] Doyle and co-workers reported that Rh$_2$(OAc)$_4$ catalyzes the reaction between α-diazo esters and aromatic azides to give α-imino esters.[167]

Secondly, the influence of different diazo derivatives on the reaction outcome was investigated (Scheme 41). Diazo compound **87** reacted smoothly with azobenzene and its *para*-methoxy and *para*-ester derivatives to give imines **118**, **134**, and **135**, respectively (65%–97%). When the *para*-methoxy substituent on the diazo compound was replaced by an ester group, the metathesis afforded imines **136** and **137** in good isolated yields (90% and 66%, respectively). Imine **138** was unstable on silica upon purification and therefore isolated in lower yield (38%). Donor/donor diazo compounds were also employed in this transformation. The reaction of 9-diazo-9*H*-fluorene with azobenzene afforded imine **139** in 53% isolated yield under the standard conditions. Extending the addition time of the diazo compound to 5 h resulted in a slightly improved yield (67%). The rationale for this is that the corresponding donor/donor carbene complex is expected to be less electrophilic at the carbene carbon and, hence, a

nucleophilic attack of the azoarene is less favored. Diazomalonate derivatives do not undergo a reaction with the catalyst and, therefore, cannot be used to synthesize imines such as **140**.

120 91% (R = H) [84%[a]]
121 97% (R = Me)
122 77% (R = OMe) [76%[a]]
123 91% (R = F)
124 84% (R = CF$_3$)[b] [54%[a]]
125 89% (R = CO$_2$C$_8$H$_{17}$)[b]

126 99% (R = OMe)
127 86% (R = CO$_2$C$_8$H$_{17}$)

128 95%

129 85%

130 0%

131 83%[b]

132 65%

133 71%
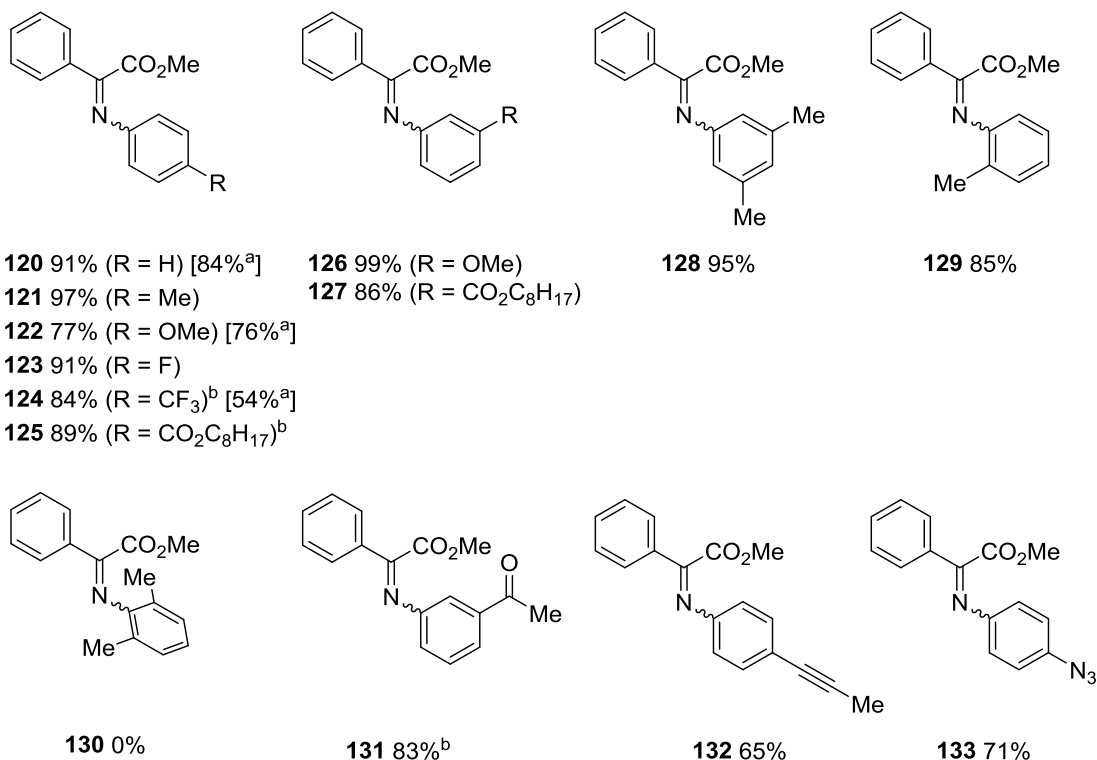
Scheme 40: Scope of azoarenes in the Rh(III)-catalyzed metathesis between diazo compound **119** and azoarenes with isolated yields. Reaction conditions: azoarene (0.25 mmol), [Cp*RhI$_2$]$_2$ (1 mol%), toluene (c = 0.08 M), rt, irradiation with blue LEDs. The solution of the diazo compound **119** (2.3–2.8 equiv. relative to the azoarene) was added over 2 h *via* syringe pump. [a] 1 mmol of azoarene and addition of the diazo compound **119** (2.3 equiv. relative to the azoarene) over 3 h *via* syringe pump. [b] At 90 °C.

118 97% (R = H)
134 69% (R = OMe)
135 65% (R = CO$_2$C$_8$H$_{17}$)[a]

136 90% (R = H)
137 66% (R = OMe)
138 50% (R = CO$_2$C$_8$H$_{17}$)[a,b]

139 53%

140 0%
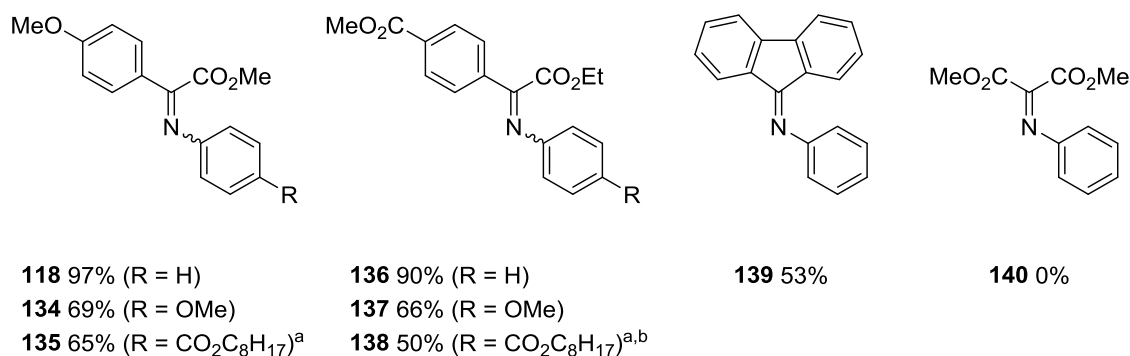
Scheme 41: Scope of diazo compounds in the Rh(III)-catalyzed metathesis between diazo compounds and azoarenes with isolated yields. Reaction conditions: azoarene (0.25 mmol), [Cp*RhI$_2$]$_2$ (1 mol%), toluene (c = 0.08 M), rt, irradiation with blue LEDs. The solution of the diazo compound (2.3–2.8 equiv. relative to the azoarene) was added over 2 h *via* syringe pump. [a] At 90 °C. [b] Conversion as determined by NMR, the product turned out to be unstable under the purification conditions.

3.2.3.3 Mechanistic Studies

In 1984, Hegedus and Kramer reported the photolytic stoichiometric reaction of chromium carbene complex **141** with (*E*)-**117** (Scheme 42).[158] Whilst the main product of the reaction, imino ether **143**, was isolated in 65% yield, small amounts of diazetodinones **144** and **145** were also isolated as a 1:1 mixture (10% yield). A detailed study suggested a [2+2]/retro-[2+2] mechanism in analogy to olefin metathesis,[159] in which the formation of **144** and **145** can be understood by migratory insertion of one of the CO ligands into the metallacycle intermediate **142**. In addition, a metal nitrene (**146**) was proposed to be formed during the reaction on account of aniline being detected in the reaction mixture after an acidic work-up.
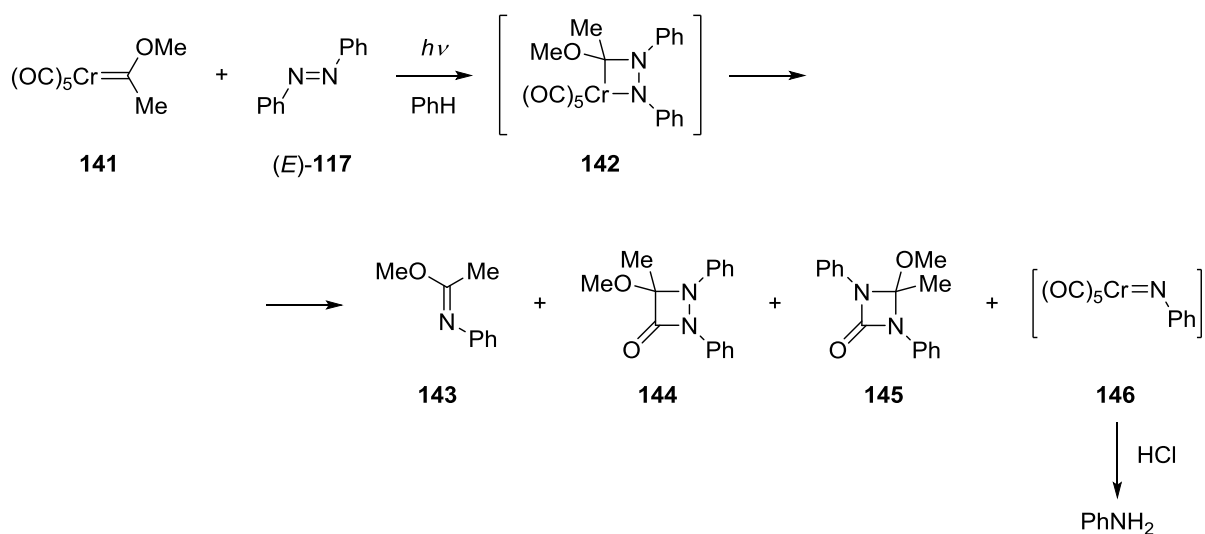
Scheme 42: Summary of the work done by Hegedus and co-workers on the photolytic stoichiometric reaction of chromium carbene complex **141** with (*E*)-**117**.
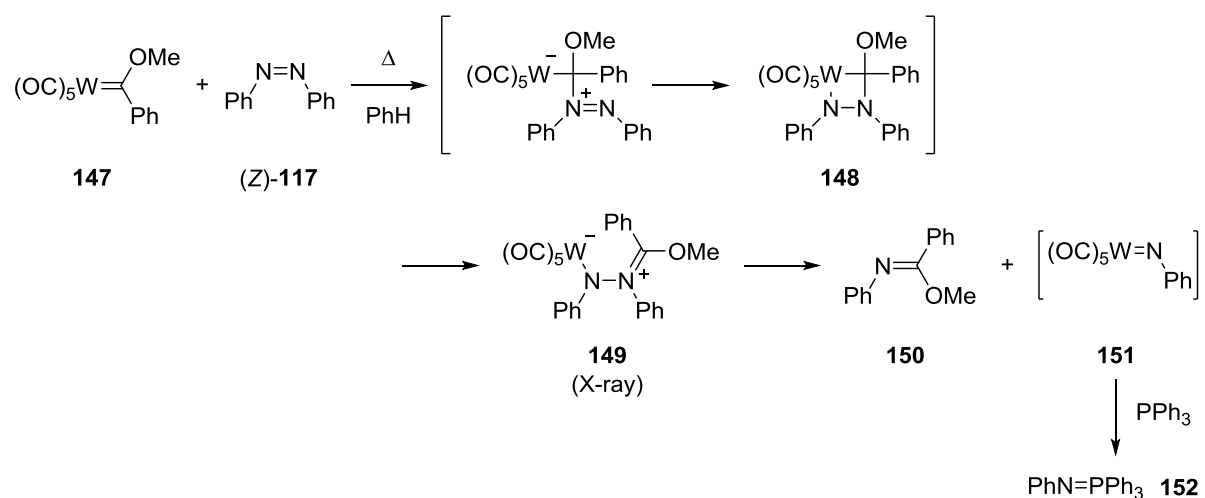
Scheme 43: Summary of the work done by McElwee-White and co-workers on the metathesis of (*Z*)-**117** and tungsten Fischer carbene complex **147**.

In 1988, McElwee-White and her group published a similar transformation between tungsten carbene complex **147** and (*Z*)-**117**, also leading to the formation of an imino ether product (**150**, Scheme 43).[160] In analogy to Hegedus' report, they were able to trap the proposed nitrene intermediate **151** with PPh$_3$.[161] In addition, zwitterionic intermediate **149** was characterized by X-ray.[163]

In light of these reports, the initial mechanistic investigations addressed the question of whether a nitrene intermediate is involved. Firstly, it is important to note that in contrast to the reports by groups of Hegedus and McElwee-White, no side products from nitrene intermediates (*i.e.*, aniline derivatives) were observed during the entire study.

When the unsymmetrically substituted azoarene **153** was used as a substrate in the metathesis reaction, the only products arising from **153** were imines **121** and **124**, which were obtained in a ≈ 1:1 ratio (Scheme 44), showing that both halves of the azoarene are incorporated into the imine products.
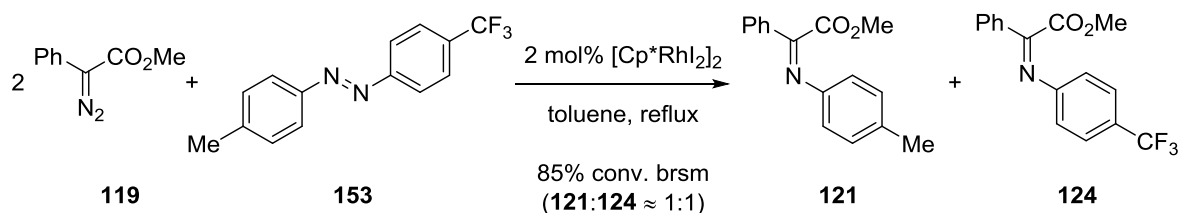
Scheme 44: Metathesis reaction of an unsymmetrically substituted azoarene (**153**). The solution of the diazo compound was added over 5 h *via* syringe pump.

Next, in a cross-over experiment, equimolar amounts of azoarenes **154** and **155** were subjected to a substoichiometric amount of diazo compound **119** under the standard conditions (Scheme 45). Due to the resulting incomplete conversion of the azoarenes, recombination of potential nitrene intermediates could result in formation of the unsymmetrically substituted azoarene **156**. However azoarene **156** was not detected by GC-MS or by NMR spectroscopy.

Lastly, an attempt to trap a potential nitrene intermediate formed from azobenzene under the standard conditions with PPh$_3$ did not furnish any traces of **152**.
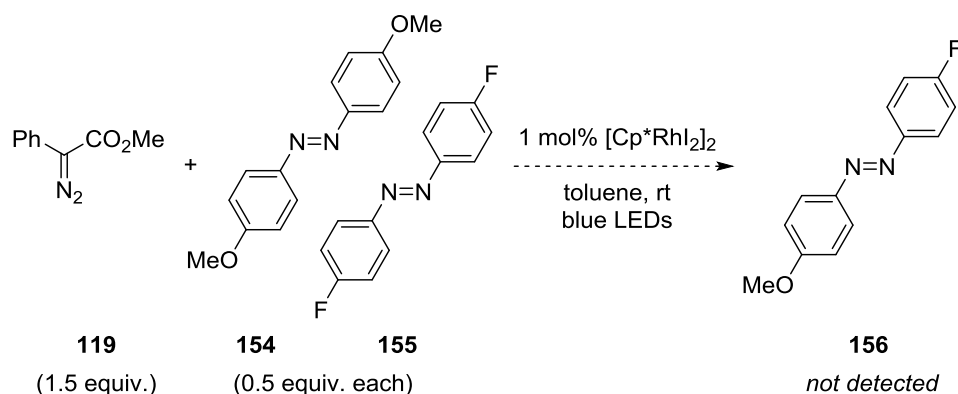
Scheme 45: Metathesis reaction of equimolar quantities of azoarenes **154** and **155** and substoichiometric amounts of diazo compound **119**. The solution of the diazo compound was added over 2 h *via* syringe pump.

These experiments provide compelling evidence that nitrene intermediates are not involved in this metathesis reaction. A different mechanism to those proposed for the stoichiometric reactions must be operative. Therefore, stoichiometric NMR experiments were conducted to detect any observable intermediates.

The first step of this transformation was proposed to be the formation of carbene complex **95**. This complex has previously been synthesized in the Fürstner group (*cf.* Section 3.1.3) and, hence, offers the possibility to study its reaction with azoarenes. In a first NMR experiment (Figure 12), 1 equiv. of **95** was generated by reaction of [Cp*RhI₂]₂ with diazo compound **87** in CD₂Cl₂ whilst cooling the sample in an ice bath. The solution of complex **95** was then cooled to −78 °C and 1 equiv. of solid (*Z*)-**116**[175] was added. The mixture was transferred into an NMR tube and inserted into the NMR spectrometer at −50 °C. At the starting point of the measurement, an ill-defined mixture was observed (*t* = 0 h, Figure 12-A). Warming this mixture to −40 °C over 45 min resulted in the slow appearance of a new set of signals (red, Figure 12-B) that were assigned to diaziridine **157**. After 3 h at −40 °C, the formation of **157** was complete (Figure 12-C). Diaziridine **157** was stable at this temperature overnight (Figure 12-D, *t* = 15 h), allowing for full collection of NMR data. Warming the sample to 25 °C resulted in the disappearance of the signals corresponding to **157** and the appearance of two sets of signals that matched an isolated sample of imine **118** (green) and (*E*)-**117** (blue, Figure 12-E). After full conversion was reached, their ratio was ≈ 2.9:1 (Figure 12-F) at 25 °C.
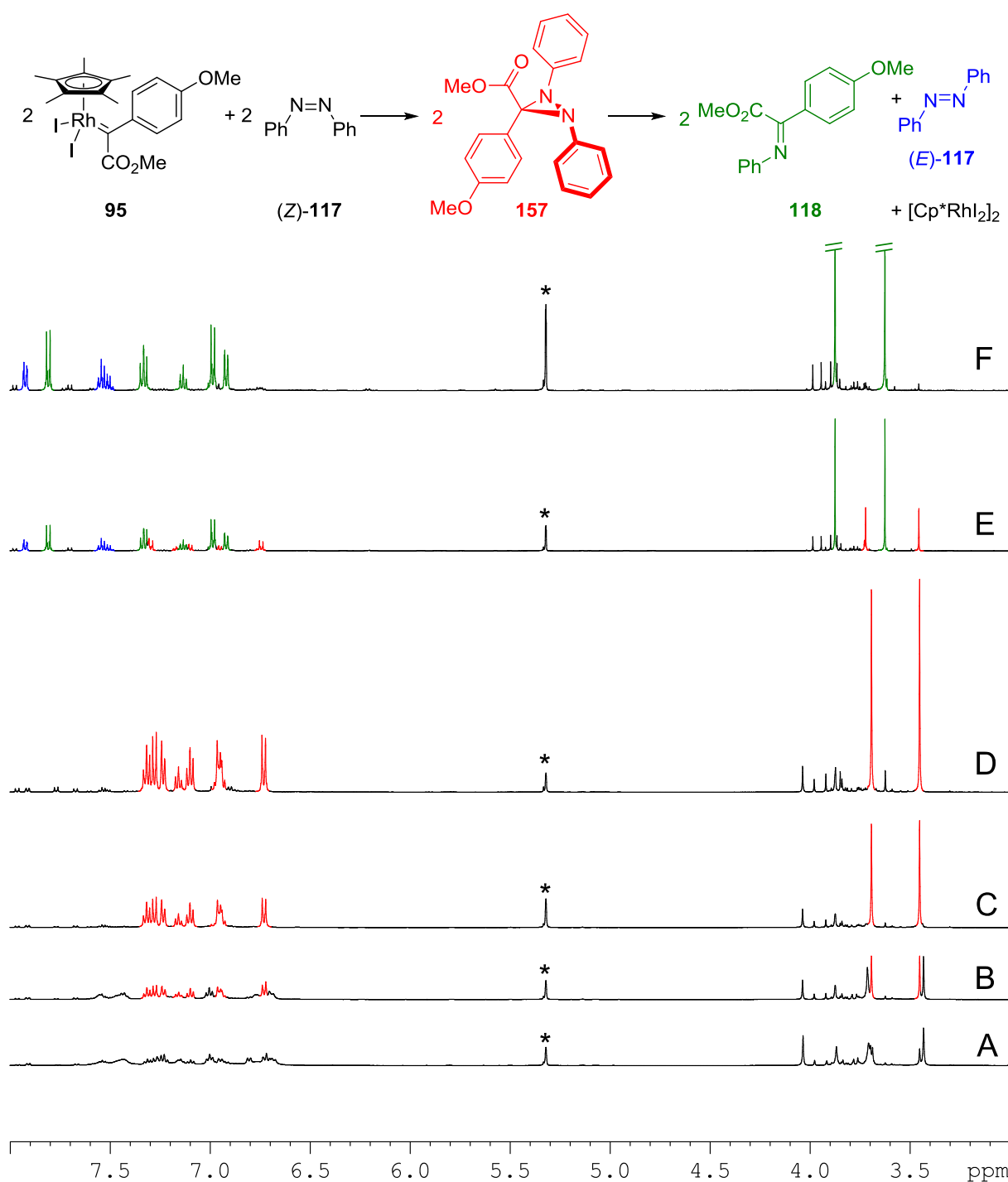
Figure 12: ^{1}H NMR spectra (500 MHz, CD$_2$Cl$_2$) of the stoichiometric (1:1) reaction of carbene complex **95** and (Z)-**117** recorded at different temperatures. For an explanation see text (* = residual CDHCl$_2$ in CD$_2$Cl$_2$). The color coding refers to the structures in the equation at the top of the figure.

The structure of **157** (red, Figure 12) was assigned on the basis of the collected NMR data: a characteristic resonance of a quaternary carbon was detected at 74.3 ppm (*cf.* Figure S3-A in the appendix for the supplementary ^{13}C{^{1}H} NMR spectrum). By ^{1}H/^{15}N HMBC NMR spectroscopy, two ^{15}N resonances were observed (−252.2 and −263.2 ppm) with very different chemical shifts

from the ones reported for the zwitterionic intermediate **149** by the McElwee-White group (δ_C = 172.0 ppm, δ_{N1} = −160.5 ppm, δ_{N2} = −248.7 ppm).[162] The absence of a Cp*Rh motif in this intermediate was established due to no scalar coupling to the rhodium metal in all spectra. The observation of two ^{15}N resonances support a *trans*-orientation of the two phenyl rings in which both nitrogen atoms are diastereotopic. This assignment is also supported by ^{1}H/^{1}H NOESY NMR experiments (Scheme 46).
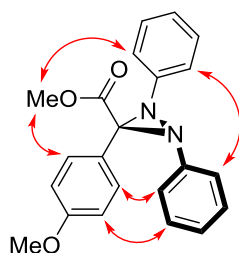
157

Scheme 46: Contacts observed by ^{1}H/^{1}H NOESY NMR spectroscopy in diaziridine **157**.

A second NMR experiment was then conducted in analogy to the previously described experiment (Figure 13): herein, 1 equiv. of solid (*Z*)-**117** were added to a solution of 2 equiv. of preformed **95** in CD$_2$Cl$_2$ whilst cooling in a dry ice bath. Again, an ill-defined mixture was observed in the NMR spectra at the starting point of the experiment (−50 °C). Warming up this mixture to −40 °C resulted in the slow appearance of the set of signals corresponding to diaziridine intermediate **157**(red). At the same time, resonances of complex **95** (dark yellow) were still present in a 1:1 ratio with **157**. Increasing the temperature to ≈ −25 °C resulted in the disappearance of the signals of **95** and **157**, while a single set of resonances assigned to imine **118** (green) appeared. This process was completed at about +15 °C. Only trace amounts of (*E*)-**117** were observed during the entire experiment.
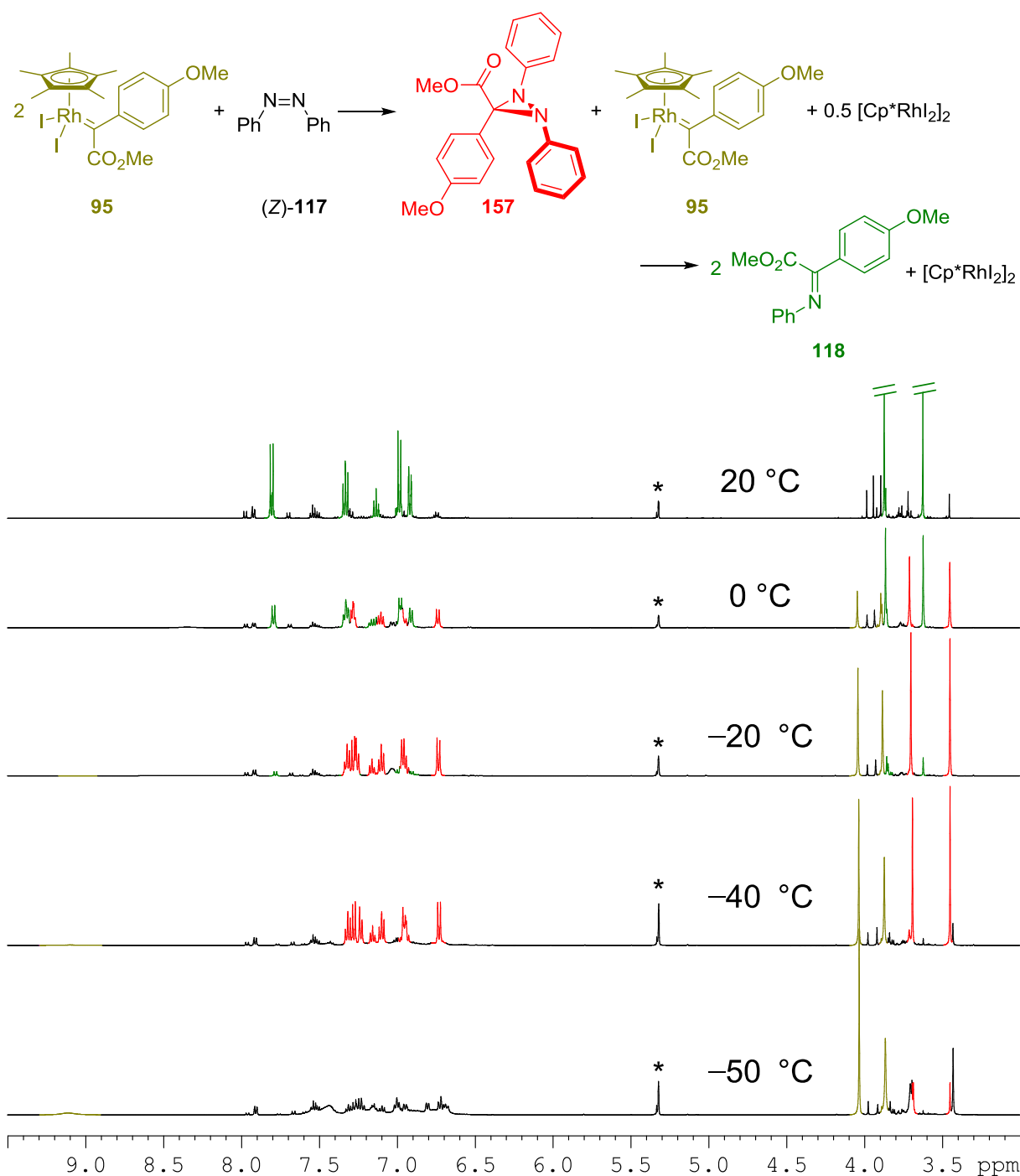
Figure 13: ^{1}H NMR spectra (500 MHz, CD$_2$Cl$_2$) of the stoichiometric (2:1) reaction of carbene complex **95** and (Z)-**117** at different temperatures. For an explanation see text (* = residual CDHCl$_2$ in CD$_2$Cl$_2$). The color coding refers to the structures in the equation at the top of the figure.

The NMR data gave rise to knowledge about the stability of **157** and allowed crystals suitable for X-ray diffraction analysis to be obtained. The X-ray data is in agreement with the NMR analysis (Figure 14) and shows that the *trans*-orientation of the two phenyl rings is retained in the solid state structure. Diaziridine **157** possesses an almost isosceles triangular core, in which the N1–N2 distance (1.481(2) Å) is only slightly longer than the C1–N1 (1.459(2) Å) and C1–N2

(1.463(3) Å) distances and all three angles are approximately 60° (N1–C1–N2 60.9(1)°, C1–N1–N2 59.7(1)°, C1–N2–N1 59.4(1)°).
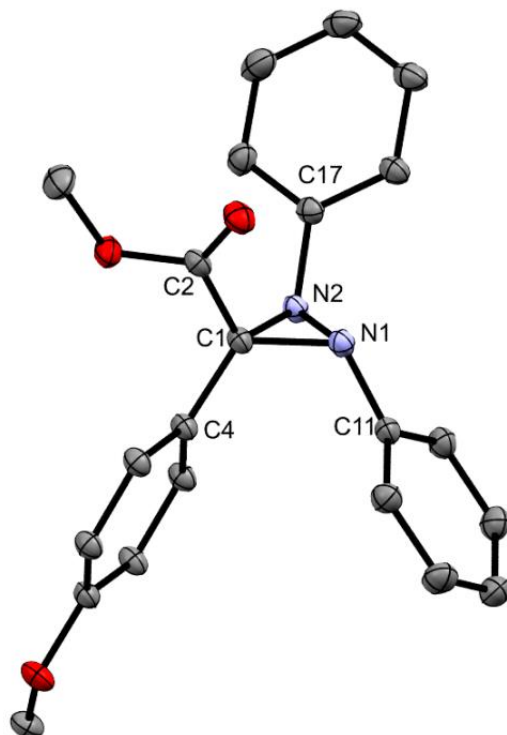
Figure 14: Molecular structure of diaziridine **157** in the solid state with ellipsoids depicted at the 50% probability level. Hydrogen atoms are omitted for clarity. Selected distances (in Å): C1–N1 1.459(2), C1–N2 1.463(2), N1–N2 1.481(2), C1–C2 1.519(2), C1–C4 1.484(2), N1–C11 1.431(2), N2–C17 1.430(2). Selected angles (in °): N1–C1–N2 60.9(1), C1–N1–N2 59.7(1), C1–N2–N1 59.4(1), C2–C1–C4 116.9(1). Selected torsion angles (in °): C11–N1–N2–C17 137.2(1), C11–N1–C1–C2 152.5(1), C11–N1–C1–C4 7.3(2), C17–N2–C1–C2 3.1(2), C17–N2–C1–C4 148.5(1).

3.2.3.4   The Proposed Catalytic Cycle

On the basis of this mechanistic investigation, a mechanism is proposed (Scheme 47).
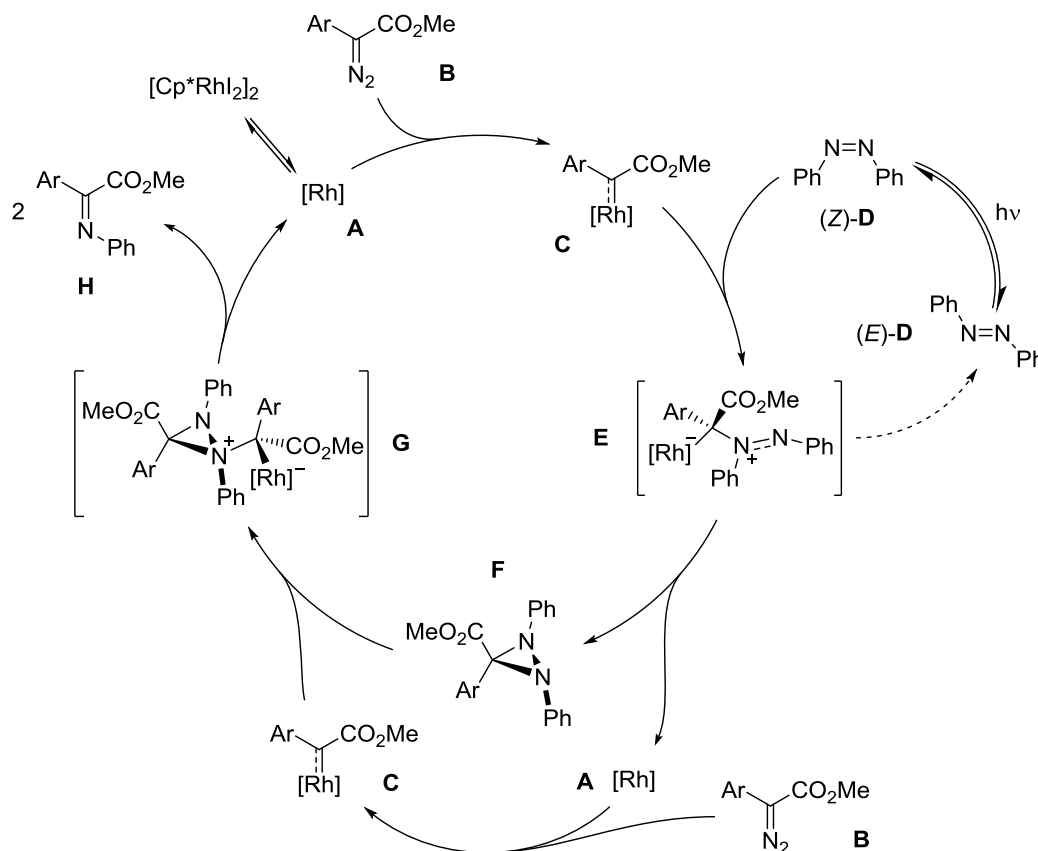
Scheme 47: Proposed catalytic cycle for the Rh(III)-catalyzed metathesis between diazo compounds and azobenzene ([Rh] = Cp*RhI$_2$).

The dimeric pre-catalyst [Cp*RhI$_2$]$_2$ first dissociates to give the active catalyst Cp*RhI$_2$ (**A**), which possesses an available coordination site on rhodium. Reaction with diazo compound **B** forms rhodium carbene complex **C**. The electrophilic carbene carbon is then attacked by one of the nitrogen atoms of (*Z*)-azobenzene ((*Z*)-**D**), which is formed from its *E*-isomer ((*E*)-**D**) under the irradiation with blue LEDs. The nucleophilic attack results in aza-ylide **E**, which undergoes ring closure to furnish the metal free diaziridine intermediate **F**. The weakened N–N bond in **E** can rotate, such that the phenyl groups adopt the observed *trans*-orientation on the three-membered ring. In addition to undergoing cyclization, ylide **E** may also dissociate to give carbene complex **C** and (*E*)-azobenzene ((*E*)-**D**). The latter isomerizes again to (*Z*)-**D** and re-enters the catalytic cycle.

The transient diaziridine **F** undergoes a nucleophilic attack onto another carbene complex **C**, which results in the formation of species **G**. If 1 equiv. of **G** breaks down, presumably *via* a cheletropic process, 2 equiv. of the product, α-imino ester **H**, are released together with catalyst **A**. The sequence **C**+**F** → **G** → **A**+**H** is supported by work of Komatsu and co-workers, who have

shown that diaziridines are nucleophilic enough to attack electrophilic species, such as ketenes, and subsequently undergo ring opening.[176]

The first stoichiometric NMR experiment (*cf.* Figure 12), however, supports a second mechanism for the formation of **H**. There, it was observed that warming 1 equiv. of diaziridine **157** results in the formation of 1 equiv. of imine **118** and 0.5 equiv. of (*E*)-**117**. Therefore, another pathway can be envisioned, in which **F** breaks down thermally to release 1 equiv. of **H** and 0.5 equiv. of (*E*)-**D** which may then re-enter the catalytic cycle (*E*)-**D** → (*Z*)-**D** → **E** → **F**. Because no nitrene intermediates were detected, the thermal breakdown of **F** presumably occurs in a bimolecular fashion. The available data show that both nucleophilic and thermal decomposition of **F** are possible, but further detailed studies are needed to clarify which mechanism operates under the conditions of catalysis.

3.2.4 Miscellaneous Reactions

3.2.4.1 *Metathesis of Other Substrates*

The metathesis methodology developed in Section 3.2.3 has so far been restricted to substrates with an azo motif. It is important to highlight that this reaction forms a diaziridine intermediate *via* a formal [2+1] cycloaddition in analogy to cyclopropanation or oxirane formation. Because the diaziridine is thermally unstable and/or the nitrogen atoms are nucleophilic enough, a further reaction is possible. Therefore, the question arises as to whether other substrates could undergo a similar process.

Four alternative substrates to azoarenes were considered. Imines have been shown to undergo metathesis mediated by imido complexes of zirconium and molybdenum.[177] Therefore, *N*-benzylideneaniline (**158**) was employed as a substrate (Scheme 48), resulting in the formation of a single diastereomer of aziridine **159** which was isolated in 68% yield. Unfortunately, the relative configuration of **159** could not be unambiguously determined by ^{1}H/^{1}H NOESY NMR experiments. But, in analogy to observations made during the oxirane syntheses (Section 3.2.2) and by Doyle *et al.*[152], the relative configuration of **159** is proposed to be as it is shown in Scheme 48. As is evident from the reaction outcome, the aziridine's nitrogen atom is not nucleophilic enough to attack another Rh(III) carbene complex or the aziridine ring is too stable to undergo thermal decomposition.

Scheme 48: Rh(III)-catalyzed aziridine formation from imine **158**. The solution of the diazo compound was added over 1 h *via* syringe pump.

The second substrate class considered was that of aromatic nitroso compounds, which have been shown to undergo a stoichiometric metathesis with Fischer carbene complexes and also with a zirconium imido complex.[178,164] The reaction of diazo compound **119** (2.2 equiv.) and nitrosobenzene (**160**) led to a complex mixture, from which four compounds were isolated (Scheme 49). The metathesis products, α-imino ester **120** and α-oxo ester **161**, were obtained in 33% and 68% isolated yield, respectively. Initially, equimolar amounts of both products were expected to be formed. The fact that a third product, (E)-**117**, is also formed resolves this puzzling observation. Two pathways for the formation of this product are envisioned: in the first scenario, intermediate (metal) nitrenes would dimerize to (E)-**117**. In the second scenario, stepwise deoxygenation of a nitroso dimer (*i.e.*, azodioxybenzene)[179] would lead ultimately to (E)-**117**, which then undergoes the azo metathesis described earlier. Such a deoxygenation process with diazo compounds has been reported for *N*-oxides[180] as well as DMSO.[181]

The fourth product isolated from this reaction was benzoylcarbamate derivative **162** (18%). Its formation can be rationalized by a two-step process that gives an oxaziridine intermediate in analogy to the diaziridine of the azo metathesis. Instead of attacking a second carbene complex, the oxaziridine undergoes a rearrangement to **162**.[182] A detailed study would be necessary to gain further insight into this transformation and increase its product selectivity, but this preliminary result shows that nitroso compounds are suitable substrates in the developed metathesis protocol and worthy a further study. A subsequent replacement of **160** by nitro benzene did not furnish any traces of potential metathesis products.

Scheme 49: Rh(III)-catalyzed reaction between diazo compound **119** and nitrosobenzene (**160**). The solution of the diazo compound was added over 2 h *via* syringe pump. The isolated yields are relative to **160**.

Lastly, carbodiimides were also considered to be potential substrates. Therefore, di-*p*-tolylcarbodiimide was subjected to the standard metathesis conditions. Although traces of possible metathesis products were detected by GC-MS (≈ 10% of **121**), the mixture was too complex to be purified and no further experiments were conducted.

3.2.4.2 Ring Expansion Reactions of the Diaziridine Intermediate

Diaziridines have been used frequently as substrates for dipolar cycloaddition and ring expansion reactions.[183] Knowing that a diaziridine is formed as an intermediate during the azo metathesis, it was postulated that one could alter its fate by interception with an appropriate substrate *via* a ring expansion reaction (Scheme 50).
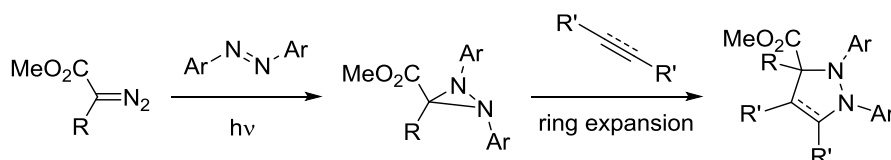
Scheme 50: Envisioned reaction sequence of intercepting the diaziridine intermediate with an appropriate partner.

Conducting the standard metathesis protocol in the presence of aromatic and aliphatic aldehydes, ketones, or electron poor alkynes gave only the imine products, and no incorporation of these reaction partners was observed.

Therefore, it was proposed that introducing unsaturation into one of the starting materials could allow the ring expansion to occur more easily in an intramolecular fashion. The β,γ-unsaturated α-diazo ester **163** was freshly prepared[184] and subjected to the metathesis conditions. Unfortunately, no diazo decomposition was observed. Rhodium acetate is known to decompose **163** and was therefore used to replace [Cp*RhI$_2$]$_2$ as a catalyst. The products formed in this reaction are shown in Scheme 51. No imine formation was observed; instead, dihydropyrazole **164** was isolated in 38% yield, when 1.0 equiv. of diazo compound **163** was used. When 2.3 equiv. of **163** were used, **164** and bicyclic product **165** were isolated in 29% and 20% yield, respectively.
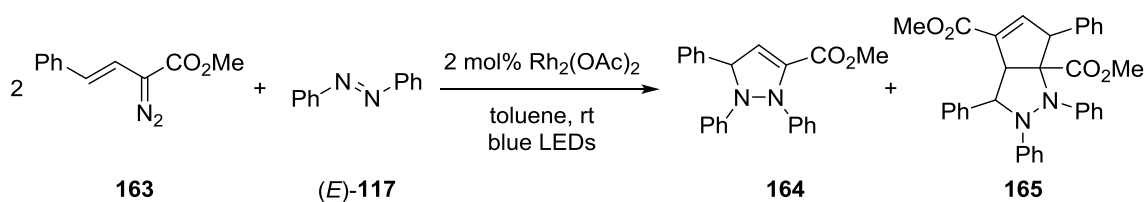

Scheme 51: Rh(II)-catalyzed metathesis reaction between a β,γ-unsaturated α-diazo ester (**163**) and (*E*)-**117**. The solution of the diazo compound was added over 2 h *via* syringe pump. For yields, see text.

The structure of **165** was assigned by single crystal X-ray diffraction analysis (Figure 15). It features a 1,2,3,3a,6,6a-hexahydrocyclopenta[*c*]pyrazole core containing one azobenzene fragment and two carbene fragments. A reasonable proposal for its formation involves cyclopropanation of the double bond of dihydropyrazole **164**, forming 2,3-diazabi-cyclo[3.1.0]hexane **167**, followed by vinylcyclopropane-cyclopentene rearrangement[185] of **167** to give bicycle **165** (Scheme 52). An excess of diazo compound **163**, with respect to (*E*)-**117**, is

required to form **165** because only after (*E*)-**117** has been consumed the less nucleophilic C–C double bond of dihydropyrazole **164** can engage in cyclopropanation.
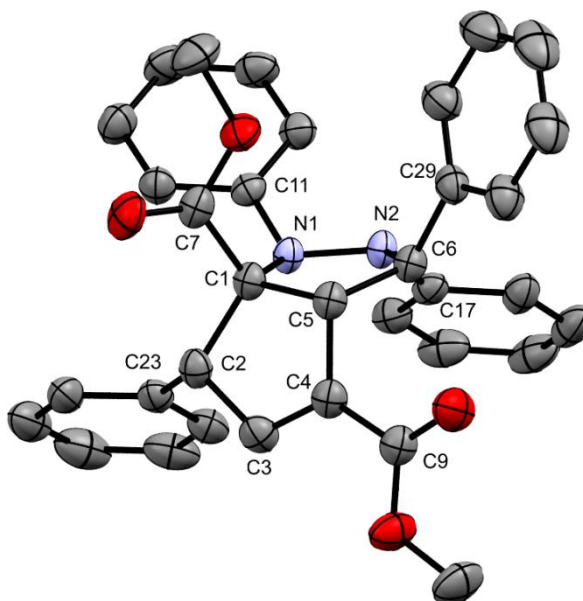
Figure 15: Molecular structure of **165** in the solid state with ellipsoids depicted at the 50% probability level. Hydrogen atoms are omitted for clarity. Selected distances (in Å): N1–N2 1.440(1), C1–N1 1.474(2), C1–C2 1.575(2), C2–C3 1.497(2), C3–C4 1.324(2), C4–C5 1.509(2), C5–C1 1.566(2), C5–C6 1.538(2), C6–N2 1.463(2).
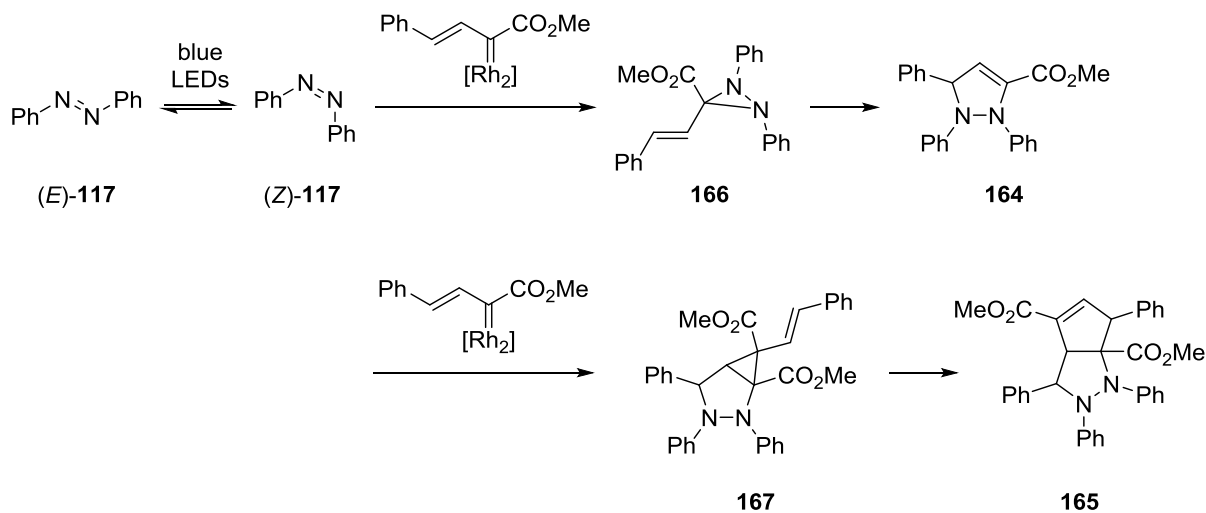
Scheme 52: Proposed sequence for the formation of **165**. [Rh$_2$] = Rh$_2$(OAc)$_4$.

This novel ring-expansion cascade process demonstrates the potential of such types of three-component cycloaddition reactions to build complex structures from simpler starting materials.[186]

3.3   Conclusions and Outlook

A detailed stoichiometric study on the Rh(III)-mediated C–H functionalization of arenes bearing a directing group was conducted for the first time. The experiments provide one of the first examples of a donor/donor diazo compound (**100**) being employed in this type of transformation, in which acceptor/acceptor diazo compounds are commonly used.[187] The study showed that a labile ligand is required to open up a free coordination site on rhodium, allowing reaction of the complex with the diazo compound. It was also found that upon halide abstraction with silver, NMR silent impurities inhibited the reaction, even though a free coordination site was available. Without these impurities, the reaction afforded, at low temperature, a mixture of two isomeric complexes. Complex **101** is the product of migratory insertion of the carbene into the Rh–C_{aryl} bond of **99** (Scheme 53). Two reaction pathways are possible: in scenario one, coordination of the diazo compound affords carbenoid complex **168** that undergoes a 1,2-aryl shift resulting in the formation of **101**. In the second scenario, **168** releases N_2 to generate a carbene complex **169** which then undergoes migratory insertion to afford **101**. At the present stage neither can be ruled out and future studies should focus on the modification of the cyclometalating ligand to slow down the reaction from **99** to **101** and stabilize the intermediates (for example, introducing a sterically demanding substituent in *ortho*-position to the Rh–C bond of **99** could prevent the migratory insertion).
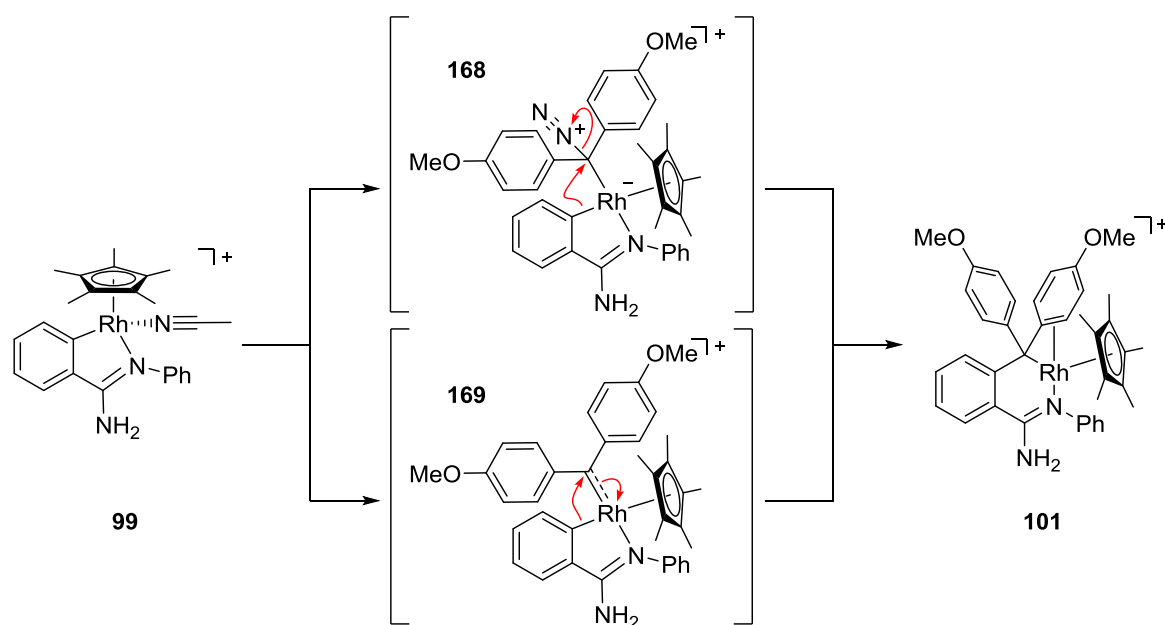
Scheme 53: Two possible mechanistic scenarios for the formation of **101** from **99**. The anion is SbF_6^- is not drawn.

Combined catalytic and crystallographic studies have shed light on the crucial role played by the anionic ligands in determining the reactivity of neutral piano-stool Rh(III) carbene complexes derived from pre-catalysts of the type [Cp*RhX$_2$]$_2$. For X = Cl, the carbene complex undergoes

facile migratory insertion to a carbenoid species **89** that cannot participate in most carbene transfer reactions. For X = I, the carbene complex **95** is stable enough to engage with a variety of nucleophiles. In the case of the analogous Ir(III) complexes, migratory insertion is not observed and they serve as good pre-catalysts. Theoretical calculations are necessary to fully rationalize why halide migration is only observed in the case of [Cp*RhCl$_2$]$_2$ and, furthermore, correlate catalytic reactivity with the ligands and the metal centers. These investigations provide much needed mechanistic insight and will likely accelerate the development of Rh(III) and Ir(III) catalysts in carbene transfer reactions.

Section 3.2.3 discussed the development of a Rh(III)-catalyzed metathesis of azoarenes and diazo compounds, which was based on the idea of switching from the usually employed cationic piano-stool Rh(III) complexes to their neutral analogs. Under irradiation with blue LEDs the reaction affords α-imino esters in a mild manner and represents a new type of reaction for donor/acceptor carbenes. The stoichiometric cleavage of N−N double bonds by transition metal complexes has been studied extensively because they are of interest in understanding the mechanisms of dinitrogen fixation.[188] On the other hand, well-defined N−N double bond cleavage reactions of azoarenes have only been occasionally reported to be followed by a C−N (double) bond forming process.[189] In contrast to azides for example, a major advantage of this methodology is the use of azoarenes as a stable, safe, and easy to synthesize starting material.[168] The method complements the existing methods to access synthetically versatile α-imino esters (*e.g.*, condensation reactions, Staudinger ligation, etc.) and allows access to compounds that would be difficult to synthesize otherwise.[190] In addition, products can be isolated in excellent yields on large scale and experimental set-ups, such as for flow chemistry, could allow for even higher material throughput.[191]

Lastly, additional experiments revealed that substrates other than azoarenes (*i.e.*, nitrosobenzene and a carbodiimide) also undergo the metathesis reaction with rhodium carbenes and that it is even possible to intercept the diaziridine intermediate *via* a ring expansion reaction. Guided especially by the latter observations, further studies could provide new synthetic routes to more complex heterocyclic structures through (enantioselective) multi-component cycloaddition reactions.

4   Summary

The first chapter of this thesis was concerned with the development of a Kumada–Tamao–Corriu-type cross-coupling reaction of *tert*-alkyl electrophiles catalyzed by a cheap and non-hygroscopic iron catalyst. Highly practical and mild reaction conditions were found to lead to a successful cross-coupling of substrates of type **37** and various *alkyl* Grignard reagents affording the direct substitution products **38** for the first time in a general manner (Scheme 54). The formation of the corresponding allenes was usually suppressed; a notable exception concerns *aryl* Grignard reagents where side reactions could not be inhibited.
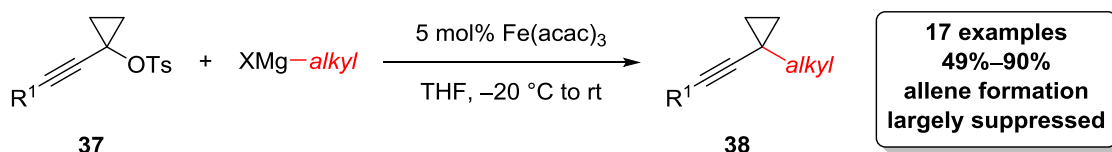
Scheme 54: Summary of the results discussed in Section 2.2.1.

Switching from the 1-alkynyl substituent to a 1-vinyl substituent resulted in a drastic change in the reaction outcome (Scheme 55). Substrates of type **170** underwent cross-coupling with a *methyl* Grignard reagent in the presence of TMEDA as an additive to afford a single cross-coupling product (**171**). On the other hand, cross-coupling **170** with higher alkyl Grignard reagents afforded the desired products **172** in varying yields along with substantial amounts of reduced and dimerized starting materials (**45** and **46**, respectively).
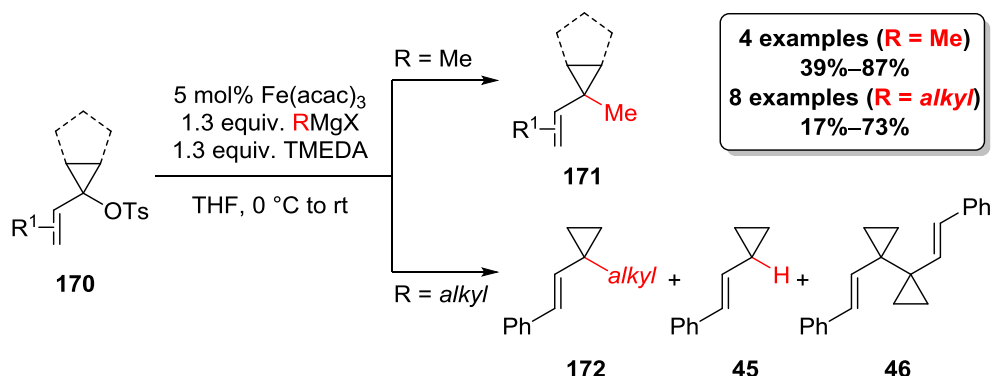
Scheme 55: Summary of the results discussed in Section 2.2.2.

Control experiments confirmed that the triple and the double bound are necessary for a successful cross-coupling to occur, consistent with pre-coordination to the catalyst. Deuterium labeling experiments showed that **45** arises from a β-hydride elimination process of the *alkyl* Grignard reagent. Further detailed mechanistic studies will address this striking difference in reactivity of 1-alkynylcyclopropyl tosylates **37** and 1-vinylcyclopropyl tosylates **170**.

In the second chapter, several aspects of modern carbene transfer reactions have been studied.

The first stoichiometric study on the Rh(III)-mediated C–H functionalization of arenes has provided valuable insight into the nature of the catalytic cycle and reactive intermediates (Scheme 56). The neutral Rh(III) halide complex **97** does not decompose diazo **100**, and neither does cationic complex **99** when generated *in situ* from **97** by halide abstraction with AgSbF₆. With pure **99** in hand, however, diazo decomposition is facile at 0 °C and leads directly to the isomeric products of migratory insertion **101** and **102**, of which the major complex **101** was characterized by X-ray crystallography. These results show that carbene formation and migratory insertion are likely to be fast steps in the catalytic cycle, and that *in situ* halide abstraction may not always lead to the envisaged reactivity.
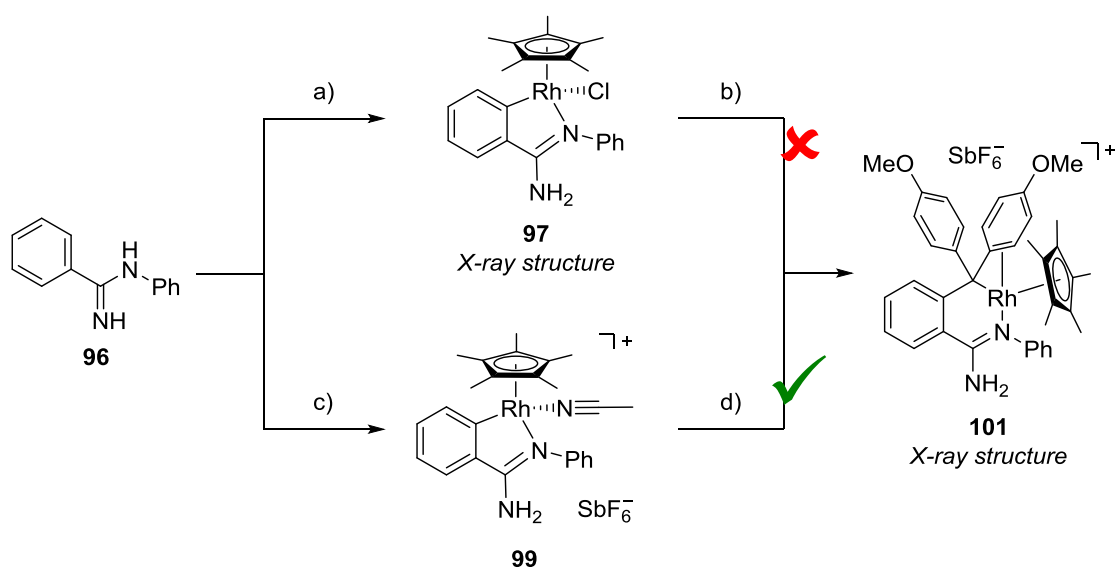
Scheme 56: Summary of the results from the study conducted in Section 3.2.1. Reaction conditions: a) [Cp*RhCl₂]₂, NaOAc, toluene, reflux, 63%; b) AgSbF₆, MeCN, rt, then **100**, CH₂Cl₂, −20 °C; c) [Cp*Rh(MeCN)₃](SbF₆)₂, NaOAc, MeCN, reflux, 80%; d) **100**, CD₂Cl₂, −20 °C.

Secondly, a thorough study was carried out for the first time on the catalytic activity of piano-stool complexes of the type [Cp*MX$_2$]$_2$ (M = Rh, Ir; X = Cl, Br, I) in carbene transfer reactions. An important influence of the halide ligand was found (Scheme 57): [Cp*RhCl$_2$]$_2$ did not catalyze many of the reactions studied (*i.e.*, cyclopopanation, Si–H insertion, and oxirane formation) and was only active for carbene insertion into the O–H bond of MeOH. The observed chloride migration in the transiently formed carbene dichlorido complex results in formation of complex **89**, which precludes typical carbene reactivity. Nevertheless, if an incoming nucleophile such as MeOH is nucleophilic enough, the carbon bound chloride can function as a leaving group resulting in formation of the same product as is formed by carbene insertion into the O–H bond (**94** and **95**). No halide migration was observed for [Cp*IrX$_2$]$_2$ and these complexes catalyzed efficiently the carbene transfer reactions studied.
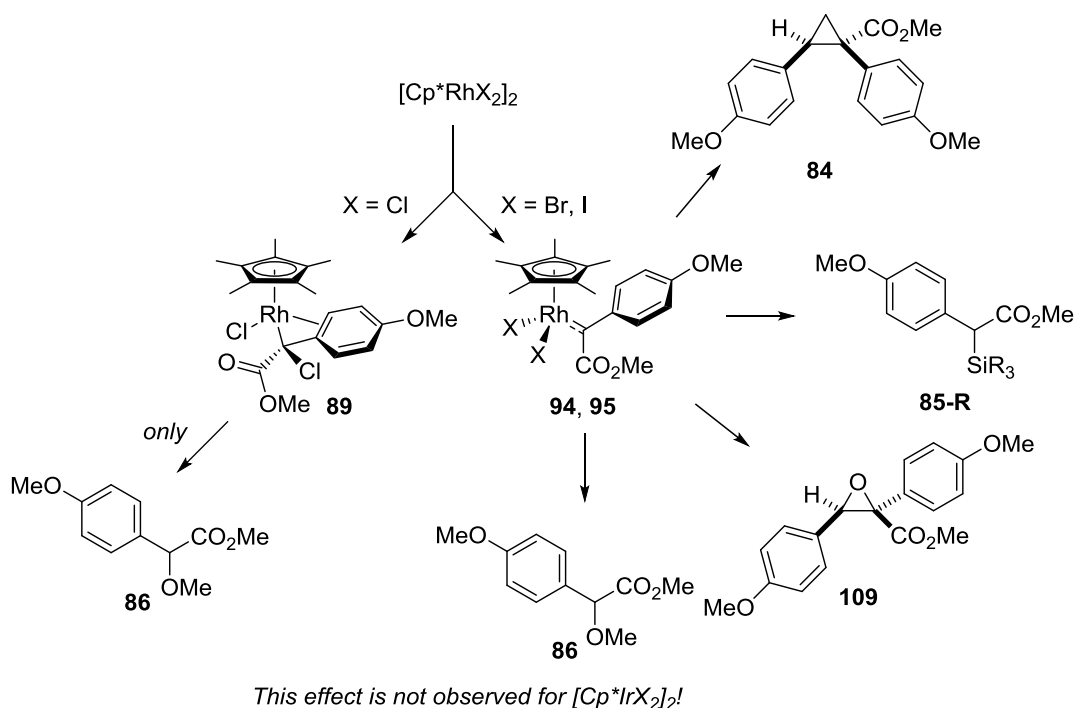
Scheme 57: Summary of the results from the study conducted in Section 3.2.2.

Thirdly, a Rh(III)-catalyzed metathesis of diazo compounds **173** and azoarenes **174** affording α-imino esters **175** under mild conditions was developed (Scheme 58). Key to the successful and scalable reaction was irradiation of the reaction mixture with commercial blue LEDs which facilitate the *E→Z* isomerization of the azoarene and sets the scene for the metathesis to occur. This transformation represents a new type of reaction of donor/acceptor carbenes and shows a broad scope with high yields and an appreciable compatibility with polar and apolar substituents giving rise to α-imino esters which could not easily be synthesized by traditional means (*e.g.*, condensation reactions, Staudinger ligation, etc.).

Mechanistic investigations argue against the intermediacy of a metal nitrene formed *via* the archetypal [2+2]/retro-[2+2] cycloaddition mechanism. Instead, reaction of rhodium carbene complex **95** and (*Z*)-azobenzene ((*Z*)-**117**) forms a transient diaziridine **157** which was characterized by X-ray crystallography. This intermediate can form the α-imino esters **175** through two possible pathways: either a metal-free decay of the three-membered ring releases the product **175** alongside (*E*)-azobenzene, which than re-enters the catalytic cycle, or the diaziridine **157** reacts with another rhodium carbene complex **95** affording a species that leads to the product and the catalyst, presumably *via* a cheletropic process.
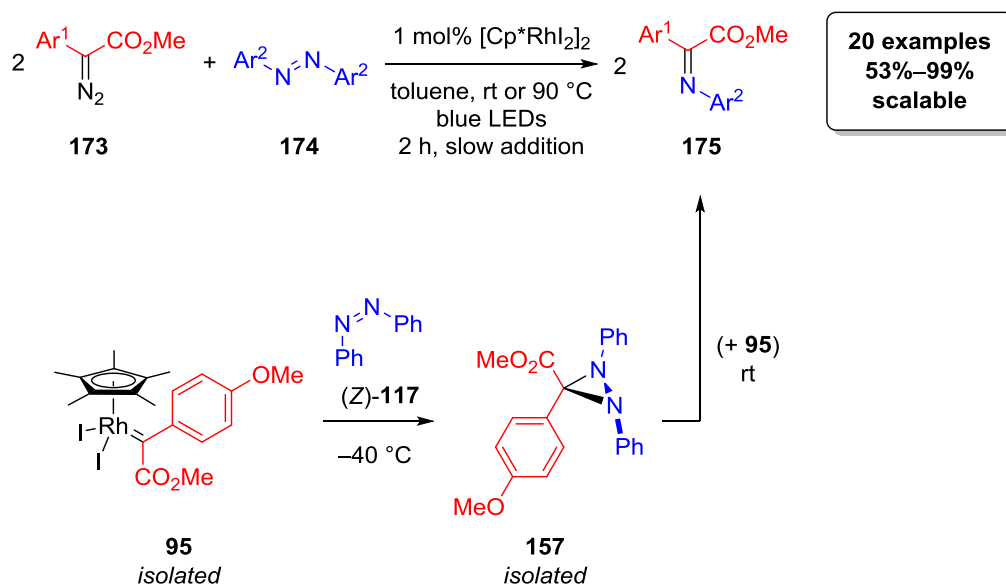
Scheme 58: Summary of the results presented in Section 3.2.3.

5 Experimental Procedures

5.1 General Experimental Details

All reactions were carried out under an argon atmosphere in flame-dried glassware unless stated otherwise.

Solvents were purified by distillation over the indicated drying agents and were transferred under argon: toluene and THF (Na/K, stored over molecular sieves), Et$_2$O (Mg/anthracene), CH$_2$Cl$_2$, DCE, and n-hexane (CaH$_2$), CD$_2$Cl$_2$ (dried and stored over molecular sieves, degassed three times by the freeze-pump-thaw method), methanol (Mg), n-pentane (Na/K, degassed three times by the freeze-pump-thaw method), NEt$_3$ and pyridine were dried by an absorption solvent purification system based on molecular sieves. TMEDA was purified by distillation over CaH$_2$ and transferred under argon.

Unless stated otherwise, all commercially available compounds (ABCR, Acros, Aldrich, TCI) were used as received. Iron(III) acetylacetonate (≥99.9% metals basis) was purchased from Sigma-Aldrich.

Flash chromatography: Merck Geduran® Si 60 (40–63 µm) or Merck Silica gel 60 (0.015–0.040 mm).

NMR: Spectra were recorded on Bruker AV VIII 300, AV 400, or AV 500 spectrometers in the indicated solvents; chemical shifts (δ) are given in ppm relative to tetramethylsilane; ^{19}F{^{1}H} NMR spectra were referenced externally to CFCl$_3$; ^{31}P NMR spectra were referenced externally to H$_3$PO$_4$; ^{15}N NMR spectra were referenced externally to MeNO$_2$. The solvent signals were used as references (CDCl$_3$: δ_C = 77.16 ppm; residual CHCl$_3$ in CDCl$_3$: δ_H = 7.26 ppm; CD$_2$Cl$_2$: δ_C = 53.84 ppm; residual CHDCl$_2$ in CD$_2$Cl$_2$: δ_H = 5.32 ppm); proton and carbon assignments were established using NOESY, HSQC, and HMBC experiments; numbering schemes as shown in the inserts.

IR: Perkin-Elmer Spectrum One spectrometer, wavenumbers ($\tilde{v}$) in cm^{-1}.

MS: EI: Finnigan MAT 8400 (70 eV), ESI: Thermo Scientific LTQ-FT or Thermo Scientific Exactive; GC-EI: Thermo Scientific Trace GC Ultra with a Thermo Scientific ISQ spectrometer; accurate mass determinations: Finnigan MAT 95, Thermo Scientific LTQ FT, or Thermo Scientific Exactive.

A self-made set-up was used for reactions carried out under irradiation with light emitted by blue LEDs (Figure 16). Two LED strips were secured to the inside of a plastic container (12 cm × 12 cm × 18 cm), of which the end was cut open (Figure 16). The LED strips were purchased from Conrad Electronic SE (www.conrad.de, SKU: 150536) and possess the following characteristics: wave length λ = 470 nm, luminous intensity I_V = 250 mcd, angle of radiation 110°, 48 LEDs per strip (3 per unit), strip length 67.2 cm, 12 V, 5.2 W.
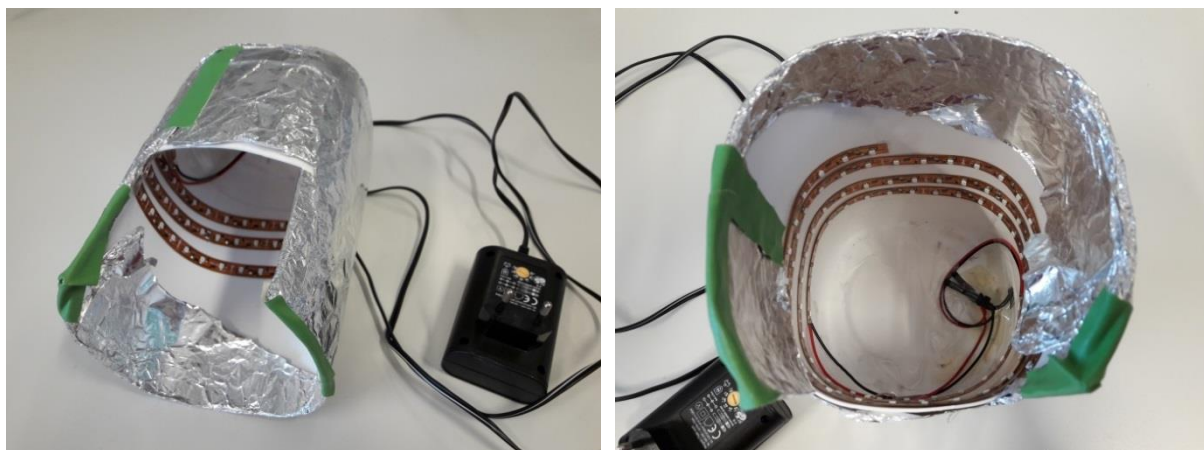
Figure 16: Self-made LED array.

5.2 Fe-Catalyzed Cross-Coupling of 1-Substituted Cyclopropyl Tosylates

5.2.1 Synthesis of Cyclopropanols

1-(5-((*tert*-Butyldimethylsilyl)oxy)pent-1-yn-1-yl)cyclopropan-1-ol (S1). MeMgCl (2.92 M in THF, 4.2 mL, 12.26 mmol) was added dropwise to a solution of 1-ethoxy-cyclopropanol (1.24 g, 12.14 mmol)[192] in THF (25 mL) at 0 °C. The resulting suspension was stirred at 0 °C for 30 min. In a separate flask, a solution of *tert*-butyldimethyl(pent-4-yn-1-yloxy)silane (2.48 g, 12.50 mmol)[193] in THF (25 mL) was treated at –78 °C with *n*-BuLi (1.6 M in *n*-hexane, 8.0 mL, 12.80 mmol). The mixture was stirred at –78 °C for 1 h and then transferred *via* cannula into the suspension of the magnesium salt of 1-ethoxycyclopropanol. Stirring was continued at room temperature overnight. The reaction was quenched with sat. aq. NH₄Cl (20 mL) and the aqueous phase extracted with EtOAc (3 × 20 mL). The combined organic layers were washed with sat. aq. NaHCO₃ (20 mL) and brine (20 mL), dried over Na₂SO₄, and concentrated *in vacuo*. The crude material was purified by flash chromatography (silica, hexanes/EtOAc, 10:1) to give the title compound as a colorless oil (2.12 g, 69%). ¹H NMR (400 MHz, CDCl₃): δ = 3.67 (t, *J* = 6.0 Hz, 2 H), 2.29 (t, *J* = 7.1 Hz, 2 H), 1.73–1.65 (m, 2 H), 1.05–1.00 (m, 2 H), 0.93–0.89 (m, 2 H), 0.89 (s, 9 H), 0.05 (s, 6 H); ¹³C{¹H} NMR (100 MHz, CDCl₃): δ = 82.7, 81.8, 61.7, 46.1, 31.8, 26.1, 18.5, 17.3, 15.3, –5.2; IR (film): $\tilde{v}$ = 3320 (br), 2929, 2953, 2857, 1471, 1234, 1102, 1066, 1007, 962, 831, 774; MS (EI): *m/z* (%) = 241 (2), 225 (2), 197 (14), 181 (23), 169 (28), 151 (13), 139 (11), 125 (17), 111 (5), 105 (25), 95 (14), 79 (26), 77 (24), 75 (100), 73 (28), 65 (4), 59 (7); HRMS (ESI+): *m/z*: calculated for C₁₄H₂₆OSiNa [M+Na]⁺: 277.15941; found: 277.15942.
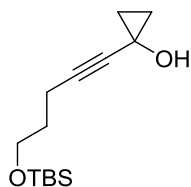
1-(4-(Benzyloxy)but-1-yn-1-yl)cyclopropan-1-ol (S2). Prepared analogously to compound **S1** as a colorless oil (593 mg, 53%). ¹H NMR (400 MHz, CDCl₃): δ = 7.40–7.26 (m, 5 H), 4.55 (s, 2 H), 3.57 (t, *J* = 7.0 Hz, 2 H), 2.53 (t, *J* = 7.0 Hz, 2 H), 2.36 (s, 1 H), 1.05–0.98 (m, 2 H), 0.97–0.90 (m, 2 H); ¹³C{¹H} NMR (100 MHz, CDCl₃): δ = 138.2, 128.6, 127.8 (2 C), 82.9, 79.7, 73.1, 68.5, 46.0, 20.4, 17.3; IR (film): $\tilde{v}$ = 3379 (br), 2912, 2864, 1354, 1363, 1233, 1096, 1019, 968, 735, 697; MS (GC-EI): *m/z* (%) = 216 [M]⁺ (<1), 187 (4), 171 (1), 159 (5), 141 (1), 129 (3), 108 (21), 91 (100), 79 (42), 65 (14), 53 (12); HRMS (ESI+): *m/z*: calculated for C₁₄H₁₆O₂Na [M+Na]⁺: 239.10425; found: 239.10407.
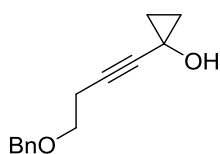
1-(5-Phenylpent-1-yn-1-yl)cyclopropan-1-ol (S3). Prepared analogously to compound **S1** as a colorless oil (1.34 g, 49%). ¹H NMR (400 MHz, CDCl₃): δ = 7.33–7.25 (m, 2 H), 7.23–7.15 (m, 3 H), 2.71 (t, *J* = 7.5 Hz, 2 H), 2.29 (s, 1 H), 2.23 (t, *J* = 7.5 Hz, 2 H), 1.83 (q, *J* = 7.5 Hz, 2 H), 1.08–0.99 (m, 2 H), 0.98–0.89 (m, 2 H); ¹³C{¹H} NMR (75 MHz, CDCl₃): δ = 141.7, 128.7, 128.5, 126.0, 82.7, 82.4, 46.1, 35.0, 30.4, 18.4,
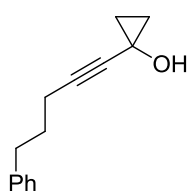
17.4; IR (film): $\tilde{v}$ = 3314 (br), 3026, 2939, 2860, 1496, 1454, 1231, 1019, 968, 744, 698; MS (GC-EI): m/z (%) = 200 [M]$^+$ (1), 185 (7), 171 (26), 157 (13), 143 (20), 128 (69), 115 (30), 109 (21), 105 (32), 96 (62), 91 (100), 79 (51), 77 (52), 65 (48), 55 (29); HRMS (ESI+): m/z: calculated for $C_{14}H_{16}ONa$ [M+Na]$^+$: 223.10933; found: 223.10943.

(*E*)-1-(5-Phenylpent-1-en-1-yl)cyclopropan-1-ol (S4). A solution of LiAlH$_4$ (1 M in THF, 3.3 mL, 3.25 mmol) was added dropwise to a solution of compound **S3** (1.04 g, 5.21 mmol) in THF (18.5 mL) and the resulting mixture was stirred at reflux temperature for 1 h. The mixture was cooled in an ice bath and the reaction was carefully quenched by slow addition of solid Na$_2$SO$_4$·10H$_2$O until gas evolution had ceased. After addition of deionized water (25 mL) the mixture was extracted with *tert*-butyl methyl ether (3 × 50 mL). The combined organic layers were dried over Na$_2$SO$_4$ and concentrated *in vacuo*. The crude material was purified by flash chromatography (silica, hexanes/*tert*-butyl methyl ether, 10:1→1:1) to give the title compound as a colorless oil (903 mg, 86%). ^{1}H NMR (300 MHz, CDCl$_3$): δ = 7.33–7.23 (m, 2 H), 7.22–7.14 (m, 3 H), 5.69 (dt, *J* = 15.4 Hz, *J* = 6.8 Hz, 1 H), 5.30 (dt, *J* = 15.4 Hz, *J* = 1.4 Hz, 1 H), 2.64 (t, *J* = 7.7 Hz, 2 H), 2.17–2.06 (m, 2 H), 1.95 (s, 1 H), 1.79–1.67 (m, 2 H), 1.04–0.97 (m, 2 H), 0.72–0.64 (m, 2 H); ^{13}C{^{1}H} NMR (75 MHz, CDCl$_3$): δ = 142.6, 134.3, 128.6, 128.4, 127.0, 125.8, 55.6, 35.5, 31.8, 31.3, 15.9; IR (film): $\tilde{v}$ = 3303 (br), 3085, 3025, 2927, 2855, 1496, 1453, 1288, 1214, 1015, 964, 743, 697; MS (GC-EI): m/z (%) = 202 [M]$^+$ (<1), 155 (2), 145 (5), 130 (25), 111 (13), 107 (17), 105 (13), 98 (30), 91 (100), 83 (63), 79 (12), 77 (17), 65 (18), 55 (21); HRMS (ESI+): m/z: calculated for $C_{14}H_{18}ONa$ [M+Na]$^+$: 225.12498; found: 225.12507.
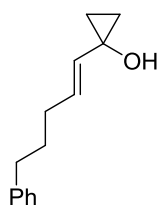
5.2.2 Synthesis of 1-Substituted Cyclopropyl Derivatives

The following tosylates were synthesized according to literature procedures: 1-vinylcyclopropyl tosylate (**40**),[194] (*E*)-1-styrylcyclopropyl tosylate (**43**),[77] 1-(cyclohex-1-en-1-yl)cyclopropyl tosylate (**S5**),[195] and 1-phenylcyclopropyl tosylate (**59**)[196].

Crystals of **43** suitable for X-ray diffraction were grown by slow evaporation from a solution in *tert*-butyl methyl ether.

1-(5-(((*tert*-Butyldimethylsilyl)oxy)pent-1-yn-1-yl)cyclopropyl pivalate (37-Piv). Et$_3$N (1.25 mL, 8.97 mmol) and DMAP (550 mg, 4.50 mmol) were successively added to a solution of compound **S1** (457 mg, 1.80 mmol) in CH$_2$Cl$_2$ (18 mL) at −78 °C. Trimethylacetyl chloride (0.25 mL, 2.03 mmol) was added dropwise. The resulting mixture was stirred at −78 °C for 1 h before it was poured onto ice water (25 mL) and the mixture was extracted with CH$_2$Cl$_2$ (3 × 20 mL). The combined extracts were dried over Na$_2$SO$_4$ and concentrated *in vacuo*. The residue was purified by flash
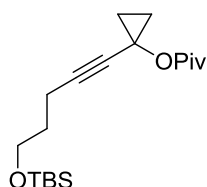
chromatography (silica, hexanes/EtOAc, 200:1) to give the title compound as a colorless oil (494 mg, 81%). ^{1}H NMR (400 MHz, CDCl$_3$): δ = 3.64 (t, J = 6.1 Hz, 2 H), 2.26 (t, J = 7.0 Hz, 2 H), 1.70–1.62 (m, 2 H), 1.15 (s, 9 H), 1.13–1.09 (m, 2 H), 1.05–0.99 (m, 2 H), 0.87 (s, 9 H), 0.03 (s, 6 H); ^{13}C{^{1}H} NMR (100 MHz, CDCl$_3$): δ = 177.7, 82.8, 78.8, 61.6, 48.3, 38.6, 31.6, 27.0, 26.1, 18.4, 15.9, 15.4, −5.2; IR (film): $\tilde{\nu}$ = 2956, 2930, 2858, 1751, 1133, 1104, 833, 775; MS (EI, %): m/z = 281 (69), 253 (11), 225 (7), 197 (15), 169 (15), 159 (53), 149 (8), 125 (9), 105 (13), 85 (22), 75 (26), 57 (1000); HRMS (ESI+): m/z: calculated for C$_{19}$H$_{34}$O$_3$SiNa [M+Na]$^+$: 361.21694, found: 361.21720.

1-(5-(($tert$-Butyldimethylsilyl)oxy)pent-1-yn-1-yl)cyclopropyl methyl carbonate (37-CO$_2$Me).

Et$_3$N (1.10 mL, 7.89 mmol) and DMAP (485 mg, 3.97 mmol) were successively added to a solution of compound **S1** (405 mg, 1.59 mmol) in CH$_2$Cl$_2$ (16 mL) at −78 °C. Methyl chloroformate (0.14 mL, 1.81 mmol) was added dropwise. The resulting mixture was stirred at −78 °C for 1 h before it was warmed to −30 °C. After 2 h, the mixture was poured onto ice water (25 mL) and extracted with CH$_2$Cl$_2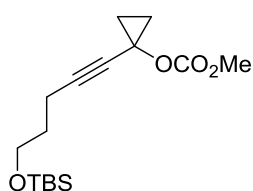$ (3 × 20 mL). The combined extracts were dried over Na$_2$SO$_4$ and concentrated *in vacuo*. The residue was purified by flash chromatography (silica, hexanes/EtOAc, 200:1) to give the title compound as a colorless oil (361 mg, 73%). ^{1}H NMR (400 MHz, CDCl$_3$): δ = 3.78 (s, 3 H), 3.64 (t, J = 6.0 Hz, 2 H), 2.28 (t, J = 7.1 Hz, 2 H), 1.72–1.63 (m, 2 H), 1.20–1.10 (m, 4 H), 0.87 (s, 9 H), 0.03 (s, 6 H); ^{13}C{^{1}H} NMR (100 MHz, CDCl$_3$): δ = 155.0, 84.2, 78.0, 61.6, 54.9, 51.4, 31.5, 26.0, 18.4, 16.0, 15.3, −5.3; IR (film): $\tilde{\nu}$ = 2954, 2930, 2857, 1764, 1440, 1274, 981, 943, 833, 775; MS (EI, %): m/z = 297 [M−Me]$^+$ (<1), 255 (68), 211 (6), 183 (15), 181 (23), 179 (29), 153 (14), 151 (10), 133 (28), 125 (10), 109 (7), 105 (29), 91 (24), 89 (100), 79 (22), 77 (19), 75 (57), 73 (28), 59 (25); HRMS (ESI+): m/z: calculated for C$_{16}$H$_{28}$O$_4$SiNa [M+Na]$^+$: 335.16491, found: 335.16493.

1-(5-(($tert$-Butyldimethylsilyl)oxy)pent-1-yn-1-yl)cyclopropyl diethyl phosphate (37-P(O)(OEt)$_2$).
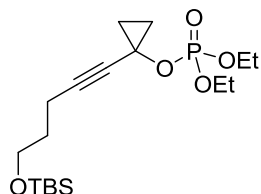
A solution of compound **S1** (424 mg, 1.67 mmol) in THF (5 mL) was added dropwise to a suspension of NaH (82 mg, 3.42 mmol) in THF (15 mL) at −78 °C. The mixture was allowed to warm to room temperature over 1 h. The resulting yellow mixture was then cooled to −78 °C and diethyl chlorophosphate (435 mg, 2.52 mmol) was added in one portion. The mixture was allowed to warm to room temperature overnight. After 7 days, sat. aq. NH$_4$Cl (10 mL) was added and the mixture extracted with EtOAc (3 × 15 mL). The combined extracts were dried over Na$_2$SO$_4$ and concentrated *in vacuo*. The residue was purified by flash chromatography (silica, hexanes/EtOAc, 10:1) to give the title compound as a colorless oil (380 mg, 58%). ^{1}H NMR (400 MHz, CDCl$_3$): δ = 4.18–4.06 (m, 4 H), 3.64 (t, J = 6.0 Hz, 2 H), 2.29 (t, J = 7.2 Hz, 2 H),

1.39–1.34 (m, 2 H), 1.28 (td, J = 7.1 Hz, J = 1.0 Hz, 6 H), 1.08–1.02 (m, 2 H), 0.87 (s, 9 H), 0.03 (s, 6 H); ^{13}C{^{1}H} NMR (100 MHz, CDCl$_3$): δ = 84.5, 78.8, 64.0 (d, J = 6.0 Hz), 61.6, 51.5 (d, J = 7.2 Hz), 31.6, 26.0, 18.4, 16.5 (d, J = 4.7 Hz), 16.2 (d, J = 7.1 Hz), 15.4, −5.2; ^{31}P{^{1}H} NMR (162 MHz, CDCl$_3$): δ = −6.62 (s); IR (film): $\tilde{v}$ = 2930, 2856, 1471, 1393, 1254, 1218, 1029, 878, 833, 770, 735; MS (EI, %): m/z = 391 [M]$^+$ (2), 375 (2), 335 (5), 334 (16), 333 (79), 305 (4), 232 (11), 211 (39), 183 (32), 179 (5), 157 (10), 156 (7), 155 (100), 151 (6), 137 (2), 123 (13), 105 (33), 103 (11), 99 (10), 95 (5), 91 (9), 89 (5), 79 (21), 78 (10), 77 (20), 75 (19), 73 (24), 59 (4).

1-(5-(((*tert*-Butyldimethylsilyl)oxy)pent-1-yn-1-yl)cyclopropyl tosylate (37-Ts/37a).
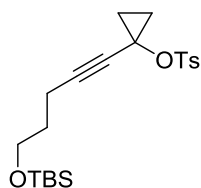
DMAP (3.80 g, 31.10 mmol) and tosyl chloride (1.90 g, 9.97 mmol) were successively added to a solution of compound **S1** (1.57 g, 6.17 mmol) in CH$_2$Cl$_2$ (60 mL). The resulting mixture was stirred at ambient temperature overnight. Sat. aq. NH$_4$Cl was added and the mixture extracted with EtOAc. The combined extracts were dried over Na$_2$SO$_4$ and concentrated *in vacuo*. The residue was purified by flash chromatography (silica, hexanes/EtOAc, 20:1) to give the title compound as a colorless oil (1.91 g, 76%). ^{1}H NMR (400 MHz, CDCl$_3$): δ = 7.86–7.81 (m, 2 H), 7.35–7.29 (m, 2 H), 3.53 (t, J = 6.0 Hz, 2 H), 2.43 (s, 3 H), 2.01 (t, J = 7.2 Hz, 2 H), 1.50–1.42 (m, 4 H), 1.09–1.04 (m, 2 H), 0.87 (s, 9 H), 0.02 (s, 6 H); ^{13}C{^{1}H} NMR (100 MHz, CDCl$_3$): δ = 144.7, 134.9, 129.5, 128.6, 86.5, 77.0, 61.6, 54.9, 31.3, 26.1, 21.8, 18.5, 16.4, 15.3, −5.2; IR (film): $\tilde{v}$ = 2922, 9954, 2857, 1366, 1253, 1208, 1173, 1096, 1063, 938, 834, 813, 776, 741, 666, 558, 583; MS (EI): m/z (%) = 351 (34), 333 (10), 307 (29), 253 (7), 229 (96), 213 (8), 195 (41), 181 (15), 169 (20), 155 (50), 149 (24), 139 (17), 125 (18), 122 (17), 111 (12), 105 (28), 93 (16), 91 (100), 79 (20), 77 (22), 75 (52), 73 (66), 65 (25); HRMS (ESI+): m/z: calculated for C$_{21}$H$_{32}$O$_{24}$SSiNa [M+Na]$^+$: 431.16828; found: 431.16848.

1-(4-(Benzyloxy)but-1-yn-1-yl)cyclopropyl tosylate (37b).
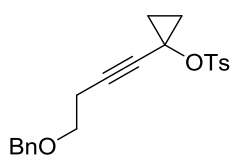
Et$_3$N (0.47 mL, 3.27 mmol) was added dropwise to a solution of compound **S2** (590 mg, 2.73 mmol) in CH$_2$Cl$_2$ (9 mL), followed by addition of DMAP (333 mg, 2.73 mmol). After stirring for 30 min, tosyl chloride (690 mg, 3.55 mmol) was added in one portion and stirring continued overnight. The yellow suspension was concentrated *in vacuo* to a volume of approximately 3 mL before it was diluted with deionized water (8 mL) and extracted with Et$_2$O (8 mL). The aqueous layer was diluted with sat. aq. NH$_4$Cl (5 mL) and extracted with Et$_2$O (6 × 5 mL). The combined organic layers were washed with deionized water (5 mL), dried over Na$_2$SO$_4$, and concentrated *in vacuo*. The residue was purified by flash chromatography (silica, hexanes/*tert*-butyl methyl ether, 5:1) to give the title compound as a colorless oil (735 mg, 73%). ^{1}H NMR (400 MHz, CDCl$_3$): δ = 7.86–7.81 (m, 2 H), 7.39–7.24 (m, 7 H), 4.49 (s, 2 H), 3.36 (t, J = 7.2 Hz, 2 H), 2.41 (s, 3 H), 2.26 (t, J = 7.2 Hz, 2 H), 1.50–1.44 (m,

2 H), 1.12–1.06 (m, 2 H); ^{13}C{^{1}H} NMR (100 MHz, CDCl$_3$): δ = 144.7, 138.1, 134.9, 129.5, 128.6 (2 C), 127.9, 127.8, 83.4, 78.1, 73.1, 68.0, 54.7, 21.8, 20.3, 16.4; IR (film): $\tilde{\nu}$ = 3064, 2864, 1365, 1174, 1096, 937, 741, 559; MS (EI): m/z (%) = 215 (9), 197 (5), 183 (5), 170 (3), 155 (12), 143 (3), 139 (5), 129 (4), 109 (4), 105 (4), 91 (100), 65 (5), 55 (1); HRMS (ESI+): m/z: calculated for C$_{21}$H$_{22}$O$_4$SNa [M+Na]$^+$: 393.11310; found: 393.11307.

1-(Hex-1-yn-1-yl)cyclopropyl tosylate (37c). Pyridine (2.7 mL, 33.38 mmol) was added to a solution of 1-(hex-1-yn-1-yl)cyclopropan-1-ol (944 mg, 6.38 mmol)[197] in CH$_2$Cl$_2$ (40 mL). After addition of tosyl chloride (1.52 g, 7.81 mmol) in one portion, the mixture was stirred for 24 h before the reaction was quenched with sat. aq. NH$_4$Cl. The aqueous phase was extracted with EtOAc and the combined organic layers were dried over Na$_2$SO$_4$ and concentrated *in vacuo*. The residue was purified by flash chromatography (silica, hexanes/EtOAc, 50:1) to give the title compound as a colorless oil (1.25 g, 63%). ^{1}H NMR (300 MHz, CD$_2$Cl$_2$): δ = 7.85–7.78 (m, 2 H), 7.40–7.32 (m, 2 H), 2.45 (s, 3 H), 1.98–1.89 (m, 2 H), 1.49–1.43 (m, 2 H), 1.32–1.20 (m, 4 H), 1.10–1.01 (m, 2 H), 0.90–0.80 (m, 3 H); ^{13}C{^{1}H} NMR (75 MHz, CD$_2$Cl$_2$): δ = 145.3, 135.1, 129.9, 128.7, 87.2, 77.1, 55.2, 30.7, 22.3, 21.8, 18.7, 16.5, 13.7; IR (film): $\tilde{\nu}$ = 2299, 3528, 2872, 1365, 1207, 1172, 1095, 1029, 936, 849, 876, 813, 781, 736, 666, 557, 582; MS (EI): m/z (%) = 292 [M]$^+$ (<1), 250 (13), 237 (12), 199 (3), 186 (6), 171 (4), 155 (64), 139 (24), 137 (10), 119 (8), 109 (74), 91 (100), 81 (12), 79 (24), 77 (8), 67 (17), 65 (16), 53 (9), 41 (12); HRMS (CI): m/z: calculated for C$_{16}$H$_{21}$O$_3$S [M]$^+$: 293.12114; found: 293.12089.
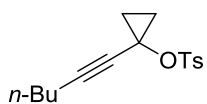
1-(Phenylethynyl)cyclopropyl tosylate (37d). Prepared analogously to compound **37b** as an off-white solid (440 mg, 38%); the spectral data matched those previously reported in the literature.[198] Crystals suitable for X-ray diffraction were grown by slow evaporation from a solution in *tert*-butyl methyl ether. ^{1}H NMR (400 MHz, CD$_2$Cl$_2$): δ = 7.88–7.83 (m, 2 H), 7.34–7.23 (m, 5 H), 7.14–7.08 (m, 2 H), 2.31 (s, 3 H), 1.64–1.57 (m, 2 H), 1.28–1.22 (m, 2 H); ^{13}C{^{1}H} NMR (100 MHz, CD$_2$Cl$_2$): δ = 145.7, 134.7, 131.9, 130.0, 129.0, 128.8, 128.5, 122.2, 86.1, 85.7, 54.9, 21.7, 17.0.
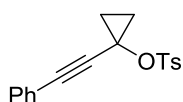
1-((Trimethylsilyl)ethynyl)cyclopropyl tosylate (37e).[199] Prepared analogously to compound **37b** as a colorless oil (893 mg, 91%). ^{1}H NMR (400 MHz, CDCl$_3$): δ = 7.89–7.83 (m, 2 H), 7.36–7.30 (m, 2 H), 2.45 (s, 3 H), 1.59–1.54 (m, 2 H), 1.21–1.16 (m, 2 H), 0.00 (s, 9 H); ^{13}C{^{1}H} NMR (100 MHz, CDCl$_3$): δ = 144.9, 134.6, 129.7, 128.6, 101.4, 90.8, 54.6, 21.9, 17.1, −0.3; IR (film): $\tilde{\nu}$ = 2961, 2173, 1599, 1368, 1300, 1250, 1205, 1171, 1095, 932, 841, 809, 760, 716, 659, 593, 558, 533; MS (GC-EI): m/z (%) = 293 (4), 253 (3), 229 (15), 197 (2), 173 (4), 165 (2), 155 (27), 153 (15), 149 (19), 139 (10), 138 (15), 125 (53), 123 (92), 97 (49), 95 (15), 91 (75), 83 (18), 75 (33), 73 (100), 67 (13), 65
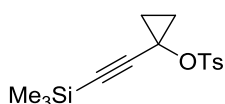
(19), 59 (33), 53 (10), 45 (14), 43 (15); HRMS (ESI+): *m/z*: calculated for $C_{15}H_{20}O_3SSiNa$ [M+Na]$^+$: 331.07947; found: 331.07952.

1-(3-Phenoxyprop-1-yn-1-yl)cyclopropyl tosylate (37n). Prepared analogously to compound **37-Ts/37a** as a colorless oil (316 mg, 68%). ^{1}H NMR (300 MHz, CDCl$_3$): δ = 7.86–7.77 (m, 2 H), 7.32–7.21 (m, 4 H), 7.01–6.92 (m, 1 H), 6.85–6.77 (m, 2 H), 4.42 (s, 2 H), 2.38 (s, 3 H), 1.54–1.44 (m, 2 H), 1.18–1.08 (m, 2 H); ^{13}C{^{1}H} NMR (75 MHz, CDCl$_3$): δ = 157.8, 145.1, 134.5, 129.6 (2 C), 128.7, 121.7, 115.0, 84.5, 81.0, 56.0, 53.8, 21.8, 16.7; IR (film): $\tilde{v}$ = 2921, 1598, 1494, 1365, 1212, 1171, 941, 874, 734, 688, 556; MS (GC-EI): *m/z* (%) = 342 [M]$^+$ (1), 248 (6), 187 (19), 170 (73), 155 (100), 145 (6), 139 (45), 131 (9), 115 (3), 103 (13), 91 (86), 77 (11), 65 (13), 52 (3); HRMS (ESI+): *m/z*: calculated for $C_{19}H_{18}O_4SNa$ [M+Na]$^+$: 365.08180; found: 365.08175.
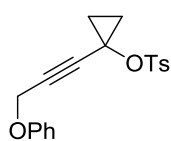
(*E*)-1-(5-Phenylpent-1-en-1-yl)cyclopropyl tosylate (S6). Prepared analogously to compound **37b** as a colorless oil (1.25 g, 80%). ^{1}H NMR (300 MHz, CD$_2$Cl$_2$): δ = 7.76–7.69 (m, 2 H), 7.35–7.23 (m, 4 H), 7.22–7.12 (m, 3 H), 5.58–5.53 (m, 2 H), 2.55 (t, *J* = 7.7 Hz, 2 H), 2.40 (s, 3 H), 1.99–1.90 (m, 2 H), 1.64–1.52 (m, 2 H), 1.32–1.24 (m, 2 H), 0.90–0.81 (m, 2 H); ^{13}C{^{1}H} NMR (75 MHz, CD$_2$Cl$_2$): δ = 145.2, 142.9, 135.8, 132.0, 130.1, 128.8, 128.7, 128.3 (2 C), 126.1, 66.0, 35.7, 31.8, 31.0, 21.7, 13.6; IR (film): $\tilde{v}$ = 3026, 2928, 2857, 1361, 1194, 1171, 1094, 909, 812, 699, 553; MS (EI): *m/z* (%) = 237 (12), 201 [M–Ts]$^+$ (28), 183 (15), 169 (6), 155 (51), 143 (19), 131 (12), 117 (9), 105 (12), 91 (100), 79 (7), 65 (7); HRMS (ESI+): *m/z*: calculated for $C_{21}H_{24}O_3SNa$ [M+Na]$^+$: 379.13384; found: 379.13414.
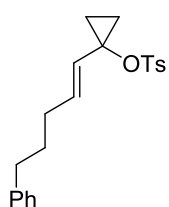
(1*R*,5*S*,6*r*)-6-(2-Chloroethyl)bicyclo[3.1.0]hexan-6-yl tosylate (S7).[200] Et$_3$N (0.23 mL, 1.64 mmol) was added dropwise to a solution of *exo*-6-(2-chloroethyl)bicyclo[3.1.0]hexan-6-ol (220 mg, 1.37 mmol)[201] in CH$_2$Cl$_2$ (4.4 mL), followed by addition of DMAP (167 mg, 1.37 mmol). After stirring for 30 min at ambient temperature, tosyl chloride (346 mg, 1.78 mmol) was added in one portion and the mixture was stirred overnight. The brown mixture was concentrated *in vacuo* and the residue was purified by flash chromatography (silica, hexanes/*tert*-butyl methyl ether, 10:1) to give the title compound as a colorless oil (398 mg, 92%). ^{1}H NMR (300 MHz, CDCl$_3$): δ = 7.79–7.72 (m, 2 H), 7.37–7.29 (m, 2 H), 3.68 (t, *J* = 7.5 Hz, 2 H), 2.45 (s, 3 H), 2.25 (t, *J* = 7.5 Hz, 2 H), 2.08–1.88 (m, 4 H), 1.83–1.70 (m, 3 H), 1.51–1.35 (m, 1 H); ^{13}C{^{1}H} NMR (75 MHz, CDCl$_3$): δ = 144.8, 135.7, 130.0, 127.5, 72.1, 40.8, 31.8, 30.4, 26.4, 25.9, 21.8; IR (film): $\tilde{v}$ = 2960, 2873, 1343, 1189, 1169, 1092, 851, 684, 662, 577; MS (EI): *m/z* (%) = 198 (6), 159 (22), 142 (10), 139 (11), 119 (9), 108 (3), 93 (30), 91 (100), 79 (4), 67 (11), 65 (14), 63 (26), 40 (10); HRMS (ESI+): *m/z*: calculated for $C_{15}H_{19}ClO_3SNa$ [M+Na]$^+$: 337.06357; found: 337.06330.
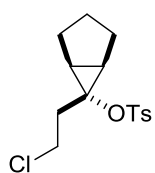
(1*R*,5*S*,6*r*)-6-Vinylbicyclo[3.1.0]hexan-6-yl tosylate (57).[200] KO*t*-Bu (184 mg, 1.91 mmol) was added to a solution of compound **S7** (400 mg, 1.27 mmol) in THF (5 mL) and the resulting yellow suspension was stirred at reflux temperature for 1.5 h. The mixture was concentrated *in vacuo* to a volume of approximately 2 mL before it was diluted with deionized water (4 mL) and extracted with *tert*-butyl methyl ether (3 × 5 mL). The aqueous layer was diluted with sat. aq. NH_4Cl (2.5 mL) and extracted with *tert*-butyl methyl ether (3 × 5 mL). The combined extracts were washed with brine (5 mL), dried over Na_2SO_4, and concentrated *in vacuo*. The residue was purified by flash chromatography (silica, hexanes/*tert*-butyl methyl ether, 10:1) to give the title compound as a colorless solid (226 mg, 64%). Crystals suitable for X-ray diffraction analysis were grown by slow evaporation from a solution in hexanes/*tert*-butyl methyl ether (10:1). M.p.: 68–69 °C; ^1H NMR (400 MHz, $CDCl_3$): δ = 7.76–7.72 (m, 2 H), 7.33–7.27 (m, 2 H), 5.81 (dd, *J* = 17.4 Hz, *J* = 10.6 Hz, 1 H), 5.51 (dd, *J* = 17.4 Hz, *J* = 1.5 Hz, 1 H), 5.34 (dd, *J* = 10.6 Hz, *J* = 1.4 Hz, 1 H), 2.43 (s, 3 H), 2.08–2.02 (m, 2 H), 1.96–1.85 (m, 2 H), 1.83–1.73 (m, 2 H), 1.68–1.56 (m, 1 H), 1.31–1.17 (m, 1 H); $^{13}C\{^1H\}$ NMR (100 MHz, $CDCl_3$): δ = 144.4, 136.0, 130.0, 129.7, 127.8, 121.7, 70.6, 31.7, 26.4, 23.7, 21.8; IR (solid): $\tilde{v}$ = 3055, 2924, 2873, 1357, 1170, 1095, 996, 861, 813, 633, 553; MS (EI): *m/z* (%) = 214 (1), 162 (6), 155 (10), 139 (4), 123 (27), 106 (7), 95 (19), 91 (32), 67 (9), 55 (100), 41 (4); HRMS (ESI+): *m/z*: calculated for $C_{15}H_{18}O_3SNa$ [M+Na]$^+$: 301.08689; found: 301.08703.
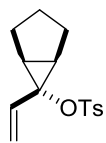
1-Phenethylcyclopropyl tosylate (58). Prepared analogously to compound **37b** from 1-phenethylcyclopropan-1-ol[202] as a colorless oil (561 mg, 86%). ^1H NMR (300 MHz, CD_2Cl_2): δ = 7.84–7.77 (m, 2 H), 7.40–7.34 (m, 2 H), 7.28–7.21 (m, 2 H), 7.20–7.13 (m, 1 H), 7.11–7.05 (m, 2 H), 2.80–2.71 (m, 2 H), 2.46 (s, 3 H), 2.03–1.95 (m, 2 H), 1.12–1.05 (m, 2 H), 0.62–0.55 (m, 2 H); $^{13}C\{^1H\}$ NMR (75 MHz, CD_2Cl_2): δ = 145.4, 141.9, 136.0, 130.3, 128.8, 128.7, 128.0, 126.3, 67.2, 38.5, 32.2, 21.8, 12.1; IR (film): $\tilde{v}$ = 3031, 2951, 2861, 1595, 1359, 1170, 1093, 1032, 838, 807, 710, 697, 553; MS (EI): *m/z* (%) = 316 [M]$^+$ (<1), 252 (1), 161 (32), 155 (24), 144 (16), 133 (18), 105 (60), 91 (100), 77 (7), 65 (10), 55 (7), 39 (3); HRMS (ESI+): *m/z*: calculated for $C_{18}H_{20}O_3SNa$ [M+Na]$^+$: 339.10254; found: 339.10242.
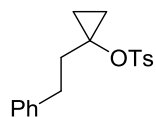
5.2.3 Grignard Reagents

Grignard reagents were purchased as ready-made solutions in THF or Et_2O from Sigma-Aldrich. They were titrated prior to use according to a literature report.[203] C_2D_5MgBr was prepared according to a literature procedure.[204]

5.2.4 Fe-Catalyzed Cross-Couplings of 1-Alkynylcyclopropyl Tosylates

Representative Procedure for the Fe-Catalyzed Cross-Coupling Reactions.

***tert*-Butyl((5-(1-hexylcyclopropyl)pent-4-yn-1-yl)oxy)dimethylsilane (38a).** *n*-Hexyl-magnesium bromide (2 M in THF, 0.24 mL, 0.480 mmol) was added dropwise over the course of 5 min to an orange solution of tosylate **37-Ts/37a** (152 mg, 0.372 mmol) and Fe(acac)$_3$ (7 mg, 0.020 mmol) in THF (4 mL) at –20 °C. After stirring for 10 min at this temperature, the brown mixture was diluted with sat. aq. NH$_4$Cl (5 mL) and the aqueous phase extracted with EtOAc (3 × 5 mL). The combined extracts were dried over Na$_2$SO$_4$, concentrated, and the residue was purified by flash chromatography (silica, hexanes) to give the title compound as a colorless oil (96 mg, 80%). ^{1}H NMR (400 MHz, CDCl$_3$): δ = 3.68 (t, J = 6.2 Hz, 2 H), 2.21 (t, J = 7.0 Hz, 2 H), 1.70–1.62 (m, 2 H), 1.57–1.47 (m, 2 H), 1.35–1.23 (m, 8 H), 0.89 (s, 9 H), 0.88 (t, J = 7.0 Hz, 3 H), 0.79–0.75 (m, 2 H), 0.52–0.47 (m, 2 H), 0.05 (s, 6 H); ^{13}C{^{1}H} NMR (100 MHz, CDCl$_3$): δ = 85.4, 76.0, 61.9, 38.7, 32.3, 32.1, 29.3, 28.0, 26.1, 22.8, 18.5, 15.3, 15.2, 14.3, 12.1, –5.2; IR (film): $\tilde{v}$ = 2954, 2927, 2856, 1470, 1463, 1254, 1103, 833, 774; MS (EI): m/z (%) = 307 (<1), 265 (100), 235 (1), 191 (14), 189 (38), 161 (6), 151 (5), 139 (3), 133 (4), 119 (26), 105 (16), 101 (18), 93 (11), 91 (19), 79 (13), 75 (96), 59 (15), 43 (11); HRMS (ESI+): m/z: calculated for C$_{20}$H$_{38}$OSiNa [M+Na]$^+$: 345.25841; found: 345.25853.
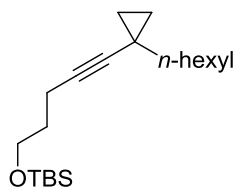
The following compounds were prepared analogously (*cf.* Table 2):

(((4-(1-Hexylcyclopropyl)but-3-yn-1-yl)oxy)methyl)benzene (38b). Colorless oil (52 mg, 74%). ^{1}H NMR (400 MHz, CDCl$_3$): δ = 7.37–7.26 (m, 5 H), 4.55 (s, 2 H), 3.55 (t, J = 7.2 Hz, 2 H), 2.46 (t, J = 7.2 Hz, 2 H), 1.57–1.47 (m, 2 H), 1.35–1.22 (m, 8 H), 0.88 (t, J = 7.0 Hz, 3 H), 0.81–0.77 (m, 2 H), 0.52–0.49 (m, 2 H); ^{13}C{^{1}H} NMR (100 MHz, CDCl$_3$): δ = 138.5, 128.5, 127.8, 127.7, 86.4, 73.0 (2 C), 69.2, 38.6, 32.0, 29.3, 27.9, 22.8, 20.4, 15.2, 14.3, 12.1; IR (film): $\tilde{v}$ = 2955, 2926, 2855, 1454, 1362, 1101, 733, 696; MS (EI): m/z (%) = 284 [M]$^+$ (1), 255 (2), 241 (2), 213 (7), 199 (54), 185 (4), 178 (4), 169 (6), 159 (23), 146 (6), 121 (6), 107 (12), 105 (16), 93 (19), 91 (100), 79 (15), 65 (6), 55 (6); HRMS (ESI+): m/z: calculated for C$_{20}$H$_{28}$ONa [M+Na]$^+$: 307.20323; found: 307.20328.
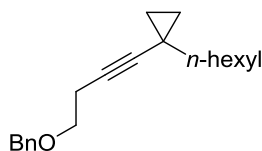
1-(Hex-1-yn-1-yl)-1-hexylcyclopropane (38c). Colorless oil (75 mg, 88%). ^{1}H NMR (400 MHz, CDCl$_3$): δ = 2.13 (t, J = 6.9 Hz, 2 H), 1.58–1.48 (m, 2 H), 1.48–1.35 (m, 4 H), 1.35–1.23 (m, 8 H), 0.90 (t, J = 7.2 Hz, 3 H), 0.89 (t, J = 6.8 Hz, 3 H), 0.80–0.74 (m, 2 H), 0.52–0.46 (m, 2 H); ^{13}C{^{1}H} NMR (100 MHz, CDCl$_3$): δ = 85.2, 76.6, 38.8, 32.1, 31.5, 29.3, 27.9, 22.8, 22.1, 18.6, 15.2, 14.3, 13.8, 12.1; IR (film): $\tilde{v}$ = 3005, 2957,
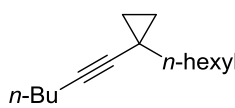
2927, 2857, 1459, 1020, 725; MS (EI): m/z (%) = 206 [M]$^+$ (2), 177 (3), 163 (3), 149 (5), 136 (24), 122 (18), 121 (32), 108 (11), 107 (77), 105 (13), 95 (12), 94 (18), 93 (69), 91 (47), 81 (17), 80 (19), 79 (100), 78 (12), 77 (35), 67 (19), 65 (14), 55 (19), 43 (20), 41 (24); HRMS (EI): m/z: calculated for $C_{15}H_{26}$ [M]$^+$: 206.20345; found: 206.20321.

((1-Hexylcyclopropyl)ethynyl)benzene (38d). Colorless oil (39 mg, 86%). ^{1}H NMR (400 MHz, CD$_2$Cl$_2$): δ = 7.38–7.32 (m, 2 H), 7.30–7.22 (m, 3 H), 1.67–1.56 (m, 2 H), 1.44–1.38 (m, 2 H), 1.38–1.25 (m, 6 H), 0.98–0.93 (m, 2 H), 0.90 (t, J = 6.9 Hz, 3 H), 0.70–0.65 (m, 2 H); ^{13}C{^{1}H} NMR (100 MHz, CD$_2$Cl$_2$): δ = 130.8, 127.6, 126.7, 123.6, 94.8, 75.9, 37.6, 31.3, 28.6, 27.3, 22.1, 14.8, 13.3, 11.8; IR (film): $\tilde{v}$ = 2955, 2926, 2855, 2223, 1598, 1491, 1022, 753, 689; MS (GC-EI): m/z (%) = 226 [M]$^+$ (9), 197 (3), 183 (4), 169 (14), 156 (100), 141 (86), 128 (30), 115 (47), 102 (5), 91 (37), 77 (15), 67 (4), 63 (4), 55 (4); HRMS (EI): m/z: calculated for $C_{17}H_{22}$ [M]$^+$: 226.17215; found: 226.17216.
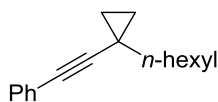
((1-Hexylcyclopropyl)ethynyl)trimethylsilane (38e). Colorless oil (35 mg, 78%). ^{1}H NMR (300 MHz, CDCl$_3$): δ = 1.61–1.45 (m, 2 H), 1.39–1.22 (m, 8 H), 0.94–0.83 (m, 5 H), 0.59–0.52 (m, 2 H), 0.13 (s, 9 H); ^{13}C{^{1}H} NMR (75 MHz, CDCl$_3$): δ = 112.6, 80.4, 38.1, 32.0, 29.2, 27.8, 22.8, 15.9, 14.3, 12.8, 0.5; IR (film): $\tilde{v}$ = 2958, 2928, 2857, 2161, 1459, 1249, 837, 758, 632; MS (GC-EI): m/z (%) = 222 [M]$^+$ (<1), 207 (25), 193 (2), 179 (4, 165 (4), 152 (14), 148 (15), 137 (70), 133 (7), 123 (10), 119 (12), 109 (10), 105 (10), 99 (10), 97 (13), 95 (7), 93 (5), 91 (6), 85 (8), 83 (10), 73 (100), 69 (5), 59 (33), 55 (4); HRMS (EI): m/z: calculated for $C_{14}H_{26}Si$ [M]$^+$: 222.18038; found: 222.18049.
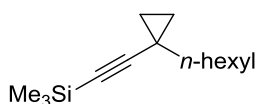
***tert*-Butyldimethyl((5-(1-methylcyclopropyl)pent-4-yn-1-yl)oxy)silane (38f).** Colorless oil (88 mg, 83%). ^{1}H NMR (400 MHz, CDCl$_3$): δ = 3.67 (t, J = 6.2 Hz, 2 H), 2.20 (t, J = 7.0 Hz, 2 H), 1.70–1.61 (m, 2 H), 1.23 (s, 3 H), 0.89 (s, 9 H), 0.82–0.77 (m, 2 H), 0.53–0.48 (m, 2 H), 0.05 (s, 6 H); ^{13}C{^{1}H} NMR (100 MHz, CDCl$_3$): δ = 86.5, 75.2, 61.9, 32.2, 26.1, 24.8, 18.5, 16.2, 15.3, 6.9, −5.2; IR (film): $\tilde{v}$ = 3006, 2954, 2857, 1472, 1463, 1254, 1103, 1068, 833, 774; MS (GC-EI): m/z (%) = 195 (17), 177 (2), 167 (4), 165 (4), 163 (3), 151 (4), 137 (7), 121 (13), 119 (55), 101 (13), 93 (15), 91 (20), 89 (14), 75 (100), 59 (17); HRMS (ESI+): m/z: calculated for $C_{15}H_{28}OSiNa$ [M+Na]$^+$: 275.18016; found: 275.18027.
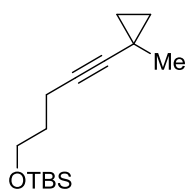
(((4-(1-Methylcyclopropyl)but-3-yn-1-yl)oxy)methyl)benzene (38g). Colorless oil (37 mg, 76%). ^{1}H NMR (400 MHz, CDCl$_3$): δ = 7.39–7.25 (m, 5 H), 4.55 (s, 2 H), 3.55 (t, J = 7.2 Hz, 2 H), 2.45 (t, J = 7.2 Hz, 2 H), 1.24 (s, 3 H), 0.85–0.78 (m, 2 H), 0.55–0.49 (m, 2 H); ^{13}C{^{1}H} NMR (100 MHz, CDCl$_3$): δ = 138.4, 128.5, 127.8 (2 C), 87.5, 73.0, 72.1, 69.1, 24.7, 20.3, 16.2, 6.9; IR (film): $\tilde{v}$ = 2961, 2930, 2908,
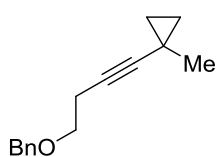
2860, 1454, 1362, 1100, 1020, 734, 696[1]; MS (GC-EI): m/z (%) = 214 [M]$^+$ (<1), 213 (4), 199 (14), 185 (5), 172 (6), 159 (10), 141 (4), 129 (3), 105 (8), 93 (17), 91 (100), 77 (19), 65 (17), 51 (5); HRMS (APPI+): m/z: calculated for $C_{15}H_{18}O$ [M]$^+$: 214.13522; found: 214.13489.

((1-Methylcyclopropyl)ethynyl)benzene (38h). Colorless oil (22 mg, 70%). The spectral data matched the previously reported values.[93] ^{1}H NMR (400 MHz, CDCl$_3$): δ = 7.41–7.34 (m, 2 H), 7.30–7.22 (m, 3 H), 3.17 (s, 3 H), 1.04–0.98 (m, 2 H), 0.71–0.66 (m, 2 H); ^{13}C{^{1}H} NMR (100 MHz, CDCl$_3$): δ = 131.8, 128.3, 127.5, 124.1, 96.4, 75.9, 24.4, 16.8, 7.4.
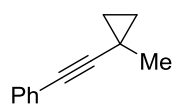
***tert*-Butyldimethyl((5-(1-((trimethylsilyl)methyl)cyclopropyl)pent-4-yn-1-yl)oxy)silane (38i).** Colorless oil (97 mg, 87%). ^{1}H NMR (400 MHz, CDCl$_3$): δ = 3.65 (t, J = 6.2 Hz, 2 H), 2.18 (t, J = 7.1 Hz, 2 H), 1.70–1.61 (m, 2 H), 0.89 (s, 9 H), 0.83–0.78 (m, 2 H), 0.69 (s, 2 H), 0.50–0.45 (m, 2 H), 0.09 (s, 9 H), 0.05 (s, 6 H); ^{13}C{^{1}H} NMR (100 MHz, CDCl$_3$): δ = 86.9, 75.4, 62.0, 32.2, 27.0, 26.1, 18.5, 17.4, 15.3, 8.5, −0.4, −5.2; IR (film): $\tilde{v}$ = 2952, 2929, 2898, 2858, 1248, 1103, 855, 830, 774; MS (EI): m/z (%) = 324 [M]$^+$ (<1), 267 (32), 239 (2), 193 (3), 179 (17), 166 (8), 161 (2), 151 (23), 149 (10), 147 (56), 133 (9), 123 (5), 99 (3), 91 (2), 73 (100), 59 (8), 45 (5); HRMS (ESI+): m/z: calculated for $C_{18}H_{36}OSi_2Na$ [M+Na]$^+$: 347.21969; found: 347.21981.
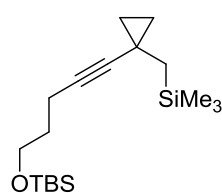
((1-(4-(Benzyloxy)but-1-yn-1-yl)cyclopropyl)methyl)trimethylsilane (38j). Colorless oil (50 mg, 86%). ^{1}H NMR (400 MHz, CDCl$_3$): δ = 7.38–7.25 (m, 5 H), 4.53 (s, 2 H), 3.54 (t, J = 7.2 Hz, 2 H), 2.44 (t, J = 7.2 Hz, 2 H), 0.85–0.80 (m, 2 H), 0.69 (s, 2 H), 0.50–0.46 (m, 2 H), 0.09 (s, 9 H); ^{13}C{^{1}H} NMR (100 MHz, CDCl$_3$): δ = 138.4, 128.5, 127.8, 127.7, 87.9, 73.0, 72.3, 69.1, 26.8, 20.3, 17.4, 8.4, −0.4; IR (film): $\tilde{v}$ = 2952, 2898, 2868, 1246, 1101, 857, 832, 734, 695, 607; MS (GC-EI): m/z (%) = 285 [M−H]$^+$ (<1), 213 (1), 199 (3), 195 (3), 181 (5), 167 (4), 155 (3), 141 (3), 135 (3), 105 (8), 103 (7), 91 (66), 75 (11), 73 (100), 65 (7), 59 (6), 45 (7); HRMS (APPI+): m/z: calculated for $C_{18}H_{26}OSi$ [M]$^+$: 286.17474; found: 286.17464.
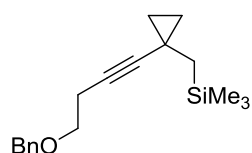
Trimethyl((1-(phenylethynyl)cyclopropyl)methyl)silane (38k). Colorless oil (41 mg, 90%). ^{1}H NMR (400 MHz, CDCl$_3$): δ = 7.30–7.23 (m, 2 H), 7.21–7.12 (m, 3 H), 0.96–0.61 (m, 2 H), 0.73 (s, 2 H), 0.58–0.53 (m, 2 H), 0.07 (s, 9 H); ^{13}C{^{1}H} NMR (100 MHz, CDCl$_3$): δ = 131.5, 128.3, 127.4, 124.3, 97.0, 76.1, 26.6, 18.0, 9.0, −0.4; IR (film): $\tilde{v}$ = 2956, 2930, 2886, 2857, 2022, 1598, 1494, 1247, 854, 844, 833, 752, 689; MS (GC-EI): m/z (%) = 228 [M]$^+$ (8), 213 (15), 197 (9), 185 (7), 169 (4), 159 (19), 154 (7), 135 (7), 115 (4), 105 (3), 73 (100), 59 (7), 45 (7); HRMS (EI): m/z: calculated for $C_{15}H_{20}Si$ [M]$^+$: 228.13343; found: 228.13337.
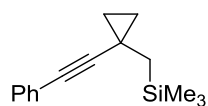
((5-(1-(2-(1,3-Dioxan-2-yl)ethyl)cyclopropyl)pent-4-yn-1-yl)oxy)(*tert*-butyl)dimethyl-silane (38l).
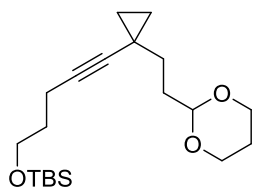
Colorless oil (66 mg, 57%). ^{1}H NMR (400 MHz, CDCl$_3$): δ = 4.59 (t, J = 5.3 Hz, 1 H), 4.13–4.05 (m, 2 H), 3.80–3.71 (m, 2 H), 3.65 (t, J = 6.1 Hz, 2 H), 2.18 (t, J = 7.1 Hz, 2 H), 2.14–2.00 (m, 1 H), 1.89–1.81 (m, 2 H), 1.69–1.61 (m, 2 H), 1.42–1.36 (m, 2 H), 1.36–1.30 (m, 1 H), 0.89 (s, 9 H), 0.80–0.76 (m, 2 H), 0.52–0.50 (m, 2 H), 0.05 (s, 6 H); ^{13}C{^{1}H} NMR (100 MHz, CDCl$_3$): δ = 102.0, 84.6, 76.6, 67.0, 61.9, 33.5, 32.9, 32.3, 26.1, 26.0, 18.5, 15.3, 15.2, 11.6, −5.2; IR (film): $\tilde{v}$ = 2953, 2928, 2854, 1471, 1379, 1287, 1146, 1137, 1103, 1006, 834, 774; MS (EI): m/z (%) = 352 [M]$^+$ (4), 351 (7), 296 (23), 295 (100), 237 (23), 221 (11), 219 (45), 193 (12), 164 (11), 163 (84), 145 (48), 143 (11), 135 (14), 133 (51), 131 (36), 129 (11), 121 (14), 119 (33), 117 (37), 115 (11), 113 (50), 105 (59), 101 (25), 100 (20), 93 (15), 91 (43), 89 (13), 87 (33), 79 (18), 77 (12), 75 (96), 73 (31), 67 (11), 59 (23); HRMS (ESI+): m/z: calculated for C$_{20}$H$_{36}$O$_3$SiNa [M+Na]$^+$: 375.23259; found: 375.23265.

2-(2-(1-(4-(Benzyloxy)but-1-yn-1-yl)cyclopropyl)ethyl)-1,3-dioxane (38m).
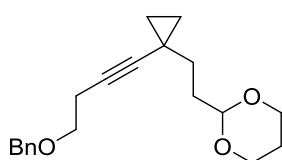
Colorless oil (52 mg, 76%). ^{1}H NMR (400 MHz, CDCl$_3$): δ = 7.42–7.35 (m, 2 H), 7.31–7.23 (m, 3 H), 4.67 (t, J = 5.3 Hz, 1 H), 4.19–4.06 (m, 2 H), 3.84–3.74 (m, 2 H), 2.18–2.03 (m, 1 H), 2.01–1.92 (m, 2 H), 1.59–1.51 (m, 2 H), 1.40–1.33 (m, 1 H), 1.04–0.98 (m, 2 H), 0.74–0.68 (m, 2 H); ^{13}C{^{1}H} NMR (100 MHz, CDCl$_3$): δ = 131.8, 128.2, 127.5, 124.0, 101.9, 94.7, 77.3, 67.0, 33.6, 32.6, 26.0, 15.8, 12.1; IR (film): $\tilde{v}$ = 2957, 2927, 2850, 1143, 1132, 1005, 891, 883, 754, 636; MS (GC-EI): m/z (%) = 256 [M]$^+$ (11), 197 (13), 182 (19), 181 (15), 180 (18), 169 (23), 168 (11), 167 (30), 165 (17), 156 (20), 155 (35), 154 (80), 153 (55), 152 (19), 142 (13), 141 (42), 129 (18), 128 (27), 127 (21), 126 (16), 115 (41), 113 (100), 100 (86), 91 (30), 87 (9), 85 (13), 77 (13), 59 (14), 55 (15); HRMS (ESI+): m/z: calculated for C$_{17}$H$_{20}$O$_2$Na [M+Na]$^+$: 279.13555; found: 279.13568.

2-(2-(1-(3-Phenoxyprop-1-yn-1-yl)cyclopropyl)ethyl)-1,3-dioxane (38n).

Colorless oil (52 mg, 76%). ^{1}H NMR (400 MHz, CDCl$_3$): δ = 7.32–7.22 (m, 2 H), 6.99–6.90 (m, 3 H), 4.64 (s, 2 H), 4.58 (t, J = 5.2 Hz, 1 H), 4.21–4.05 (m, 2 H), 3.78–3.69 (m, 2 H), 2.13–2.00 (m, 1 H), 1.88–1.80 (m, 2 H), 1.46–1.40 (m, 2 H), 1.36–1.29 (m, 1 H), 0.90–0.85 (m, 2 H), 0.62–0.56 (m, 2 H); ^{13}C{^{1}H} NMR (100 MHz, CDCl$_3$): δ = 158.0, 129.8, 129.5, 121.3, 115.1, 101.8, 92.6, 71.7, 67.0, 56.7, 33.4, 32.2, 26.0, 15.5, 11.5; IR (film): $\tilde{v}$ = 2958, 2927, 2854, 1598, 1494, 1377, 1236, 1214, 1144, 1134, 891, 878, 752, 690; MS (GC-EI): m/z (%) = 385 [M−H]$^+$ (<1), 193 (7), 151 (1), 135 (34), 119 (19), 117 (21), 115 (11), 107 (35), 105 (20), 91 (100), 87 (34), 79 (60), 77 (43), 65 (29), 59 (19), 55 (19); HRMS (ESI+): m/z: calculated for C$_{18}$H$_{22}$O$_3$Na [M+Na]$^+$: 309.14611; found: 309.14623.

2-(2-(1-(Phenylethynyl)cyclopropyl)ethyl)-1,3-dioxane (38o). Colorless oil (39 mg, 76%).

^{1}H NMR (400 MHz, CDCl$_3$): δ = 7.32–7.22 (m, 2 H), 6.99–6.90 (m, 3 H), 4.64 (s, 2 H), 4.58 (t, J = 5.2 Hz, 1 H), 4.21–4.05 (m, 2 H), 3.78–3.69 (m, 2 H), 2.13–2.00 (m, 1 H), 1.88–1.80 (m, 2 H), 1.46–1.40 (m, 2 H), 1.36–1.29 (m, 1 H), 0.90–0.85 (m, 2 H), 0.62–0.56 (m, 2 H); ^{13}C{^{1}H} NMR (100 MHz, CDCl$_3$): δ = 158.0, 129.8, 129.5, 121.3, 115.1, 101.8, 92.6, 71.7, 67.0, 56.7, 33.4, 32.2, 26.0, 15.5, 11.5; IR (film): $\tilde{v}$ = 2958, 2927, 2854, 1598, 1494, 1377, 1236, 1214, 1144, 1134, 891, 878, 752, 690; MS (GC-EI): m/z (%) = 385 [M−H]$^+$ (<1), 193 (7), 151 (1), 135 (34), 119 (19), 117 (21), 115 (11), 107 (35), 105 (20), 91 (100), 87 (34), 79 (60), 77 (43), 65 (29), 59 (19), 55 (19); HRMS (ESI+): m/z: calculated for C$_{18}$H$_{22}$O$_3$Na [M+Na]$^+$: 309.14611; found: 309.14623.

***tert*-Butyldimethyl((5-(1-phenethylcyclopropyl)pent-4-yn-1-yl)oxy)silane (38p).** Isolated as a $\approx$ 4:1 mixture with the corresponding allene **39p**. An analytically pure sample was obtained by preparative HPLC as a colorless oil (36 mg, 49%). ^{1}H NMR (400 MHz, CDCl$_3$): δ = 7.31–7.24 (m, 2 H), 7.23–7.14 (m, 3 H), 3.71 (t, J = 6.2 Hz, 2 H), 2.90–2.82 (m, 2 H), 2.26 (t, J = 7.0 Hz, 2 H), 1.75–1.66 (m, 2 H), 1.64–1.55 (m, 2 H), 0.90 (s, 9 H), 0.82–0.77 (m, 2 H), 0.51–0.46 (m, 2 H), 0.07 (s, 6 H); ^{13}C{^{1}H} NMR (100 MHz, CDCl$_3$): δ = 142.5, 128.6, 128.4, 125.8, 84.9, 76.8, 61.9, 40.9, 34.4, 32.3, 26.1, 18.5, 15.3, 15.2, 12.1, −5.1; IR (film): $\tilde{v}$ = 2951, 2928, 2857, 1254, 1105, 835, 776, 669; MS (GC-EI): m/z (%) = 327 (<1), 285 (55), 267 (2), 257 (2), 239 (2), 209 (26), 181 (26), 167 (19), 155 (9), 141 (13), 131 (16), 117 (15), 109 (39), 101 (20), 91 (100), 75 (99), 73 (22), 59 (17); HRMS (ESI+): m/z: calculated for C$_{22}$H$_{34}$OSiNa [M+Na]$^+$: 365.22711; found: 365.22722.
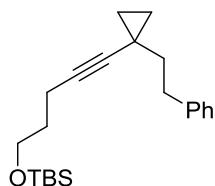
***tert*-Butyl((4-(cyclopropylidenemethylene)-6-phenylhexyl)oxy)dimethylsilane (39p).** An analytically pure sample was obtained by preparative HPLC as a colorless oil (9 mg, 12%). ^{1}H NMR (500 MHz, CDCl$_3$): δ = 7.30–7.24 (m, 2 H), 7.21–7.14 (m, 3 H), 3.63 (t, J = 6.5 Hz, 2 H), 2.76–2.70 (m, 2 H), 2.36–2.30 (m, 2 H), 2.09 (t, J = 7.5 Hz, 2 H), 1.70–1.63 (m, 2 H), 1.44–1.39 (m, 4 H), 0.89 (s, 9 H), 0.51–0.46 (m, 2 H), 0.04 (s, 6 H); ^{13}C{^{1}H} NMR (125 MHz, CDCl$_3$): δ = 186.4, 142.6, 128.5, 128.4, 125.8, 107.3, 79.4, 63.0, 35.3, 34.4, 31.1, 29.8, 26.1, 18.5, 6.7, −5.1; IR (film): $\tilde{v}$ = 2952, 2930, 2857, 1255, 1101, 835, 776, 698; MS (GC-EI): m/z (%) = 342 [M]$^+$ (<1), 285 (6), 267 (2), 223 (6), 209 (10), 195 (10), 181 (29), 169 (31), 167 (40), 155 (10), 141 (22), 129 (11), 119 (15), 117 (17), 115 (12), 105 (15), 93 (16), 91 (100), 89 (14), 77 (11), 75 (65), 73 (49), 59 (16); HRMS (APPI+): m/z: calculated for C$_{22}$H$_{35}$OSi [M+H]$^+$: 343.24517; found: 343.24521.
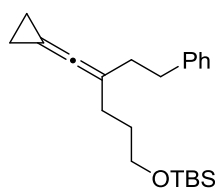
((5-([1,1'-Bi(cyclopropan)]-1-yl)pent-4-yn-1-yl)oxy)(*tert*-butyl)dimethylsilane (38q).
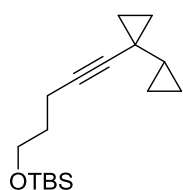
Colorless oil (70 mg, 59%). ^{1}H NMR (400 MHz, CDCl$_3$): δ = 3.67 (t, J = 6.2 Hz, 2 H), 2.20 (t, J = 7.0 Hz, 2 H), 1.70–1.61 (m, 2 H), 0.89 (s, 9 H), 0.84–0.73 (m, 1 H), 0.77–0.74 (m, 2 H), 0.56–0.52 (m, 2 H), 0.40–0.34 (m, 2 H), 0.28–0.23 (m, 2 H), 0.05 (s, 6 H); ^{13}C{^{1}H} NMR (100 MHz, CDCl$_3$): δ = 84.4, 76.2, 61.9, 32.3, 26.1, 18.5, 16.4, 15.3, 14.1, 13.0, 2.8, −5.2; IR (film): $\tilde{v}$ = 2952, 2929, 2857, 1471, 1254, 1103, 1069, 1017, 833, 774; MS (GC-EI): m/z (%) = 221 (20), 193 (6), 175 (5), 163 (7), 149 (5), 145 (18), 135 (6), 119 (12), 117 (22), 115 (11), 105 (17), 101 (16), 91 (27), 89 (17), 79 (11), 77 (11), 75 (100), 73 (21), 59 (21); HRMS (CI): m/z: calculated for C$_{17}$H$_{31}$OSi [M+H]$^+$: 279.21442; found: 279.21414.

(1-(4-(Benzyloxy)but-1-yn-1-yl)cyclopropyl)benzene (38r) and **(4-(benzyloxy)-1-cyclo-propylidenebut-1-en-2-yl)benzene (39r).** Colorless oil (40 mg, 66% combined yield, **38r**:**39r** ≈ 1.3:1); distinct signals of the alkyne are marked * and those of the allene **. ^{1}H NMR (400 MHz, CDCl$_3$): δ = 7.41–7.25 (m, overlapping), 7.21–7.15 (m, overlapping), 4.57* (s, 2 H), 4.54** (s, 2 H), 3.72* (t, J = 7.2 Hz, 2 H), 3.62** (t, J = 7.1 Hz, 2 H), 2.86** (t, J = 7.1 Hz, 2 H), 2.56* (t, J = 7.2 Hz, 2 H), 1.71–1.65** (m, 2 H), 1.65–1.59** (m, 2 H), 1.41–1.35* (2 H), 1.23–1.18* (m, 2 H); ^{13}C{^{1}H} NMR (100 MHz, CDCl$_3$): δ = 188.9**, 142.5*, 138.6**, 138.3*, 137.8**, 128.6, 128.5 (2 C), 128.4, 127.8 (3 C), 127.7, 126.4, 126.0, 125.9, 125.6, 104.9**, 85.1*, 80.1**, 75.1*, 73.2**, 73.1*, 69.4**, 69.0*, 30.8**, 20.5*, 20.2*, 15.8*, 8.3**; IR (film): $\tilde{v}$ = 3060, 3028, 3008, 2912, 2858, 2006, 1600, 1496, 1453, 1272, 1100, 1027, 752, 734, 694; MS* (GC-EI): m/z (%) = 276 [M]$^+$ (0.97), 247 (1.75), 231 (1.13), 215 (1.38), 185 (2.54), 170 (8.74), 155 (18.39), 153 (12.25), 143 (13.23), 141 (13.00), 129 (15.55), 128 (15.68), 117 (14.86), 115 (21.73), 106 (18.46), 105 (24.21), 92 (33.99), 91 (100.00), 79 (11.29), 78 (12.03), 77 (36.46), 65 (15.70), 51 (14.46); MS** (GC-EI): m/z (%) = 276 [M]$^+$ (2), 243 (1), 231 (1), 215 (2), 185 (11), 170 (8), 155 (20), 153 (12), 143 (13), 141 (16), 129 (20), 128 (16), 117 (18), 115 (26), 106 (17), 105 (22), 92 (32), 91 (100), 79 (12), 78 (15), 77 (38), 65 (17), 51 (15); HRMS (APPI+): m/z: calculated for C$_{20}$H$_{20}$O [M]$^+$: 276.15087; found: 276.15041.
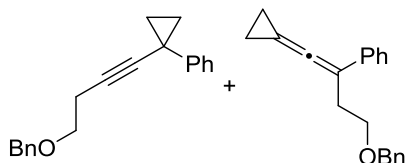
((1-Phenylcyclopropyl)ethynyl)benzene (38s) and **(2-cyclopropylideneethene-1,1-diyl)di-benzene (39s).** Colorless oil (32 mg, 73% combined yield, **38s**:**39s** ≈ 7.3:1); distinct signals of the alkyne are marked * and those of the allene **. ^{1}H NMR (400 MHz, CDCl$_3$): δ = 7.49–7.19 (m, overlapping), 1.75** (s, 4 H), 1.60–1.53* (m, 2 H), 1.39–1.33* (m, 2 H); ^{13}C{^{1}H} NMR (100 MHz, CDCl$_3$): δ = 190.4**, 142.0*, 137.9**, 131.9, 128.6, 128.5, 128.4, 128.3, 127.8, 127.0, 126.2, 125.6, 123.8*, 111.9**, 93.9*, 79.2**, 78.5*, 20.7*, 16.4*, 9.1**; IR (film): $\tilde{v}$ = 3082, 3058, 3024, 2234,
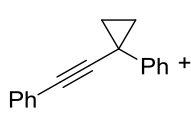
2215, 2001, 1597, 1490, 1442, 1000, 954, 751, 689, 556; MS* (GC-EI): m/z (%) = 218 [M]$^+$ (100), 217 (78), 215 (36), 203 (53), 202 (82), 190 (13), 189 (37), 165 (5), 163 (7), 141 (9), 139 (9), 129 (5), 115 (25), 108 (13), 107 (10), 101 (12), 95 (20), 94 (11), 91 (11), 77 (6), 63 (6); MS** (GC-EI): m/z (%) = 218 [M]$^+$ (100), 217 (89), 215 (34), 203 (45), 202 (68), 192 (13), 191 (12), 189 (20), 178 (11), 165 (15), 141 (7), 139 (7), 129 (4), 115 (18), 108 (8), 107 (16), 101 (23), 95 (15), 94 (10), 91 (6), 77 (5), 63 (5); HRMS (APPI+): m/z: calculated for $C_{17}H_{14}$ [M]$^+$: 218.10900; found: 218.10861.

5.2.5 Fe-Catalyzed Cross-Couplings of 1-Vinylcyclopropyl Tosylates

Representative Procedure for the Optimization of the Fe-Catalyzed Cross-Coupling Reactions of 1-Vinylcyclopropyl Tosylates (*cf.* Table 3).

1-Methoxy-4-(2-(1-vinylcyclopropyl)ethyl)benzene (42). Tosylate **40** (119 mg, 0.499 mmol) and Fe(acac)$_3$ (8.8 mg, 0.025 mmol) were dissolved in dry THF (5 mL) and the solution was cooled in an ice bath. A premixed solution of 2-(4-methoxyphenyl)ethylmagnesium chloride (**41**, 0.2 M in THF, 3 mL, 0.599 mmol) and TMEDA (90 μL, 0.599 mmol) was added *via* syringe pump over the course of 30 min. After consumption of the starting material, as indicated by TLC, 1,3,5-trimethoxybenzene (24.7 mg, 0.147 mmol), sat. aq. NH$_4$Cl (4 mL), and deionized water (2 mL) were subsequently added. The aqueous phase was extracted with *tert*-butyl methyl ether (3 × 4 mL). The combined organic layers were dried over Na$_2$SO$_4$ and concentrated *in vacuo*. The crude material was analyzed by ^{1}H NMR spectroscopy. ^{1}H NMR (400 MHz, CDCl$_3$): δ = 7.12–7.07 (m, 2 H), 6.84–6.80 (m, 2 H), 5.63 (dd, J = 17.4 Hz, J = 10.7 Hz, 1 H), 5.00 (dd, J = 17.4 Hz, J = 1.3 Hz, 1 H), 4.97 (dd, J = 10.7 Hz, J = 1.3 Hz, 1 H), 3.79 (s, 3 H), 2.67–2.61 (m, 2 H), 1.72–1.65 (m, 2 H), 0.63–0.53 (m, 4 H); ^{13}C{^{1}H}-NMR (100 MHz, CDCl$_3$): δ = 157.8, 143.8, 135.0, 129.3, 113.8, 111.0, 55.4, 38.5, 32.6, 22.6, 14.3; IR (film): $\tilde{v}$ = 3076, 2998, 2933, 2858, 2834, 1512, 1245, 1039; MS (GC-EI): m/z (%) = 202 [M]$^+$ (7.55), 187 (2.20), 173 (5.46), 160 (2.35), 134 (7.59), 121 (100.00), 108 (1.58), 91 (5.01), 77 (5.43), 65 (1.59), 53 (1.01); HRMS (EI): m/z: calculated for $C_{14}H_{18}O$ [M]$^+$: 202.13577, found: 202.13587.
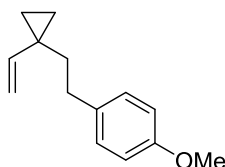
Representative Procedure for the Fe-Catalyzed Cross-Coupling Reactions of (*E*)-1-Styryl-cyclopropyl Tosylate (43).

(*E*)-(2-(1-Methylcyclopropyl)vinyl)benzene (44h). Tosylate **43** (60 mg, 0.191 mmol) and Fe(acac)$_3$ (3.4 mg, 0.010 mmol) were dissolved in dry THF (1.9 mL) and the solution was cooled in an ice bath. A premixed solution of MeMgCl (0.5 M in THF, 0.46 mL, 0.229 mmol) and TMEDA (34 μL, 0.229 mmol) was added *via* syringe pump over the course of 30 min. The resulting brown-red solution was stirred at 0 °C for 2.5 h.
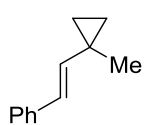
The reaction was quenched with sat. aq. NH$_4$Cl (3 mL) and deionized water (1.5 mL) and the aqueous phase was extracted with *tert*-butyl methyl ether (3 × 4 mL). The combined organic layers were dried over Na$_2$SO$_4$ and concentrated *in vacuo*. The residue was purified by flash chromatography (silica, *n*-pentane/Et$_2$O, 100:1) to give compound **44h** as a colorless oil (24 mg, 79%). ^{1}H NMR (300 MHz, CD$_2$Cl$_2$): δ = 7.36–7.23 (m, 2 H), 7.20–7.12 (m, 3 H), 6.34 (d, *J* = 16.0 Hz, 1 H), 5.86 (d, *J* = 16.0 Hz, 1 H), 1.29 (s, 3 H), 0.75–0.65 (m, 4 H); ^{13}C{^{1}H} NMR (75 MHz, CD$_2$Cl$_2$): δ = 139.2, 138.5, 128.9, 126.9, 126.0, 125.7, 21.6, 18.1, 15.9; IR (film): $\tilde{v}$ = 3077, 3024, 2956, 1648, 1602, 1492, 1447, 1425, 1385, 1073, 1014, 935, 960, 846, 804, 743, 690, 591, 523, 411; MS (GC-EI): *m/z* (%) = 158 [M]$^+$ (16), 143 (100), 128 (74), 115 (25), 102 (5), 91 (13), 77 (13), 65 (7), 51 (7); HRMS (EI): *m/z*: calculated for C$_{12}$H$_{14}$ [M]$^+$: 158.10955; found: 158.10938.

The following compounds were prepared analogously (*cf.* Table 4):

(*E*)-(2-(1-Hexylcyclopropyl)vinyl)benzene (44a). Colorless oil (20 mg, 62% combined yield, **44a**:**45**[92] ≈ 1:2.3); distinct signals of **44a** are marked * and those of **45** **. ^{1}H NMR (400 MHz, CDCl$_3$): δ = 7.35–7.25 (m, overlapping), 7.20–7.14 (m, overlapping), 6.47** (d, *J* = 15.8 Hz, 1 H), 6.27* (d, *J* = 16.1 Hz, 1 H), 6.03* (d, *J* = 16.1 Hz, 1 H), 5.73** (dd, *J* = 15.8 Hz, *J* = 9.0 Hz, 1 H), 1.62–1.52** (m, 1 H), 1.52–1.37* (m, 4 H), 1.36–1.27* (m, 6 H), 0.89* (t, *J* = 6.9 Hz, 3 H), 0.86–0.79** (m, 2 H), 0.71–0.66* (m, 2 H), 0.65–0.60* (m, 2 H), 0.54–0.48** (m, 2 H); ^{13}C{^{1}H} NMR (100 MHz, CDCl$_3$): δ = 138.1*, 137.9**, 136.7*, 135.1**, 128.6 (2 C), 127.5**, 126.7 (2 C), 126.3*, 125.8, 125.7, 36.8*, 32.0*, 29.8*, 27.3*, 22.8*, 22.6*, 14.7 (2 C), 14.3**, 7.4**; IR (film): $\tilde{v}$ = 3081, 3024, 2926, 2855, 1650, 1490, 1448, 953, 742, 691, 516; MS* (GC-EI, %): *m/z* = 228 [M]$^+$ (2), 157 (2), 143 (100), 128 (26), 115 (10), 104 (2), 91 (12), 77 (3), 65 (2), 55 (2); HRMS* (EI): *m/z*: calculated for C$_{17}$H$_{24}$ [M]$^+$: 228.18780, found: 228.18758.

(*E*)-(2-(1-Ethylcyclopropyl)vinyl)benzene (44b). Colorless oil (6 mg, 17%). ^{1}H NMR (400 MHz, CDCl$_3$): δ = 7.35–7.24 (m, 4 H), 7.20–7.14 (m, 1 H), 6.29 (dd, *J* = 16.1 Hz, *J* = 3.0 Hz, 1 H), 5.99 (dd, *J* = 16.1 Hz, *J* = 3.0 Hz, 1 H), 1.54 (q, *J* = 7.4 Hz, 2 H), 0.98 (t, *J* = 7.4 Hz, 3 H), 0.71–0.60 (m, 4 H); ^{13}C{^{1}H} NMR (100 MHz, CDCl$_3$): δ = 138.1, 136.4, 128.6, 126.7, 126.3, 125.8, 29.2, 23.6, 14.5, 11.4; IR (film): $\tilde{v}$ = 3078, 3025, 2999, 2963, 2930, 2874, 1645, 1602, 1494, 1448, 1376, 1046, 1015, 963, 939, 818, 746, 692, 538; MS (GC-EI): *m/z* (%) = 171 [M]$^+$ (2), 143 (100), 128 (48), 115 (13), 102 (2), 91 (5); HRMS (APPI+): *m/z*: calculated for C$_{13}$H$_{16}$ [M]$^+$: 172.12465; found: 172.12436.

(E)-(2-(1-(Ethyl-d_5)cyclopropyl)vinyl)benzene ([D$_5$]-44b). Colorless oil (5 mg, 16%). ^{1}H NMR (400 MHz, CDCl$_3$): δ = 7.38–7.25 (m, 4 H), 7.22–7.15 (m, 1 H), 6.30 (d, J = 16.1 Hz, 1 H), 5.98 (d, J = 16.1 Hz, 1 H), 0.71–0.61 (m, 4 H); ^{13}C{^{1}H} NMR (100 MHz, CDCl$_3$): δ = 138.1, 136.5, 128.6, 126.7, 126.3, 125.8, 23.4, 14.4; IR (film): $\tilde{v}$ = 3077, 3026, 3000, 2220, 1646, 1601, 1493, 1448, 1056, 1016, 962, 941, 744, 692, 531; MS (GC-EI): m/z (%) = 177 [M]$^+$ (4), 143 (100), 128 (44), 115 (13), 102 (3), 91 (8), 77 (5), 65 (5), 51 (4); HRMS (EI): m/z: calculated for C$_{13}$H$_{11}$D$_5$ [M]$^+$: 177.15604; found: 177.15583.

(E)-(2-(1-Neopentylcyclopropyl)vinyl)benzene (44c). Colorless oil (12 mg, 30%). ^{1}H NMR (400 MHz, CDCl$_3$): δ = 7.34–7.25 (m, 4 H), 7.20–7.14 (m, 1 H), 6.50 (d, J = 16.0 Hz, 1 H), 6.14 (d, J = 16.0 Hz, 1 H), 1.46 (s, 2 H), 0.95 (s, 9 H), 0.78–0.74 (m, 2 H), 0.62–0.57 (m, 2 H); ^{13}C{^{1}H} NMR (100 MHz, CDCl$_3$): δ = 138.2, 137.2, 128.6, 126.7, 125.9, 124.8, 52.5, 33.0, 30.8, 21.2, 14.9; IR (film): $\tilde{v}$ = 3080, 3025, 2949, 2902, 1476, 1363, 963, 738, 691; MS (GC-EI, %): m/z = 214 [M]$^+$ (3), 157 (4), 143 (100), 128 (22), 115 (10), 91 (11), 77 (5), 65 (3), 57 (58), 41 (12) ; HRMS (EI): m/z: calculated for C$_{16}$H$_{22}$ [M]$^+$: 214.17215, found: 214.17203.

(E)-Trimethyl((1-styrylcyclopropyl)methyl)silane (44d). Colorless oil (16 mg, 36%). ^{1}H-NMR (400 MHz, CDCl$_3$): δ = 7.33–7.25 (m, 4 H), 7.20–7.14 (m, 1 H), 6.23 (d, J = 15.9 Hz, 1 H), 6.05 (d, J = 15.9 Hz, 1 H), 0.90 (s, 2 H), 0.77–0.72 (m, 2 H), 0.64–0.60 (m, 2 H), 0.06 (s, 9 H); ^{13}C{^{1}H} NMR (100 MHz, CDCl$_3$): δ = 138.2, 138.0, 128.7, 126.7, 126.0, 125.8, 25.1, 20.0, 16.6, 0.3; IR (film): $\tilde{v}$ = 3025, 2952, 2894, 1246, 962, 833, 742, 690, 524; MS (GC-EI, %): m/z = 230 [M]$^+$ (4), 215 (1), 156 (12), 143 (22), 128 (8), 115 (4), 91 (4), 73 (100), 65 (1), 59 (7), 45 (9); HRMS (EI): m/z: calculated for C$_{15}$H$_{22}$Si [M]$^+$: 230.14908, found: 230.14894.

(E)-2-(2-(1-Styrylcyclopropyl)ethyl)-1,3-dioxane (44e). Colorless oil (18 mg, 37%). ^{1}H NMR (400 MHz, CDCl$_3$): δ = 7.34–7.24 (m, 4 H), 7.19–7.14 (m, 1 H), 6.30 (d, J = 16.0 Hz, 1 H), 5.99 (d, J = 16.0 Hz, 1 H), 4.56 (t, J = 5.1 Hz, 1 H), 4.10 (ddd, J = 11.8 Hz, J = 5.0 Hz, J = 1.3 Hz, 2 H), 3.80–3.71 (m, 2 H), 2.15–2.00 (m, 1 H), 1.80–1.72 (m, 2 H), 1.64–1.57 (m, 2 H), 1.37–1.30 (m, 1 H), 0.73–0.62 (m, 4 H); ^{13}C{^{1}H} NMR (100 MHz, CDCl$_3$): δ = 137.9, 135.9, 128.6, 126.7 (2 C), 125.9, 102.3, 67.0, 33.0, 30.6, 26.0, 22.1, 14.7; IR (film): $\tilde{v}$ = 2958, 2850, 1133, 1085, 1046, 1004, 963, 937, 885, 745, 693; MS (GC-EI, %): m/z = 258 [M]$^+$ (7), 182 (33), 182 (33), 156 (75), 141 (53), 128 (58), 113 (33), 100 (100), 91 (41), 87 (37), 77 (14), 65 (8), 59 (17), 41 (14), 31 (16); HRMS (ESI+): m/z: calculated for C$_{17}$H$_{22}$O$_2$Na [M+Na]$^+$: 281.15120, found: 281.15140.

(E)-(2-(1-Isobutylcyclopropyl)vinyl)benzene (44f). Colorless oil (21 mg, 54%). ^{1}H NMR (400 MHz, CDCl$_3$): δ = 7.35–7.25 (m, 4 H), 7.20–7.14 (m, 1 H), 6.26 (d, J = 16.0 Hz, 1 H), 6.20 (d, J = 16.0 Hz, 1 H), 1.89 (sept, J = 6.7 Hz, 1 H), 1.39 (d, J = 7.2 Hz, 2 H), 0.93 (d, J = 6.7 Hz, 6 H), 0.75–0.70 (m, 2 H), 0.62–0.58 (m, 2 H); ^{13}C{^{1}H} NMR (100 MHz, CDCl$_3$): δ = 138.0, 136.2, 128.6, 126.8, 126.4, 125.9, 46.6, 27.3, 23.3, 21.3, 14.7; IR (film): $\tilde{v}$ = 3079, 3025, 2952, 2901, 2868, 1646, 1599, 1467, 1494, 1448, 1365, 1383, 1172, 1048, 1073, 1017, 961, 809, 743, 692, 534; MS (GC-EI, %): m/z = 200 [M]$^+$ (4), 171 (1), 143 (100), 128 (32), 115 (13), 91 (14), 77 (5), 65 (3); HRMS (EI): m/z: calculated for C$_{15}$H$_{20}$ [M]$^+$: 200.15650, found: 200.15637.
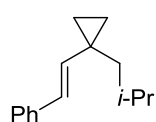
(E)-1-Styryl-1,1'-bi(cyclopropane) (44g). Colorless oil (26 mg, 73%). ^{1}H NMR (400 MHz, CDCl$_3$): δ = 7.37–7.32 (m, 2 H), 7.32–7.26 (m, 2 H), 7.20– 7.15 (m, 1 H), 6.62 (d, J = 15.9 Hz, 1 H), 5.94 (d, J = 15.9 Hz, 1 H), 1.33–1.24 (m, 1 H), 0.60–0.55 (m, 4 H), 0.51–0.45 (m, 2 H), 0.11–0.50 (m, 2 H); ^{13}C{^{1}H} NMR (100 MHz, CDCl$_3$): δ = 138.5, 138.1, 128.6, 126.7, 126.2, 125.8, 23.2, 13.6, 12.1, 2.4; IR (film): $\tilde{v}$ = 3079, 3004, 1645, 1601, 1494, 1448, 1423, 1290, 1099, 1072, 1047, 1017, 959, 936, 870, 823, 744, 691, 592, 537, 480; MS (GC-EI, %): m/z = 184 [M]$^+$ (21), 169 (100), 155 (43), 143 (69, 141 (73), 128 (93), 115 (52), 102 (12), 91 (67), 77 (28), 65 (12), 51 (11); HRMS (EI): m/z: calculated for C$_{14}$H$_{16}$ [M]$^+$: 184.12520, found: 184.12503.
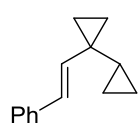
(E)-(2-(Cyclopropyl-1-d)vinyl)benzene ([D]-45). Colorless oil (6 mg, 20%). ^{1}H NMR (400 MHz, CDCl$_3$): δ = 7.36–7.25 (m, 4 H), 7.21–7.14 (m, 1 H), 6.47 (d, J = 15.8 Hz, 1 H), 5.73 (dt, J = 15.8 Hz, J = 4.5 Hz, 1 H), 0.85–0.79 (m, 2 H), 0.54–0.48 (m, 2 H); ^{13}C{^{1}H} NMR (100 MHz, CDCl$_3$): δ = 137.9, 135.0, 128.6, 127.5, 126.7, 125.7, 7.3; IR (film): $\tilde{v}$ = 3077, 3026, 3000, 2220, 1646, 1601, 1493, 1448, 1056, 1016, 962, 941, 744, 692, 531; MS (GC-EI): m/z (%)= 145 [M]$^+$ (49), 144 (43), 143 (12), 130 (100), 129 (96), 128 (50), 116 (26), 115 (25), 102 (7), 91 (13), 89 (8), 77 (12), 71 (12), 67 (10), 66 (11), 65 (12), 63 (12), 51 (14), 39 (12); HRMS (APPI+): m/z: calculated for C$_{11}$H$_{11}$D [M]$^+$: 145.09963, found: 145.09947.
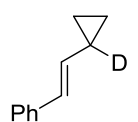
1,1'-Di((E)-styryl)-1,1'-bi(cyclopropane) (46). Colorless solid (7 mg, 26%). Crystals suitable for X-ray diffraction analysis were grown by slow evaporation of a solution in hexanes. M.p.: 65 °C; ^{1}H NMR (400 MHz, CDCl$_3$): δ = 7.34–7.23 (m, 4 H), 7.18–7.13 (m, 1 H), 6.46 (d, J = 16.2 Hz, 1 H), 6.07 (d, J = 16.2 Hz, 1 H), 0.83–0.75 (m, 4 H); ^{13}C{^{1}H} NMR (100 MHz, CDCl$_3$): δ = 138.1, 136.5, 128.6, 127.1, 126.7, 125.9, 25.1, 13.9; IR (solid): $\tilde{v}$ = 3077, 3019, 2997, 1643, 1493, 1053, 965, 948, 749, 690, 538; MS (GC-EI): m/z (%) = 286 [M]$^+$ (23), 258 (8), 243 (6), 228 (9), 215 (7), 195 (92), 182 (62), 167 (100), 154 (44), 141 (44), 128 (66), 115 (62), 103 (11), 91 (96), 77 (20), 65 (14); HRMS (EI): m/z: calculated for C$_{22}$H$_{22}$ [M]$^+$: 286.17215; found: 286.17201.
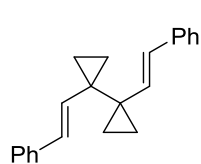
(E)-(5-(1-Methylcyclopropyl)pent-4-en-1-yl)benzene (54). Colorless oil (48 mg, 86%). ^{1}H NMR (400 MHz, CDCl$_3$): δ = 7.32–7.24 (m, 2 H), 7.22–7.14 (m, 3 H), 5.37 (dt, J = 15.4 Hz, J = 6.8 Hz, 1 H), 5.08 (d, J = 15.4 Hz, 1 H), 2.62 (t, J = 7.5 Hz, 2 H), 2.05 (q, J = 7.5 Hz, 2 H), 1.69 (apparent quint, J = 7.5 Hz, 2 H), 1.15 (s, 3 H), 0.55–0.48 (m, 4 H); ^{13}C{^{1}H} NMR (100 MHz, CDCl$_3$): δ = 142.8, 138.3, 128.6, 128.4, 125.7, 125.6, 35.5, 32.3, 31.6, 21.8, 17.0, 15.0; IR (film): $\tilde{v}$ = 3075, 3026, 2929, 2856, 1604, 1496, 1453, 1384, 1084, 1013, 965, 932, 742, 697, 575, 487; MS (GC-EI): m/z (%) = 200 [M]$^+$ (3), 185 (1), 171 (3), 143 (5), 130 (19), 117 (12), 109 (12), 104 (58), 91 (52), 81 (100), 67 (35), 55 (12), 41 (12); HRMS (EI): m/z: calculated for C$_{15}$H$_{20}$ [M]$^+$: 200.15650; found: 200.15665.
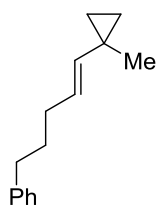
1-(1-Methylcyclopropyl)cyclohex-1-ene (55). Colorless oil (13 mg, 48%). ^{1}H NMR (400 MHz, CDCl$_3$): δ = 5.51–5.46 (m, 1 H), 2.02–1.95 (m, 2 H), 1.94–1.88 (m, 2 H), 1.63–1.48 (m, 4 H), 1.12 (s, 3 H), 0.59–0.54 (m, 2 H), 0.34–0.30 (m, 2 H); ^{13}C{^{1}H} NMR (100 MHz, CDCl$_3$): δ = 141.3, 120.2, 26.0, 25.4, 24.0, 23.3, 22.8, 21.5, 12.6; IR (film): $\tilde{v}$ = 3076, 3001, 2924, 2858, 2837, 1448, 1424, 1376, 1313, 1264, 1136, 1082, 1039, 1010, 932, 919, 862, 840, 795, 735, 545, 463, 434; MS (GC-EI): m/z (%) = 136 [M]$^+$ (5), 121 (66), 107 (34), 105 (7), 93 (73), 79 (100), 67 (38), 55 (17), 41 (20); HRMS (EI): m/z: calculated for C$_{10}$H$_{16}$ [M]$^+$: 136.12520; found: 136.12534.
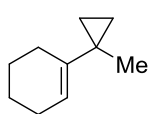
(1R,5S,6s)-6-Methyl-6-vinylbicyclo[3.1.0]hexane (56). Colorless oil (10 mg, 39%). ^{1}H NMR (500 MHz, CDCl$_3$): δ = 5.78 (dd, J = 17.4 Hz, J = 10.7 Hz, 1 H), 5.15 (dd, J = 17.4 Hz, J = 2.0 Hz, 1 H), 5.11 (dd, J = 10.7 Hz, J = 2.0 Hz, 1 H), 1.92–1.79 (m, 2 H), 1.81–1.71 (m, 1 H), 1.71–1.64 (m, 2 H), 1.45–1.35 (m, 1 H), 1.35–1.33 (m, 2 H), 1.08 (s, 3 H); ^{13}C{^{1}H} NMR (126 MHz, CDCl$_3$): δ = 138.6, 114.7, 34.3, 26.1, 25.9 (2 C), 24.2; IR (film): $\tilde{v}$ = 3007, 2926, 2860, 1446, 914; MS (GC-EI): m/z (%) = 122 [M]$^+$ (16), 107 (44), 93 (37), 91 (28), 81 (31), 79 (100), 77 (29), 67 (27), 65 (14), 53 (24); HRMS (EI): m/z: calculated for C$_9$H$_{14}$ [M]$^+$: 122.10955; found: 122.10942.

5.3 Reactivity of Piano-Stool Rh(III) & Ir(III) Carbene Complexes

5.3.1 Synthesis of Rhodium Complexes

$[Cp*RhCl_2]_2$ and $[Cp*Rh(MeCN)_3](SbF_6)_2$ were purchased from Strem Chemicals. $[Cp*IrCl_2]_2$ and $[Cp*IrI_2]_2$ were purchased from Sigma-Aldrich. All four complexes were used as received. The following rhodium complexes were synthesized according to literature procedures: $[Cp*RhI_2]_2$,[205] $[Cp*RhBr_2]_2$.[206]

Chloro[2-(*N*′-phenylcarbamimidoyl-κ*N*′)phenyl](η⁵-pentamethylcyclopentadienyl)-

rhodium(III) (97). *N*-Phenylbenzamidine (**96**, 33.2 mg, 0.169 mmol), $[Cp*RhCl_2]_2$ (49.5 mg, 0.080 mmol) and NaOAc (41.0 mg, 0.500 mmol) were stirred in toluene (3 mL) at reflux temperature overnight. The solvent was removed *in vacuo* and the residue was extracted with CH_2Cl_2 (5 × 3 mL). The solution was concentrated until a precipitate formed which was collected by filtration and dried *in vacuo* to give **97** as an orange powder (47 mg, 63%). Crystals suitable for X-ray diffraction were grown by slow diffusion of *n*-pentane into a solution of **97** in CH_2Cl_2. M.p.: >250 °C; ¹H NMR (400 MHz, CD_2Cl_2): δ = 7.72 (dd, *J* = 7.6 Hz, *J* = 0.9 Hz, 1 H, H4), 7.51 (s br, 2 H, H11), 7.42 (t, *J* = 7.8 Hz, 2 H, H12), 7.24 (dd, *J* = 7.7 Hz, *J* = 1.2 Hz, 1 H, H7), 7.23–7.17 (m, 1 H, H13), 7.13 (td, *J* = 7.4 Hz, *J* = 1.0 Hz, 1 H, H5), 6.80 (t, *J* = 7.5 Hz, 1 H, H6), 5.26 (s br, 2 H, N$\underline{H}_2$), 1.32 (s, 15 H, H2); ¹³C{¹H} NMR (100 MHz, CD_2Cl_2): δ = 179.3 (d, *J* = 32.2 Hz, C3), 164.5 (d, *J* = 2.9 Hz, C9), 147.8 (C10), 141.3 (C8), 136.9 (C4), 130.6 (C5), 129.7 (s br, C12), 125.8 (C13), 125.0 (s br, C11), 124.4 (C7), 122.5 (C6), 95.5 (d, *J* = 6.5 Hz, C1), 8.8 (C2); IR (solid): $\tilde{\nu}$ = 3420, 3299, 3240, 3214, 3191, 3173, 1631, 1588, 1488, 1418, 738, 702; HRMS (EI): *m/z*: calculated For $C_{23}H_{26}N_2ClRh$ $[M]^+$: 468.08325; found: 468.08340.
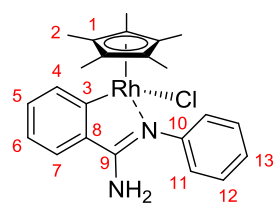
(Acetonitrile)[2-(*N*′-phenylcarbamimidoyl-κ*N*′)phenyl](η⁵-pentamethylcyclopentadi-

enyl)rhodium(III) hexafluoroantimonate (99). $[Cp*Rh(MeCN)_3](SbF_6)_2$ (51.1 mg, 0.061 mmol), NaOAc (50.3 mg, 0.613 mmol) and *N*-phenyl-benzamidine (**96**, 12.7 mg, 0.065 mmol) were stirred in MeCN (5 mL) at reflux temperature for 1 h. The solvent was removed *in vacuo*. The residue was extracted with CH_2Cl_2 (4 × 2 mL) and filtered over Celite. The solvent was removed *in vacuo* and the residue was washed with Et_2O (2 × 0.5 mL). Upon drying *in vacuo*, the residue solidified and complex **99** was obtained as a red orange powder (35 mg, 80%). ¹H NMR (400 MHz, CD_2Cl_2): δ = 7.82 (dd, *J* = 7.6 Hz, *J* = 0.6 Hz, 1 H, H4), 7.60–7.53 (m, 2 H, H12), 7.40 (td, *J* = 7.4 Hz, *J* = 1.3 Hz, 1 H, H5), 7.37–7.31 (m, 2 H, H7, H13), 7.27–7.17 (m, 3 H, H6, H11), 5.67 (s br, 2 H, N$\underline{H}_2$), 2.27 (s, 3 H, H15), 1.40 (s, 15 H, H2); ¹³C{¹H} NMR (100 MHz, CD_2Cl_2): δ = 174.5 (d, *J* = 30.2 Hz, C3), 165.7 (d, *J* = 2.9 Hz, C9), 146.4 (C10), 141.1 (C8), 136.7 (C4), 130.7 (C12), 127.1 (C13), 124.9 (C7), 124.4 (C11), 124.2 (C6), 122.6 (s br, C14), 97.9 (d, *J* = 6.5 Hz, C1), 8.8 (C2), 3.9 (C15); IR (solid):
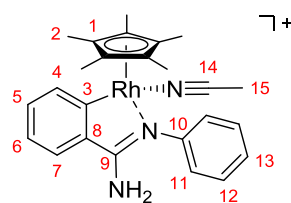
$\tilde{v}$ = 3488, 3396, 3058, 2975, 2912, 1629, 1586, 1546, 1488, 1450, 1414, 1024, 731, 653; HRMS (ESI): m/z: calculated For $C_{25}H_{29}N_3Rh$ [M−SbF$_6$]$^+$: 474.14110; found: 474.14154.

[Bis(4-methoxyphenyl)(2-(N'-phenylcarbamimidoyl-κN')phenyl)methyl](η⁵-pentamethyl-cyclopentadienyl)rhodium(III) hexafluoroantimonate (101).
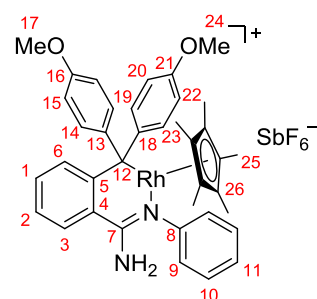
A solution of diazo compound **100** (7.7 mg, 0.030 mmol) in CD_2Cl_2 (0.5 mL) was added dropwise to a solution of complex **99** (20.5 mg, 0.029 mmol) in CD_2Cl_2 (1.0 mL) at −20 °C. The solution was stirred at that temperature for 5 min before it was transferred into an NMR tube. ^{1}H NMR (400 MHz, CD_2Cl_2, 273 K): δ = 7.89–7.81 (m, 1 H, H3), 7.49–7.38 (m, 3 H, H1, H2, H6), 7.34–7.27 (m, 2 H, H10), 7.26–7.16 (m, 1 H, H20), 7.19–7.12 (m, 3 H, H11, H14), 7.06 (dd, J = 8.0 Hz, J = 2.8 Hz, 1 H, H22), 6.82 (d, J = 8.9 Hz, 2 H, H15), 6.70 (dd, J = 8.0 Hz, J = 2.5 Hz, 1 H, H23), 6.65 (dd, J = 9.2 Hz, J = 2.4 Hz, 1 H, H19), 6.02 (s br, 2 H, H9), 5.72 (s br, 1 H, N$\underline{H}_2$), 5.23 (s br, 1 H, N$\underline{H}_2$), 4.00 (s, 3 H, H24), 3.82 (s, 3 H, H17), 0.98 (s, 15 H, H25); ^{13}C{^{1}H} NMR (100 MHz, CD_2Cl_2, 273 K): δ = 163.1 (C21), 159.8 (C7), 158.9 (C16), 148.2 (C8), 143.0 (C4), 138.6 (C13), 133.3 (C6), 132.5 (C11), 131.7 (C1), 131.2 (C19), 130.0 (C10), 128.9 (C3), 127.4 (C2), 126.7 (C14), 126.0 (C20), 124.3 (C9), 113.1 (C15), 109.9 (C22), 106.7 (C18), 105.6 (C23), 99.5 (d, J = 7.2 Hz, C26), 96.7 (d, J = 6.3 Hz, C5), 71.4 (d, J = 14.3 Hz, C12), 56.4 (C24), 55.6 (C17), 8.6 (C25); HRMS (ESI+): m/z: calculated for $C_{38}H_{40}N_2O_2Rh$ [M−SbF$_6$]$^+$: 659.21393; found: 659.21414.

In CD_2Cl_2 solution complex **101** is in equilibrium with the isomeric complex **102**. The ratio **101**:**102** was determined to be ≈ 2.5:1. Spectral data for **102**: ^{1}H NMR (400 MHz, CD_2Cl_2, 273 K): δ = 7.73 (ddd, J = 8.4 Hz, J = 6.7 Hz, J = 1.4 Hz, 1 H, H2), 7.65 (dd, J = 9.0 Hz, J = 1.4 Hz, 1 H, H6), 7.52–7.46 (m, 2 H, H14), 7.49–7.38 (m, 1 H, H11), 7.34–7.27 (m, 2 H, H10), 7.24–7.15 (m, 1 H, H1), 7.19–7.12 (m, 1 H, H3), 7.08 (s br, 1 H, C7–N$\underline{H}$–C8), 7.05–6.98 (m, 2 H, H9), 6.89–6.81 (m, 3 H, H15, H19), 6.57 (dd, J = 8.4 Hz, J = 2.5 Hz, 1 H, H23), 6.34 (dd, J = 8.4 Hz, J = 2.8 Hz, 1 H, H20), 6.30 (dd, J = 8.6 Hz, J = 2.8 Hz, 1 H, H22), 6.12 (s br, 1 H, C7–N$\underline{H}$), 3.77 (s, 3 H, H17), 3.42 (s, 3 H, H24), 1.39 (s, 15 H, H25); ^{13}C{^{1}H} NMR (100 MHz, CD_2Cl_2, 273 K): δ = 165.8 (C8), 158.9 (C7), 158.0 (C16), 157.4 (C21), 138.0 (C13), 136.6 (C18), 134.4 (C6), 133.0 (C19), 132.4 (C14), 132.3 (C11), 129.5 (C3), 128.7 (C10, C23), 127.1 (C2), 126.6 (C9), 126.1 (C1), 115.9 (C4), 114.2 (C20), 113.5 (C15), 112.4 (C22), 97.6 (d, J = 6.9 Hz, C26), 91.8 (d, J = 4.2 Hz, C5), 84.1 (d, J = 13.2 Hz, C12), 55.4 (C17), 55.2 (C24), 8.8 (C25).
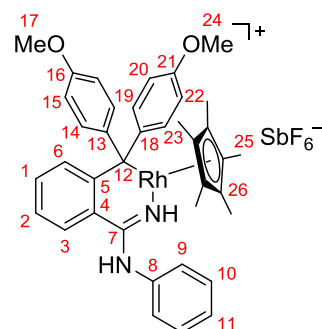
5.3.2 Synthesis of Diazo Compounds

The following diazo compounds were synthesized according to literature procedures: methyl 2-diazo-2-(4-methoxyphenyl)acetate (**87**),[207] bis(4-methoxyphenyl)diazomethane (**100**),[120]

methyl 4-(1-diazo-2-ethoxy-2-oxoethyl)benzoate (**104**),[208] methyl 2-diazo-2-phenylacetate (**119**),[207] and 9-diazo-9*H*-fluorene.[209]

5.3.3 Ir(III)-Catalyzed Cyclopropanation of 4-Methoxystyrene

Methyl (*E*)-1,2-bis(4-methoxyphenyl)cyclopropane-1-carboxylate (84). Diazo compound **87** (20.0 mg, 0.097 mmol) was added to a solution of [Cp*IrCl$_2$]$_2$ (1.0 mg, 1.3 µmol) and 4-methoxystyrene (120 mg, 0.894 mmol) in CH$_2$Cl$_2$ (3 mL) and the resulting mixture was stirred at 40 °C. After consumption of the starting material, as indicated by TLC, the mixture was concentrated *in vacuo*. The residue was purified by flash chromatography (silica, hexanes/EtOAc, 5:1) to give the title compound as a colorless oil (19 mg, 63%). The spectral data matched the previously reported values.[210] ^{1}H NMR (400 MHz, CDCl$_3$): δ = 6.96–6.91 (m, 2 H), 6.71–6.68 (m, 2 H), 6.68–6.66 (m, 2 H), 6.64–6.59 (m, 2 H), 3.73 (s, 3 H), 3.71 (s, 3 H), 3.65 (s, 3 H), 3.02 (dd, *J* = 9.4 Hz, *J* = 7.3 Hz, 1 H), 2.10 (dd, *J* = 9.4 Hz, *J* = 4.8 Hz, 1 H), 1.75 (dd, *J* = 7.3 Hz, *J* = 4.8 Hz, 1 H); ^{13}C{^{1}H} NMR (100 MHz, CDCl$_3$): δ = 174.9, 158.5, 158.2, 133.1, 129.2, 128.6, 127.1, 113.3 (2 C), 55.2 (2 C), 52.7, 36.4, 32.9, 21.0.
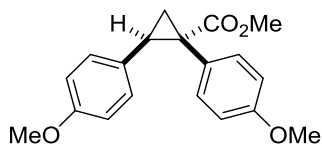
Methyl 4-((*E*)-1-(ethoxycarbonyl)-2-(4-methoxyphenyl)cyclopropyl)benzoate (105). A solution of diazo compound **104** (49.3 mg, 0.199 mmol) in CH$_2$Cl$_2$ (2 mL) was added *via* syringe pump over the course of 1 h to a solution of [Cp*IrI$_2$]$_2$ (2.3 mg, 2.0 µmol) and 4-methoxystyrene (0.26 mL, 1.96 mmol) in CH$_2$Cl$_2$ (1 mL). After consumption of the starting material, as indicated by TLC, the mixture was concentrated *in vacuo*. The residue was purified by flash chromatography (silica, hexanes/EtOAc, 5:1→5:2) to give the title compound as a light orange oil (41 mg, 58%). ^{1}H NMR (400 MHz, CDCl$_3$): δ = 7.83–7.78 (m, 2 H), 7.13–7.08 (m, 2 H), 6.71–6.67 (m, 2 H), 6.62–6.57 (m, 2 H), 4.20–4.06 (m, 2 H), 3.86 (s, 3 H), 3.69 (s, 3 H), 3.09 (dd, *J* = 9.4 Hz, *J* = 7.3 Hz, 1 H), 2.13 (dd, *J* = 9.4 Hz, *J* = 5.0 Hz, 1 H), 1.84 (dd, *J* = 7.3 Hz, *J* = 5.0 Hz, 1 H), 1.16 (t, *J* = 7.1 Hz, 3 H); ^{13}C{^{1}H} NMR (100 MHz, CDCl$_3$): δ = 173.3, 167.2, 158.4, 140.7, 132.1, 129.1, 129.1, 128.8, 127.9, 113.5, 61.5, 55.3, 52.2, 37.2, 32.9, 20.1, 14.3; IR (film): $\tilde{\nu}$ = 2982, 2953, 2907, 2837, 1711, 1611, 1514, 1436, 1275, 1173, 159, 1103, 1020, 831, 706; MS (EI, %): *m*/*z* = 534 [M]$^+$ (100), 325 (26), 308 (61), 281 (66, 279 (29), 265 (11), 249 (35), 221 (31), 207 (10), 189 (13), 178 (19), 165 (21), 145 (11), 137 (12), 121 (13), 115 (13); HRMS (ESI+): *m*/*z*: calculated for C$_{21}$H$_{22}$O$_5$Na [M+Na]$^+$: 377.13594, found: 377.13562.
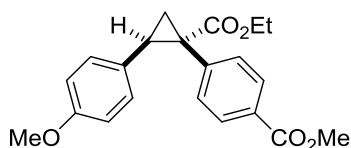
5.3.4 Ir(III)-Catalyzed Insertion of α-Diazo Esters into Si−H Bonds

Methyl 2-(4-methoxyphenyl)-2-(triethylsilyl)acetate (85-Et). Solid diazo compound **87** (20.0 mg, 0.097 mmol) was added to a solution of [Cp*IrCl$_2$]$_2$ (1.0 mg, 1.3 μmol) and triethylsilane (0.15 mL, 0.939 mmol) in DCE (3 mL) and the solution was heated to 80 °C. After consumption of the starting material, as indicated by TLC, the reaction mixture was concentrated *in vacuo*. The residue was purified by flash chromatography (silica, hexanes/EtOAc, 20:1) to give the title compound as a yellow oil (14 mg, 49%). The spectral data matched the previously reported values.[211] ^{1}H NMR (400 MHz, CDCl$_3$): δ = 7.29–7.23 (m, 2 H), 6.86–6.80 (m, 2 H), 3.78 (s, 3 H), 3.66 (s, 3 H), 3.47 (s, 1 H), 0.90 (t, J = 7.9 Hz, 9 H), 0.63–0.52 (m, 6 H); ^{13}C{^{1}H} NMR (100 MHz, CDCl$_3$): δ = 174.2, 157.7, 129.6, 128.7, 113.7, 55.4, 51.5, 41.7, 7.2, 2.8.
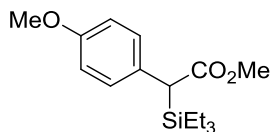
Methyl 4-(2-ethoxy-2-oxo-1-(triethylsilyl)ethyl)benzoate (106). A solution of diazo compound **104** (49.7 mg, 0.200 mmol) in DCE (2 mL) was added *via* syringe pump over the course of 1 h to a solution of [Cp*IrI$_2$]$_2$ (2.7 mg, 2.3 μmol) and triethylsilane (0.32 mL, 2.00 mmol) in DCE (1 mL). After consumption of the starting material, as indicated by TLC, the reaction mixture was concentrated *in vacuo*. The residue was purified by flash chromatography (silica, hexanes/EtOAc, 10:1) to give the title compound as a colorless oil (26 mg, 39%). ^{1}H NMR (400 MHz, CDCl$_3$): δ = 7.95–7.90 (m, 2 H), 7.48–7.43 (m, 2 H), 4.20–4.06 (m, 2 H), 3.87 (s, 3 H), 3.62 (s, 1 H), 1.27 (t, J = 7.1 Hz, 3 H), 0.90 (t, J = 7.9 Hz, 9 H), 0.64–0.55 (m, 6 H); ^{13}C{^{1}H} NMR (100 MHz, CDCl$_3$): δ = 172.7, 167.3, 143.1, 129.6, 128.9, 127.9, 60.8, 52.2, 43.7, 14.5, 7.2, 3.1; IR (film): $\tilde{\nu}$ = 2953, 2911, 2878, 1717, 1608, 1435, 1272, 1146, 1106, 1019, 704; MS (GC-EI, %): m/z = 336 [M]$^+$ (7), 279 (10), 249 (2), 191 (5), 176 (60), 149 (23), 145 (51), 131 (34), 121 (11), 118 (21), 117 (12), 115 (16), 105 (11), 103 (41), 91 (16), 90 (14), 89 (26), 87 (48), 77 (11), 75 (30), 59 (29); HRMS (ESI+): m/z: calculated for C$_{18}$H$_{28}$O$_4$SiNa [M+Na]$^+$: 359.16491, found: 359.16473.
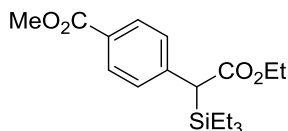
5.3.5 Rh(III)-Catalyzed Oxirane Formation from Aldehydes

Representative Procedure for the Rh-Catalyzed Epoxidation Reactions.

Methyl (*Z*)-2,3-diphenyloxirane-2-carboxylate (107). A solution of diazo compound **119** (67.3 mg, 0.382 mmol) in CH$_2$Cl$_2$ (2 mL) was added *via* syringe pump over the course of 1 h to a solution of benzaldehyde (26.0 mg, 0.250 mmol) and [Cp*RhI$_2$]$_2$ (2.8 mg, 1.2 μmol) in CH$_2$Cl$_2$ (1 mL). After consumption of the starting material, as indicated by TLC, the mixture was concentrated *in vacuo*. The residue was purified by flash chromatography (silica, hexanes/EtOAc, 20:1→10:1) to give the title compound as a colorless oil (39 mg, 63%). The spectral data matched the previously reported values.[154] ^{1}H
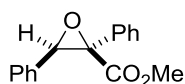
NMR (400 MHz, CDCl$_3$): δ = 7.67–7.63 (m, 2 H), 7.45–7.33 (m, 8 H), 4.16 (s, 1 H), 3.55 (s, 3 H); ^{13}C{^{1}H} NMR (100 MHz, CDCl$_3$): δ = 167.2, 134.8, 133.9, 129.0, 128.8, 128.7, 128.5, 126.3, 126.1, 67.2, 66.0, 52.4.

The following compounds were prepared analogously (*cf.* Scheme 36):

Methyl (*Z*)-3-(4-methoxyphenyl)-2-phenyloxirane-2-carboxylate (108). Colorless oil (62 mg, 96%). The spectral data matched the previously reported values.[154] ^{1}H NMR (400 MHz, CDCl$_3$): δ = 7.66–7.61 (m, 2 H), 7.43–7.35 (m, 3 H), 7.34–7.29 (m, 2 H), 6.92–6.87 (m, 2 H), 4.10 (s, 1 H), 3.82 (s, 3 H), 3.58 (s, 3 H); ^{13}C{^{1}H} NMR (100 MHz, CDCl$_3$): δ = 167.4, 160.0, 134.9, 128.9, 128.7, 127.4, 126.3, 125.9, 114.0, 67.2, 65.9, 55.4, 52.4.
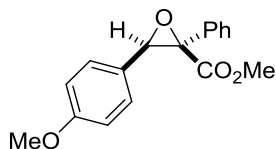
Methyl (*Z*)-2,3-bis(4-methoxyphenyl)oxirane-2-carboxylate (109). Colorless oil (65 mg, 83%). The spectral data matched the previously reported values.[154] Crystals suitable for X-ray diffraction were grown by slow diffusion of hexanes into a solution in EtOAc at 5 °C. ^{1}H NMR (400 MHz, CDCl$_3$): δ = 7.57–7.52 (m, 2 H), 7.34–7.28 (m, 2 H), 6.95–6.91 (m, 2 H), 6.91–6.86 (m, 2 H), 4.09 (s, 1 H), 3.82 (s, 3 H), 3.81 (s, 3 H), 3.57 (s, 3 H); ^{13}C{^{1}H} NMR (100 MHz, CDCl$_3$): δ = 191.0, 167.6, 160.1, 159.9, 127.7, 127.4, 126.9, 125.9, 114.1, 113.9, 67.0, 65.8, 55.5, 55.4, 52.3.
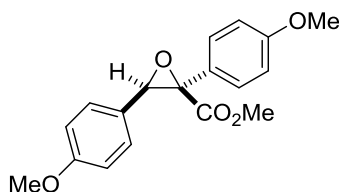
Ethyl (*Z*)-3-(4-(methoxycarbonyl)phenyl)-2-phenyloxirane-2-carboxylate (110). Colorless oil (69 mg, 85%). ^{1}H NMR (400 MHz, CDCl$_3$): δ = 8.08–8.02 (m, 2 H), 7.67–7.61 (m, 2 H), 7.51–7.46 (m, 2 H), 7.45–7.39 (m, 3 H), 4.19 (s, 1 H), 3.93 (s, 3 H), 3.54 (s, 3 H); ^{13}C{^{1}H} NMR (100 MHz, CDCl$_3$): δ = 166.9, 166.8, 138.9, 134.4, 130.6, 129.8, 129.2, 128.8, 126.3, 126.2, 67.3, 65.4, 52.5, 52.4; IR (film): $\tilde{\nu}$ = 3063, 3032, 3001, 2953, 1717, 1613, 1435, 1274, 1216, 1193, 1167, 1101, 757, 738, 696; MS (EI, %): *m/z* = 312 [M]$^+$ (1), 284 (2), 281 (3), 253 (1), 225 (<1), 221 (<1), 194 (1), 193 (1), 179 (100), 165 (4), 148 (4), 133 (2), 120 (1), 105 (17), 89 (3), 77 (7), 63 (1); HRMS (ESI+): *m/z*: calculated for C$_{18}$H$_{16}$O$_5$Na [M+Na]$^+$: 335.08899, found: 335.08869.
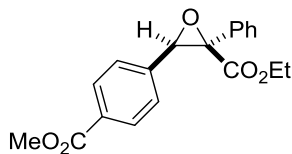
Methyl (*Z*)-2-phenyl-3-((*E*)-styryl)oxirane-2-carboxylate (111). Colorless oil (58 mg, 88%). The spectral data matched the previously reported values.[154] ^{1}H NMR (400 MHz, CDCl$_3$): δ = 7.62–7.58 (m, 2 H), 7.43–7.27 (m, 8 H), 6.90 (d, *J* = 16.0 Hz, 1 H), 6.09 (dd, *J* = 16.0 Hz, *J* = 7.9 Hz, 1 H), 3.82 (s, 3 H), 3.73 (dd, *J* = 7.9 Hz, *J* = 0.6 Hz, 1 H); ^{13}C{^{1}H} NMR (100 MHz, CDCl$_3$): δ = 168.3, 137.5, 135.9, 134.9, 128.9, 128.7, 128.6, 126.9, 126.7, 122.0, 65.9, 65.6, 52.9.
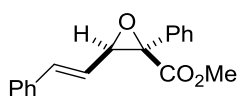
Methyl (*Z*)-3-((*E*)-but-1-en-1-yl)-2-phenyloxirane-2-carboxylate (112). Colorless oil (64 mg, 99%). ^{1}H NMR (400 MHz, CDCl$_3$): δ = 7.60–7.53 (m, 2 H), 7.41–7.30 (m, 3 H), 6.11 (dt, *J* = 15.5 Hz, *J* = 6.4 Hz, 1 H), 5.33 (ddt, *J* = 15.5 Hz, *J* = 8.1 Hz, *J* = 1.6 Hz, 1 H), 3.81 (s, 3 H), 3.53 (d, *J* = 8.1 Hz, 1 H), 2.19–2.08 (m, 2 H), 1.02 (t,
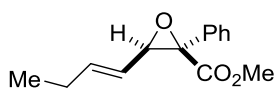
J = 7.5 Hz, 3 H); ^{13}C{^{1}H} NMR (100 MHz, CDCl$_3$): δ = 168.5, 142.1, 135.2, 128.7, 128.5, 126.7, 122.0, 65.8, 65.2, 52.7, 25.7, 13.2; IR (film): $\tilde{\nu}$ = 2964, 1736, 1435, 1302, 1279, 1200, 1112, 966, 753, 697, 640; MS (GC-EI, %): m/z = 232 [M]$^+$ (<1), 216 (1), 187 (4), 173 (8), 157 (6), 155 (7), 145 (25), 129 (15), 117 (12), 115 (16), 105 (51), 99 (100), 91 (15), 77 (42), 67 (24); HRMS (ESI+): m/z: calculated for C$_{14}$H$_{16}$O$_3$Na [M+Na]$^+$: 255.09916, found: 255.09906.

5.3.6 Ir(III)-Catalyzed Insertion of α-Diazo Esters into O–H Bonds

Methyl 2-methoxy-2-(4-methoxyphenyl)acetate (86). Diazo compound **87** (20.0 mg, 0.097 mmol) was added in portions to a solution of [Cp*IrCl$_2$]$_2$ (1.0 mg, 1.3 µmol) and methanol (39 µL, 0.970 mmol) in n-pentane (3 mL). After consumption of the starting material, as indicated by TLC, the reaction mixture was concentrated *in vacuo*. The residue was purified by flash chromatography (silica, hexanes/EtOAc, 10:1→5:1) to give the title compound as a light yellow oil (15 mg, 74%). The spectral data matched the previously reported values.[121] ^{1}H NMR (400 MHz, CDCl$_3$): δ = 7.38–7.32 (m, 2 H), 6.92–6.86 (m, 2 H), 4.72 (s, 1 H), 3.80 (s, 3 H), 3.71 (s, 3 H), 3.37 (s, 3 H); ^{13}C{^{1}H} NMR (100 MHz, CDCl$_3$): δ = 171.5, 160.1, 128.7, 128.3, 114.2, 82.2, 57.2, 55.4, 52.4.
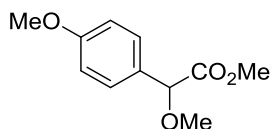
Methyl 4-(2-ethoxy-1-methoxy-2-oxoethyl)benzoate (113). Prepared analogously to **86** as a light orange oil (48 mg, 90%). The spectral data matched the previously reported values.[212] ^{1}H NMR (400 MHz, CDCl$_3$): δ = 8.06–8.01 (m, 2 H), 7.56–7.51 (m, 2 H), 4.81 (s, 1 H), 4.24–4.19 (m, 2 H), 3.91 (s, 3 H), 3.43 (s, 3 H), 1.21 (t, J = 7.1 Hz, 3 H); ^{13}C{^{1}H} NMR (100 MHz, CDCl$_3$): δ = 170.2, 166.9, 141.4, 130.6, 130.0, 127.2, 82.4, 61.7, 57.7, 52.3, 14.2.
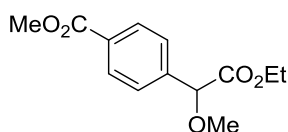
5.3.7 Synthesis of Azoarene Derivatives

Azobenzene was purchased from TCI Chemicals and used without further purification. The following azoarenes were synthesized according to literature procedures: (*Z*)-1,2-diphenyldiazene ((*Z*)-azobenzene, (*Z*)-**117**),[175] (*E*)-1,2-bis(4-methoxyphenyl)diazene (**154**),[213] (*E*)-1,2-bis(4-fluorophenyl)diazene (**155**),[213] (*E*)-1,2-bis(4-(trifluoromethyl)phenyl)di-azene,[214] (*E*)-1,2-bis(3,5-dimethylphenyl)diazene,[213] (*E*)-1,2-di-*p*-tolyldiazene,[213] dioctyl 4,4'-(diazene-1,2-diyl)(*E*)-dibenzoate,[215] (*E*)-1,2-bis(2,6-dimethylphenyl)diazene,[216] (*E*)-1,2-bis(3-methoxyphenyl)diazene,[213,214] (*E*)-1-(*p*-tolyl)-2-(4-(trifluoromethyl)phenyl)diazene (**153**),[189d] (*E*)-1,2-di-*o*-tolyl-diazene,[213] (*E*)-1,1'-(diazene-1,2-diylbis(3,1-phenylene))bis(ethan-1-one),[213] and (*E*)-1,2-bis(4-azidophenyl)diazene.[217]

Dioctyl 3,3'-(diazene-1,2-diyl)(*E*)-dibenzoate (S8). n-Octanol (1.1 mL, 6.99 mmol) and pyridine (1.0 mL, 12.36 mmol) were added to a solution of (*E*)-3,3'-(diazene-1,2-diyl)dibenzoyl chlo-ride (897 mg, 2.92 mmol)[218] in toluene (30 mL) and
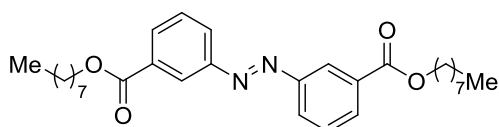
the resulting mixture was stirred at reflux temperature for 3 h. The mixture was poured onto ice-water mixture (150 mL) and the aqueous phase was extracted with toluene (3 × 60 mL). The combined organic layers were washed with HCl (2 M, 60 mL) and deionized water (2 × 40 mL), dried over Na_2SO_4, and concentrated *in vacuo*. The crude material was purified by flash chromatography (silica, hexanes/EtOAc, 20:1) to give the title compound as a bright orange solid (1.28 g, 89%). M.p.: 45–46 °C; ^{1}H NMR (400 MHz, CDCl₃): δ = 8.60 (t, *J* = 1.7 Hz, 2 H), 8.18 (dt, *J* = 7.8 Hz, *J* = 1.4 Hz, 2 H), 8.12 (ddd, *J* = 7.9 Hz, *J* = 2.0 Hz, *J* = 1.2 Hz, 2 H), 7.61 (t, *J* = 7.9 Hz, 2 H), 4.38 (t, *J* = 6.7 Hz, 4 H), 1.86–1.76 (m, 4 H), 1.53–1.22 (m, 20 H), 0.88 (t, *J* = 6.9 Hz, 6 H); ^{13}C{^{1}H} NMR (100 MHz, CDCl₃): δ = 166.2, 152.6, 132.2, 132.0, 129.4, 126.7, 124.7, 65.7, 31.9, 29.4, 29.3, 28.9, 26.2, 22.8, 14.2; IR (film): $\tilde{v}$ = 2949, 2920, 2853, 1718, 1467, 1441, 1285, 1269, 1210, 1153, 1103, 969, 924, 754, 688; MS (EI, %): *m/z* = 495 (33), 494 [M]⁺ (100), 365 (23), 261 (4), 253 (5), 123 (7), 105 (22), 91 (18), 69 (12); HRMS (ESI+): *m/z*: calculated for $C_{30}H_{42}N_2O_4Na$ [M+Na]⁺: 517.30368, found: 517.30345.

(*E*)-1,2-Bis(4-(prop-1-yn-1-yl)phenyl)diazene (S9). A mixture of 4-(prop-1-yn-1-yl)aniline

(401 mg, 3.06 mmol),[219] CuBr (32.6 mg, 0.23 mmol), and pyridine (0.06 mL, 0.74 mmol) in toluene (12 mL) was stirred under air at 60 °C. After 7 h, the solvent was evaporated and the crude material was purified by flash chromatography (silica, hexanes/EtOAc, 30:1→20:1) to give the title compound as an orange solid (355 mg, 90%). M.p.: 194–195 °C; ^{1}H NMR (400 MHz, CDCl₃): δ = 7.89–7.78 (m, 4 H), 7.56–7. 47(m, 4 H), 2.09 (s, 6 H); ^{13}C{^{1}H} NMR (100 MHz, CDCl₃): δ = 151.5, 132.4, 127.1, 123.0, 89.0, 79.8, 4.7; IR (film): $\tilde{v}$ = 2913, 2251, 2212, 1594, 1494, 1404, 1153, 1100, 846, 558; MS (GC-EI, %): *m/z* = 258 [M]⁺ (21), 143 (20), 130 (2), 115 (100), 103 (1), 89 (20), 77 (2), 65 (13), 63 (11); HRMS (ESI+): *m/z*: calculated for $C_{18}H_{15}N_2$ [M+H]⁺: 259.12297, found: 259.12296.

5.3.8   Rh(III)-Catalyzed Metathesis of α-Diazo Esters and Azoarenes

Representative Procedure for the Rh(III)-Catalyzed Metathesis between Diazo Compounds and Azoarenes Performed at Ambient Temperature.

Methyl (*Z*)-2-phenyl-2-(phenylimino)acetate (120). A solution of diazo compound **119**

(113.2 mg, 0.643 mmol) in toluene (2 mL) was added *via* syringe pump over the course of 2 h to a solution of azobenzene **117** (44.8 mg, 0.250 mmol) and [Cp*RhI₂]₂ (2.3 mg, 2.3 µmol) in toluene (3 mL) during constant irradiation of the mixture with the light emitted by blue LEDs (Figure S1 in the appendix). After consumption of the starting material, as indicated by TLC, the mixture was concentrated *in vacuo*. The residue was purified by flash chromatography (silica, hexanes/EtOAc, 20:1 + 1% Et₃N) to give the title compound as an orange oil (107 mg, mixture of two geometric isomers (95:5), 91%). The
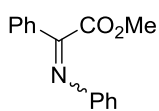
spectral data of the major isomer matched the previously reported values.[167] ^{1}H NMR (400 MHz, CDCl$_3$): δ = 7.90–7.85 (m, 2 H), 7.56–7.44 (m, 3 H), 7.37–7.31 (m, 2 H), 7.17–7.11 (m, 1 H), 6.99–6.94 (m, 2 H), 3.64 (s, 3 H); ^{13}C{^{1}H} NMR (100 MHz, CDCl$_3$): δ = 165.6, 160.1, 150.2, 134.0, 132.0, 129.0, 128.9, 128.1, 125.1, 119.6, 52.0.

The following compounds were prepared analogously (*cf.* Scheme 40 and Scheme 41):

Methyl (*Z*)-2-(4-methoxyphenyl)-2-(phenylimino)acetate (118). Yellow oil (130 mg, isolated as a single isomer, 97%). Crystals suitable for X-ray diffraction were grown by slow diffusion of *n*-pentane into a solution in CH$_2$Cl$_2$ at −20 °C. ^{1}H NMR (400 MHz, CD$_2$Cl$_2$): δ = 7.85–7.80 (m, 2 H), 7.35–7.29 (m, 2 H), 7.15–7.09 (m, 1 H), 7.00–6.93 (m, 2 H), 3.88 (s, 3 H), 3.63 (s, 3 H); ^{13}C{^{1}H} NMR (100 MHz, CD$_2$Cl$_2$): δ = 165.9, 163.1, 159.6, 150.8, 130.1, 129.3, 126.9, 125.1, 120.0, 114.5, 55.9, 52.1; IR (film): $\tilde{v}$ = 2953, 2839, 1735, 1602, 1591, 1513, 1259, 1164, 1016; MS (GC-EI, %): *m/z* =269 [M]$^+$ (9), 211 (15), 210 (100), 195 (5), 167 (9), 133 (6), 103 (3), 90 (5), 77 (55), 63 (4), 51 (21); HRMS (ESI+): *m/z*: calculated for C$_{16}$H$_{16}$NO$_3$ [M+H]$^+$: 270.11239, found: 270.11247.

Methyl (*Z*)-2-phenyl-2-(*p*-tolylimino)acetate (121). Orange oil (124 mg, mixture of two geometric isomers (94:6), 97%). The spectral data of the major isomer are given. ^{1}H NMR (400 MHz, CDCl$_3$): δ = 7.90–7.84 (m, 2 H), 7.55–7.43 (m, 3 H), 7.17–7.11 (m, 2 H), 6.92–6.87 (m, 2 H), 3.68 (s, 3 H), 2.34 (s, 3 H); ^{13}C{^{1}H} NMR (100 MHz, CDCl$_3$): δ = 165.9, 159.7, 147.6, 134.8, 134.1, 131.8, 129.6, 128.8, 128.0, 119.7, 52.0, 21.1; IR (film): $\tilde{v}$ = 3027, 2952, 2923, 1732, 1624, 1504, 1449, 1433, 1301, 1225, 1194, 1166, 1009, 908, 838, 729; MS (GC-EI, %): *m/z* = 253 [M]$^+$ (8), 195 (16), 194 (100), 165 (1), 152 (<1), 116 (1), 103 (3), 97 (2), 91 (36), 77 (5), 65 (30), 63 (5), 51 (5), 39 (8); HRMS (ESI+): *m/z*: calculated for C$_{16}$H$_{16}$NO$_2$ [M+H]$^+$: 254.11755, found: 254.11727.
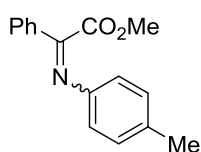
Methyl (*Z*)-2-((4-methoxyphenyl)imino)-2-phenylacetate (122). Yellow solid (103 mg, mixture of two geometric isomers (93:7), 77%). The spectral data of the major isomer matched the previously reported values.[167] ^{1}H NMR (400 MHz, CDCl$_3$): δ = 7.89–7.83 (m, 2 H), 7.54–7.42 (m, 3 H), 7.00–6.94 (m, 2 H), 6.92–6.85 (m, 2 H), 3.81 (s, 3 H), 3.70 (s, 3 H); ^{13}C{^{1}H} NMR (100 MHz, CDCl$_3$): δ = 166.3, 159.3, 157.5, 143.3, 134.3, 131.7, 128.8, 128.0, 121.3, 114.3, 55.6, 52.1.

Methyl (*Z*)-2-((4-fluorophenyl)imino)-2-phenylacetate (123). Yellow oil (119 mg, mixture of two geometric isomers (94:6), 91%). The spectral data of the major isomer are given. ^{1}H NMR (400 MHz, CDCl$_3$): δ = 7.88–7.84 (m, 2 H), 7.56–7.50 (m, 1 H), 7.50–7.44 (m, 2 H), 7.07–7.00 (m, 2 H), 6.97–6.90 (m, 2 H), 3.67 (s); ^{13}C{^{1}H} NMR (100 MHz, CDCl$_3$): δ = 165.6, 160.6, 160.5 (d, $^1J_{CF}$ = 243.8 Hz),146.3 (d, $^4J_{CF}$ = 2.8 Hz), 133.8, 132.1, 128.9, 128.1, 121.3 (d, $^3J_{CF}$ = 8.1 Hz), 115.8 (d, $^2J_{CF}$ = 22.5 Hz), 52.1; ^{19}F{^{1}H}-NMR (282 MHz, CDCl$_3$): δ = −118.4 (s); IR (film): $\tilde{v}$ = 3066, 3031, 2953, 1732, 1499,
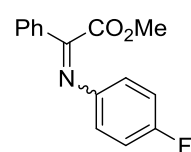
1229, 1214, 1192, 1170, 1009, 844, 769, 689; MS (EI, %): m/z = 257 [M]$^+$ (12), 240 (2), 199 (13), 198 (100), 181 (1), 151 (1.03), 104 (1), 103 (1), 95 (14), 91 (5), 77 (6), 75 (7); HRMS (ESI+): m/z: calculated for $C_{15}H_{12}NO_2F$ [M+H]$^+$: 258.09248, found: 258.09232.

Methyl (*Z*)-2-((3-methoxyphenyl)imino)-2-phenylacetate (126). Yellow oil (135 mg, mixture of two geometric isomers (98:2), 99%). The spectral data of the major isomer are given. ^{1}H NMR (400 MHz, CDCl$_3$): δ = 7.90–7.84 (m, 2 H), 7.55–7.50 (m, 1 H), 7.50–7.44 (m, 2 H), 7.26–7.20 (m, 1 H), 6.71 (ddd, ^3J = 8.4 Hz, ^4J = 2.4 Hz, ^4J = 1.0 Hz, 1 H), 7.25–7.20 (m, 2 H), 3.80 (s, 3 H), 3.67 (s, 3 H); ^{13}C{^{1}H} NMR (100 MHz, CDCl$_3$): δ = 165.6, 160.2, 160.1, 151.5, 133.9, 132.0, 129.9, 128.9, 128.1, 111.7, 111.3, 105.4, 55.4, 52.1; IR (film): $\tilde{v}$ = 3064, 3003, 2952, 2835, 1731, 1592, 1579, 1480, 1432, 1210, 1139, 1009, 776, 688; MS (GC-EI, %): m/z = 269 [M]$^+$ (11), 211 (15), 210 (100), 195 (2), 167 (2), 107 (10), 105 (5), 92 (20), 77 (24), 64 (11), 51 (2); HRMS (ESI+/−): m/z: calculated for $C_{16}H_{16}NO_3$ [M+H$^+$]$^+$: 270.11247, found: 270.11198.
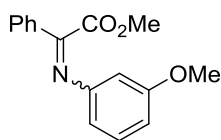
Octyl (*Z*)-3-((2-methoxy-2-oxo-1-phenylethylidene)amino)benzoate (127). Yellow oil (169 mg, isolated as a single isomer, 86%). ^{1}H NMR (400 MHz, CDCl$_3$): δ = 7.91–7.86 (m, 2 H), 7.84 (ddd, J = 7.8 Hz, J = 1.5 Hz, J = 1.2 Hz, 1 H), 7.68–7.64 (m, 1 H), 7.57–7.51 (m, 1 H), 7.51–7.45 (m, 2 H), 7.41 (td, J = 7.8 Hz, J = 0.3 Hz, 1 H), 7.15 (ddd, J = 7.8 Hz, J = 2.2 Hz, J = 1.1 Hz, 1 H), 4.31 (t, J = 6.7 Hz, 2 H), 3.66 (s, 3 H), 1.81–1.71 (m, 2 H), 1.49–1.39 (m, 2 H), 1.39–1.20 (m, 8 H), 0.88 (t, J = 6.8 Hz, 3 H); ^{13}C{^{1}H} NMR (100 MHz, CDCl$_3$): δ = 166.4, 165.2, 160.9, 150.2, 133.7, 132.2, 131.5, 129.1, 128.9, 128.2, 126.3, 124.1, 120.8, 65.4, 52.1, 31.9, 29.4, 29.3, 28.8, 26.2, 22.8, 14.2; IR (film): $\tilde{v}$ = 2953, 2926, 2855, 1736, 1717, 1625, 1580, 1450, 1433, 1266, 1171, 1103, 1011, 757, 688; MS (EI, %): m/z = 396 (2), 395 [M]$^+$ (7), 337 (24), 336 (100), 266 (3), 224 (15), 179 (4), 65 (1); HRMS (ESI+): m/z: calculated for $C_{24}H_{30}NO_4$ [M+H]$^+$: 396.21693, found: 396.21668.
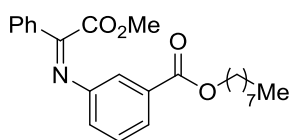
Methyl (*Z*)-2-((3,5-dimethylphenyl)imino)-2-phenylacetate (128). Orange-yellow oil (130 mg, mixture of two geometric isomers (94:6), 95%). The spectral data of the major isomer are given. ^{1}H NMR (400 MHz, CDCl$_3$): δ = 7.89–7.83 (m, 2 H), 7.55–7.43 (m, 3 H), 6.81–6.77 (m, 1 H), 6.63–6.58 (m, 2 H), 3.68 (s, 3 H), 2.31 (s, 6 H); ^{13}C{^{1}H} NMR (100 MHz, CDCl$_3$): δ = 165.8, 159.5, 150.1, 138.7, 134.1, 131.8, 128.8, 128.1, 126.9, 117.4, 51.9, 21.4; IR (film): $\tilde{v}$ = 2950, 2917, 1732, 1603, 1588, 1449, 1432, 1317, 1280, 1208, 1142, 1025, 848, 687; MS (GC-EI, %): m/z = 267 [M]$^+$ (10), 209 (16), 208 (100), 193 (1), 166 (<1), 105 (15), 103 (11), 97 (5), 79 (13), 77 (16), 65 (2), 51 (2); HRMS (ESI+): m/z: calculated for $C_{17}H_{18}NO_2$ [M+H]$^+$: 268.13320, found: 268.13299.
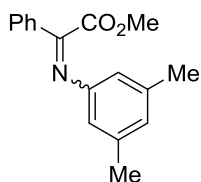
Methyl (*Z*)-2-phenyl-2-(*o*-tolylimino)acetate (129). Yellow oil (109 mg, isolated as a single isomer, 85%). ^{1}H NMR (400 MHz, CDCl$_3$): δ = 7.94–7.89 (m, 2 H), 7.54–7.45 (m, 3 H), 7.22–7.18 (m, 1 H), 7.16–7.10 (m, 1 H), 7.05 (td, *J* = 7.4 Hz, *J* = 1.2 Hz, 1 H), 6.74–6.70 (m, 1 H), 3.61 (s, 3 H), 2.22 (s, 3 H); ^{13}C{^{1}H} NMR (100 MHz, CDCl$_3$): δ = 165.5, 159.5, 149.1, 133.9, 131.9, 130.3, 129.3, 128.9, 128.1, 126.3, 125.0, 117.5, 51.9, 18.1; IR (film): $\tilde{v}$ = 3064, 3025, 2951, 1733, 1629, 1596, 1578, 1484, 1449, 1433, 1304, 1229, 1203, 1171, 1111, 1009, 754, 689; MS (GC-EI, %): *m/z* = 253 [M]$^+$ (13), 195 (15), 194 (100), 167 (6), 165 (3), 152 (1), 116 (4), 103 (3), 91 (40), 89 (9), 77 (4), 65 (32), 51 (4); HRMS (ESI+): *m/z*: calculated for C$_{16}$H$_{16}$NO$_2$ [M+H]$^+$: 254.11755, found: 254.11744.
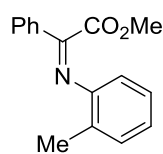
Methyl (*Z*)-2-phenyl-2-((4-(prop-1-yn-1-yl)phenyl)imino)acetate (132). Orange oil (90 mg, mixture of two geometric isomers (93:7), 65%). The spectral data of the major isomer is given. ^{1}H NMR (400 MHz, CDCl$_3$): δ = 7.90–7.83 (m, 2 H), 7.56–7.50 (m, 1 H), 7.50–7.43 (m, 2 H), 7.40–7.34 (m, 2 H), 6.92–6.85 (m, 2 H), 3.64 (s, 3 H), 2.06 (s, 3 H); ^{13}C{^{1}H} NMR (100 MHz, CDCl$_3$): δ = 165.4, 160.1, 149.4, 133.8, 132.3, 132.1, 128.9, 128.2, 120.8, 119.7, 85.8, 79.7, 52.1, 4.5; IR (film): $\tilde{v}$ = 3062, 3035, 2951, 2915, 2850, 1731, 1623, 1498, 1226, 1195, 1165, 1007, 848, 688, 561; MS (GC-EI, %): *m/z* = 277 [M]$^+$ (23), 219 (16), 218 (100), 203 (1), 140 (<1), 115 (14), 109 (1), 89 (5), 77 (1), 65 (2), 63 (2); HRMS (ESI+): *m/z*: calculated for C$_{18}$H$_{16}$NO$_2$ [M+H]$^+$: 278.11755, found: 278.11757.
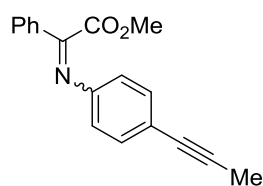
Methyl (*Z*)-2-((4-azidophenyl)imino)-2-phenylacetate (133). Yellow oil (100 mg, mixture of two geometric isomers (93:7), 71%). The spectral data of the major isomer is given. ^{1}H NMR (400 MHz, CDCl$_3$): δ = 7.89–7.83 (m, 2 H), 7.56–7.50 (m, 1 H), 7.50–7.44 (m, 2 H), 7.04–6.96 (m, 4 H), 3.69 (s, 3 H); ^{13}C{^{1}H} NMR (100 MHz, CDCl$_3$): δ = 165.6, 160.4, 147.2, 136.9, 133.8, 132.1, 128.9, 128.1, 121.4, 119.7, 52.2; IR (film): $\tilde{v}$ = 3062, 3035, 2951, 2108, 2077, 1731, 1621, 1497, 1294, 1226, 1195, 1166, 1006, 841, 688, 674, 556; MS (EI, %): *m/z* = 280 [M]$^+$ (10), 253 (17), 252 (100), 221 (8), 208 (6), 207 (36), 194 (5), 193 (30), 192 (19), 180 (10), 168 (3), 167 (4), 166 (5), 141 (1), 140 (3), 139 (2), 129 (1), 120 (1), 118 (3), 115 (2), 106 (9), 105 (5), 104 (4), 103 (3), 97 (2), 90 (29), 80 (21), 77 (10), 63 (12); HRMS (ESI+): *m/z*: calculated for C$_{15}$H$_{13}$N$_4$O$_2$ [M+H]$^+$: 281.10330, found: 281.10347.
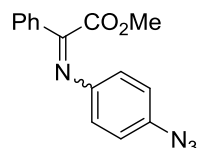
Methyl (*Z*)-2-(4-methoxyphenyl)-2-((4-methoxyphenyl)imino)acetate (134). Yellow solid (103 mg, mixture of two geometric isomers (85:15), 69%). The spectral data of the major isomer is given. M.p.: 91-92 °C; ^{1}H NMR (400 MHz, CDCl$_3$): δ = 7.84–7.77 (m, 2 H), 7.00–6.91 (m, 4 H), 6.90–6.83 (m, 2 H), 3.87 (s, 3 H), 3.80 (s, 3 H), 3.67 (s, 3 H); ^{13}C{^{1}H} NMR (100 MHz, CDCl$_3$): δ = 166.4, 162.5, 158.7, 157.2, 143.6, 129.8, 127.0, 121.3, 114.3, 114.2, 55.6, 55.5, 52.0; IR (film): $\tilde{v}$ = 3012, 2973, 2953, 2937, 2914, 2839, 1729, 1604, 1594, 1572, 1510, 1498, 1452, 1309, 1244, 1160, 1022, 842, 510; MS (EI, %): *m/z* = 299
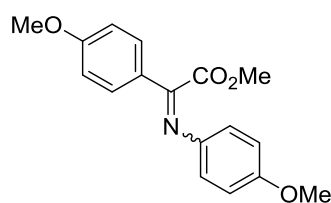
[M]+ (19), 241 (15), 240 (100), 225 (6), 197 (5), 154 (<1), 120 (2), 92 (4), 77 (3); HRMS (GC-EI): m/z: calculated for $C_{17}H_{17}NO_4$ [M]+: 299.11521, found: 299.11523.

Methyl (*Z*)-4-(2-ethoxy-2-oxo-1-(phenylimino)ethyl)benzoate (136). Yellow oil (140 mg, mixture of two geometric isomers (96:4), 90%). The spectral data of the major isomer is given. ^{1}H NMR (400 MHz, CDCl$_3$): δ = 8.16–8.10 (m, 2 H), 7.99–7.94 (m, 2 H), 7.36–7.30 (m, 2 H), 7.19–7.13 (m, 1 H), 6.99–6.94 (m, 2 H), 4.14 (q, J = 7.1 Hz, 2 H), 3.95 (s, 3 H), 0.99 (t, J = 7.1 Hz, 3 H); ^{13}C{^{1}H} NMR (100 MHz, CDCl$_3$): δ = 166.5, 164.6, 159.4, 150.0, 137.8, 132.9, 130.0, 129.0, 128.1, 125.4, 119.6, 61.8, 52.5, 13.8; IR (film): $\tilde{v}$ = 2983, 2953, 1721, 1624, 1435, 1274, 1223, 1187, 1106, 1014, 761, 696; MS (GC-EI, %): m/z = 311 [M]+ (3), 280 (1), 239 (13), 238 (74), 179 (6), 152 (2), 130 (3), 104 (4), 77 (100), 51 (13); HRMS (ESI+): m/z: calculated for $C_{18}H_{17}NO_4Na$ [M+Na]+: 334.10498, found: 334.10484.
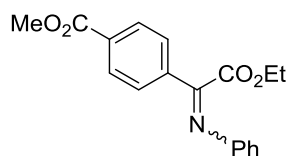
Methyl (*Z*)-4-(2-ethoxy-1-((4-methoxyphenyl)imino)-2-oxoethyl)benzoate (137). Yellow solid (113 mg, mixture of two geometric isomers (94:6), 66%). The spectral data of the major isomer is given. M.p.: 75–76 °C; ^{1}H NMR (400 MHz, CDCl$_3$): δ = 8.14–8.09 (m, 2 H), 7.97–7.91 (m, 2 H), 7.01–6.95 (m, 2 H), 6.92–6.86 (m, 2 H), 4.20 (q, J = 7.1 Hz, 2 H), 3.95 (s, 3 H), 3.81 (s, 3 H), 1.09 (t, J = 7.1 Hz, 3 H); ^{13}C{^{1}H} NMR (100 MHz, CDCl$_3$): δ = 166.6, 165.4, 158.5, 157.8, 143.0, 138.2, 132.6, 130.0, 127.9, 121.4, 114.3, 61.8, 55.6, 52.5, 14.0; IR (film): $\tilde{v}$ = 3007, 2981, 2959, 2838, 1713, 1630, 1499, 1434, 1288, 1240, 1224, 1189, 1105, 1014, 708; MS (EI, %): m/z = 341 [M]+ (14), 269 (16), 268 (100), 253 (2), 225 (2), 209 (3), 166 (<1), 119 (1), 92 (4), 77 (4); HRMS (GC-EI): m/z: calculated for $C_{19}H_{19}NO_5$ [M]+: 341.12577, found: 341.12566.
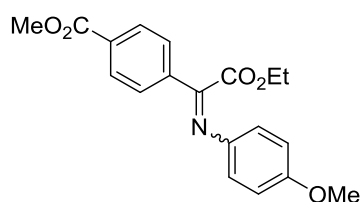
N-Phenyl-9*H*-fluoren-9-imine (139). Yellow oil (53 mg, 53%). The spectral data matched the previously reported values.[220] ^{1}H NMR (400 MHz, CDCl$_3$): δ = 7.90 (d, J = 7.5 Hz, 1 H), 7.60–7.52 (m, 2 H), 7.47–7.35 (m, 3 H), 7.35–7.24 (m, 2 H), 7.23–7.14 (m, 1 H), 7.01–6.94 (m, 2 H), 6.88 (td, J = 7.6 Hz, J = 1.0 Hz, 1 H), 6.54 (d, J = 7.7 Hz, 1 H); ^{13}C{^{1}H} NMR (100 MHz, CDCl$_3$): δ = 163.0, 151.9, 143.9, 142.0, 137.6, 132.0, 131.9, 131.3, 129.4, 128.5, 127.8, 127.2, 124.1, 123.4, 120.3, 119.7, 118.4.
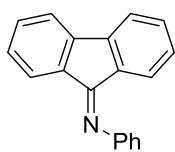
Representative Procedure for the Rh(III)-Catalyzed Metathesis between Diazo Compounds and Azoarenes at Elevated Temperature.

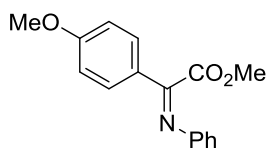**Octyl (*Z*)-4-((2-methoxy-2-oxo-1-phenylethylidene)amino)benzoate (125).** A solution of diazo compound **119** (101.5 mg, 0.576 mmol) in toluene (2 mL) was added *via* syringe pump over the course of 2 h to a solution of dioctyl 4,4'-(diazene-1,2-diyl)(*E*)-dibenzoate (**S8**, 122.9 mg, 0.248 mmol) and [Cp*RhI$_2$]$_2$ (2.2 mg, 2.2 μmol) in toluene (13 mL) at 90 °C under
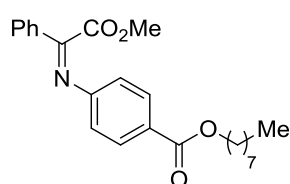
constant irradiation with the light emitted by a blue LED (Figure S2 in the appendix). After consumption of the starting material, as indicated by TLC, the mixture was concentrated *in vacuo*. The residue was purified by flash chromatography (silica, hexanes/EtOAc, 20:1 + 1% Et$_3$N) to give the title compound as an orange oil (175 mg, isolated as a single isomer, 89%). ^{1}H NMR (400 MHz, CDCl$_3$): δ = 8.06–8.00 (m, 2 H), 7.90–7.85 (m, 2 H), 7.58–7.51 (m, 1 H), 7.51–7.45 (m, 2 H), 7.01–6.95 (m, 2 H), 4.31 (t, J = 6.7 Hz), 3.63 (s, 3 H), 1.77 (quint, J = 6.8 Hz), 1.52–1.23 (m, 12 H), 0.89 (t, J = 6.9 Hz); ^{13}C{^{1}H} NMR (100 MHz, CDCl$_3$): δ = 166.5, 164.9, 160.6, 154.3, 133.5, 132.4, 130.7, 129.0, 128.3, 127.1, 119.4, 65.2, 52.2, 31.9, 29.4, 29.3, 28.9, 26.2, 22.8, 14.2; IR (film): $\tilde{\nu}$ = 2953, 2926, 2855, 1736, 1713, 1598, 1269, 1227, 1196, 1163, 1099, 1009, 861, 772, 689; MS (EI, %): m/z = 395 [M]$^+$ (10), 337 (23), 336 (100), 266 (6), 224 (17), 179 (7), 104 (<1), 103 (<1), 76 (2), 65 (1); HRMS (ESI+): m/z: calculated for C$_{24}$H$_{30}$NO$_4$ [M+H]$^+$: 396.216934, found: 396.21649.

The following compounds were prepared analogously (*cf.* Scheme 40 and Scheme 41):

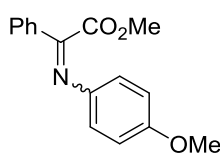**Methyl (*Z*)-2-phenyl-2-((4-(trifluoromethyl)phenyl)imino)acetate (124).** Orange oil (128 mg, mixture of two geometric isomers (94:6), 84%). The spectral data of the major isomer are given. ^{1}H NMR (400 MHz, CDCl$_3$): δ = 7.91–7.46 (m, 2 H), 7.63–7.58 (m, 2 H), 7.58–7.53 (m, 1 H), 7.53–7.46 (m, 2 H), 7.06–7.01 (m, 2 H), 3.65 (s, 3 H); ^{13}C{^{1}H} NMR (100 MHz, CDCl$_3$): δ = 164.8, 161.1, 153.2, 133.4, 132.5, 129.0, 128.3, 127.0 (q, ^2J = 32.4 Hz), 126.3 (q, ^3J = 3.7 Hz), 124.4 (q, ^1J = 270.7 Hz), 119.8, 52.2; ^{19}F{^{1}H} NMR (282 MHz, CDCl$_3$): δ = −62.1; IR (film): $\tilde{\nu}$ = 3065, 3054, 2955, 1735, 1608, 1319, 1230, 1163, 1063, 1015, 1009, 852, 689; MS (GC-EI, %): m/z = 307 [M]$^+$ (5), 288 (2), 249 (15), 248 (100), 228 (3), 208 (2), 172 (1), 145 (41), 125 (10), 103 (10), 95 (21), 77 (29), 51 (5); HRMS (ESI+): m/z: calculated for C$_{16}$H$_{13}$NO$_2$F$_3$ [M+H]$^+$: 308.08929, found: 308.08901.

Methyl (*Z*)-2-((3-acetylphenyl)imino)-2-phenylacetate (131). Orange oil (116 mg, isolated as a single isomer, 83%). ^{1}H NMR (400 MHz, CDCl$_3$): δ = 7.90–7.85 (m, 2 H), 7.76 (ddd, J = 7.8 Hz, J = 1.7 Hz, J = 1.1 Hz, 1 H), 7.58–7.52 (m, 2 H), 7.52–7.46 (m, 2 H), 7.44 (t, J = 7.8 Hz, 1 H), 7.17 (ddd, J = 7.8 Hz, J = 2.2 Hz, J = 1.0 Hz, 1 H), 3.65 (s, 3 H), 2.60 (s, 3 H); ^{13}C{^{1}H} NMR (100 MHz, CDCl$_3$): δ = 197.8, 165.2, 161.1, 150.4, 138.0, 133.6, 132.3, 129.4, 129.0, 128.2, 124.9, 124.3, 119.8, 52.1, 26.9; IR (film): $\tilde{\nu}$ = 3063, 3004, 2952, 1732, 1683, 1624, 1578, 1429, 1262, 1216, 1163, 1010, 687; MS (GC-EI, %): m/z = 281 [M]$^+$ (7), 223 (16), 222 (100), 179 (2), 119 (5), 104 (7), 103 (5), 91 (40), 77 (21), 76 (32), 65 (12), 50 (10), 43 (29); HRMS (ESI+): m/z: calculated for C$_{17}$H$_{16}$NO$_3$ [M+H]$^+$: 282.11247, found: 282.11272.

Octyl (*Z*)-4-((2-methoxy-1-(4-methoxyphenyl)-2-oxoethylidene)amino)benzoate (135).
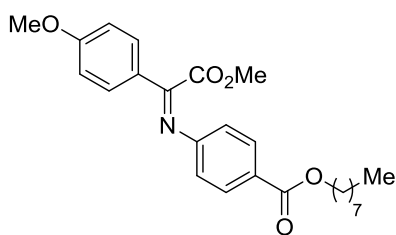
Orange oil (138 mg, isolated as a single isomer, 65%). ^{1}H NMR (400 MHz, CDCl$_3$): δ = 8.05–7.99 (m, 2 H), 7.86–7.79 (m, 2 H), 7.00–6.93 (m, 4 H), 4.30 (t, *J* = 6.7 Hz), 3.88 (s, 3 H), 3.61 (s, 3 H), 1.77 (quint, *J* = 6.9 Hz), 1.50–1.40 (m, 2 H), 1.40–1.22 (m, 10 H), 0.89 (t, *J* = 6.9 Hz); ^{13}C{^{1}H} NMR (100 MHz, CDCl$_3$): δ = 166.6, 165.1, 163.0, 159.8, 154.6, 130.7, 130.2, 126.8, 126.2, 119.6, 114.4, 65.2, 55.6, 52.1, 31.9, 29.4, 29.3, 28.9, 26.2, 22.8, 14.2; IR (film): $\tilde{v}$ = 2953, 2927, 2855, 1736, 1712, 1592, 1573, 1513, 1256, 1229, 1158, 1112, 1098, 1017, 839, 772, 704; MS (EI, %): *m/z* = 425 [M]$^+$ (3), 425 (9), 368 (4), 367 (22), 366 (100), 296 4), 254 (14), 209 (5), 118 (1), 76 (<1); HRMS (ESI+): *m/z*: calculated for C$_{25}$H$_{32}$NO$_5$ [M+H]$^+$: 426.22750, found: 426.22704.

Methyl (*Z*)-4-(2-ethoxy-1-((4-((octyloxy)carbonyl)phenyl)imino)-2-oxoethyl)benzoate
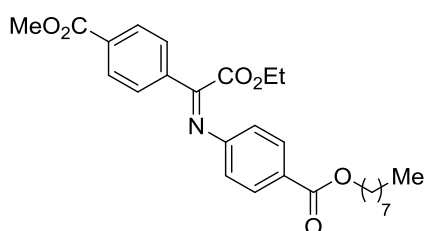
(138). Brown oil (138 mg, isolated as a single isomer, 38%). ^{1}H NMR (400 MHz, CDCl$_3$): δ = 8.17–8.11 (m, 2 H), 8.06–8.00 (m, 2 H), 7.99–7.94 (m, 2 H), 7.02–6.96 (m, 2 H), 4.14 (q, *J* = 7.2 Hz, 2 H), 4.31 (t, *J* = 6.7 Hz, 2 H), 3.96 (s, 3 H), 1.83–1.71 (m, 2 H), 1.50–1.40 (m, 2 H), 1.40–1.22 (m, 8 H), 0.88 (t, *J* = 6.8 Hz, 3 H); ^{13}C{^{1}H} NMR (100 MHz, CDCl$_3$): δ = 166.4 (2 C), 164.0, 159.9, 154.0, 137.3, 133.2, 130.7, 130.1, 128.3, 127.3, 119.3, 65.3, 62.0, 52.6, 31.9, 29.4, 29.3, 28.9, 26.2, 22.8, 14.2, 13.9; IR (film): $\tilde{v}$ = 2954, 2927, 2856, 1715, 1600, 1268, 1189, 1164, 1100, 1014, 869, 772, 700; MS (EI, %): *m/z* = 467 [M]$^+$ (5), 436 (2), 395 (24), 394 (100), 338 (4), 282 (12), 237 (4), 179 (<1), 121 (<1), 76 (1); HRMS (ESI+): *m/z*: calculated for C$_{27}$H$_{33}$NO$_6$Na [M+Na]$^+$: 490.22001, found: 490.22002.

5.3.9 Mechanistic Experiments on the Azo Metathesis

Stoichiometric NMR Experiments. A cold (0 °C) solution of diazo compound **87** (9.1 mg, 0.044 mmol) in degassed CD$_2$Cl$_2$ (0.5 mL) was added dropwise to a cold (0 °C) solution of [Cp*RhI$_2$]$_2$ (21.6 mg, 0.022 mmol) in degassed CD$_2$Cl$_2$ (1 mL). The mixture was stirred for 10 min whilst cooling in an ice bath before it was cooled to −78 °C and solid (*Z*)-**117** (8.5 mg, 0.047 mmol) was added in one portion. After 5 min, this mixture was transferred to a pre-cooled (−78 °C) NMR tube. ^{1}H NMR (500 MHz, CD$_2$Cl$_2$, 233 K): δ = 7.35–7.29 (m, 2 H, H22), 7.29–7.25 (m, 2 H, H3), 7.25–7.21 (m, 2 H, H21), 7.19–7.13 (m, 1 H, H23), 7.13–7.07 (m, 2 H, H12), 6.98–6.92 (m, 3 H, H11, H13), 6.76–6.70 (m, 2 H, H4), 3.69 (s, 3 H, H6), 3.45 (s, 3 H, H8); ^{13}C{^{1}H} NMR (125 MHz, CD$_2$Cl$_2$, 233 K): δ = 166.4 (C7), 159.9 (C5), 148.3 (C20), 147.1 (C10), 129.9 (C3), 128.6 (C22), 128.2 (C12), 125.0 (C23), 124.1 (C13), 122.5 (C2), 120.7 (C11), 120.0 (C21), 113.1 (C4), 73.4 (C1), 55.2 (C6), 52.9 (C8); ^{15}N NMR (50 Hz, CD$_2$Cl$_2$, 233 K): δ = −252.2, −263.2 (the ^{15}N resonances were observed by ^{1}H/^{15}N HMBC NMR spectroscopy); HRMS (ESI+): *m/z*: calculated for C$_{22}$H$_{21}$N$_2$O$_3$ [M+H]$^+$: 361.15467, found: 361.15439.

Methyl 3-(4-methoxyphenyl)-1,2-diphenyldiaziridine-3-carboxylate (157). A cold (0 °C) solution of diazo compound **87** (9.4 mg, 0.046 mmol) in degassed CD$_2$Cl$_2$ (0.5 mL) was added dropwise to an ice-cold solution of [Cp*RhI$_2$]$_2$ (22.4 mg, 0.023 mmol) in degassed CD$_2$Cl$_2$ (1 mL) and the resulting mixture was stirred for 15 min whilst cooling in an ice bath. The mixture was cooled to −78 °C before solid (*Z*)-**117** (8.8 mg, 0.048 mmol) was added in one portion and the resulting mixture was stored at −40 °C overnight. The mixture was layered with pre-cooled (−40 °C) and carefully degassed *n*-pentane (1.5 mL) and stored at the same temperature, which resulted in precipitation of a red solid. The mother liquor was transferred into another pre-cooled (−40 °C) Schlenk tube, layered with pre-cooled (−40 °C) *n*-pentane (2 mL), and slowly cooled to −78 °C to give the title compound in the form of small colorless crystals suitable for X-ray diffraction.
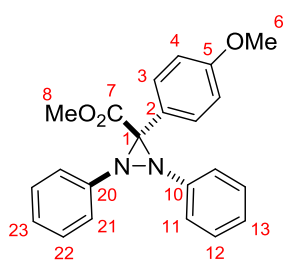
5.3.10 Rh(III)-Catalyzed Reaction of α-Diazo Ester 119 and an Aryl Imine

Methyl (*E*)-1,2,3-triphenylaziridine-2-carboxylate (159). A solution of diazo compound **119** (66.1 mg, 0.375 mmol) in CH$_2$Cl$_2$ (2 mL) was added *via* syringe pump over the course of 1 h to a solution of benzylideneaniline (44.6 mg, 0.246 mmol) and [Cp*RhI$_2$]$_2$ (2.3 mg, 2.3 μmol) in CH$_2$Cl$_2$ (1 mL). After consumption of the starting material, as indicated by TLC, the reaction mixture was concentrated *in vacuo*. The residue was purified by flash chromatography (silica, hexanes/EtOAc, 10:1) to give the title compound as a colorless solid (55 mg, 68%). This compound has been described previously in the literature without any characterization data.[152] M.p.: 105–106 °C; ^{1}H NMR (400 MHz, CDCl$_3$): δ = 7.35–7.28 (m, 4 H), 7.25–7.11 (m, 8 H), 7.09–7.03 (m, 3 H), 4.49 (s, 1 H), 3.55 (s, 3 H); ^{13}C{^{1}H} NMR (100 MHz, CDCl$_3$): δ = 168.6, 149.6, 134.9, 134.1, 129.5, 129.3, 128.0, 127.9, 127.7 (2 C), 127.6, 123.1, 119.2, 57.1, 52.8, 52.1; IR (solid): $\tilde{v}$ = 3062, 3028, 3007, 2953, 1723, 1597, 1488, 1454, 1431, 1272, 1229, 1211, 1147, 1075, 1018, 761, 694; MS (EI, %): m/z = 330 (23), 329 [M]$^+$ (95), 328 (72), 314 (14), 298 (31), 297 (18), 271 (21), 270 (99), 269 (99), 252 (4), 237 (13), 236 (7), 193 (9), 182 (9), 181 (16), 180 (100), 178 (12), 167 (39), 166 (14), 165 (38), 152 (14), 135 (6), 134 (6), 121 (23), 105 (3), 104 (3), 89 (7), 77 (26); HRMS (ESI+): m/z: calculated for C$_{22}$H$_{20}$NO$_2$ [M+H]$^+$: 330.14885, found: 330.14878.
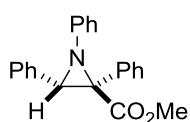
5.3.11 Rh(III)-Catalyzed Metathesis of α-Diazo Ester 119 and Nitrosobenzene

A solution of diazo compound **119** (103.3 mg, 0.586 mmol) in toluene (2 mL) was added *via* syringe pump over the course of 2 h to a solution of nitrosobenzene (28.6 mg, 0.267 mmol) and [Cp*RhI$_2$]$_2$ (9.7 mg, 0.01 mmol) in toluene (3 mL). After consumption of the starting material, as indicated by TLC, the reaction mixture was concentrated *in vacuo*. The residue was purified by flash chromatography (silica, hexanes/EtOAc, 20:1→5:1) to give the following compounds.

(*E*)-Azobenzide ((*E*)-117). Red-orange oil (5 mg, 21%). The spectral data matched those of a commercial sample. ^{1}H NMR (400 MHz, CDCl$_3$): δ = 7.96–7.90 (m, 4 H), 7.57–7.45 (m, 6 H).
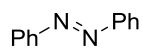
Methyl (*Z*)-2-phenyl-2-(phenylimino)acetate (120). Orange oil (20 mg, mixture of two geometric isomers (95:5), 33%). The spectral data of the major isomer matched the previously reported values.[167] ^{1}H NMR (400 MHz, CDCl$_3$): δ = 7.90–7.85 (m, 2 H), 7.56–7.44 (m, 3 H), 7.37–7.31 (m, 2 H), 7.17–7.11 (m, 1 H), 6.99–6.94 (m, 2 H), 3.64 (s, 3 H); ^{13}C{^{1}H} NMR (100 MHz, CDCl$_3$): δ = 165.6, 160.1, 150.2, 134.0, 132.0, 129.0, 128.9, 128.1, 125.1, 119.6, 52.0.
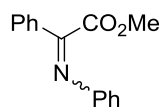
Methyl 2-oxo-2-phenylacetate (161). Red orange oil (30 mg, 68%). The spectral data matched those of a commercial sample. ^{1}H NMR (400 MHz, CDCl$_3$): δ = 8.05–7.99 (m, 2 H), 7.70–7.63 (m, 1 H), 7.55–7.48 (m, 2 H), 3.98 (s, 3 H); ^{13}C{^{1}H} NMR (100 MHz, CDCl$_3$): δ = 186.2, 164.2, 135.1, 132.6, 130.2, 129.1, 52.9.
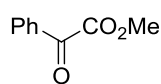
Methyl benzoyl(phenyl)carbamate (162). Off-white oil (12 mg, 18%). ^{1}H NMR (400 MHz, CDCl$_3$): δ = 7.74–7.68 (m, 2 H), 7.54–7.48 (m, 1 H), 7.45–7.38 (m, 4 H), 7.38–7.32 (m, 1 H), 7.28–7.22 (m, 2 H), 3.68 (s, 3 H); ^{13}C{^{1}H} NMR (100 MHz, CDCl$_3$): δ = 172.2, 155.4, 138.8, 135.7, 132.2, 129.4, 128.5, 128.4, 128.2, 128.1, 54.0; IR (film): $\tilde{v}$ = 3062, 3035, 2955, 1735, 1682, 1596, 1492, 1437, 1253, 1054, 692; MS (EI, %): m/z = 255 [M]$^+$ (10), 197 (2), 196 (2), 168 (1), 119 (14), 106 (7), 105 (1002), 91 (2), 77 (32), 65 (2), 51 (6); HRMS (ESI+): m/z: calculated for C$_{15}$H$_{13}$NO$_3$Na [M+Na]$^+$: 278.07876, found: 278.07887.
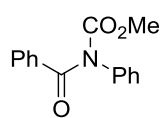
5.3.12 Rh(II)-Catalyzed Metathesis of Diazo Ester 163 and Azobenzene

A solution of freshly prepared diazo compound **163** (117.5 mg, 0.581 mmol) in toluene (2 mL) was added *via* syringe pump over the course of 2 h to a solution of azobenzene **117** (45.5 mg, 0.250 mmol) and Rh$_2$(OAc)$_4$ (2.4 mg, 5.4 μmol) in toluene (3 mL) during constant irradiation of the mixture with the light emitted by blue LEDs (Figure S1 in the appendix). After consumption of the starting material, as indicated by TLC, the mixture was concentrated *in vacuo*. The residue was purified by flash chromatography (silica, hexanes/EtOAc, 20:1) to give following compounds.

Methyl 1,2,5-triphenyl-2,5-dihydro-1*H*-pyrazole-3-carboxylate (164). Yellow oil (26 mg, 29%). ^{1}H NMR (400 MHz, CDCl$_3$): δ = 7.38–7.19 (m, 11 H), 7.10–6.97 (m, 4 H), 6.44 (d, *J* = 3.5 Hz, 1 H), 5.36 (d, *J* = 3.5 Hz, 1 H), 3.81 (s, 3 H); ^{13}C{^{1}H} NMR (100 MHz, CDCl$_3$): δ = 161.8, 154.3, 148.8, 140.7, 137.3, 129.3, 129.0, 128.8, 127.8, 126.4, 124.1, 122.5, 122.2, 120.1, 115.8, 77.2, 52.5; IR (film): $\tilde{v}$ = 3060, 3024, 2838, 2952, 1733, 1593, 1486, 1453, 1319, 1230, 1204, 1152, 1068, 751, 695; MS (EI, %): m/z = 357 (4), 356
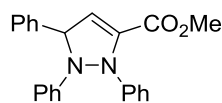
(18), 355 [M]⁺ (20), 280 (18), 279 (100), 219 (5), 206 (3), 180 (6), 165 (1), 144 (1), 117 (2), 116 (2), 104 (2), 91 (2), 77 (14); HRMS (ESI+): *m/z*: calculated for $C_{23}H_{21}N_2O_2$ [M+H]⁺: 357.15975, found: 357.15986.

Dimethyl 1,2,3,6-tetraphenyl-2,3,3a,6-tetrahydrocyclopenta[*c*]pyrazole-4,6a(1*H*)-dicarboxylate (165). Yellow solid (26 mg, 20%). Crystals suitable for X-ray diffraction were grown by slow diffusion of *n*-pentane into a solution in CH_2Cl_2 at room temperature. ¹H NMR (400 MHz, CDCl₃): δ = 7.79–7.71 (m, 2 H), 7.46–7.38 (m, 2 H), 7.36–7.30 (m, 2 H), 7.30–7.20 (m, 5 H), 7.17–7.10 (m, 2 H), 6.99–6.90 (m, 2 H), 6.86–6.79 (m, 1 H), 6.74 (t, *J* = 2.2 Hz, 1 H), 6.69–6.63 (m, 1 H), 6.60–6.53 (m, 2 H), 5.36 (d, *J* = 3.5 Hz, 1 H), 5.66 (s, 1 H), 5.45 (t, *J* = 2.1 Hz, 1 H), 4.39 (q, *J* = 2.0 Hz, 1 H), 3.79 (s, 3 H), 2.91 (s, 3 H); ¹³C{¹H} NMR (100 MHz, CDCl₃): δ = 172.8, 164.5, 149.1, 147.3, 147.1, 142.9, 137.3, 133.1, 131.2, 128.6, 128.2, 128.2, 128.1, 128.1, 126.9, 126.6, 119.5, 119.4, 114.7, 83.6, 77.2, 70.9, 68.1, 57.1, 52.0, 51.8; IR (solid): $\tilde{v}$ = 3060, 3033, 2950, 1723, 1709, 1592, 1488, 1438, 1265, 1232, 1105, 745, 694; MS (EI, %): *m/z* = 532 (8), 531 (37), 530 [M]⁺ (100), 515 (8), 472 (5), 471 (15), 453 (12), 379 (1), 368 (2), 355 (2), 348 (2), 334 (2), 290 (31), 273 (8), 272 (45), 271 (11), 258 (5), 230 (10), 206 (2, 204 (2), 202 (1), 181 (23), 180 (25), 128 (4), 104 (3), 77 (15); HRMS (ESI+): *m/z*: calculated for $C_{34}H_{31}N_2O_4$ [M+H]⁺: 531.22783, found: 531.22772.
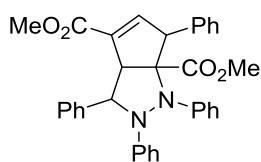
6 References and Notes

[1]   K. J. Laidler, *Pure Appl. Chem.* **1996**, *68*, 149.

[2]   J. J. Berzelius, *Årsberättelse om framstegen i fysik och kemi [Annual report on progress in physics and chemistry]*, Stockholm (Sweden), **1835**.

[3]   M. W. Roberts, *Catal. Lett.* **2000**, *67*, 1.

[4]   I. Chorkendorff, J. W. Niemantsverdriet, *Concepts of Modern Catalysis and Kinetics*, WILEY-VCH, Weinheim (Germany), **2007**.

[5]   B. Lindström, L. J. Pettersson, *CATTECH* **2003**, *7*, 130.

[6]   J. Hagen, *Industrial Catalysis. A Practical Approach*, WILEY-VCH, Weinheim (Germany), **2015**.

[7]   a) F. Diederich, A. de Meijere (Eds.) *Metal-Catalyzed Cross-Coupling Reactions*, WILEY-VCH, Weinheim (Germany), **2004**; b) M. Beller, C. Bolm, *Transition Metals for Organic Synthesis. Building Blocks and Fine Chemicals*, WILEY-VCH, Weinheim (Germany), **2006**.

[8]   a) M. Beller, A. Zapf in *Handbook of Organopalladium Chemistry for Organic Synthesis* (Ed.: E.-i. Negishi), John Wiley & Sons, Inc., New York (USA), **2002**; b) A. Zapf, M. Beller, *Top. Catal.* **2002**, *19*, 101.

[9]   A. D. Schlüter, Z. Bo in *Handbook of Organopalladium Chemistry for Organic Synthesis* (Ed.: E.-i. Negishi), John Wiley & Sons, Inc., New York (USA), **2002**.

[10]   K. C. Nicolaou, E. J. Sorensen, *Classics in Total Synthesis*, WILEY-VCH, Weinheim (Germany), **2008**.

[11]   "The Nobel Prize in Chemistry 2010", Nobelprize.org, Nobel Media AB 2014, can be found under http://www.nobelprize.org/nobel_prizes/chemistry/laureates/2010/, accessed on Mar 13, 2018.

[12]   K. S. Egorova, V. P. Ananikov, *Angew. Chem. Int. Ed.* **2016**, *55*, 12150.

[13]   Values based on www.infomine.com. The stated values are the average of the last three month period (Oct–Dec 2017). In the case of iron, the price is based on iron ore pellets. See also: S. Enthaler, K. Junge, M. Beller, *Angew. Chem. Int. Ed.* **2008**, *47*, 3317.

[14]   European Medicines Agency, *Guideline on the Specification Limits for Residues of Metal Catalysts or Metal Reagents. EMEA/CHMP/SWP/4446/2000*, London (UK), **2008**.

[15]   A. Piontek, E. Bisz, M. Szostak, *Angew. Chem. Int. Ed.,* doi:10.1002/anie.201800364.

[16]   A. Fürstner, A. Leitner, G. Seidel, *Org. Synth.* **2005**, *81*, 33.

[17]   C.-L. Sun, A. Fürstner, *Angew. Chem. Int. Ed.* **2013**, *52*, 13071.

[18]   C.-X. Zhuo, A. Fürstner, *Angew. Chem. Int. Ed.* **2016**, *55*, 6051.

[19]   a) C. Bolm, J. Legros, J. Le Paih, L. Zani, *Chem. Rev.* **2004**, *104*, 6217; b) I. Bauer, H.-J. Knölker, *Chem. Rev.* **2015**, *115*, 3170.

[20]   a) B. Plietker (Ed.) *Iron Catalysis in Organic Chemistry. Reactions and Applications*, WILEY-VCH, Weinheim (Germany), **2008**; b) B. Plietker (Ed.) *Top. Organomet. Chem.*, *Vol. 33*, Springer, Heidelberg, **2011**; c) E. Nakamura, T. Hatakeyama, S. Ito, K. Ishizuka, L. Ilies, M. Nakamura, *Org. React.* **2013**, *83*, 1; d) I. Marek, Z. Rappoport (Eds.) *The Chemistry of Organoiron Compounds*, Wiley, Chichester (UK), **2014**; e) E. Bauer (Ed.) *Top. Organomet. Chem.*, *Vol. 50*, Springer, Cham (CH), **2015**.

[21]   a) H. Shinokubo, K. Oshima, *Eur. J. Org. Chem.* **2004**, *2004*, 2081; b) A. Fürstner, R. Martin, *Chem. Lett.* **2005**, *34*, 624; c) E. B. Bauer, *Curr. Org. Chem.* **2008**, *12*, 1341; d) B. D. Sherry, A. Fürstner, *Acc. Chem. Res.* **2008**, *41*, 1500; e) W. M. Czaplik, M. Mayer, J. Cvengros, A. Jacobi von Wangelin, *ChemSusChem* **2009**, *2*, 396; f) O. Kuzmina, A. Steib, A. Moyeux, G. Cahiez, P. Knochel, *Synthesis* **2015**, *47*, 1696; g) A. Guérinot, J. Cossy, *Top. Curr. Chem.* **2016**, *374*, 49; h) W. M. Czaplik, M. Mayer, S. Grupe, A. Jacobi von Wangelin, *Pure Appl. Chem.* **2010**, *82*, 2968; i) A. Correa, O. García Mancheño, C. Bolm, *Chem. Soc. Rev.* **2008**, *37*, 1108.

[22]   Special issue on "Earth Abundant Metals in Homogeneous Catalysis" in Accounts of Chemical Research: P. J. Chirik, R. Morris, *Acc. Chem. Res.* **2015**, *48*, 2495.

[23]   Special issue on "Iron Catalysis" in Israel Journal of Chemistry: C. Darcel, J.-B. Sortais, *Isr. J. Chem.* **2017**, *57*, 1069.

[24]   C–H functionalization processes: a) G. Cera, L. Ackermann, *Top. Curr. Chem.* **2016**, *374*, 57; b) R. Shang, L. Ilies, E. Nakamura, *Chem. Rev.* **2017**, *117*, 9086.

[25]   C–O Bond activation reactions: a) T. Mesganaw, N. K. Garg, *Org. Process Res. Dev.* **2012**, *17*, 29; b) E. Bisz, M. Szostak, *ChemSusChem* **2017**, *10*, 3964.

[26]   Low-valent Fe-catalyzed C–C bond forming reactions: E. Nakamura, N. Yoshikai, *J. Org. Chem.* **2010**, *75*, 6061.

[27]   Fe-promoted radical reactions: A. Gualandi, L. Mengozzi, P. G. Cozzi, *Asian J. Org. Chem.* **2017**, *6*, 1160.

[28]   Applications in total synthesis: J. Legros, B. Figadère, *Nat. Prod. Rep.* **2015**, *32*, 1541.

[29]   a) P. Knochel, T. Thaler, C. Diene, *Isr. J. Chem.* **2010**, *50*, 547; b) R. M. Bullock (Ed.) *Catalysis without Precious Metals*, WILEY-VCH, Weinheim (Germany), **2010**; c) R. Jana, T. P. Pathak, M. S. Sigman, *Chem. Rev.* **2011**, *111*, 1417.

[30]   M. S. Kharasch, E. K. Fields, *J. Am. Chem. Soc.* **1941**, *63*, 2316.

[31]   Although Kharasch's and Fields' report is usually cited as the first Fe-catalyzed coupling reaction, it seems that Michailenko and co-workers have reported the first Fe-catalyzed homocoupling of PhMgBr and BnMgBr in the early 1920s, see: a) J. I. Michailenko, M.

Sassypkina, *Chemisches Zentralblatt* **1923**, *94*, 1014; b) J. I. Michailenko, N. P. Protassowa, *Chemisches Zentralblatt* **1923**, *94*, 1014.

[32]   G. Vavon, P. Mottez, *C. R. Hebd. Seances Acad. Sci.* **1944**, *218*, 557.

[33]   W. C. Percival, R. B. Wagner, N. C. Cook, *J. Am. Chem. Soc.* **1953**, *75*, 3731.

[34]   J. Cason, K. W. Kraus, *J. Org. Chem.* **1961**, *26*, 1768.

[35]   J. Cason, K. W. Kraus, *J. Org. Chem.* **1961**, *26*, 1772.

[36]   a) M. Tamura, J. K. Kochi, *J. Am. Chem. Soc.* **1971**, *93*, 1487; b) M. Tamura, J. K. Kochi, *Synthesis* **1971**, *1971*, 303; c) M. Tamura, J. K. Kochi, *J. Organomet. Chem.* **1971**, *31*, 289.

[37]   S. M. Neumann, J. K. Kochi, *J. Org. Chem.* **1975**, *40*, 599.

[38]   a) K. Tamao, K. Sumitani, M. Kumada, *J. Am. Chem. Soc.* **1972**, *94*, 4374; b) R. J. P. Corriu, J. P. Masse, *J. Chem. Soc., Chem. Commun.* **1972**, 144a.

[39]   a) M. Hanack, T. Baessler, W. Eymann, W. E. Heyd, R. Kopp, *J. Am. Chem. Soc.* **1974**, *96*, 6686; b) H. M. Walborsky, R. B. Banks, *J. Org. Chem.* **1981**, *46*, 5074; c) G. A. Molander, B. J. Rahn, D. C. Shubert, S. E. Bonde, *Tetrahedron Lett.* **1983**, *24*, 5449; d) U. H. Brinker, L. König, *Chem. Ber.* **1983**, *116*, 882; e) D. J. Wustrow, L. D. Wise, *Synthesis* **1991**, *1991*, 993; f) G. Cahiez, S. Marquais, *Pure Appl. Chem.* **1996**, *68*, 669; g) A. Fürstner, H. Brunner, *Tetrahedron Lett.* **1996**, *37*, 7009.

[40]   a) J.-L. Fabre, M. Julia, J.-N. Verpeaux, *Tetrahedron Lett.* **1982**, *23*, 2469; b) J.-L. Fabre, M. Julia, J.-N. Verpeaux, *Bull. Soc. Chim. Fr.* **1985**, 772; c) E. Alvarez, T. Cuvigny, C. Du Hervé Penhoat, M. Julia, *Tetrahedron* **1988**, *44*, 111; d) E. Alvarez, T. Cuvigny, C. Du Hervé Penhoat, M. Julia, *Tetrahedron* **1988**, *44*, 119.

[41]   a) V. Fiandanese, G. Marchese, V. Martina, L. Ronzini, *Tetrahedron Lett.* **1984**, *25*, 4805; b) K. Ritter, M. Hanack, *Tetrahedron Lett.* **1985**, *26*, 1285; c) C. Cardellicchio, V. Fiandanese, G. Marchese, L. Ronzini, *Tetrahedron Lett.* **1987**, *28*, 2053; d) C. K. Reddy, P. Knochel, *Angew. Chem. Int. Ed.* **1996**, *35*, 1700; e) M. M. Dell'Anna, P. Mastrorilli, C. F. Nobile, G. Marchese, M. R. Taurino, *J. Mol. Catal. A: Chem.* **2000**, *161*, 239.

[42]   C. Cardellicchio, V. Fiandanese, G. Marchese, L. Ronzini, *Tetrahedron Lett.* **1985**, *26*, 3595.

[43]   a) A. Yanagisawa, N. Nomura, H. Yamamoto, *Synlett* **1991**, *1991*, 513; b) A. Yanagisawa, N. Nomura, H. Yamamoto, *Tetrahedron* **1994**, *50*, 6017.

[44]   For an Fe-catalyzed reaction of diketene with Grignard reagents, see: T. Fujisawa, T. Sato, Y. Gotoh, M. Kawashima, T. Kawara, *Bull. Chem. Soc. Jpn.* **1982**, *55*, 3555.

[45]   G. Cahiez, H. Avedissian, *Synthesis* **1998**, *1998*, 1199.

[46]   P. Knochel, W. Dohle, N. Gommermann, F. F. Kneisel, F. Kopp, T. Korn, I. Sapountzis, V. A. Vu, *Angew. Chem. Int. Ed.* **2003**, *42*, 4302.

[47]   a) A. Fürstner, A. Leitner, *Angew. Chem. Int. Ed.* **2002**, *41*, 609; b) A. Fürstner, A. Leitner, M. Méndez, H. Krause, *J. Am. Chem. Soc.* **2002**, *124*, 13856.

[48]   For an Fe-catalyzed arylation of heteroaryl halides, see: J. Quintin, X. Franck, R. Hocquemiller, B. Figadère, *Tetrahedron Lett.* **2002**, *43*, 3547.

[49]   *Cf.* reference 30, and: M. S. Kharasch, W. Nudenberg, S. Archer, *J. Am. Chem. Soc.* **1943**, *65*, 495.

[50]   T. Hatakeyama, M. Nakamura, *J. Am. Chem. Soc.* **2007**, *129*, 9844.

[51]   T. Hatakeyama, S. Hashimoto, K. Ishizuka, M. Nakamura, *J. Am. Chem. Soc.* **2009**, *131*, 11949.

[52]   A. Fürstner, *ACS Cent. Sci.* **2016**, *2*, 778.

[53]   a) B. Hölzer, R. W. Hoffmann, *Chem. Commun.* **2003**, 732; b) A. Guérinot, S. Reymond, J. Cossy, *Angew. Chem. Int. Ed.* **2007**, *46*, 6521; c) J. Kleimark, A. Hedström, P.-F. Larsson, C. Johansson, P.-O. Norrby, *ChemCatChem* **2009**, *1*, 152; d) D. Noda, Y. Sunada, T. Hatakeyama, M. Nakamura, H. Nagashima, *J. Am. Chem. Soc.* **2009**, *131*, 6078; e) S. L. Daifuku, M. H. Al-Afyouni, B. E. R. Snyder, J. L. Kneebone, M. L. Neidig, *J. Am. Chem. Soc.* **2014**, *136*, 9132; f) A. Hedström, Z. Izakian, I. Vreto, C.-J. Wallentin, P.-O. Norrby, *Chem. Eur. J.* **2015**, *21*, 5946; g) S. L. Daifuku, J. L. Kneebone, B. E. R. Snyder, M. L. Neidig, *J. Am. Chem. Soc.* **2015**, *137*, 11432; h) C. Cassani, G. Bergonzini, C.-J. Wallentin, *ACS Catal.* **2016**, *6*, 1640; i) A. Bekhradnia, P.-O. Norrby, *Dalton Trans.* **2015**, *44*, 3959.

[54]   a) D. Schröder, S. Shaik, H. Schwarz, *Acc. Chem. Res.* **2000**, *33*, 139; b) J. N. Harvey, R. Poli, K. M. Smith, *Coord. Chem. Rev.* **2003**, *238-239*, 347.

[55]   S. H. Carpenter, M. L. Neidig, *Isr. J. Chem.* **2017**, *57*, 1106.

[56]   T. L. Mako, J. A. Byers, *Inorg. Chem. Front.* **2016**, *3*, 766.

[57]   R. S. Smith, J. K. Kochi, *J. Org. Chem.* **1976**, *41*, 502.

[58]   R. B. Bedford, *Acc. Chem. Res.* **2015**, *48*, 1485.

[59]   A. Fürstner, H. Krause, C. W. Lehmann, *Angew. Chem. Int. Ed.* **2006**, *45*, 440.

[60]   M. H. Al-Afyouni, K. L. Fillman, W. W. Brennessel, M. L. Neidig, *J. Am. Chem. Soc.* **2014**, *136*, 15457.

[61]   S. B. Muñoz Iii, S. L. Daifuku, W. W. Brennessel, M. L. Neidig, *J. Am. Chem. Soc.* **2016**, *138*, 7492.

[62]   R. Martin, A. Fürstner, *Angew. Chem. Int. Ed.* **2004**, *43*, 3955.

[63]   A. Fürstner, R. Martin, H. Krause, G. Seidel, R. Goddard, C. W. Lehmann, *J. Am. Chem. Soc.* **2008**, *130*, 8773.

[64]   a) J. Terao, N. Kambe, *Acc. Chem. Res.* **2008**, *41*, 1545; b) N. Kambe, T. Iwasaki, J. Terao, *Chem. Soc. Rev.* **2011**, *40*, 4937.

[65]   R. Jana, T. P. Pathak, M. S. Sigman, *Chem. Rev.* **2011**, *111*, 1417.

[66]   A. Rudolph, M. Lautens, *Angew. Chem. Int. Ed.* **2009**, *48*, 2656.

[67]   a) R. B. Bedford, D. W. Bruce, R. M. Frost, J. W. Goodby, M. Hird, *Chem. Commun.* **2004**, 2822; b) T. Nagano, T. Hayashi, *Org. Lett.* **2004**, *6*, 1297.

[68]   M. Nakamura, K. Matsuo, S. Ito, E. Nakamura, *J. Am. Chem. Soc.* **2004**, *126*, 3686.

[69]   Cross-coupling of *tert*-alkyl halides catalyzed by metals other than iron are also rare, see: a) P. Zhang, H. Le, R. E. Kyne, J. P. Morken, *J. Am. Chem. Soc.* **2011**, *133*, 9716; b) S. L. Zultanski, G. C. Fu, *J. Am. Chem. Soc.* **2013**, *135*, 624; c) X. Wang, S. Wang, W. Xue, H. Gong, *J. Am. Chem. Soc.* **2015**, *137*, 11562; d) K. Yotsuji, N. Hoshiya, T. Kobayashi, H. Fukuda, H. Abe, M. Arisawa, S. Shuto, *Adv. Synth. Catal.* **2015**, *357*, 1022.

[70]   Y. Nishii, K. Wakasugi, Y. Tanabe, *Synlett* **1998**, *1998*, 67.

[71]   a) D. J. Pasto, G. F. Hennion, R. H. Shults, A. Waterhouse, S.-K. Chou, *J. Org. Chem.* **1976**, *41*, 3496; b) D. J. Pasto, S.-K. Chou, A. Waterhouse, R. H. Shults, G. F. Hennion, *J. Org. Chem.* **1978**, *43*, 1385.

[72]   A. S. K. Hashmi, G. Szeimies, *Chem. Ber.* **1994**, *127*, 1075.

[73]   S. N. Kessler, J.-E. Bäckvall, *Angew. Chem. Int. Ed.* **2016**, *55*, 3734.

[74]   A. Fürstner, M. Méndez, *Angew. Chem. Int. Ed.* **2003**, *42*, 5355.

[75]   a) P. R. O. de Montellano, *J. Chem. Soc., Chem. Commun.* **1973**, 709; b) A. Doutheau, A. Saba, J. Gore, G. Quash, *Tetrahedron Lett.* **1982**, *23*, 2461; c) A. C. Oehlschlager, E. Czyzewska, *Tetrahedron Lett.* **1983**, *24*, 5587; d) C. R. Johnson, D. S. Dhanoa, *J. Org. Chem.* **1987**, *52*, 1885; e) J. A. Marshall, K. G. Pinney, *J. Org. Chem.* **1993**, *58*, 7180; f) F. Bertozzi, P. Crotti, F. Macchia, M. Pineschi, A. Arnold, B. L. Feringa, *Tetrahedron Lett.* **1999**, *40*, 4893; g) R. K. Dieter, L. E. Nice, *Tetrahedron Lett.* **1999**, *40*, 4293; h) C. Spino, S. Fréchette, *Tetrahedron Lett.* **2000**, *41*, 8033.

[76]   B. D. Sherry, A. Fürstner, *Chem. Commun.* **2009**, 7116.

[77]   A. Stolle, J. Ollivier, P. P. Piras, J. Salaün, A. de Meijere, *J. Am. Chem. Soc.* **1992**, *114*, 4051.

[78]   In the case of more involved reaction cascades, a net propargylic substitution has also been observed under copper catalysis, although the proposed mechanism suggests a carbocupration of an intermediate vinylidenecyclopropane. See: D.-Y. Li, Y. Wei, M. Shi, *Chem. Eur. J.* **2013**, *19*, 15682.

[79]   The screening of the leaving groups was conducted by Helga Krause.

[80]   Because the product in this transformation is opposite to what is expected from the corresponding copper catalysis (*i.e.*, allenes), potential copper impurities in the iron complex are considered to be negligible. See also: S. L. Buchwald, C. Bolm, *Angew. Chem. Int. Ed.* **2009**, *48*, 5586.

[81]   a) K. G. Dongol, H. Koh, M. Sau, C. L. L. Chai, *Adv. Synth. Catal.* **2007**, *349*, 1015; b) Y. Gartia, S. Pulla, P. Ramidi, C. C. Farris, Z. Nima, D. E. Jones, A. S. Biris, A. Ghosh, *Catal. Lett.* **2012**, *142*, 1397; c) T. Hatakeyama, T. Hashimoto, K. K. A. D. S. Kathriarachchi, T.

Zenmyo, H. Seike, M. Nakamura, *Angew. Chem. Int. Ed.* **2012**, *51*, 8834; d) S. Luo, D.-G. Yu, R.-Y. Zhu, X. Wang, L. Wang, Z.-J. Shi, *Chem. Commun.* **2013**, *49*, 7794.

[82] M. Guisan-Ceinos, F. Tato, E. Bunuel, P. Calle, D. J. Càrdenas, *Chem. Sci.* **2013**, *4*, 1098.

[83] a) B. Scheiper, M. Bonnekessel, H. Krause, A. Fürstner, *J. Org. Chem.* **2004**, *69*, 3943; b) G. Seidel, D. Laurich, A. Fürstner, *J. Org. Chem.* **2004**, *69*, 3950; c) A. L. Silberstein, S. D. Ramgren, N. K. Garg, *Org. Lett.* **2012**, *14*, 3796; d) T. Agrawal, S. P. Cook, *Org. Lett.* **2013**, *15*, 96; e) X. Chen, Z.-J. Quan, X.-C. Wang, *Appl. Organometal. Chem.* **2015**, *29*, 296; f) A. Piontek, M. Szostak, *Eur. J. Org. Chem.* **2017**, *2017*, 7271.

[84] S. Ito, Y.-i. Fujiwara, E. Nakamura, M. Nakamura, *Org. Lett.* **2009**, *11*, 4306.

[85] The reactions of entries 1, 3, 6, 9, 12, 14, 16, and 17 were conducted by Helga Krause. The full characterization of the products was obtained by Daniel J. Tindall.

[86] a) J. B. Lambert, *Tetrahedron* **1990**, *46*, 2677; b) J. B. Lambert, Y. Zhao, R. W. Emblidge, L. A. Salvador, X. Liu, J.-H. So, E. C. Chelius, *Acc. Chem. Res.* **1999**, *32*, 183.

[87] H. Krause, A. Fürstner, *unpublished results*.

[88] R. B. Bedford, D. W. Bruce, R. M. Frost, M. Hird, *Chem. Commun.* **2005**, 4161.

[89] G. Cahiez, V. Habiak, C. Duplais, A. Moyeux, *Angew. Chem. Int. Ed.* **2007**, *46*, 4364.

[90] K. G. Dongol, H. Koh, M. Sau, C. L. L. Chai, *Adv. Synth. Catal.* **2007**, *349*, 1015.

[91] a) N. Boudet, S. Sase, P. Sinha, C.-Y. Liu, A. Krasovskiy, P. Knochel, *J. Am. Chem. Soc.* **2007**, *129*, 12358; b) T. Hatakeyama, Y. Yoshimoto, T. Gabriel, M. Nakamura, *Org. Lett.* **2008**, *10*, 5341; c) F. M. Piller, A. Metzger, M. A. Schade, B. A. Haag, A. Gavryushin, P. Knochel, *Chem. Eur. J.* **2009**, *15*, 7192.

[92] a) G. Zuo, J. Louie, *Angew. Chem. Int. Ed.* **2004**, *43*, 2277; b) C. Vila, M. Giannerini, V. Hornillos, M. Fañanás-Mastral, B. L. Feringa, *Chem. Sci.* **2014**, *5*, 1361.

[93] S. Ma, Q. He, *Tetrahedron* **2006**, *62*, 2769.

[94] a) E. O. Fischer, H. Werner, *Angew. Chem. Int. Ed.* **1963**, *2*, 80; b) C. P. Casey, C. R. Cyr, *J. Am. Chem. Soc.* **1973**, *95*, 2248; c) P. Boudjouk, S. Lin, *J. Organomet. Chem.* **1978**, *155*, C13-C16; d) H.-J. Knölker, *Chem. Soc. Rev.* **1999**, *28*, 151; e) H. S. Clayton, J. R. Moss, M. E. Dry, *J. Organomet. Chem.* **2003**, *688*, 181; f) I. Bauer, H.-J. Knölker in *Iron Catalysis in Organic Chemistry. Reactions and Applications* (Ed.: B. Plietker), WILEY-VCH, Weinheim (Germany), **2008**; g) M. Mayer, A. Welther, A. Jacobi von Wangelin, *ChemCatChem* **2011**, *3*, 1567; h) A. Casitas, H. Krause, R. Goddard, A. Fürstner, *Angew. Chem. Int. Ed.* **2015**, *54*, 1521; i) A. Casitas, H. Krause, S. Lutz, R. Goddard, E. Bill, A. Fürstner, *Organometallics* **2018**, *37*, 729.

[95] I. D. Gridnev, *Coord. Chem. Rev.* **2008**, *252*, 1798.

[96] S. Gülak, A. Jacobi von Wangelin, *Angew. Chem. Int. Ed.* **2012**, *51*, 1357.

[97] Y. Yu, J. M. Smith, C. J. Flaschenriem, P. L. Holland, *Inorg. Chem.* **2006**, *45*, 5742.

[98]   a) C. J. Suckling, *Angew. Chem. Int. Ed.* **1988**, *27*, 537; b) J. Salaün in *Current Medicinal Chemistry* (Ed.: Atta-ur-Rahman), Bentham Science Publisher BV, Schipol (NL), **1995**, pp. 511–542; c) J. Salaün, *Top. Curr. Chem.* **2000**, *207*, 1; d) R. Faust, *Angew. Chem. Int. Ed.* **2001**, *40*, 2251; e) O. G. Kulinkovich, *Cyclopropanes in Organic Synthesis*, John Wiley & Sons, Inc., Hoboken (USA), **2015**.

[99]   J. Corbett, WO 2004/013110 (A1), **2004**.

[100]   a) S. S. Lee, W. Shen, X. Zheng, I. C. Jacobsen, WO 2012/083105 (A1), **2012**; b) J. Green, D. M. Wilson, L. C. C. Kong, S. K. Das, C. Poisson, J. J. Court, Q. Tang, P. Li, P. N. Collier, N. Waal, D. J. Lauffer, W. Dorsch, WO 2012/006055 (A2), **2012**.

[101]   F. F. van Goor, W. L. Burton, WO 2011/050325, **2011**.

[102]   S. A. M. Jeanmart, D. Bonvalot, F. Perruccio, S. V. Wendeborn, H. Nussbaumer, R. Rajan, R. Titulaer, WO 2013/144224 (A1), **2013**.

[103]   S. Y. Kim, S. I. Lee, S. Y. Choi, Y. K. Chung, *Angew. Chem. Int. Ed.* **2008**, *47*, 4914.

[104]   a) F. Inagaki, K. Sugikubo, Y. Miyashita, C. Mukai, *Angew. Chem. Int. Ed.* **2010**, *49*, 2206; b) Y. Oonishi, A. Hosotani, Y. Sato, *J. Am. Chem. Soc.* **2011**, *133*, 10386.

[105]   H. A. Wegner, *Dissertation*, Georg-August-Universität Göttingen, Göttingen (Germany), **2004**.

[106]   a) R. Paulissen, H. Reimlinger, E. Hayez, A. J. Hubert, P. Teyssié, *Tetrahedron Lett.* **1973**, *14*, 2233; b) A. J. Hubert, A. F. Noels, A. J. Anciaux, P. Teyssié, *Synthesis* **1976**, *1976*, 600.

[107]   M. P. Doyle, M. A. McKervey, T. Ye, *Modern Catalytic Methods for Organic Synthesis with Diazo Compounds: From Cyclopropanes to Ylides*, Wiley, New York (USA), **1998**.

[108]   P. A. Evans (Ed.) *Modern Rhodium-Catalyzed Organic Reactions*, WILEY-VCH, Weinheim (Germany), **2005**.

[109]   a) H. M. L. Davies, R. E. J. Beckwith, *Chem. Rev.* **2003**, *103*, 2861; b) H. M. L. Davies, E. G. Antoulinakis, *Org. React.* **2004**, *57*, 1; c) F. A. Cotton, C. A. Murillo, R. A. Walton (Eds.) *Multiple Bonds Between Metal Atoms*, Carlos A. Murillo, Boston (USA), **2005**; d) H. M. L. Davies, J. R. Manning, *Nature* **2008**, *451*, 417; e) H. M. L. Davies, J. R. Denton, *Chem. Soc. Rev.* **2009**, *38*, 3061; f) H. M. L. Davies, *Top. Curr. Chem.* **2010**, *292*, 303; g) H. M. L. Davies, D. Morton, *Chem. Soc. Rev.* **2011**, *40*, 1857; h) H. M. L. Davies, P. M. Pelphrey, *Org. React.* **2011**, *75*, 75; i) H. M. L. Davies, Y. Lian, *Acc. Chem. Res.* **2012**, *45*, 923.

[110]   a) M. P. Doyle, *Chem. Rev.* **1986**, *86*, 919; b) M. P. Doyle, D. C. Forbes, *Chem. Rev.* **1998**, *98*, 911; c) M. P. Doyle, D. J. Timmons in *Multiple Bonds Between Metal Atoms* (Eds.: F. A. Cotton, C. A. Murillo, R. A. Walton), Carlos A. Murillo, Boston (USA), **2005**, pp. 591–632; d) M. P. Doyle, *J. Org. Chem.* **2006**, *71*, 9253; e) M. P. Doyle, R. Duffy, M. Ratnikov, L. Zhou, *Chem. Rev.* **2010**, *110*, 704.

[111]   a) A. Padwa, M. D. Weingarten, *Chem. Rev.* **1996**, *96*, 223; b) A. Padwa, *Chem. Soc. Rev.* **2009**, *38*, 3072.

[112]   a) T. Ye, M. A. McKervey, *Chem. Rev.* **1994**, *94*, 1091; b) H. Lebel, J.-F. Marcoux, C. Molinaro, A. B. Charette, *Chem. Rev.* **2003**, *103*, 977; c) P. M. P. Gois, C. A. M. Afonso, *Eur. J. Org. Chem.* **2004**, *2004*, 3773; d) Z. Zhang, J. Wang, *Tetrahedron* **2008**, *64*, 6577; e) Y. Zhang, J. Wang, *Coord. Chem. Rev.* **2010**, *254*, 941; f) S.-F. Zhu, Q.-L. Zhou, *Acc. Chem. Res.* **2012**, *45*, 1365; g) D. Gillingham, N. Fei, *Chem. Soc. Rev.* **2013**, *42*, 4918; h) X. Guo, W.-H. Hu, *Acc. Chem. Res.* **2013**, *46*, 2427; i) G. K. Murphy, C. Stewart, F. G. West, *Tetrahedron* **2013**, *69*, 2667; j) A. Ford, H. Miel, A. Ring, C. N. Slattery, A. R. Maguire, M. A. McKervey, *Chem. Rev.* **2015**, *115*, 9981; k) A. DeAngelis, R. Panish, J. M. Fox, *Acc. Chem. Res.* **2016**, *49*, 115.

[113]   a) J. Barluenga, C. Valdés, *Angew. Chem. Int. Ed.* **2011**, *50*, 7486; b) Z. Shao, H. Zhang, *Chem. Soc. Rev.* **2012**, *41*, 560; c) P. Anbarasan, D. Yadagiri, S. Rajasekar, *Synthesis* **2014**, *46*, 3004; d) H. M. L. Davies, J. S. Alford, *Chem. Soc. Rev.* **2014**, *43*, 5151; e) Y. Wang, X. Lei, Y. Tang, *Synlett* **2015**, *26*, 2051; f) M. Jia, S. Ma, *Angew. Chem. Int. Ed.* **2016**, *55*, 9134.

[114]   K. H. Dötz, J. Stendel, *Chem. Rev.* **2009**, *109*, 3227.

[115]   R. R. Schrock, *Chem. Rev.* **2009**, *109*, 3211.

[116]   J. F. Berry, *Dalton Trans.* **2012**, *41*, 700.

[117]   E. Nakamura, N. Yoshikai, M. Yamanaka, *J. Am. Chem. Soc.* **2002**, *124*, 7181.

[118]   K. P. Kornecki, J. F. Briones, V. Boyarskikh, F. Fullilove, J. Autschbach, K. E. Schrote, K. M. Lancaster, H. M. L. Davies, J. F. Berry, *Science* **2013**, *342*, 351.

[119]   J. P. Snyder, A. Padwa, T. Stengel, A. J. Arduengo, A. Jockisch, H.-J. Kim, *J. Am. Chem. Soc.* **2001**, *123*, 11318.

[120]   C. Werlé, R. Goddard, A. Fürstner, *Angew. Chem. Int. Ed.* **2015**, *54*, 15452.

[121]   C. Werlé, R. Goddard, P. Philipps, C. Farès, A. Fürstner, *J. Am. Chem. Soc.* **2016**, *138*, 3797.

[122]   J. Hansen, J. Autschbach, H. M. L. Davies, *J. Org. Chem.* **2009**, *74*, 6555.

[123]   L. R. Collins, M. van Gastel, F. Neese, A. Fürstner, *manuscript in preparation*.

[124]   C. Werlé, R. Goddard, P. Philipps, C. Farès, A. Fürstner, *Angew. Chem. Int. Ed.* **2016**, *55*, 10760.

[125]   For reviews, see references 109g and 110e. For two selected examples addressing this matter, see: a) K. Liao, S. Negretti, D. G. Musaev, J. Bacsa, H. M. L. Davies, *Nature* **2016**, *533*, 230; b) K. Liao, W. Liu, Z. L. Niemeyer, Z. Ren, J. Bacsa, D. G. Musaev, M. S. Sigman, H. M. L. Davies, *ACS Catal.* **2017**, *8*, 678. For an outlook on undirected, homogeneous C–H bond functionalization, see: J. F. Hartwig, M. A. Larsen, *ACS Cent. Sci.* **2016**, *2*, 281.

[126]   R. H. Crabtree, A. Lei, *Chem. Rev.* **2017**, *117*, 8481.

[127] a) Z. Shi, D. C. Koester, M. Boultadakis-Arapinis, F. Glorius, *J. Am. Chem. Soc.* **2013**, *135*, 12204; b) W. Ai, X. Yang, Y. Wu, X. Wang, Y. Li, Y. Yang, B. Zhou, *Chem. Eur. J.* **2014**, *20*, 17653; c) F. Hu, Y. Xia, F. Ye, Z. Liu, C. Ma, Y. Zhang, J. Wang, *Angew. Chem. Int. Ed.* **2014**, *53*, 1364; d) J. Jeong, P. Patel, H. Hwang, S. Chang, *Org. Lett.* **2014**, *16*, 4598; e) Y. Liang, K. Yu, B. Li, S. Xu, H. Song, B. Wang, *Chem. Commun.* **2014**, *50*, 6130; f) J. Shi, Y. Yan, Q. Li, H. E. Xu, W. Yi, *Chem. Commun.* **2014**, *50*, 6483; g) B. Ye, N. Cramer, *Angew. Chem. Int. Ed.* **2014**, *53*, 7896; h) Y. Zhang, J. Zheng, S. Cui, *J. Org. Chem.* **2014**, *79*, 6490; i) Y. Cheng, C. Bolm, *Angew. Chem. Int. Ed.* **2015**, *54*, 12349; j) I. E. Iagafarova, D. V. Vorobyeva, A. S. Peregudov, S. N. Osipov, *Eur. J. Org. Chem.* **2015**, *2015*, 4950; k) S. Sharma, S. H. Han, S. Han, W. Ji, J. Oh, S.-Y. Lee, J. S. Oh, Y. H. Jung, I. S. Kim, *Org. Lett.* **2015**, *17*, 2852; l) L. Wang, Z. Li, X. Qu, W.-M. Peng, S.-Q. Hu, H.-B. Wang, *Tetrahedron Lett.* **2015**, *56*, 6214; m) Y. Yang, X. Wang, Y. Li, B. Zhou, *Angew. Chem. Int. Ed.* **2015**, *54*, 15400; n) S. Yu, S. Liu, Y. Lan, B. Wan, X. Li, *J. Am. Chem. Soc.* **2015**, *137*, 1623; o) B. Zhou, Z. Chen, Y. Yang, W. Ai, H. Tang, Y. Wu, W. Zhu, Y. Li, *Angew. Chem. Int. Ed.* **2015**, *54*, 12121; p) J. Zhou, J. Shi, X. Liu, J. Jia, H. Song, H. E. Xu, W. Yi, *Chem. Commun.* **2015**, *51*, 5868; q) Y.-S. Lu, W.-Y. Yu, *Org. Lett.* **2016**, *18*, 1350; r) K. S. Halskov, H. S. Roth, J. A. Ellman, *Angew. Chem.* **2017**, *129*, 9311; s) B. Zhang, B. Li, X. Zhang, X. Fan, *Org. Lett.* **2017**, *19*, 2294.

[128] W.-W. Chan, S.-F. Lo, Z. Zhou, W.-Y. Yu, *J. Am. Chem. Soc.* **2012**, *134*, 13565.

[129] T. K. Hyster, K. E. Ruhl, T. Rovis, *J. Am. Chem. Soc.* **2013**, *135*, 5364.

[130] a) D. A. Colby, A. S. Tsai, R. G. Bergman, J. A. Ellman, *Acc. Chem. Res.* **2012**, *45*, 814; b) G. Song, F. Wang, X. Li, *Chem. Soc. Rev.* **2012**, *41*, 3651; c) N. Kuhl, N. Schröder, F. Glorius, *Adv. Synth. Catal.* **2014**, *356*, 1443.

[131] a) A. Vigalok, D. Milstein, *Organometallics* **2000**, *19*, 2061; b) R. Cohen, B. Rybtchinski, M. Gandelman, H. Rozenberg, J. M. L. Martin, D. Milstein, *J. Am. Chem. Soc.* **2003**, *125*, 6532.

[132] D. Zhao, J. H. Kim, L. Stegemann, C. A. Strassert, F. Glorius, *Angew. Chem. Int. Ed.* **2015**, *54*, 4508.

[133] S.-S. Zhang, C.-Y. Jiang, J.-Q. Wu, X.-G. Liu, Q. Li, Z.-S. Huang, D. Li, H. Wang, *Chem. Commun.* **2015**, *51*, 10240.

[134] Y. Xia, D. Qiu, J. Wang, *Chem. Rev.* **2017**, *117*, 13810.

[135] a) F.-N. Ng, Y.-F. Lau, Z. Zhou, W.-Y. Yu, *Org. Lett.* **2015**, *17*, 1676; b) L. Qiu, D. Huang, G. Xu, Z. Dai, J. Sun, *Org. Lett.* **2015**, *17*, 1810.

[136] a) H. J. Callot, C. Piechocki, *Tetrahedron Lett.* **1980**, *21*, 3489; b) H. J. Callot, F. Metz, C. Piechocki, *Tetrahedron* **1982**, *38*, 2365; c) S. O'Malley, T. Kodadek, *Tetrahedron Lett.* **1991**, *32*, 2445; d) T. Hayashi, T. Kato, T. Kaneko, T. Asai, H. Ogoshi, *J. Organomet. Chem.* **1994**, *473*, 323; e) V. Lo, H.-Y. Thu, Y.-M. Chan, T.-L. Lam, W.-Y. Yu, C.-M. Che, *Synlett*

2012, *23*, 2753; f) N. M. G. Franssen, M. Finger, J. N. H. Reek, B. de Bruin, *Dalton Trans.* **2013**, *42*, 4139.

[137]   Ò. Torres, A. Pla-Quintana, *Tetrahedron Lett.* **2016**, *57*, 3881.

[138]   J. R. Rumble, *CRC Handbook of Chemistry and Physics*. Internet Version 2018, CRC Press/Taylor & Francis, Boca Raton (USA).

[139]   T. W. Hanks, R. A. Ekeland, K. Emerson, R. D. Larsen, P. W. Jennings, *Organometallics* **1987**, *6*, 28.

[140]   P. Bergamini, E. Costa, S. Sostero, A. G. Orpen, P. G. Pringle, *Organometallics* **1991**, *10*, 2989.

[141]   J. Maxwell, T. Kodadek, *Organometallics* **1991**, *10*, 4.

[142]   a) D. Tapu, D. A. Dixon, C. Roe, *Chem. Rev.* **2009**, *109*, 3385; b) L. Falivene, L. Cavallo, *Coord. Chem. Rev.* **2017**, *344*, 101; c) K. Yamamoto, C. P. Gordon, W.-C. Liao, C. Copéret, C. Raynaud, O. Eisenstein, *Angew. Chem. Int. Ed.* **2017**, *56*, 10127.

[143]   N. Wiberg, E. Wiberg, A. F. Holleman, *Lehrbuch der Anorganischen Chemie*, de Gruyter, Berlin (Germany), **2007**.

[144]   F. Weinhold, C. R. Landis, *Valency and Bonding. A Natural Bond Orbital Donor-Acceptor Perspective*, Cambridge University Press, Cambridge (UK), **2005**.

[145]   Z. Qi, S. Yu, X. Li, *Org. Lett.* **2016**, *18*, 700.

[146]   H. Günther, *NMR Spectroscopy. Basic Principles, Concepts, and Applications in Chemistry*, WILEY-VCH, Weinheim (Germany), **2013**.

[147]   The crystals suitable for X-ray crystallography were obtained by Dr. Christophe Werlé.

[148]   D. Panichakul, Y. Su, Y. Li, W. Deng, J. Zhao, X. Li, *Organometallics* **2008**, *27*, 6390.

[149]   a) For a review on iridium carbene chemistry, see: A. G. Schafer, S. B. Blakey, *Chem. Soc. Rev.* **2015**, *44*, 5969; b) For a recent advance, see: N. M. Weldy, A. G. Schafer, C. P. Owens, C. J. Herting, A. Varela-Alvarez, S. Chen, Z. L. Niemeyer, D. G. Musaev, M. S. Sigman, H. M. L. Davies, S. B. Blakey, *Chem. Sci.* **2016**, *7*, 3142.

[150]   C. Werlé, *Final Report: Transition Metal Carbene Chemistry*, Mülheim a. d. Ruhr (Germany), **2016**.

[151]   Y. Liu, *Curr. Org. Chem.* **2015**, *20*, 19.

[152]   M. P. Doyle, W.-H. Hu, D. J. Timmons, *Org. Lett.* **2001**, *3*, 933.

[153]   H. M. L. Davies, J. DeMeese, *Tetrahedron Lett.* **2001**, *42*, 6803.

[154]   Z. Wang, J. Wen, Q.-W. Bi, X.-Q. Xu, Z.-Q. Shen, X.-X. Li, Z. Chen, *Tetrahedron Lett.* **2014**, *55*, 2969.

[155]   V. K. Aggarwal, C. L. Winn, *Acc. Chem. Res.* **2004**, *37*, 611.

[156]   A. Caballero, P. J. Pérez, *Chem. Eur. J.* **2017**, *23*, 14389.

[157]   J.-Y. Son, S. Kim, W. H. Jeon, P. H. Lee, *Org. Lett.* **2015**, *17*, 2518.

[158] L. S. Hegedus, A. Kramer, *Organometallics* **1984**, *3*, 1263.

[159] L. S. Hegedus, B. R. Lundmark, *J. Am. Chem. Soc.* **1989**, *111*, 9194.

[160] H. F. Sleiman, L. McElwee-White, *J. Am. Chem. Soc.* **1988**, *110*, 8700.

[161] H. F. Sleiman, S. Mercer, L. McElwee-White, *J. Am. Chem. Soc.* **1989**, *111*, 8007.

[162] C. T. Maxey, H. F. Sleiman, S. T. Massey, L. McElwee-White, *J. Am. Chem. Soc.* **1992**, *114*, 5153.

[163] S. T. Massey, N. D. R. Barnett, K. A. Abboud, L. McElwee-White, *Organometallics* **1996**, *15*, 4625.

[164] W. J. Peng, A. S. Gamble, J. L. Templeton, M. Brookhart, *Inorg. Chem.* **1990**, *29*, 463.

[165] F. H. Allen, O. Kennard, D. G. Watson, L. Brammer, A. G. Orpen, R. Taylor, *J. Chem. Soc., Perkin Trans. 2* **1987**, S1.

[166] a) P. Gu, X.-P. Wu, Y. Su, X.-Q. Li, P. Xue, R. Li, *Synlett* **2014**, *25*, 535; b) Y. Qian, C. Jing, C. Zhai, W.-H. Hu, *Adv. Synth. Catal.* **2012**, *354*, 301; c) H. Huang, Y. Wang, Z. Chen, W.-H. Hu, *Synlett* **2005**, 2498.

[167] M. D. Mandler, P. M. Truong, P. Y. Zavalij, M. P. Doyle, *Org. Lett.* **2014**, *16*, 740.

[168] a) E. Merino, *Chem. Soc. Rev.* **2011**, *40*, 3835; b) E. Léonard, F. Mangin, C. Villette, M. Billamboz, C. Len, *Catal. Sci. Technol.* **2016**, *6*, 379.

[169] H. M. D. Bandara, S. C. Burdette, *Chem. Soc. Rev.* **2012**, *41*, 1809.

[170] D. Bleger, J. Schwarz, A. M. Brouwer, S. Hecht, *J. Am. Chem. Soc.* **2012**, *134*, 20597.

[171] In the photostationary state, the isomer ratio of azobenzene is *Z:E* = 37:63, *cf.*: E. Fischer, M. Frankel, R. Wolovsky, *J. Chem. Phys.* **1955**, *23*, 1367.

[172] For another recent example in which blue LEDs were required for a successful reaction of azobenzene after isomerization, see: H. Ikeda, K. Nishi, H. Tsurugi, K. Mashima, *Chem. Commun.* **2018**, *54*, 3709.

[173] a) H. M. L. Davies, G. H. Lee, *Org. Lett.* **2004**, *6*, 1233; b) J. F. Briones, J. Hansen, K. I. Hardcastle, J. Autschbach, H. M. L. Davies, *J. Am. Chem. Soc.* **2010**, *132*, 17211; c) J. F. Briones, H. M. L. Davies, *Org. Lett.* **2011**, *13*, 3984; d) J. F. Briones, H. M. L. Davies, *Tetrahedron* **2011**, *67*, 4313.

[174] For a review on transition metal-catalyzed N-atom transfer reactions of azides, see: T. G. Driver, *Org. Biomol. Chem.* **2010**, *8*, 3831.

[175] A. H. Cook, *J. Chem. Soc.* **1938**, 876.

[176] M. Komatsu, N. Nishikaze, M. Sakamoto, Y. Ohshiro, T. Agawa, *J. Org. Chem.* **1974**, *39*, 3198.

[177] a) G. K. Cantrell, T. Y. Meyer, *J. Am. Chem. Soc.* **1998**, *120*, 8035; b) R. L. Zuckerman, S. W. Krska, R. G. Bergman, *J. Am. Chem. Soc.* **2000**, *122*, 751.

[178] a) S. A. Blum, R. G. Bergman, *Organometallics* **2004**, *23*, 4003; b) J. W. Herndon, L. A. McMullen, *J. Organomet. Chem.* **1989**, *368*, 83; c) R. S. Pilato, G. D. Williams, G. L. Geoffroy, A. L. Rheingold, *Inorg. Chem.* **1988**, *27*, 3665.

[179] D. Beaudoin, J. D. Wuest, *Chem. Rev.* **2016**, *116*, 258.

[180] a) Y. Yu, Q. Sha, H. Cui, K. S. Chandler, M. P. Doyle, *Org. Lett.* **2018**, *20*, 776; b) J. Jeong, D. Lee, S. Chang, *Chem. Commun.* **2015**, *51*, 7035.

[181] N. R. O'Connor, P. Bolgar, B. M. Stoltz, *Tetrahedron Lett.* **2016**, *57*, 849.

[182] K. S. Williamson, D. J. Michaelis, T. P. Yoon, *Chem. Rev.* **2014**, *114*, 8016.

[183] a) H. W. Heine, T. R. Hoye, P. G. Williard, R. C. Hoye, *J. Org. Chem.* **1973**, *38*, 2984; b) A. V. Shevtsov, V. V. Kuznetsov, A. A. Kislukhin, V. Y. Petukhova, Y. A. Strelenko, N. N. Makhova, K. A. Lyssenko, *J. Heterocyclic Chem.* **2006**, *43*, 881; c) A. V. Shevtsov, A. A. Kislukhin, V. V. Kuznetsov, V. Y. Petukhova, V. A. Maslennikov, A. O. Borissova, K. A. Lyssenko, N. N. Makhova, *Mendeleev Commun.* **2007**, *17*, 119; d) Y. S. Syroeshkina, V. V. Kuznetsov, V. V. Kachala, N. N. Makhova, *J. Heterocyclic Chem.* **2009**, *46*, 1195; e) N. N. Makhova, A. V. Shevtsov, V. Y. Petukhova, *Russ. Chem. Rev.* **2011**, *80*, 1035; f) M. Kamuf, F. Rominger, O. Trapp, *Eur. J. Org. Chem.* **2012**, *2012*, 4733.

[184] J. R. Manning, H. M. L. Davies, *Org. Synth.* **2007**, *84*, 334.

[185] A. Thakur, J. Louie in *Molecular Rearrangements in Organic Synthesis* (Ed.: C. M. Rojas), Wiley, Hoboken (USA), **2015**.

[186] For a selected example of a Rh(II)-catalyzed reaction of DEAD and a carbonyl yilde, see: A. DeAngelis, M. T. Taylor, J. M. Fox, *J. Am. Chem. Soc.* **2009**, *131*, 1101.

[187] For an example of insertion of donor/donor diazo compounds into C–H bonds, see: S. Xu, G. Wu, F. Ye, X. Wang, H. Li, X. Zhao, Y. Zhang, J. Wang, *Angew. Chem. Int. Ed.* **2015**, *54*, 4669.

[188] a) M. Hidai, Y. Mizobe, *Chem. Rev.* **1995**, *95*, 1115; b) B. A. MacKay, M. D. Fryzuk, *Chem. Rev.* **2004**, *104*, 385; c) N. Hazari, *Chem. Soc. Rev.* **2010**, *39*, 4044.

[189] a) A. Spencer, *J. Organomet. Chem.* **1985**, *295*, 199; b) X. Yan, X. Yi, C. Xi, *Org. Chem. Front.* **2014**, *1*, 657; c) G. Hong, D. Mao, X. Zhu, S. Wu, L. Wang, *Org. Chem. Front.* **2015**, *2*, 985; d) X. Yi, C. Xi, *Org. Lett.* **2015**, *17*, 5836; e) Z. W. Gilbert, R. J. Hue, I. A. Tonks, *Nat. Chem.* **2016**, *8*, 63.

[190] B. Eftekhari-Sis, M. Zirak, *Chem. Rev.* **2017**, *117*, 8326.

[191] a) J. Britton, C. L. Raston, *Chem. Soc. Rev.* **2017**, *46*, 1250; b) M. B. Plutschack, B. Pieber, K. Gilmore, P. H. Seeberger, *Chem. Rev.* **2017**, *117*, 11796.

[192] F. Kleinbeck, F. D. Toste, *J. Am. Chem. Soc.* **2009**, *131*, 9178.

[193] E. D. Slack, C. M. Gabriel, B. H. Lipshutz, *Angew. Chem. Int. Ed.* **2014**, *53*, 14051.

[194] O. S. Ojo, P. A. Inglesby, D. E. Negru, P. A. Evans, *Org. Chem. Front.* **2014**, *1*, 821.

[195]   L. G. Quan, H. G. Lee, J. K. Cha, *Org. Lett.* **2007**, *9*, 4439.

[196]   J. Salaün, *J. Org. Chem.* **1978**, *43*, 2809.

[197]   J. Ollivier, P. Dorizon, P. P. Pirasa, A. de Meijere, J. Salaün, *Inorg. Chim. Acta* **1994**, *222*, 37.

[198]   J. Salaün, *J. Org. Chem.* **1976**, *41*, 1237.

[199]   S. Bräse, S. Schömenauer, G. McGaffin, A. Stolle, A. de Meijere, *Chem. Eur. J.* **1996**, *2*, 545.

[200]   F. Lecornué, F. Charnay-Pouget, J. Ollivier, *Synlett* **2006**, *2006*, 1407.

[201]   F. Lecornué, J. Ollivier, *Chem. Commun.* **2003**, *42*, 584.

[202]   a) D. Rosa, A. Orellana, *Chem. Commun.* **2013**, *49*, 5420; b) S. Ren, C. Feng, T.-P. Loh, *Org. Biomol. Chem.* **2015**, *13*, 5105.

[203]   A. Krasovskiy, P. Knochel, *Synthesis* **2006**, *2006*, 890.

[204]   W. M. Czaplik, S. Grupe, M. Mayer, A. Jacobi von Wangelin, *Chem. Commun.* **2010**, *46*, 6350.

[205]   W. D. Jones, F. J. Feher, *Inorg. Chem.* **1984**, *23*, 2376.

[206]   D. S. Gill, P. M. Maitlis, *J. Organomet. Chem.* **1975**, *87*, 359.

[207]   R. Hrdina, L. Guénée, D. Moraleda, J. Lacour, *Organometallics* **2013**, *32*, 473.

[208]   F. Ye, S. Qu, L. Zhou, C. Peng, C. Wang, J. Cheng, M. L. Hossain, Y. Liu, Y. Zhang, Z.-X. Wang, J. Wang, *J. Am. Chem. Soc.* **2015**, *137*, 4435.

[209]   F. Friscourt, C. J. Fahrni, G.-J. Boons, *Chem. Eur. J.* **2015**, *21*, 13996.

[210]   H. M. L. Davies, S. A. Panaro, *Tetrahedron* **2000**, *56*, 4871.

[211]   Z. Qu, W. Shi, J. Wang, *J. Org. Chem.* **2001**, *66*, 8139.

[212]   X. Liu, J. F. Hartwig, *J. Am. Chem. Soc.* **2004**, *126*, 5182.

[213]   C. Zhang, N. Jiao, *Angew. Chem. Int. Ed.* **2010**, *49*, 6174.

[214]   X. Geng, C. Wang, *Org. Lett.* **2015**, *17*, 2434.

[215]   C. Bornholdt, *Dissertation*, Christian-Albrechts-Universität, Kiel (Germany), **2008**.

[216]   a) L. Zhang, J. Xia, Q. Li, X. Li, S. Wang, *Organometallics* **2011**, *30*, 375; b) K. Seth, S. R. Roy, A. Kumar, A. K. Chakraborti, *Catal. Sci. Technol.* **2016**, *6*, 2892.

[217]   T. Doiuchi, T. Nakaya, M. Imoto, *Makromol. Chem.* **1972**, *161*, 231.

[218]   M. Y. Qui, J. C. Zhang, W. Y. Shi, Q. C. Jia, Y. S. Niu, *Asian J. Chem.* **2012**, *24*, 2295.

[219]   a) N. G. Pschirer, U. H. F. Bunz, *Tetrahedron Lett.* **1999**, *40*, 2481; b) S. Schaubach, *Dissertation*, Technische Universität Dortmund, Dortmund (Germany), **2016**.

[220]   S. Liu, Y. Yu, L. S. Liebeskind, *Org. Lett.* **2007**, *9*, 1947.

7 Appendix

7.1 Experimental Set-Up for the Azo Metathesis
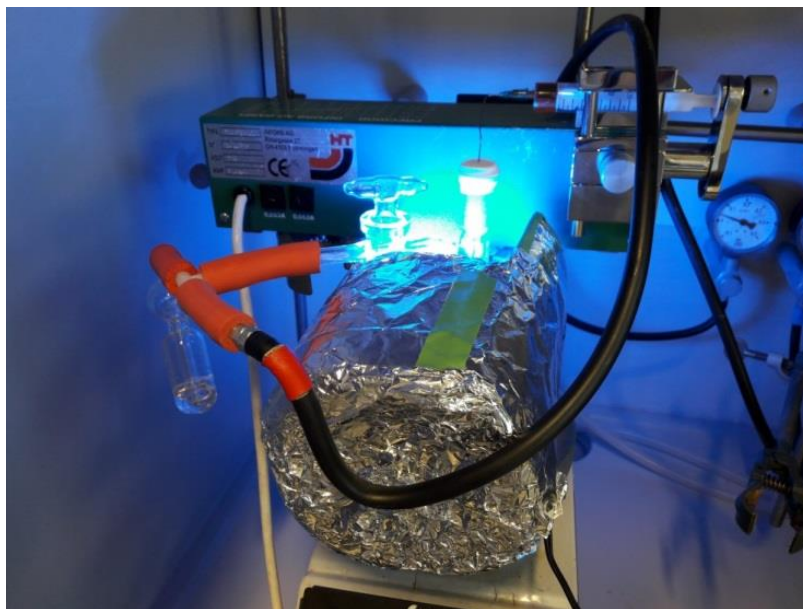
Figure S1: Experimental set-up for the Rh-catalyzed metathesis between diazo compounds and azoarenes performed at ambient temperature: Schlenk flask with septum in the center, syringe pump (in green) with syringe in the back, self-made LED array (*cf.* Figure 16) wrapped in aluminum foil, and argon supply (black tubing).
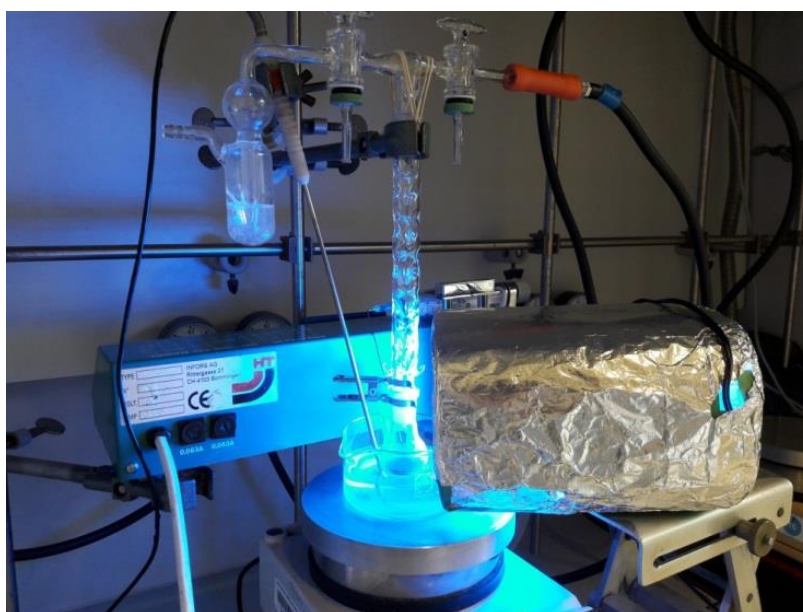
Figure S2: Experimental set-up for the Rh-catalyzed metathesis between diazo compounds and azoarenes at elevated temperatures: two-neck Schlenk flask in oil bath with septum and vigreux column (center), syringe pump (in green) with syringe in the back, self-made LED array (*cf.* Figure 16) wrapped in aluminum foil, and argon supply (black tubing).

7.2 Supplementary NMR Spectra
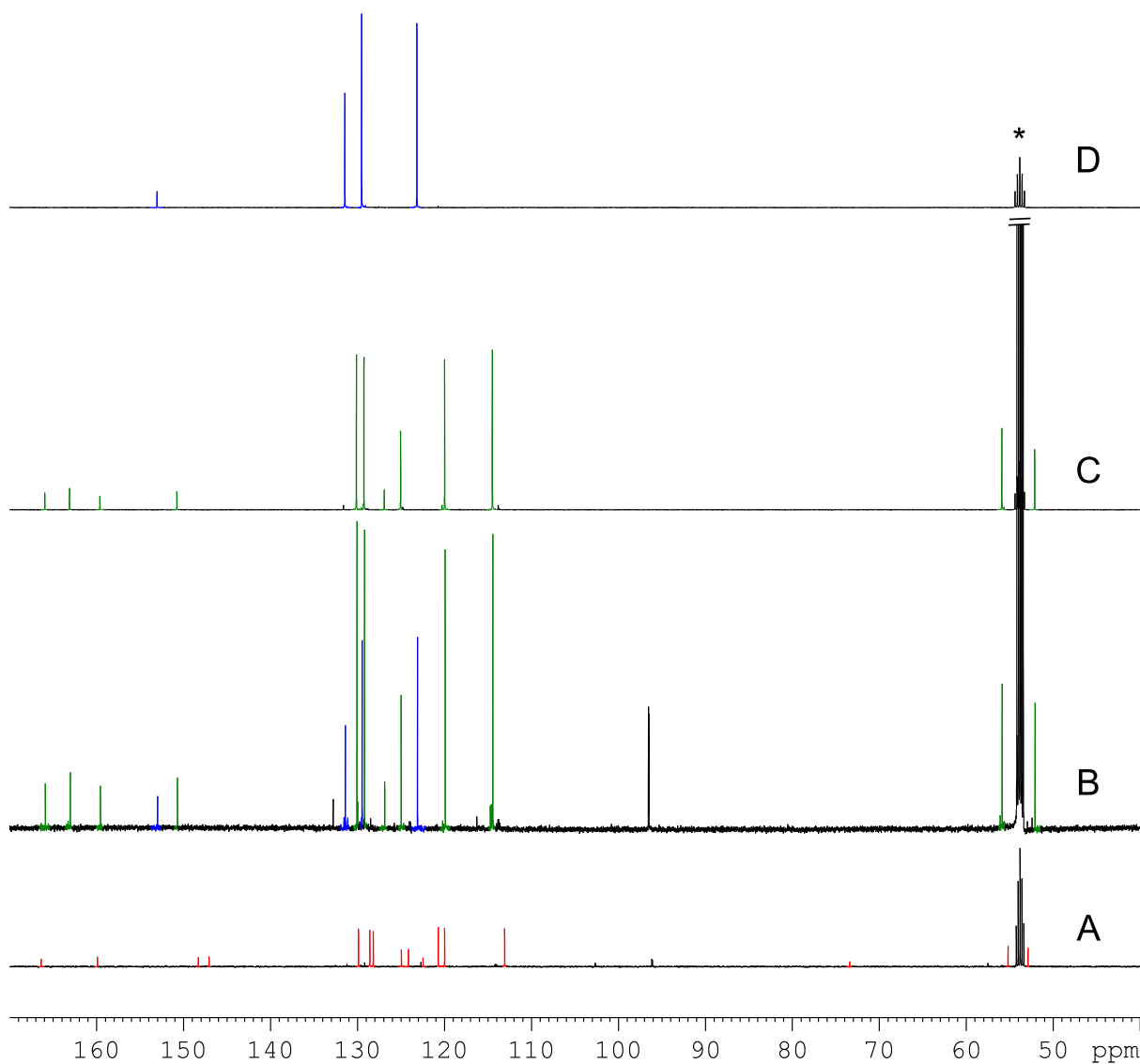
Figure S3: $^{13}C\{^1H\}$ NMR spectra (500 MHz, CD_2Cl_2) of A: the stoichiometric (1:1) reaction of carbene complex **95** and (*Z*)-**117** at −40 °C (*t* = 3 h), B: the same reaction mixture after warming to 25 °C (*cf*. Figure 12-F), C: an isolated sample of imine **118**, and D: an isolated sample of (*E*)-**117** (* = residual $CDHCl_2$ in CD_2Cl_2). Color coding refers to the structures in the equation at the top of Figure 12.

7.3 Crystallographic Data

7.3.1 Crystal Data and Structure Refinement of Alkynyl Tosylate 37d

Empirical formula	$C_{18}H_{16}O_3S$
Color	colorless
Formula weight	312.37 g·mol^{-1}
Temperature	100 K
Wavelength	0.71073 Å
Crystal system	orthorhombic
Space group	Pbca (№ 61)
Unit cell dimensions	a = 7.2040(16) Å $\quad$ α = 90°
	b = 20.271(4) Å $\quad$ β = 90°
	c = 21.103(5) Å $\quad$ γ = 90°
Volume	3081.7(12) Å^3
Z	8
Density (calculated)	1.347 Mg·m^{-3}
Absorption coefficient	0.220 mm^{-1}
F(000)	1312 e
Crystal size	0.341 × 0.173 × 0.010 mm^3
θ range for data collection	1.930 to 30.616°.
Index ranges	$-10 \le h \le 10$, $-29 \le k \le 28$, $-30 \le l \le 30$
Reflections collected	79443
Independent reflections	4735 [R_{int} = 0.0821]
Reflections with I>2σ(I)	3573
Completeness to θ = 25.242°	100.0%
Absorption correction	Gaussian
Max. and min. transmission	0.99777 and 0.95308
Refinement method	Full-matrix least-squares on F^2
Data / restraints / parameters	4735 / 0 / 200
Goodness-of-fit on F^2	1.155
Final R indices [I>2σ(I)]	R_1 = 0.0413 $\qquad$ wR_2 = 0.1167
R indices (all data)	R_1 = 0.0668 $\qquad$ wR_2 = 0.1459
Largest diff. peak and hole	0.560 and -0.595 e·Å^{-3}

CCDC 1472161 contains the supplementary crystallographic data for this compound. These data can be obtained free of charge from The Cambridge Crystallographic Data Centre *via* www.ccdc.cam.ac.uk/data_request/cif.

7.3.2 Crystal Data and Structure Refinement of Alkenyl Toslyate 43

Empirical formula	$C_{18}H_{18}O_3S$
Color	colorless
Formula weight	314.38 g·mol^{-1}
Temperature	200 K
Wavelength	0.71073 Å
Crystal system	monoclinic
Space group	P2$_1$/c (№ 14)
Unit cell dimensions	a = 21.541(3) Å α = 90°
	b = 7.4591(9) Å β = 106.055(2)°
	c = 20.595(2) Å γ = 90°
Volume	3180.1(6) Å^3
Z	8
Density (calculated)	1.313 Mg·m^{-3}
Absorption coefficient	0.213 mm^{-1}
F(000)	1328 e
Crystal size	0.290 × 0.167 × 0.081 mm^3
θ range for data collection	2.903 to 31.070°
Index ranges	$-31 \le h \le 31$, $-10 \le k \le 10$, $-29 \le l \le 29$
Reflections collected	91654
Independent reflections	10169 [R$_{int}$ = 0.0259]
Reflections with I>2σ(I)	8602
Completeness to θ = 25.242°	99.8%
Absorption correction	Gaussian
Max. and min. transmission	0.98449 and 0.96298
Refinement method	Full-matrix least-squares on F^2
Data / restraints / parameters	10169 / 0 / 399
Goodness-of-fit on F^2	1.059
Final R indices [I>2σ(I)]	R$_1$ = 0.0495 wR$_2$ = 0.1363
R indices (all data)	R$_1$ = 0.0586 wR$_2$ = 0.1448
Largest diff. peak and hole	0.956 and -0.350 e·Å^{-3}

CCDC 1472070 contains the supplementary crystallographic data for this compound. These data can be obtained free of charge from The Cambridge Crystallographic Data Centre *via* www.ccdc.cam.ac.uk/data_request/cif.

7.3.3 Crystal Data and Structure Refinement of Dimer 46

Empirical formula	$C_{22}H_{22}$
Color	colorless
Formula weight	$286.39 \text{ g·mol}^{-1}$
Temperature	100 K
Wavelength	0.71073 Å
Crystal system	orthorhombic
Space group	Aba2 (№ 41)
Unit cell dimensions	$a = 11.026(2)$ Å $\quad \alpha = 90°$
	$b = 21.404(4)$ Å $\quad \beta = 90°$
	$c = 7.0746(14)$ Å $\quad \gamma = 90°$
Volume	$1669.6(6) \text{ Å}^3$
Z	4
Density (calculated)	1.139 Mg·m^{-3}
Absorption coefficient	0.064 mm^{-1}
F(000)	616 e
Crystal size	$0.180 \times 0.100 \times 0.030 \text{ mm}^3$
θ range for data collection	3.552 to 31.006°
Index ranges	$-15 \leq h \leq 15, -30 \leq k \leq 30, -10 \leq l \leq 10$
Reflections collected	23686
Independent reflections	2652 [R_{int} = 0.0336]
Reflections with I>2σ(I)	2534
Completeness to θ = 25.242°	99.8%
Absorption correction	Gaussian
Max. and min. transmission	0.99821 and 0.98810
Refinement method	Full-matrix least-squares on F^2
Data / restraints / parameters	2652 / 1 / 107
Goodness-of-fit on F^2	1.056
Final R indices [I>2σ(I)]	$R_1 = 0.0328$ $\quad$ $wR_2 = 0.0874$
R indices (all data)	$R_1 = 0.0352$ $\quad$ $wR_2 = 0.0890$
Largest diff. peak and hole	0.307 and -0.194 e·Å^{-3}

CCDC 1472067 contains the supplementary crystallographic data for this compound. These data can be obtained free of charge from The Cambridge Crystallographic Data Centre *via* www.ccdc.cam.ac.uk/data_request/cif.

7.3.4 Crystal Data and Structure Refinement of Bicyclic Tosylate 57

Empirical formula	$C_{15}H_{18}O_3S$
Color	colorless
Formula weight	278.35 g·mol^{-1}
Temperature	100 K
Wavelength	0.71073 Å
Crystal system	monoclinic
Space group	P2$_1$/c (№ 14)
Unit cell dimensions	a = 6.0865(19) Å α = 90°
	b = 15.313(5) Å β = 90.171(5)°
	c = 15.003(5) Å γ = 90°
Volume	1398.3(7) Å^3
Z	4
Density (calculated)	1.322 Mg·m^{-3}
Absorption coefficient	0.233 mm^{-1}
F(000)	592 e
Crystal size	0.390 × 0.376 × 0.140 mm^3
θ range for data collection	3.347 to 36.623°
Index ranges	$-10 \le h \le 10$, $-25 \le k \le 25$, $-25 \le l \le 25$
Reflections collected	54108
Independent reflections	6852 [R$_{int}$ = 0.0253]
Reflections with I>2σ(I)	6046
Completeness to θ = 25.242°	99.8%
Absorption correction	Gaussian
Max. and min. transmission	0.97286 and 0.93654
Refinement method	Full-matrix least-squares on F^2
Data / restraints / parameters	6852 / 0 / 173
Goodness-of-fit on F^2	1.051
Final R indices [I>2σ(I)]	R$_1$ = 0.0303 wR$_2$ = 0.0878
R indices (all data)	R$_1$ = 0.0360 wR$_2$ = 0.0920
Largest diff. peak and hole	0.599 and -0.345 e·Å^{-3}

CCDC 1472069 contains the supplementary crystallographic data for this compound. These data can be obtained free of charge from The Cambridge Crystallographic Data Centre *via* www.ccdc.cam.ac.uk/data_request/cif.

7.3.5 Crystal Data and Structure Refinement of Rhodium Complex 97

Empirical formula	$C_{23}H_{26}ClN_2Rh$
Color	red
Formula weight	468.82 g·mol^{-1}
Temperature	100(2) K
Wavelength	0.71073 Å
Crystal system	tetragonal
Space group	$P4_2/n$, (№ 86)
Unit cell dimensions	a = 18.496(2) Å $\quad \alpha = 90°$
	b = 18.496(2) Å $\quad \beta = 90°$
	c = 11.9141(18) Å $\quad \gamma = 90°$
Volume	4076.0(11) Å^3
Z	8
Density (calculated)	1.528 Mg·m^{-3}
Absorption coefficient	0.979 mm^{-1}
F(000)	1920 e
Crystal size	0.14 × 0.12 × 0.10 mm^3
θ range for data collection	2.788 to 33.189°
Index ranges	$-28 \leq h \leq 28, -28 \leq k \leq 28, -18 \leq l \leq 16$
Reflections collected	79410
Independent reflections	7814 [R_{int} = 0.0654]
Reflections with I>2σ(I)	5737
Completeness to θ = 25.242°	99.9%
Absorption correction	Gaussian
Max. and min. transmission	0.91 and 0.88
Refinement method	Full-matrix least-squares on F^2
Data / restraints / parameters	7814 / 0 / 257
Goodness-of-fit on F^2	1.065
Final R indices [I>2σ(I)]	R_1 = 0.0362 $\quad$ wR^2 = 0.0793
R indices (all data)	R_1 = 0.0622 $\quad$ wR^2 = 0.0906
Largest diff. peak and hole	1.4 and -1.2 e·Å^{-3}

Table S1: Atomic coordinates and equivalent isotropic displacement parameters (Å^2) for **97**. U_{eq} is defined as one third of the trace of the orthogonalized U_{ij} tensor.

	x	y	z	U_{eq}
Rh(1)	0.6765(1)	0.4665(1)	0.8159(1)	0.014(1)
Cl(1)	0.6277(1)	0.3633(1)	0.9171(1)	0.021(1)
N(1)	0.6414(1)	0.5356(1)	0.9446(1)	0.016(1)
N(2)	0.5433(1)	0.6030(1)	1.0158(2)	0.020(1)
C(1)	0.5745(1)	0.5592(1)	0.9390(2)	0.016(1)
C(2)	0.5340(1)	0.5336(1)	0.8403(2)	0.016(1)
C(3)	0.5738(1)	0.4869(1)	0.7691(2)	0.016(1)
C(4)	0.5368(1)	0.4546(1)	0.6804(2)	0.019(1)
C(5)	0.4638(1)	0.4694(1)	0.6606(2)	0.021(1)
C(6)	0.4261(1)	0.5165(1)	0.7305(2)	0.019(1)
C(7)	0.4606(1)	0.5486(1)	0.8209(2)	0.017(1)
C(8)	0.6878(1)	0.5540(1)	1.0361(2)	0.020(1)
C(9)	0.7074(1)	0.6256(1)	1.0566(2)	0.027(1)
C(10)	0.7571(1)	0.6413(2)	1.1417(2)	0.035(1)
C(11)	0.7862(1)	0.5862(2)	1.2059(2)	0.037(1)
C(12)	0.7669(1)	0.5147(2)	1.1851(2)	0.031(1)
C(13)	0.7182(1)	0.4986(1)	1.0999(2)	0.024(1)
C(14)	0.7850(1)	0.4129(1)	0.7876(2)	0.018(1)
C(15)	0.7979(1)	0.4861(1)	0.8123(2)	0.018(1)
C(16)	0.7580(1)	0.5291(1)	0.7313(2)	0.018(1)
C(17)	0.7256(1)	0.4808(1)	0.6509(2)	0.018(1)
C(18)	0.7371(1)	0.4088(1)	0.6903(2)	0.018(1)
C(19)	0.8136(1)	0.3478(1)	0.8479(2)	0.023(1)
C(20)	0.8451(1)	0.5172(1)	0.9021(2)	0.023(1)
C(21)	0.7632(1)	0.6096(1)	0.7209(2)	0.025(1)
C(22)	0.6898(1)	0.5023(1)	0.5433(2)	0.024(1)
C(23)	0.7137(1)	0.3399(1)	0.6356(2)	0.022(1)

Table S2: Bond lengths [Å] and angles [°] for **97**.

Rh(1)-Cl(1)	2.4318(6)	Rh(1)-N(1)	2.0991(17)
Rh(1)-C(3)	2.0162(19)	Rh(1)-C(14)	2.263(2)
Rh(1)-C(15)	2.275(2)	Rh(1)-C(16)	2.152(2)
Rh(1)-C(17)	2.181(2)	Rh(1)-C(18)	2.152(2)
N(1)-C(1)	1.315(2)	N(1)-C(8)	1.429(3)
N(2)-C(1)	1.351(3)	C(1)-C(2)	1.472(3)
C(2)-C(3)	1.416(3)	C(2)-C(7)	1.405(3)
C(3)-C(4)	1.393(3)	C(4)-C(5)	1.396(3)
C(5)-C(6)	1.392(3)	C(6)-C(7)	1.386(3)
C(8)-C(9)	1.394(3)	C(8)-C(13)	1.395(3)
C(9)-C(10)	1.400(3)	C(10)-C(11)	1.383(4)
C(11)-C(12)	1.391(4)	C(12)-C(13)	1.391(3)
C(14)-C(15)	1.405(3)	C(14)-C(18)	1.461(3)
C(14)-C(19)	1.498(3)	C(15)-C(16)	1.453(3)
C(15)-C(20)	1.496(3)	C(16)-C(17)	1.441(3)
C(16)-C(21)	1.496(3)	C(17)-C(18)	1.428(3)
C(17)-C(22)	1.497(3)	C(18)-C(23)	1.495(3)

N(1)-Rh(1)-Cl(1)	90.03(5)	N(1)-Rh(1)-C(14)	130.50(7)
N(1)-Rh(1)-C(15)	102.81(7)	N(1)-Rh(1)-C(16)	103.34(7)
N(1)-Rh(1)-C(17)	135.48(7)	N(1)-Rh(1)-C(18)	166.06(7)
C(3)-Rh(1)-Cl(1)	86.22(6)	C(3)-Rh(1)-N(1)	78.23(7)
C(3)-Rh(1)-C(14)	151.26(8)	C(3)-Rh(1)-C(15)	153.56(8)
C(3)-Rh(1)-C(16)	115.46(8)	C(3)-Rh(1)-C(17)	96.92(8)
C(3)-Rh(1)-C(18)	113.08(8)	C(14)-Rh(1)-Cl(1)	93.42(5)
C(14)-Rh(1)-C(15)	36.08(7)	C(15)-Rh(1)-Cl(1)	120.06(5)
C(16)-Rh(1)-Cl(1)	156.24(5)	C(16)-Rh(1)-C(14)	62.94(7)
C(16)-Rh(1)-C(15)	38.19(8)	C(16)-Rh(1)-C(17)	38.85(8)
C(16)-Rh(1)-C(18)	64.95(8)	C(17)-Rh(1)-Cl(1)	134.18(6)
C(17)-Rh(1)-C(14)	63.27(7)	C(17)-Rh(1)-C(15)	63.46(7)
C(18)-Rh(1)-Cl(1)	98.60(6)	C(18)-Rh(1)-C(14)	38.54(7)
C(18)-Rh(1)-C(15)	63.37(7)	C(18)-Rh(1)-C(17)	38.47(7)
C(1)-N(1)-Rh(1)	117.19(14)	C(1)-N(1)-C(8)	121.62(17)
C(8)-N(1)-Rh(1)	121.16(12)	N(1)-C(1)-N(2)	124.53(19)
N(1)-C(1)-C(2)	114.31(18)	N(2)-C(1)-C(2)	121.15(18)
C(3)-C(2)-C(1)	114.26(17)	C(7)-C(2)-C(1)	123.97(18)
C(7)-C(2)-C(3)	121.59(18)	C(2)-C(3)-Rh(1)	116.00(14)
C(4)-C(3)-Rh(1)	126.32(15)	C(4)-C(3)-C(2)	117.40(18)
C(3)-C(4)-C(5)	121.27(19)	C(6)-C(5)-C(4)	120.37(19)
C(7)-C(6)-C(5)	120.10(19)	C(6)-C(7)-C(2)	119.24(19)
C(9)-C(8)-N(1)	121.1(2)	C(9)-C(8)-C(13)	119.9(2)
C(13)-C(8)-N(1)	118.78(19)	C(8)-C(9)-C(10)	119.6(2)
C(11)-C(10)-C(9)	120.3(2)	C(10)-C(11)-C(12)	120.1(2)
C(13)-C(12)-C(11)	120.0(2)	C(12)-C(13)-C(8)	120.1(2)
C(15)-C(14)-Rh(1)	72.40(11)	C(15)-C(14)-C(18)	108.60(18)
C(15)-C(14)-C(19)	127.86(19)	C(18)-C(14)-Rh(1)	66.61(11)
C(18)-C(14)-C(19)	123.54(19)	C(19)-C(14)-Rh(1)	126.39(15)
C(14)-C(15)-Rh(1)	71.52(11)	C(14)-C(15)-C(16)	107.62(18)
C(14)-C(15)-C(20)	128.28(19)	C(16)-C(15)-Rh(1)	66.33(11)
C(16)-C(15)-C(20)	124.08(19)	C(20)-C(15)-Rh(1)	128.62(14)
C(15)-C(16)-Rh(1)	75.48(12)	C(15)-C(16)-C(21)	124.57(19)
C(17)-C(16)-Rh(1)	71.68(12)	C(17)-C(16)-C(15)	108.23(17)
C(17)-C(16)-C(21)	126.1(2)	C(21)-C(16)-Rh(1)	128.29(14)
C(16)-C(17)-Rh(1)	69.48(12)	C(16)-C(17)-C(22)	126.03(19)
C(18)-C(17)-Rh(1)	69.66(11)	C(18)-C(17)-C(16)	107.31(18)
C(18)-C(17)-C(22)	126.60(19)	C(22)-C(17)-Rh(1)	128.31(14)
C(14)-C(18)-Rh(1)	74.85(11)	C(14)-C(18)-C(23)	124.46(18)
C(17)-C(18)-Rh(1)	71.87(11)	C(17)-C(18)-C(14)	107.67(18)
C(17)-C(18)-C(23)	127.43(19)	C(23)-C(18)-Rh(1)	125.02(14)

Symmetry transformations used to generate equivalent atoms: —

Table S3: Anisotropic displacement parameters (Å^2) for **97**. The anisotropic displacement factor exponent takes the form: $-2\pi^2[\, h^2 \, a^{*2}U_{11} + \ldots + 2\, h\, k\, a^*\, b^*\, U_{12}\,]$.

	U_{11}	U_{22}	U_{33}	U_{23}	U_{13}	U_{12}
Rh(1)	0.013(1)	0.014(1)	0.014(1)	0.000(1)	0.000(1)	0.001(1)
Cl(1)	0.019(1)	0.019(1)	0.024(1)	0.004(1)	0.004(1)	0.002(1)
N(1)	0.014(1)	0.019(1)	0.016(1)	−0.002(1)	0.000(1)	0.001(1)
N(2)	0.016(1)	0.024(1)	0.018(1)	−0.004(1)	0.000(1)	0.002(1)
C(1)	0.016(1)	0.016(1)	0.018(1)	0.003(1)	0.001(1)	−0.001(1)
C(2)	0.016(1)	0.015(1)	0.017(1)	0.002(1)	0.000(1)	−0.001(1)
C(3)	0.016(1)	0.015(1)	0.017(1)	0.002(1)	−0.002(1)	0.000(1)
C(4)	0.017(1)	0.018(1)	0.021(1)	0.000(1)	−0.002(1)	0.000(1)
C(5)	0.019(1)	0.020(1)	0.024(1)	−0.001(1)	−0.005(1)	−0.002(1)
C(6)	0.015(1)	0.022(1)	0.021(1)	0.004(1)	−0.002(1)	−0.001(1)
C(7)	0.017(1)	0.016(1)	0.019(1)	0.003(1)	0.001(1)	0.001(1)
C(8)	0.014(1)	0.029(1)	0.015(1)	−0.006(1)	0.001(1)	0.002(1)
C(9)	0.021(1)	0.031(1)	0.029(1)	−0.011(1)	−0.004(1)	0.005(1)
C(10)	0.025(1)	0.041(1)	0.039(2)	−0.025(1)	−0.009(1)	0.006(1)
C(11)	0.024(1)	0.058(2)	0.031(1)	−0.017(1)	−0.011(1)	0.009(1)
C(12)	0.020(1)	0.053(2)	0.019(1)	0.002(1)	−0.002(1)	0.008(1)
C(13)	0.018(1)	0.035(1)	0.018(1)	0.001(1)	0.001(1)	0.001(1)
C(14)	0.015(1)	0.021(1)	0.016(1)	0.001(1)	0.001(1)	0.002(1)
C(15)	0.014(1)	0.022(1)	0.017(1)	−0.002(1)	0.002(1)	−0.001(1)
C(16)	0.016(1)	0.019(1)	0.017(1)	−0.002(1)	0.003(1)	0.002(1)
C(17)	0.017(1)	0.021(1)	0.015(1)	0.001(1)	0.001(1)	0.002(1)
C(18)	0.016(1)	0.020(1)	0.016(1)	0.000(1)	0.001(1)	0.001(1)
C(19)	0.019(1)	0.023(1)	0.025(1)	0.006(1)	−0.001(1)	0.004(1)
C(20)	0.017(1)	0.030(1)	0.021(1)	−0.006(1)	0.001(1)	−0.002(1)
C(21)	0.026(1)	0.017(1)	0.032(1)	−0.001(1)	0.005(1)	0.000(1)
C(22)	0.024(1)	0.029(1)	0.018(1)	0.004(1)	−0.002(1)	0.002(1)
C(23)	0.024(1)	0.020(1)	0.023(1)	−0.004(1)	−0.001(1)	0.002(1)

Table S4: Hydrogen coordinates and isotropic displacement parameters ($\mathring{A}^2$) for **97**.

	x	y	z	U_{eq}
H(2A)	0.5646(16)	0.6071(15)	1.076(2)	0.032(8)
H(2B)	0.4978(16)	0.6066(15)	1.017(3)	0.034(8)
H(4)	0.5616	0.4220	0.6325	0.022
H(5)	0.4398	0.4472	0.5991	0.025
H(6)	0.3766	0.5266	0.7162	0.023
H(7)	0.4350	0.5805	0.8691	0.021
H(9)	0.6870	0.6636	1.0131	0.032
H(10)	0.7710	0.6899	1.1555	0.042
H(11)	0.8194	0.5971	1.2643	0.045
H(12)	0.7871	0.4769	1.2292	0.037
H(13)	0.7055	0.4497	1.0851	0.028
H(19A)	0.8453	0.3633	0.9093	0.034
H(19B)	0.8411	0.3177	0.7953	0.034
H(19C)	0.7731	0.3198	0.8785	0.034
H(20A)	0.8204	0.5581	0.9377	0.034
H(20B)	0.8906	0.5339	0.8688	0.034
H(20C)	0.8553	0.4801	0.9586	0.034
H(21A)	0.7245	0.6272	0.6720	0.037
H(21B)	0.8102	0.6226	0.6886	0.037
H(21C)	0.7584	0.6316	0.7953	0.037
H(22A)	0.6544	0.4654	0.5217	0.036
H(22B)	0.7263	0.5070	0.4842	0.036
H(22C)	0.6651	0.5488	0.5534	0.036
H(23A)	0.7065	0.3027	0.6931	0.033
H(23B)	0.7509	0.3239	0.5827	0.033
H(23C)	0.6682	0.3480	0.5952	0.033

7.3.6 Crystal Data and Structure Refinement of Rhodium Complex 101

Empirical formula	$C_{39}H_{42}Cl_2F_6N_2O_2RhSb$
Color	green
Formula weight	980.30 g·mol^{-1}
Temperature	100(2) K
Wavelength	0.71073 Å
Crystal system	monoclinic
Space group	P2$_1$/n (№ 14)
Unit cell dimensions	a = 13.991(2) Å α = 90°
	b = 19.610(3) Å β = 99.514(3)°
	c = 14.167(2) Å γ = 90°
Volume	3833.5(10) Å^3
Z	4
Density (calculated)	1.699 Mg·m^{-3}
Absorption coefficient	1.341 mm^{-1}
F(000)	1960 e
Crystal size	0.081 × 0.051 × 0.032 mm^3
θ range for data collection	2.469 to 33.588°
Index ranges	$-21 \leq h \leq 21$, $-30 \leq k \leq 30$, $-21 \leq l \leq 21$
Reflections collected	130444
Independent reflections	15025 [R$_{int}$ = 0.1073]
Reflections with I>2σ(I)	10648
Completeness to θ = 25.242°	99.9%
Absorption correction	Gaussian
Max. and min. transmission	0.97909 and 0.92097
Refinement method	Full-matrix least-squares on F^2
Data / restraints / parameters	15025 / 0 / 531
Goodness-of-fit on F^2	1.018
Final R indices [I>2σ(I)]	R$_1$ = 0.0387 wR$_2$ = 0.0907
R indices (all data)	R$_1$ = 0.0724 wR$_2$ = 0.1039
Largest diff. peak and hole	1.006 and -1.366 e·Å^{-3}

CCDC 1575834 contains the supplementary crystallographic data for this compound. These data can be obtained free of charge from The Cambridge Crystallographic Data Centre *via* www.ccdc.cam.ac.uk/data_request/cif.

7.3.7 Crystal Data and Structure Refinement of Oxirane 109

Empirical formula	$C_{18}H_{18}O_5$
Color	colorless
Formula weight	314.32 g·mol^{-1}
Temperature	200 K
Wavelength	0.71073 Å
Crystal system	monoclinic
Space group	C2/c (№ 15)
Unit cell dimensions	a = 37.6824(14) Å α = 90°
	b = 7.8512(14) Å β = 105.473(9)°
	c = 11.2312(16) Å γ = 90°
Volume	3202.3(8) Å^3
Z	8
Density (calculated)	1.304 Mg·m^{-3}
Absorption coefficient	0.095 mm^{-1}
F(000)	1328 e
Crystal size	0.14 × 0.14 × 0.07 mm
θ range for data collection	2.654 to 33.186°
Index ranges	$-57 \le h \le 57, -12 \le k \le 12, -17 \le l \le 17$
Reflections collected	52073
Independent reflections	6096 [R$_{int}$ = 0.0448]
Reflections with I>2σ(I)	4509
Completeness to θ = 25.242°	99.2%
Absorption correction	Gaussian
Max. and min. transmission	0.99 and 0.99
Refinement method	Full-matrix least-squares on F^2
Data / restraints / parameters	6096 / 0 / 211
Goodness-of-fit on F^2	1.124
Final R indices [I>2σ(I)]	R$_1$ = 0.0829 wR$_2$ = 0.2336
R indices (all data)	R$_1$ = 0.1071 wR$_2$ = 0.2460
Largest diff. peak and hole	0.4 and -0.3 e·Å^{-3}

CCDC 1575460 contains the supplementary crystallographic data for this compound. These data can be obtained free of charge from The Cambridge Crystallographic Data Centre *via* www.ccdc.cam.ac.uk/data_request/cif.

7.3.8 Crystal Data and Structure Refinement of Imine 118

Empirical formula	$C_{16}H_{15}NO_3$
Color	pale yellow
Formula weight	269.29 g·mol^{-1}
Temperature	100 K
Wavelength	0.71073 Å
Crystal system	monoclinic
Space group	$P2_1/n$ (№ 14)
Unit cell dimensions	$a = 12.2325(16)$ Å $\quad \alpha = 90°$
	$b = 8.0485(10)$ Å $\quad \beta = 100.216(2)°$
	$c = 14.1715(18)$ Å $\quad \gamma = 90°$
Volume	1373.1(3) Å^3
Z	4
Density (calculated)	1.303 Mg·m^{-3}
Absorption coefficient	0.090 mm^{-1}
F(000)	568 e
Crystal size	0.174 × 0.147 × 0.072 mm^3
θ range for data collection	2.029 to 32.714°
Index ranges	$-18 \le h \le 18$, $-12 \le k \le 12$, $-21 \le l \le 21$
Reflections collected	43994
Independent reflections	5051 [$R_{int} = 0.0372$]
Reflections with I>2σ(I)	4247
Completeness to θ = 25.242°	100.0%
Absorption correction	Gaussian
Max. and min. transmission	1.00 and 0.99
Refinement method	Full-matrix least-squares on F^2
Data / restraints / parameters	5051 / 0 / 241
Goodness-of-fit on F^2	1.080
Final R indices [I>2σ(I)]	$R_1 = 0.0388$ $\quad$ $wR_2 = 0.1114$
R indices (all data)	$R_1 = 0.0481$ $\quad$ $wR_2 = 0.1226$
Largest diff. peak and hole	0.5 and -0.3 e·Å^{-3}

Table S5: Atomic coordinates and equivalent isotropic displacement parameters (Å^2) for **118**.
U_{eq} is defined as one third of the trace of the orthogonalized U_{ij} tensor.

	x	y	z	U_{eq}
O(1)	0.2889(1)	0.9698(1)	0.4891(1)	0.020(1)
O(2)	0.1254(1)	1.0786(1)	0.5106(1)	0.016(1)
O(3)	0.0682(1)	0.8531(1)	0.9251(1)	0.019(1)
N(1)	0.1370(1)	0.6676(1)	0.4991(1)	0.016(1)
C(1)	0.1576(1)	0.7973(1)	0.5514(1)	0.013(1)
C(2)	0.1996(1)	0.9571(1)	0.5127(1)	0.013(1)
C(3)	0.1577(1)	1.2374(1)	0.4756(1)	0.019(1)
C(4)	0.1421(1)	0.8003(1)	0.6520(1)	0.013(1)
C(5)	0.1885(1)	0.9272(1)	0.7143(1)	0.016(1)
C(6)	0.1660(1)	0.9375(1)	0.8064(1)	0.017(1)
C(7)	0.0931(1)	0.8237(1)	0.8369(1)	0.015(1)
C(8)	0.0507(1)	0.6919(1)	0.7775(1)	0.016(1)
C(9)	0.0760(1)	0.6806(1)	0.6861(1)	0.015(1)
C(10)	-0.0140(1)	0.7476(1)	0.9548(1)	0.021(1)
C(11)	0.1400(1)	0.6754(1)	0.3995(1)	0.015(1)
C(12)	0.0620(1)	0.7702(1)	0.3381(1)	0.017(1)
C(13)	0.0610(1)	0.7663(1)	0.2396(1)	0.019(1)
C(14)	0.1371(1)	0.6697(1)	0.2020(1)	0.018(1)
C(15)	0.2146(1)	0.5755(1)	0.2633(1)	0.018(1)
C(16)	0.2155(1)	0.5764(1)	0.3616(1)	0.017(1)

Table S6: Bond lengths [Å] and angles [°] for **118**.

O(1)-C(2)	1.2028(10)	O(2)-C(2)	1.3312(10)
O(2)-C(3)	1.4507(10)	O(3)-C(7)	1.3592(10)
O(3)-C(10)	1.4346(11)	N(1)-C(1)	1.2798(11)
N(1)-C(11)	1.4200(11)	C(1)-C(2)	1.5217(11)
C(1)-C(4)	1.4713(11)	C(3)-H(3A)	0.974(14)
C(3)-H(3B)	0.947(14)	C(3)-H(3C)	1.014(15)
C(4)-C(5)	1.4029(12)	C(4)-C(9)	1.3975(11)
C(5)-H(5)	0.995(14)	C(5)-C(6)	1.3829(12)
C(6)-H(6)	0.986(15)	C(6)-C(7)	1.3992(11)
C(7)-C(8)	1.3961(12)	C(8)-H(8)	0.983(14)
C(8)-C(9)	1.3881(12)	C(9)-H(9)	0.981(13)
C(10)-H(10A)	0.988(14)	C(10)-H(10B)	0.981(15)
C(10)-H(10C)	1.001(14)	C(11)-C(12)	1.3979(12)
C(11)-C(16)	1.3978(12)	C(12)-H(12)	0.946(13)
C(12)-C(13)	1.3927(13)	C(13)-H(13)	0.982(15)
C(13)-C(14)	1.3903(12)	C(14)-H(14)	0.968(14)
C(14)-C(15)	1.3919(13)	C(15)-H(15)	0.963(13)
C(15)-C(16)	1.3903(13)	C(16)-H(16)	1.003(14)
C(2)-O(2)-C(3)	115.41(6)	C(7)-O(3)-C(10)	116.70(7)
C(1)-N(1)-C(11)	120.15(7)	N(1)-C(1)-C(2)	121.70(7)
N(1)-C(1)-C(4)	121.87(7)	C(4)-C(1)-C(2)	116.43(7)
O(1)-C(2)-O(2)	125.51(7)	O(1)-C(2)-C(1)	123.59(7)
O(2)-C(2)-C(1)	110.89(6)	O(2)-C(3)-H(3A)	104.7(8)

O(2)-C(3)-H(3B)	111.3(9)	O(2)-C(3)-H(3C)	110.2(8)
H(3A)-C(3)-H(3B)	112.2(12)	H(3A)-C(3)-H(3C)	111.9(11)
H(3B)-C(3)-H(3C)	106.6(11)	C(5)-C(4)-C(1)	120.96(7)
C(9)-C(4)-C(1)	120.40(7)	C(9)-C(4)-C(5)	118.56(7)
C(4)-C(5)-H(5)	119.3(8)	C(6)-C(5)-C(4)	120.81(7)
C(6)-C(5)-H(5)	119.9(8)	C(5)-C(6)-H(6)	122.2(8)
C(5)-C(6)-C(7)	119.78(8)	C(7)-C(6)-H(6)	117.9(8)
O(3)-C(7)-C(6)	115.45(7)	O(3)-C(7)-C(8)	124.54(7)
C(8)-C(7)-C(6)	120.01(8)	C(7)-C(8)-H(8)	120.1(8)
C(9)-C(8)-C(7)	119.48(7)	C(9)-C(8)-H(8)	120.4(8)
C(4)-C(9)-H(9)	121.0(8)	C(8)-C(9)-C(4)	121.09(7)
C(8)-C(9)-H(9)	117.8(8)	O(3)-C(10)-H(10A)	110.2(8)
O(3)-C(10)-H(10B)	104.8(9)	O(3)-C(10)-H(10C)	111.3(8)
H(10A)-C(10)-H(10B)	111.5(12)	H(10A)-C(10)-H(10C)	109.8(12)
H(10B)-C(10)-H(10C)	109.2(12)	C(12)-C(11)-N(1)	120.55(7)
C(16)-C(11)-N(1)	119.44(7)	C(16)-C(11)-C(12)	119.78(8)
C(11)-C(12)-H(12)	119.7(8)	C(13)-C(12)-C(11)	119.67(8)
C(13)-C(12)-H(12)	120.5(8)	C(12)-C(13)-H(13)	120.1(9)
C(14)-C(13)-C(12)	120.62(8)	C(14)-C(13)-H(13)	119.3(9)
C(13)-C(14)-H(14)	120.8(8)	C(13)-C(14)-C(15)	119.56(8)
C(15)-C(14)-H(14)	119.6(8)	C(14)-C(15)-H(15)	118.9(8)
C(16)-C(15)-C(14)	120.41(8)	C(16)-C(15)-H(15)	120.7(8)
C(11)-C(16)-H(16)	119.7(8)	C(15)-C(16)-C(11)	119.94(8)
C(15)-C(16)-H(16)	120.3(8)		

Symmetry transformations used to generate equivalent atoms: —

Table S7: Anisotropic displacement parameters (Å^2) for **118**. The anisotropic displacement factor exponent takes the form: $-2\pi^2[\,h^2\,a^{*2}U_{11} + ... + 2\,h\,k\,a^*\,b^*\,U_{12}\,]$.

	U_{11}	U_{22}	U_{33}	U_{23}	U_{13}	U_{12}
O(1)	0.016(1)	0.019(1)	0.028(1)	0.001(1)	0.011(1)	−0.001(1)
O(2)	0.015(1)	0.011(1)	0.022(1)	0.004(1)	0.005(1)	0.001(1)
O(3)	0.019(1)	0.023(1)	0.015(1)	0.001(1)	0.007(1)	−0.002(1)
N(1)	0.021(1)	0.012(1)	0.017(1)	0.001(1)	0.005(1)	−0.001(1)
C(1)	0.013(1)	0.012(1)	0.015(1)	0.002(1)	0.004(1)	0.000(1)
C(2)	0.014(1)	0.012(1)	0.013(1)	0.000(1)	0.003(1)	−0.001(1)
C(3)	0.019(1)	0.012(1)	0.024(1)	0.005(1)	0.002(1)	−0.002(1)
C(4)	0.012(1)	0.012(1)	0.015(1)	0.002(1)	0.003(1)	0.000(1)
C(5)	0.016(1)	0.016(1)	0.016(1)	0.001(1)	0.004(1)	−0.005(1)
C(6)	0.018(1)	0.017(1)	0.016(1)	−0.001(1)	0.003(1)	−0.005(1)
C(7)	0.013(1)	0.017(1)	0.014(1)	0.003(1)	0.003(1)	0.001(1)
C(8)	0.014(1)	0.016(1)	0.017(1)	0.004(1)	0.004(1)	−0.002(1)
C(9)	0.015(1)	0.012(1)	0.016(1)	0.002(1)	0.002(1)	−0.002(1)
C(10)	0.018(1)	0.028(1)	0.019(1)	0.006(1)	0.008(1)	0.001(1)
C(11)	0.018(1)	0.011(1)	0.017(1)	−0.001(1)	0.005(1)	−0.003(1)
C(12)	0.018(1)	0.016(1)	0.018(1)	−0.002(1)	0.005(1)	0.002(1)
C(13)	0.019(1)	0.020(1)	0.018(1)	−0.002(1)	0.003(1)	0.002(1)
C(14)	0.019(1)	0.019(1)	0.017(1)	−0.004(1)	0.005(1)	−0.001(1)
C(15)	0.019(1)	0.015(1)	0.023(1)	−0.002(1)	0.008(1)	0.001(1)
C(16)	0.017(1)	0.013(1)	0.021(1)	0.001(1)	0.006(1)	0.000(1)

Table S8: Hydrogen coordinates and isotropic displacement parameters (Å^2) for **118**.

	x	y	z	U$_{eq}$
H(3A)	0.1031(11)	1.3158(17)	0.4914(10)	0.025(3)
H(3B)	0.2311(12)	1.2662(18)	0.5044(10)	0.024(3)
H(3C)	0.1567(12)	1.2315(18)	0.4040(11)	0.029(3)
H(5)	0.2377(11)	1.0110(17)	0.6916(10)	0.025(3)
H(6)	0.1966(12)	1.0266(18)	0.8511(10)	0.028(3)
H(8)	0.0011(11)	0.6100(17)	0.7996(9)	0.023(3)
H(9)	0.0430(11)	0.5890(16)	0.6450(9)	0.021(3)
H(10A)	−0.0821(12)	0.7465(18)	0.9055(10)	0.026(3)
H(10B)	−0.0278(12)	0.796(2)	1.0150(11)	0.035(4)
H(10C)	0.0144(11)	0.6316(18)	0.9672(10)	0.027(3)
H(12)	0.0084(11)	0.8327(16)	0.3634(9)	0.021(3)
H(13)	0.0060(12)	0.8317(18)	0.1961(11)	0.032(4)
H(14)	0.1370(11)	0.6674(16)	0.1337(10)	0.023(3)
H(15)	0.2668(11)	0.5087(17)	0.2364(10)	0.023(3)
H(16)	0.2716(11)	0.5088(17)	0.4057(10)	0.026(3)

7.3.9 Crystal Data and Structure Refinement of Diazridine 157

Empirical formula	$C_{22}H_{20}N_2O_3$
Color	colorless
Formula weight	360.40 g·mol^{-1}
Temperature	100(2) K
Wavelength	0.71073 Å
Crystal system	monoclinic
Space group	$P2_1/n$ (№ 14)
Unit cell dimensions	a = 10.248(2) Å α = 90°
	b = 9.5803(19) Å β = 92.79(3)°
	c = 18.801(4) Å γ = 90°
Volume	1843.8(6) Å^3
Z	4
Density (calculated)	1.298 Mg·m^{-3}
Absorption coefficient	0.087 mm^{-1}
F(000)	760 e
Crystal size	0.36 × 0.25 × 0.15 mm^3
θ range for data collection	2.912 to 33.111°
Index ranges	$-15 \le h \le 15, -14 \le k \le 14, -28 \le l \le 28$
Reflections collected	38159
Independent reflections	6970 [R_{int} = 0.0786]
Reflections with I>2σ(I)	5483
Completeness to θ = 25.242°	99.6%
Absorption correction	Gaussian
Max. and min. transmission	0.99 and 0.97
Refinement method	Full-matrix least-squares on F^2
Data / restraints / parameters	6970 / 0 / 246
Goodness-of-fit on F^2	1.136
Final R indices [I>2σ(I)]	R_1 = 0.0724 wR_2 = 0.1664
R indices (all data)	R_1 = 0.0927 wR_2 = 0.1771
Largest diff. peak and hole	0.6 and -0.4 e·Å^{-3}

CCDC 1575838 contains the supplementary crystallographic data for this compound. These data can be obtained free of charge from The Cambridge Crystallographic Data Centre *via* www.ccdc.cam.ac.uk/data_request/cif.

7.3.10 Crystal Data and Structure Refinement of Bicycle 165

Empirical formula	$C_{34}H_{30}N_2O_4$
Color	colorless
Formula weight	530.60 g·mol^{-1}
Temperature	200(2) K
Wavelength	1.54178 Å
Crystal system	triclinic
Space group	P$\bar{1}$ (№ 2)
Unit cell dimensions	a = 9.6316(3) Å $\quad$ α = 78.635(2)°
	b = 15.2985(5) Å $\quad$ β = 84.6930(10)°
	c = 19.2607(7) Å $\quad$ γ = 87.861(2)°
Volume	2769.94(16) Å^3
Z	4
Density (calculated)	1.272 Mg·m^{-3}
Absorption coefficient	0.670 mm^{-1}
F(000)	1120 e
Crystal size	0.257 × 0.203 × 0.140 mm^3
θ range for data collection	4.611 to 63.589°
Index ranges	$-11 \leq h \leq 11$, $-17 \leq k \leq 17$, $-22 \leq l \leq 22$
Reflections collected	78293
Independent reflections	8693 [R$_{int}$ = 0.0328]
Reflections with I>2σ(I)	7840
Completeness to θ = 63.589°	95.6%
Absorption correction	Gaussian
Max. and min. transmission	0.93 and 0.87
Refinement method	Full-matrix least-squares on F^2
Data / restraints / parameters	8693 / 0 / 725
Goodness-of-fit on F^2	1.027
Final R indices [I>2σ(I)]	R$_1$ = 0.0341 $\quad$ wR$_2$ = 0.0839
R indices (all data)	R$_1$ = 0.0381 $\quad$ wR$_2$ = 0.0867
Largest diff. peak and hole	0.2 and −0.2 e·Å^{-3}

Table S9: Atomic coordinates and equivalent isotropic displacement parameters (Å^2) for **165**. U_{eq} is defined as one third of the trace of the orthogonalized U_{ij} tensor.

	x	y	z	U_{eq}
O(1)	1.1519(1)	0.2735(1)	0.3135(1)	0.048(1)
O(2)	0.9964(1)	0.1709(1)	0.3674(1)	0.041(1)
O(3)	0.6297(1)	0.3424(1)	0.1663(1)	0.049(1)
O(4)	0.7580(1)	0.3673(1)	0.0615(1)	0.046(1)
N(1)	0.9990(1)	0.1054(1)	0.2440(1)	0.027(1)
N(2)	0.8545(1)	0.0829(1)	0.2469(1)	0.029(1)
C(1)	1.0133(1)	0.2014(1)	0.2421(1)	0.029(1)
C(2)	1.1016(1)	0.2525(1)	0.1744(1)	0.032(1)
C(3)	0.9922(1)	0.2955(1)	0.1277(1)	0.035(1)
C(4)	0.8650(1)	0.2910(1)	0.1605(1)	0.031(1)
C(5)	0.8615(1)	0.2406(1)	0.2363(1)	0.029(1)
C(6)	0.7639(1)	0.1604(1)	0.2530(1)	0.030(1)
C(7)	1.0654(1)	0.2197(1)	0.3109(1)	0.033(1)
C(8)	1.0444(2)	0.1730(1)	0.4359(1)	0.056(1)
C(9)	0.7383(1)	0.3354(1)	0.1311(1)	0.034(1)
C(10)	0.6392(2)	0.4117(1)	0.0279(1)	0.055(1)
C(11)	1.0821(1)	0.0415(1)	0.2867(1)	0.029(1)
C(12)	1.2220(1)	0.0594(1)	0.2916(1)	0.034(1)
C(13)	1.3060(2)	−0.0029(1)	0.3312(1)	0.042(1)
C(14)	1.2543(2)	−0.0847(1)	0.3657(1)	0.046(1)
C(15)	1.1165(2)	−0.1031(1)	0.3602(1)	0.041(1)
C(16)	1.0306(1)	−0.0411(1)	0.3213(1)	0.034(1)
C(17)	0.8206(1)	0.0277(1)	0.2004(1)	0.030(1)
C(18)	0.9217(2)	−0.0186(1)	0.1646(1)	0.036(1)
C(19)	0.8822(2)	−0.0767(1)	0.1235(1)	0.046(1)
C(20)	0.7426(2)	−0.0906(1)	0.1180(1)	0.052(1)
C(21)	0.6425(2)	−0.0459(1)	0.1542(1)	0.050(1)
C(22)	0.6796(2)	0.0127(1)	0.1953(1)	0.039(1)
C(23)	1.2101(1)	0.2005(1)	0.1364(1)	0.031(1)
C(24)	1.1697(2)	0.1404(1)	0.0972(1)	0.038(1)
C(25)	1.2687(2)	0.0922(1)	0.0625(1)	0.050(1)
C(26)	1.4087(2)	0.1055(1)	0.0652(1)	0.056(1)
C(27)	1.4500(2)	0.1670(1)	0.1021(1)	0.052(1)
C(28)	1.3516(1)	0.2144(1)	0.1379(1)	0.040(1)
C(29)	0.6729(1)	0.1508(1)	0.3228(1)	0.035(1)
C(30)	0.5555(1)	0.2069(1)	0.3257(1)	0.045(1)
C(31)	0.4661(2)	0.1990(1)	0.3869(1)	0.055(1)
C(32)	0.4936(2)	0.1367(1)	0.4457(1)	0.060(1)
C(33)	0.6104(2)	0.0816(1)	0.4442(1)	0.056(1)
C(34)	0.7000(2)	0.0881(1)	0.3825(1)	0.044(1)
O(5)	0.7191(1)	0.4648(1)	0.7904(1)	0.041(1)
O(6)	0.8386(1)	0.5269(1)	0.8618(1)	0.043(1)
O(7)	1.0523(1)	0.6040(1)	0.5530(1)	0.059(1)
O(8)	1.2526(1)	0.6373(1)	0.5903(1)	0.045(1)
N(3)	0.9630(1)	0.3617(1)	0.7648(1)	0.028(1)
N(4)	0.9635(1)	0.3532(1)	0.6921(1)	0.028(1)
C(41)	0.9633(1)	0.4563(1)	0.7709(1)	0.029(1)
C(42)	1.1021(1)	0.4884(1)	0.7948(1)	0.032(1)
C(43)	1.1763(1)	0.5343(1)	0.7261(1)	0.032(1)

C(44)	1.0971(1)	0.5466(1)	0.6720(1)	0.030(1)
C(45)	0.9545(1)	0.5079(1)	0.6928(1)	0.030(1)
C(46)	0.9161(1)	0.4379(1)	0.6505(1)	0.030(1)
C(47)	0.8349(1)	0.4852(1)	0.8152(1)	0.032(1)
C(48)	0.5911(2)	0.5054(1)	0.8153(1)	0.056(1)
C(49)	1.1299(1)	0.5975(1)	0.5992(1)	0.035(1)
C(50)	1.2911(2)	0.6863(1)	0.5193(1)	0.055(1)
C(51)	0.8896(1)	0.2961(1)	0.8154(1)	0.030(1)
C(52)	0.8758(2)	0.3016(1)	0.8872(1)	0.038(1)
C(53)	0.8054(2)	0.2362(1)	0.9367(1)	0.050(1)
C(54)	0.7492(2)	0.1646(1)	0.9161(1)	0.055(1)
C(55)	0.7670(2)	0.1572(1)	0.8456(1)	0.046(1)
C(56)	0.8378(1)	0.2214(1)	0.7955(1)	0.036(1)
C(57)	1.0803(1)	0.3070(1)	0.6657(1)	0.028(1)
C(58)	1.1586(1)	0.2476(1)	0.7121(1)	0.031(1)
C(59)	1.2672(1)	0.1981(1)	0.6861(1)	0.038(1)
C(60)	1.3003(2)	0.2056(1)	0.6140(1)	0.044(1)
C(61)	1.2217(2)	0.2632(1)	0.5677(1)	0.043(1)
C(62)	1.1118(1)	0.3130(1)	0.5925(1)	0.036(1)
C(63)	1.1917(1)	0.4217(1)	0.8408(1)	0.037(1)
C(64)	1.1806(2)	0.4153(1)	0.9142(1)	0.057(1)
C(65)	1.2706(2)	0.3573(2)	0.9555(1)	0.077(1)
C(66)	1.3709(2)	0.3075(1)	0.9242(1)	0.077(1)
C(67)	1.3820(2)	0.3141(1)	0.8522(1)	0.065(1)
C(68)	1.2931(2)	0.3708(1)	0.8106(1)	0.044(1)
C(69)	0.7631(1)	0.4408(1)	0.6364(1)	0.037(1)
C(70)	0.6754(1)	0.3704(1)	0.6594(1)	0.043(1)
C(71)	0.5361(2)	0.3773(1)	0.6441(1)	0.056(1)
C(72)	0.4854(2)	0.4542(2)	0.6058(1)	0.075(1)
C(73)	0.5721(2)	0.5239(2)	0.5820(2)	0.099(1)
C(74)	0.7109(2)	0.5180(1)	0.5966(1)	0.073(1)

Table S10: Bond lengths [Å] and angles [°] for **165**.

O(1)-C(7)	1.2038(16)	O(2)-C(7)	1.3302(17)
O(2)-C(8)	1.4447(17)	O(3)-C(9)	1.2047(16)
O(4)-C(9)	1.3323(17)	O(4)-C(10)	1.4477(17)
N(1)-N(2)	1.4396(14)	N(1)-C(1)	1.4736(16)
N(1)-C(11)	1.4207(16)	N(2)-C(6)	1.4624(16)
N(2)-C(17)	1.4118(16)	C(1)-C(2)	1.5747(18)
C(1)-C(5)	1.5655(16)	C(1)-C(7)	1.5368(17)
C(2)-C(3)	1.4967(18)	C(2)-C(23)	1.5117(17)
C(3)-C(4)	1.3235(19)	C(4)-C(5)	1.5089(18)
C(4)-C(9)	1.4777(18)	C(5)-C(6)	1.5384(18)
C(6)-C(29)	1.5202(18)	C(11)-C(12)	1.4000(18)
C(11)-C(16)	1.3931(19)	C(12)-C(13)	1.3832(19)
C(13)-C(14)	1.384(2)	C(14)-C(15)	1.384(2)
C(15)-C(16)	1.3867(19)	C(17)-C(18)	1.3942(19)
C(17)-C(22)	1.4011(19)	C(18)-C(19)	1.3860(19)
C(19)-C(20)	1.386(2)	C(20)-C(21)	1.377(2)
C(21)-C(22)	1.385(2)	C(23)-C(24)	1.3872(19)
C(23)-C(28)	1.3909(19)	C(24)-C(25)	1.386(2)

C(25)-C(26)	1.379(3)	C(26)-C(27)	1.376(3)
C(27)-C(28)	1.387(2)	C(29)-C(30)	1.398(2)
C(29)-C(34)	1.382(2)	C(30)-C(31)	1.383(2)
C(31)-C(32)	1.369(3)	C(32)-C(33)	1.382(3)
C(33)-C(34)	1.392(2)	O(5)-C(47)	1.3246(16)
O(5)-C(48)	1.4450(17)	O(6)-C(47)	1.2029(16)
O(7)-C(49)	1.2006(16)	O(8)-C(49)	1.3304(16)
O(8)-C(50)	1.4472(18)	N(3)-N(4)	1.4318(14)
N(3)-C(41)	1.4747(15)	N(3)-C(51)	1.4122(16)
N(4)-C(46)	1.4640(16)	N(4)-C(57)	1.4145(16)
C(41)-C(42)	1.5788(17)	C(41)-C(45)	1.5638(17)
C(41)-C(47)	1.5376(17)	C(42)-C(43)	1.5009(18)
C(42)-C(63)	1.5129(18)	C(43)-C(44)	1.3274(18)
C(44)-C(45)	1.5038(17)	C(44)-C(49)	1.4756(19)
C(45)-C(46)	1.5418(17)	C(46)-C(69)	1.5200(17)
C(51)-C(52)	1.3952(19)	C(51)-C(56)	1.3972(19)
C(52)-C(53)	1.387(2)	C(53)-C(54)	1.381(2)
C(54)-C(55)	1.378(2)	C(55)-C(56)	1.385(2)
C(57)-C(58)	1.3967(18)	C(57)-C(62)	1.4000(18)
C(58)-C(59)	1.3835(18)	C(59)-C(60)	1.378(2)
C(60)-C(61)	1.382(2)	C(61)-C(62)	1.385(2)
C(63)-C(64)	1.393(2)	C(63)-C(68)	1.385(2)
C(64)-C(65)	1.401(3)	C(65)-C(66)	1.377(3)
C(66)-C(67)	1.365(3)	C(67)-C(68)	1.388(2)
C(69)-C(70)	1.371(2)	C(69)-C(74)	1.381(2)
C(70)-C(71)	1.396(2)	C(71)-C(72)	1.359(3)
C(72)-C(73)	1.360(3)	C(73)-C(74)	1.387(3)
C(7)-O(2)-C(8)	116.90(11)	C(9)-O(4)-C(10)	116.32(11)
N(2)-N(1)-C(1)	110.81(9)	C(11)-N(1)-N(2)	114.88(10)
C(11)-N(1)-C(1)	120.48(9)	N(1)-N(2)-C(6)	110.83(9)
C(17)-N(2)-N(1)	116.49(9)	C(17)-N(2)-C(6)	117.92(10)
N(1)-C(1)-C(2)	114.47(10)	N(1)-C(1)-C(5)	104.35(9)
N(1)-C(1)-C(7)	112.28(10)	C(5)-C(1)-C(2)	105.39(10)
C(7)-C(1)-C(2)	111.41(10)	C(7)-C(1)-C(5)	108.26(10)
C(3)-C(2)-C(1)	103.03(10)	C(3)-C(2)-C(23)	112.87(11)
C(23)-C(2)-C(1)	118.45(10)	C(4)-C(3)-C(2)	113.36(12)
C(3)-C(4)-C(5)	112.62(11)	C(3)-C(4)-C(9)	126.00(12)
C(9)-C(4)-C(5)	121.19(11)	C(4)-C(5)-C(1)	103.32(10)
C(4)-C(5)-C(6)	114.08(10)	C(6)-C(5)-C(1)	106.41(10)
N(2)-C(6)-C(5)	105.15(9)	N(2)-C(6)-C(29)	114.03(11)
C(29)-C(6)-C(5)	115.43(10)	O(1)-C(7)-O(2)	124.50(12)
O(1)-C(7)-C(1)	125.01(13)	O(2)-C(7)-C(1)	110.41(11)
O(3)-C(9)-O(4)	123.81(12)	O(3)-C(9)-C(4)	123.86(12)
O(4)-C(9)-C(4)	112.32(11)	C(12)-C(11)-N(1)	119.68(11)
C(16)-C(11)-N(1)	121.80(11)	C(16)-C(11)-C(12)	118.44(12)
C(13)-C(12)-C(11)	120.67(13)	C(12)-C(13)-C(14)	120.73(13)
C(13)-C(14)-C(15)	118.75(13)	C(14)-C(15)-C(16)	121.23(14)
C(15)-C(16)-C(11)	120.17(13)	C(18)-C(17)-N(2)	122.45(11)
C(18)-C(17)-C(22)	118.79(12)	C(22)-C(17)-N(2)	118.49(12)
C(19)-C(18)-C(17)	120.05(14)	C(18)-C(19)-C(20)	120.89(15)
C(21)-C(20)-C(19)	119.17(13)	C(20)-C(21)-C(22)	120.88(14)
C(21)-C(22)-C(17)	120.20(14)	C(24)-C(23)-C(2)	120.25(11)
C(24)-C(23)-C(28)	118.83(12)	C(28)-C(23)-C(2)	120.88(12)

C(25)-C(24)-C(23)	120.56(14)	C(26)-C(25)-C(24)	120.10(15)
C(27)-C(26)-C(25)	119.84(14)	C(26)-C(27)-C(28)	120.37(15)
C(27)-C(28)-C(23)	120.25(15)	C(30)-C(29)-C(6)	117.99(13)
C(34)-C(29)-C(6)	122.89(12)	C(34)-C(29)-C(30)	119.11(13)
C(31)-C(30)-C(29)	120.57(16)	C(32)-C(31)-C(30)	119.90(16)
C(31)-C(32)-C(33)	120.32(15)	C(32)-C(33)-C(34)	120.22(17)
C(29)-C(34)-C(33)	119.87(15)	C(47)-O(5)-C(48)	116.61(11)
C(49)-O(8)-C(50)	115.41(11)	N(4)-N(3)-C(41)	110.93(9)
C(51)-N(3)-N(4)	116.10(10)	C(51)-N(3)-C(41)	122.86(10)
N(3)-N(4)-C(46)	108.82(9)	C(57)-N(4)-N(3)	115.33(9)
C(57)-N(4)-C(46)	119.98(10)	N(3)-C(41)-C(42)	115.38(10)
N(3)-C(41)-C(45)	103.80(9)	N(3)-C(41)-C(47)	113.65(10)
C(45)-C(41)-C(42)	105.08(10)	C(47)-C(41)-C(42)	110.95(10)
C(47)-C(41)-C(45)	106.96(10)	C(43)-C(42)-C(41)	103.22(10)
C(43)-C(42)-C(63)	114.34(11)	C(63)-C(42)-C(41)	119.17(11)
C(44)-C(43)-C(42)	113.12(11)	C(43)-C(44)-C(45)	112.56(11)
C(43)-C(44)-C(49)	127.86(12)	C(49)-C(44)-C(45)	119.41(11)
C(44)-C(45)-C(41)	103.98(10)	C(44)-C(45)-C(46)	114.95(10)
C(46)-C(45)-C(41)	105.68(10)	N(4)-C(46)-C(45)	103.92(9)
N(4)-C(46)-C(69)	114.38(11)	C(69)-C(46)-C(45)	113.89(10)
O(5)-C(47)-C(41)	110.14(10)	O(6)-C(47)-O(5)	124.58(12)
O(6)-C(47)-C(41)	124.99(12)	O(7)-C(49)-O(8)	123.36(13)
O(7)-C(49)-C(44)	123.34(12)	O(8)-C(49)-C(44)	113.27(11)
C(52)-C(51)-N(3)	120.47(12)	C(52)-C(51)-C(56)	118.55(12)
C(56)-C(51)-N(3)	120.83(11)	C(53)-C(52)-C(51)	120.18(13)
C(54)-C(53)-C(52)	120.81(14)	C(55)-C(54)-C(53)	119.23(14)
C(54)-C(55)-C(56)	120.79(14)	C(55)-C(56)-C(51)	120.32(13)
C(58)-C(57)-N(4)	120.46(11)	C(58)-C(57)-C(62)	118.33(11)
C(62)-C(57)-N(4)	120.92(11)	C(59)-C(58)-C(57)	120.47(12)
C(60)-C(59)-C(58)	121.10(13)	C(59)-C(60)-C(61)	118.75(13)
C(60)-C(61)-C(62)	121.24(13)	C(61)-C(62)-C(57)	120.08(12)
C(64)-C(63)-C(42)	120.37(14)	C(68)-C(63)-C(42)	120.86(12)
C(68)-C(63)-C(64)	118.60(14)	C(63)-C(64)-C(65)	119.52(19)
C(66)-C(65)-C(64)	120.80(18)	C(67)-C(66)-C(65)	119.61(16)
C(66)-C(67)-C(68)	120.4(2)	C(63)-C(68)-C(67)	121.11(16)
C(70)-C(69)-C(46)	123.76(12)	C(70)-C(69)-C(74)	118.31(14)
C(74)-C(69)-C(46)	117.91(14)	C(69)-C(70)-C(71)	120.81(15)
C(72)-C(71)-C(70)	120.30(17)	C(71)-C(72)-C(73)	119.31(16)
C(72)-C(73)-C(74)	121.04(19)	C(69)-C(74)-C(73)	120.22(19)

Symmetry transformations used to generate equivalent atoms: —

Table S11: Anisotropic displacement parameters (Å^2) for **165**. The anisotropic displacement factor exponent takes the form: $-2\pi^2[\,h^2\,a^{*2}U_{11} + \ldots + 2\,h\,k\,a^*\,b^*\,U_{12}\,]$.

	U_{11}	U_{22}	U_{33}	U_{23}	U_{13}	U_{12}
O(1)	0.049(1)	0.042(1)	0.058(1)	−0.015(1)	−0.018(1)	−0.010(1)
O(2)	0.043(1)	0.049(1)	0.033(1)	−0.014(1)	−0.006(1)	−0.004(1)
O(3)	0.034(1)	0.057(1)	0.051(1)	−0.002(1)	−0.001(1)	0.013(1)
O(4)	0.044(1)	0.056(1)	0.038(1)	−0.005(1)	−0.007(1)	0.018(1)
N(1)	0.024(1)	0.025(1)	0.034(1)	−0.006(1)	−0.005(1)	−0.001(1)
N(2)	0.025(1)	0.029(1)	0.035(1)	−0.009(1)	−0.005(1)	−0.003(1)
C(1)	0.029(1)	0.025(1)	0.035(1)	−0.009(1)	−0.005(1)	0.000(1)
C(2)	0.028(1)	0.026(1)	0.040(1)	−0.006(1)	−0.003(1)	−0.002(1)
C(3)	0.035(1)	0.028(1)	0.040(1)	−0.002(1)	−0.001(1)	0.003(1)
C(4)	0.032(1)	0.024(1)	0.038(1)	−0.008(1)	−0.004(1)	0.001(1)
C(5)	0.028(1)	0.028(1)	0.034(1)	−0.010(1)	−0.004(1)	0.001(1)
C(6)	0.027(1)	0.030(1)	0.033(1)	−0.008(1)	−0.005(1)	0.000(1)
C(7)	0.031(1)	0.029(1)	0.042(1)	−0.012(1)	−0.009(1)	0.003(1)
C(8)	0.065(1)	0.069(1)	0.038(1)	−0.017(1)	−0.016(1)	0.004(1)
C(9)	0.033(1)	0.029(1)	0.040(1)	−0.009(1)	−0.005(1)	0.003(1)
C(10)	0.053(1)	0.063(1)	0.049(1)	−0.006(1)	−0.019(1)	0.021(1)
C(11)	0.032(1)	0.027(1)	0.027(1)	−0.008(1)	−0.004(1)	0.001(1)
C(12)	0.032(1)	0.031(1)	0.037(1)	−0.003(1)	−0.004(1)	−0.001(1)
C(13)	0.035(1)	0.044(1)	0.046(1)	−0.005(1)	−0.011(1)	0.003(1)
C(14)	0.051(1)	0.038(1)	0.046(1)	0.001(1)	−0.017(1)	0.007(1)
C(15)	0.056(1)	0.030(1)	0.038(1)	0.000(1)	−0.010(1)	−0.004(1)
C(16)	0.038(1)	0.031(1)	0.033(1)	−0.006(1)	−0.006(1)	−0.004(1)
C(17)	0.037(1)	0.024(1)	0.030(1)	−0.002(1)	−0.009(1)	−0.004(1)
C(18)	0.046(1)	0.029(1)	0.033(1)	−0.006(1)	−0.006(1)	−0.003(1)
C(19)	0.074(1)	0.032(1)	0.035(1)	−0.010(1)	−0.010(1)	−0.001(1)
C(20)	0.084(1)	0.034(1)	0.042(1)	−0.007(1)	−0.027(1)	−0.013(1)
C(21)	0.058(1)	0.038(1)	0.055(1)	0.002(1)	−0.031(1)	−0.013(1)
C(22)	0.039(1)	0.032(1)	0.046(1)	−0.003(1)	−0.015(1)	−0.005(1)
C(23)	0.030(1)	0.028(1)	0.032(1)	0.002(1)	−0.003(1)	0.001(1)
C(24)	0.043(1)	0.032(1)	0.035(1)	−0.001(1)	−0.001(1)	−0.002(1)
C(25)	0.074(1)	0.036(1)	0.036(1)	−0.003(1)	0.007(1)	0.004(1)
C(26)	0.060(1)	0.051(1)	0.046(1)	0.004(1)	0.014(1)	0.023(1)
C(27)	0.033(1)	0.063(1)	0.048(1)	0.010(1)	0.003(1)	0.012(1)
C(28)	0.031(1)	0.045(1)	0.039(1)	0.003(1)	−0.005(1)	0.001(1)
C(29)	0.030(1)	0.039(1)	0.038(1)	−0.012(1)	0.000(1)	−0.007(1)
C(30)	0.034(1)	0.052(1)	0.049(1)	−0.016(1)	0.002(1)	0.000(1)
C(31)	0.041(1)	0.068(1)	0.059(1)	−0.026(1)	0.010(1)	−0.001(1)
C(32)	0.054(1)	0.077(1)	0.052(1)	−0.030(1)	0.017(1)	−0.013(1)
C(33)	0.064(1)	0.064(1)	0.039(1)	−0.008(1)	0.005(1)	−0.014(1)
C(34)	0.043(1)	0.048(1)	0.041(1)	−0.009(1)	0.002(1)	−0.006(1)
O(5)	0.027(1)	0.044(1)	0.054(1)	−0.018(1)	−0.001(1)	0.002(1)
O(6)	0.046(1)	0.040(1)	0.047(1)	−0.019(1)	0.002(1)	−0.002(1)
O(7)	0.052(1)	0.071(1)	0.047(1)	0.018(1)	−0.021(1)	−0.019(1)
O(8)	0.040(1)	0.046(1)	0.044(1)	0.008(1)	−0.007(1)	−0.014(1)
N(3)	0.032(1)	0.024(1)	0.028(1)	−0.005(1)	−0.001(1)	−0.002(1)
N(4)	0.029(1)	0.027(1)	0.029(1)	−0.005(1)	−0.005(1)	0.000(1)
C(41)	0.029(1)	0.023(1)	0.034(1)	−0.005(1)	−0.004(1)	−0.002(1)
C(42)	0.033(1)	0.029(1)	0.034(1)	−0.007(1)	−0.006(1)	−0.003(1)
C(43)	0.029(1)	0.025(1)	0.041(1)	−0.003(1)	−0.006(1)	−0.004(1)

C(44)	0.029(1)	0.023(1)	0.038(1)	−0.001(1)	−0.007(1)	0.000(1)
C(45)	0.027(1)	0.025(1)	0.036(1)	−0.003(1)	−0.007(1)	0.001(1)
C(46)	0.029(1)	0.028(1)	0.033(1)	−0.002(1)	−0.007(1)	−0.001(1)
C(47)	0.035(1)	0.022(1)	0.038(1)	−0.004(1)	−0.002(1)	−0.001(1)
C(48)	0.031(1)	0.062(1)	0.076(1)	−0.022(1)	0.003(1)	0.008(1)
C(49)	0.033(1)	0.029(1)	0.041(1)	0.001(1)	−0.009(1)	−0.002(1)
C(50)	0.049(1)	0.056(1)	0.050(1)	0.014(1)	−0.001(1)	−0.014(1)
C(51)	0.027(1)	0.025(1)	0.036(1)	−0.004(1)	0.002(1)	0.002(1)
C(52)	0.047(1)	0.028(1)	0.038(1)	−0.007(1)	0.005(1)	0.001(1)
C(53)	0.066(1)	0.035(1)	0.042(1)	−0.005(1)	0.019(1)	0.002(1)
C(54)	0.062(1)	0.034(1)	0.061(1)	−0.002(1)	0.028(1)	−0.006(1)
C(55)	0.044(1)	0.029(1)	0.063(1)	−0.009(1)	0.009(1)	−0.008(1)
C(56)	0.035(1)	0.029(1)	0.043(1)	−0.008(1)	0.000(1)	−0.001(1)
C(57)	0.028(1)	0.024(1)	0.032(1)	−0.007(1)	−0.004(1)	−0.005(1)
C(58)	0.035(1)	0.027(1)	0.030(1)	−0.005(1)	−0.003(1)	−0.001(1)
C(59)	0.039(1)	0.033(1)	0.043(1)	−0.008(1)	−0.007(1)	0.005(1)
C(60)	0.042(1)	0.045(1)	0.046(1)	−0.019(1)	−0.001(1)	0.007(1)
C(61)	0.048(1)	0.053(1)	0.033(1)	−0.017(1)	−0.001(1)	0.001(1)
C(62)	0.040(1)	0.040(1)	0.031(1)	−0.008(1)	−0.009(1)	0.001(1)
C(63)	0.038(1)	0.035(1)	0.037(1)	0.002(1)	−0.012(1)	−0.014(1)
C(64)	0.055(1)	0.076(1)	0.038(1)	0.005(1)	−0.010(1)	−0.025(1)
C(65)	0.079(1)	0.093(2)	0.048(1)	0.031(1)	−0.034(1)	−0.046(1)
C(66)	0.075(1)	0.052(1)	0.098(2)	0.029(1)	−0.055(1)	−0.022(1)
C(67)	0.062(1)	0.035(1)	0.099(2)	0.001(1)	−0.042(1)	0.000(1)
C(68)	0.045(1)	0.032(1)	0.057(1)	−0.004(1)	−0.020(1)	−0.003(1)
C(69)	0.032(1)	0.039(1)	0.042(1)	−0.011(1)	−0.011(1)	0.001(1)
C(70)	0.035(1)	0.050(1)	0.047(1)	−0.012(1)	−0.008(1)	−0.006(1)
C(71)	0.035(1)	0.076(1)	0.064(1)	−0.027(1)	−0.003(1)	−0.014(1)
C(72)	0.036(1)	0.088(2)	0.111(2)	−0.032(1)	−0.031(1)	0.010(1)
C(73)	0.062(1)	0.069(1)	0.168(3)	0.000(2)	−0.068(2)	0.009(1)
C(74)	0.052(1)	0.049(1)	0.117(2)	0.008(1)	−0.046(1)	−0.002(1)

Table S12: Hydrogen coordinates and isotropic displacement parameters ($Å^2$) for **165**.

	x	y	z	U_{eq}
H(2)	1.1507	0.3014	0.1892	0.038
H(3)	1.0122	0.3232	0.0793	0.042
H(5)	0.8388	0.2816	0.2704	0.035
H(6)	0.7001	0.1678	0.2140	0.036
H(8A)	0.9814	0.1388	0.4735	0.083
H(8B)	1.0458	0.2350	0.4424	0.083
H(8C)	1.1387	0.1469	0.4383	0.083
H(10A)	0.6101	0.4631	0.0495	0.083
H(10B)	0.5621	0.3700	0.0345	0.083
H(10C)	0.6649	0.4320	-0.0230	0.083
H(12)	1.2596	0.1148	0.2676	0.041
H(13)	1.4002	0.0107	0.3348	0.050
H(14)	1.3123	-0.1276	0.3926	0.055
H(15)	1.0801	-0.1591	0.3836	0.050
H(16)	0.9363	-0.0550	0.3182	0.041
H(18)	1.0178	-0.0103	0.1684	0.043

H(19)	0.9517	-0.1073	0.0987	0.056
H(20)	0.7163	-0.1304	0.0896	0.062
H(21)	0.5466	-0.0555	0.1508	0.060
H(22)	0.6094	0.0427	0.2202	0.047
H(24)	1.0734	0.1322	0.0940	0.045
H(25)	1.2400	0.0499	0.0369	0.060
H(26)	1.4765	0.0723	0.0416	0.067
H(27)	1.5465	0.1771	0.1031	0.062
H(28)	1.3810	0.2565	0.1635	0.048
H(30)	0.5369	0.2508	0.2851	0.054
H(31)	0.3857	0.2367	0.3882	0.066
H(32)	0.4322	0.1313	0.4878	0.072
H(33)	0.6296	0.0390	0.4855	0.067
H(34)	0.7795	0.0496	0.3814	0.053
H(42)	1.0741	0.5360	0.8225	0.038
H(43)	1.2704	0.5526	0.7217	0.038
H(45)	0.8816	0.5564	0.6909	0.036
H(46)	0.9731	0.4490	0.6036	0.036
H(48A)	0.5177	0.4993	0.7847	0.084
H(48B)	0.6058	0.5688	0.8140	0.084
H(48C)	0.5630	0.4757	0.8642	0.084
H(50A)	1.2956	0.6457	0.4857	0.082
H(50B)	1.3826	0.7129	0.5180	0.082
H(50C)	1.2214	0.7336	0.5063	0.082
H(52)	0.9148	0.3502	0.9022	0.046
H(53)	0.7957	0.2408	0.9854	0.060
H(54)	0.6989	0.1210	0.9501	0.066
H(55)	0.7302	0.1074	0.8313	0.055
H(56)	0.8513	0.2146	0.7473	0.043
H(58)	1.1372	0.2412	0.7620	0.037
H(59)	1.3199	0.1582	0.7184	0.045
H(60)	1.3757	0.1719	0.5965	0.052
H(61)	1.2433	0.2686	0.5179	0.052
H(62)	1.0578	0.3512	0.5598	0.044
H(64)	1.1124	0.4500	0.9362	0.069
H(65)	1.2624	0.3523	1.0056	0.092
H(66)	1.4321	0.2687	0.9526	0.093
H(67)	1.4509	0.2797	0.8305	0.078
H(68)	1.3020	0.3747	0.7606	0.053
H(70)	0.7098	0.3163	0.6861	0.052
H(71)	0.4765	0.3281	0.6606	0.067
H(72)	0.3904	0.4591	0.5958	0.090
H(73)	0.5371	0.5776	0.5549	0.119
H(74)	0.7702	0.5672	0.5791	0.088

8 Danksagungen

Zunächst gilt mein Dank Herrn Prof. Dr. Alois Fürstner für die Aufnahme in seinen Arbeitskreis, die spannenden und herausfordernden Themenstellungen, das entgegengebrachte Vertrauen, die Bereitstellung ausgezeichneter Arbeitsbedingungen und für die mir gewährte Freiheit bei der Durchführung dieser Arbeit. Ich danke außerdem Herrn Prof. Dr. Nobert Krause von der TU Dortmund für die Übernahme des Zweitgutachtens.

Für die gute Zusammenarbeit in beiden Projekten danke ich Helga und Christophe. Monika Lickfeld danke ich für ihre Hilfe bei allen organisatorischen Angelegenheiten. Ebenfalls möchte ich mich bei Christian, Karin, Rosi, Saskia und Sebastian für die großartige Unterstützung bedanken. Haltet den Laden weiter am Laufen! ;)

Ohne die Unterstützung der analytischen Abteilungen des Max-Planck-Instituts für Kohlenforschung wäre mir eine erfolgreiche Anfertigung dieser Arbeit nicht möglich gewesen. Deshalb gilt mein Dank zunächst der Abteilung für Massenspektrometrie (namentlich Marion Blumenthal, Dirk Kampen, Simone Marcus und Daniel Margold) und der HPLC-Abteilung (Alfred Deege und seinem Team). Petra und Christophe, Euch danke ich für die zuverlässige Messung und gewissenhafte Auswertung der anvertrauten NMR-Proben. Elke Dreher, Angelika Dreier, Dr. Richard Goddard und Jörg Rust danke ich für die Bestimmung der Kristallstrukturen.

Meinen Kollegen in Box 5 und im Büro (Alberto, Aurélien, Christian, Christophe, Dragoş, Fabio, Jakub, Johanna, Karin, Pol, Sylvester und Yong) möchte ich für ihre (z. T. sehr humorvolle) Unterstützung in vielen praktischen und theoretischen Aspekten des Arbeitsalltags danken. Karin, Du hast mit Deiner Unterstützung und mit der Organisation eines reibungslosen Ablaufs im Labor entscheidend zum Erfolg dieser Arbeit beigetragen. Danke!

Weiterhin möchte ich ehemaligen und aktuellen Mitgliedern der Arbeitsgruppe danken, die neben dem wissenschaftlichen Austausch auch für unvergessliche Erlebnisse beim Bouldern, Essen, Fußball, Geburtstagsfeiern, Geocaching, Hochseilgärten, Kanufahrten, Klettern, Kochen, Museumsbesuchen, Party machen, Radtouren, Reisen, Saunagängen, Squash, Trinken, Umzüge, Wandern, Weihnachtsmarktbesuche, usw. verantwortlich waren.

Besonders hervorheben möchte ich meine Kletterpartner Aileen, Lauren, Lee und Nico. Mit Euch konnte ich mein Hobby während meiner Zeit in Mülheim weiter betreiben, in neue Schwierigkeitsgrade vorsteigen und so den Kopf immer wieder frei bekommen. Es hat mir sehr viel Spaß gemacht!

Mein ganz besonderer Dank gilt Dragoş und Lee. Ihr habt mich jeglicher Hinsicht unterstützt und mich viel gelehrt. Für diese Unterstützung danke ich Euch sehr. Nicht zuletzt danke ich Euch auch für die kritisch-konstruktive Korrektur dieser Arbeit sowie die *Myriade* an Anmerkungen und Verbesserungsvorschlägen.

Der größte Dank allerdings gilt meiner Familie. Sie unterstützte mich immer und half mir den richtigen Weg zu finden. Unendlich dankbar bin ich dabei meinen Eltern. Ich habe Euch so viel zu verdanken; auf Eure Unterstützung konnte ich mich immer verlassen und Ihr habt es mir ermöglicht, diesen Weg einzuschlagen. Vielen Dank! Deshalb widme ich Euch diese Arbeit.